Alandijany, Thamir Abdulaziz A. (2018) *Distinct temporal regulation of intrinsic and innate intracellular immunity to Herpes Simplex Virus type 1 (HSV-1) infection.* PhD thesis.

https://theses.gla.ac.uk/30662/

Distinct Temporal Regulation of Intrinsic and Innate Intracellular Immunity to Herpes Simplex Virus type 1 (HSV-1) Infection

Thamir Abdulaziz A Alandijany

A thesis presented for the degree of Doctor of Philosophy in the College of Medical, Veterinary, and Life Sciences

MRC-University of Glasgow Center for Virus Research

Institute of Infection Immunity and Inflammation

University of Glasgow

2018

Abstract

Intrinsic and innate immunity play pivotal roles in limiting the replication of invading viral pathogens. Intrinsic immunity is constitutive and mediated by pre-existing host cell restriction factors (e.g., promyelocytic leukemia-nuclear body (PML-NB) constituent proteins) which directly confer antiviral properties. On the other hand, innate immunity is inducible and upregulated in response to infection. Pattern recognition receptors (PRRs) (e.g., interferon gamma inducible protein 16 (IFI16)) sense pathogen-associated molecular patterns (PAMPs) and induce downstream signaling cascades leading to the induction of Interferon-stimulated gene (ISG) products that confer antiviral properties. These two arms of immunity represent the first line of intracellular defense to HSV-1 infection. Indeed, rapid recruitment of intrinsic and innate immune factors to viral DNA (vDNA) has a significant bearing on the outcome of infection. However, the spatial and temporal regulation of this recruitment remains poorly defined due to the technical challenges associated with vDNA detection at multiplicities of infection (MOI) that do not saturate intrinsic host factors. Utilizing 5-Ethynyl-2'-deoxyuridine (EdU) labeling of HSV-1 DNA in combination with click chemistry, we directly visualized input viral genomes under low MOI conditions (MOI of ≤ 3 PFU/cell) at 30-90 minutes post-addition of virus (mpi). This protocol is sensitive, specific, and compatible with indirect immunofluorescence (IF) staining protocols, providing a valuable assay to investigate the temporal recruitment of immune regulators to infecting vDNA.

Upon entry of vDNA into the nucleus, PML-NB associated restriction factors (e.g., PML, SP100, and Daxx) were rapidly recruited to infecting viral genome foci. This process occurred in a PML-dependent manner and led to genome entrapment and silencing within PML-NBs. Interestingly, genome entrapment was observed during both wild-type (WT) and ICP0-null mutant (ΔICP0) HSV-1 infection. During WT HSV-1 infection, ICP0 induced PML degradation and the dispersal of PML-NB restriction factors, highlighting the importance of ICP0 to release viral genomes entrapped within PML-NBs to stimulate the onset of lytic HSV-1 replication. During ΔICP0 HSV-1 infection,

vDNA remained stably entrapped within PML-NBs leading to a repression in viral gene expression and a restriction in plaque formation. Importantly, IFI16 was not stably recruited to vDNA entrapped within PML-NBs, and ISG expression was not induced under low MOI conditions that do not saturate PML-NB intrinsic host defenses. These data demonstrate that vDNA entry into the nucleus alone is not sufficient to stimulate the induction of innate immunity.

Saturation of intrinsic host defenses under high MOI conditions stimulated the stable recruitment of IFI16 to infecting viral genomes, and induced ISG expression in a PML-, IFI16-, and Janus-associated kinase (JAK)-dependent manner. The induction of this innate immune response was dependent on the onset of vDNA replication, as treatment of the infected cell monolayers with phosphonoacetic acid (PAA), a vDNA polymerase inhibitor, inhibited ISG induction in a dose-dependent manner. Unlike PML depletion, inhibition of JAK signaling failed to relieve the plaque formation defect of ΔICP0 HSV-1, but instead significantly enhanced virus yields.

Collectively, these data, for the first time, demonstrate a temporal and sequential induction of intrinsic and innate immunity during HSV-1 infection. Intrinsic immunity is induced within minutes of nuclear infection to restrict the initiation of viral gene transcription and the onset of lytic replication. Escape from this intrinsic repression and initiation of vDNA replication, which takes several hours, triggers the induction of innate immunity. ISG products establish an antiviral state within infected and neighboring uninfected cells to constrict viral propagation and limit the spread of infection. We identify dual roles for PML in the regulation of intrinsic and innate immunity to HSV-1 infection. However, these host defenses are counteracted by the viral ubiquitin ligase ICP0, which targets PML for degradation to promote vDNA release from PML-NBs in order to evade intrinsic viral genome silencing from the onset of nuclear infection.

Contents

Supplementary materials

ALANDIJANY T, ROBERTS APE, CONN KL, LONEY C, MCFARLANE S, ORR A AND BOUTELL C. 2018. Distinct temporal roles for the promyelocytic leukaemia (PML) protein in the sequential regulation of intracellular host immunity to HSV-1 infection. PLoS pathogens 14: e1006769.

List of figures

List of tables

Acknowledgements

Author's declaration

Author's Declaration All the results presented in this thesis were obtained by the author's own efforts, unless stated otherwise.

List of abbreviations

ACG	Acyclovir
ATRX	Alpha-thalassemia mental retardation X-linked
BHK	Baby hamster kidney cells
BrdU	Bromodeoxyuridine
CBP	CREB binding protein
cDNA	Complementary DNA
cDCs	Conventional dendritic cells
CENP	Centromere protein
CIITA	Class II transactivator
cGAMP	Cyclic guanosine monophosphate–adenosine monophosphate
cGAS	cGAMP synthase
ChIP	Chromosome immune-precipitation
Ctrl	Control
CMV	Cytomegalovirus
DAI	DNA-dependent activator of interferon regulatory factors
Daxx	Human death-domain associated protein
Dil	Dilution
DMEM	Dulbecco's Modified Eagle Medium
DMSO	Dimethyl sulfoxide
DNA	Deoxyribonucleic acid
DNA-PKcs	DNA-dependent protein kinase
Ds	Double strand
DTT	DL-Dithiothreitol
E	Early
EBV	Epstein-Barr virus
EdA	5-Ethynyl-2'-deoxyadenosine
EdC	5-Ethynyl-2'-deoxycytidine
EdU	5-Ethynyl-2'-deoxyuridine
EGTA	Ethylene glycol tetraacetic acid
ER	Endoplasmic reticulum
eYFP	Enhanced Yellow Fluorescent Protein

E2FBP1	E2F-binding protein 1
FCS	Fetal calf serum
FISH	Fluorescent in situ hybridization
G	Glycoprotein
GMEM	Glasgow modified Eagle's medium
HaCaT	A spontaneously transformed aneuploid immortal keratinocyte cell line from adult human skin
HC	Host cell factor
HCl	Hydrogen chloride
HDAC	Histone deacetylase
HEK-293t	Human embryonic kidney cells immortalized by insertion of hTERT
HEL	Human embryonic lung
HFt	Human Fibroblasts immortalized by insertion of hTERT
HHV	Human herpesviruses
HIN-200	DNA-binding hematopoietic interferon-inducible nuclear proteins with 200-amino acids repeat
Hpi	Hours post-infection
HS	Human serum
HSV	Herpes Simplex Virus type
HSV-1^{EdU}	EdU-labeled WT HSV-1
hTERT	Human telomerase reverse transcriptase
ICP	Infected cell protein
IE	Immediate early
IF	Indirect immunofluorescence
IFI16	Interferon gamma inducible protein 16
IFN	Interferon
IFNAR	IFNα/ß receptor
IFNGR	IFNγ receptor
IKKε	Inhibitor of NFκB epsilon
IL	Interleukin
IRF	IFN-regulatory factor
ISG	IFN-stimulated gene
ISGF3	IFN-stimulated gene factor 3

IU	International unit
JAK	Janus-associated kinase
K	Lysine
kDa	Kilo Dalton
L	Late
LATs	Latency-associated transcripts
LSD1	Lysine-specific histone demethylase 1A
MAVS	Adaptor protein mitochondrial antiviral signaling protein
MDA	Melanoma differentiation-associated gene
MEFs	Mouse embryonic fibroblasts
MgCl2	Magnesium chloride
Mg	Milligram
MHC	Major histocompatibility complex
Ml	Milliliter
Mm	Millimeter
MOI	Multiplicity of infection
MORC	Microrchidia family CW-type zinc finger
Mpi	Minutes post-infection
mRNA	Messenger RNA
NaCl	Sodium Chloride
NFκB	Nuclear factor kappa-light-chain-enhancer of activated B cells
Ng	Nanogram
NK	Natural killer
NLS	Nuclear localization signal
Ns	Non-significant
N-CoR	Nuclear receptor co-repressor
OAS	2-5 Oligoadenylate synthetase
Oct	Octamer-binding protein
Ori	Origin of replication
ORF	Open reading frame
PAA	Phosphonoacetic acid
PAGE	Polyacrylamide gel electrophoresis
PAH	Paired amphipathic helices

PAMPs	Pathogen-associated molecular pattern
PBS	Phosphate buffered saline
pDCs	Plasmacytoid dendritic cells
PFU	Plaque forming unit
PIAS	Protein Inhibitor of Activated STAT
PML	Promyelocytic leukemia protein
PML-NB	PML-nuclear body
Pol III	RNA polymerase III
PRRs	Pattern recognition receptors
PY	Pyrin
qPCR	Quantitative polymerase chain reaction
RIG	Retinoic acid inducible gene
RING	Really interesting new gene
RNA	Ribonucleic acid
RNase	Ribonuclease
RNF	Ring finger protein
RPE	Retinal pigmented epithelial cells immortalized hTERT
Rpm	Revolutions per minute
RQ	Relative quantitation
RT	Reverse transcription
Rux	Ruxolitinib
SAE	SUMO-activating enzymes
SAOS	Human bone osteosarcoma epithelial cells
SD	Standard deviation
SDS	Sodium dodecyl sulfate
SENP	SUMO-specific proteases
shRNA	Short hairpin RNA
SIM	Sumo-interacting motif
SLS	SIM-like sequence
Sp100	Speckled protein of 100 kDa
STAT	Signal transducers and activators of transcription
STING	Stimulator of interferon genes
STUbL	SUMO-targeted ubiquitin ligases

Ss	Single strand
SUMO	Small ubiquitin-like modifiers
TBK1	TANK binding kinase 1
TBP	TATA-binding protein
TF	Transcription factor
Th	T helper
Tk	Thymidine kinase
TLR	Toll-like receptor
TNFα	Tumor-necrosis factors α
TPB	Tryptose Phosphate Broth
TPCK	Tosyl phenylalanyl chloromethyl ketone
TRIM	Tripartite motif
TYK	Tyrosine kinase
Ubc9	SUMO E2 conjugating enzyme
Ub	Ubiquitin
U_L	Unique long
U_s	Unique short
USP7	Ubiquitin-specific protease 7
UV	Ultraviolet
U2OS	Human bone osteosarcoma epithelial cells
vDNA	Viral DNA
Vhs	Virion host shutoff
VP	Virion protein
VSV	Varicella-zoster virus
W	Weighted
WB	Western blot
WT	Wild type
ZAP	Zinc finger antiviral protein
3D	3 dimensional
μg	Microgram
μM	Micromolar
ΔICP0	ICP0-null mutant HSV-1
$\Delta ICP0^{EdU}$	EdU-labeled ΔICP0 HSV-1

1. Introduction

When host cells are invaded by viruses, cells deploy multifaceted defense mechanisms to control infection and minimize the damage they may cause. These antiviral responses can be classified into three main branches of immunity: intrinsic, innate, and adaptive. Intrinsic immune responses refer to pre-existing cellular defenses conferred by proteins (host cell restriction factors) that can directly and immediately control viral replication. In contrast, innate and adaptive immune responses are conferred by proteins and cells that are induced and upregulated in response to infection (Hannoun et al. 2016, Scherer and Stamminger 2016, Yan and Chen 2012).

Efficient restriction of invading viral pathogens relies on both constitutive and induced arms of host immunity. Viruses, however, have evolved multiple strategies to evade these immune defenses. The molecular basis of these viral-host interactions has been extensively studied (Lanfranca et al. 2014, Orzalli and Knipe 2014, Zheng 2018, Bieniasz 2004, Boutell and Everett 2013, Yan and Chen 2012). This literature review will focus on the mechanisms employed by host cells to control herpes simplex virus type 1 (HSV-1) infection, as well as the strategies employed by the virus to counteract these immune responses. Particular attention will be given to promyelocytic leukemia-nuclear body (PML-NB) constituent proteins and Interferon γ-inducible Protein (IFI16) due to their key role in regulating intrinsic and innate immune responses during herpesvirus infection, respectively. The central role of the viral infected cell protein 0 (ICP0) to evade these immune mechanisms during HSV-1 infection is also discussed.

1.1. An overview of HSV-1 infection

HSV-1 infection is a common viral infection. Worldwide, 3.7 billion people (< 50 years old) are infected with HSV-1. Virus transmission occurs via direct

contact with infected individuals who are shedding the virus (Fields et al. 2013). Vertical transmission from infected mothers to their children during pregnancy is another route for viral transmission, although rare (Baldwin and Whitley 1989). HSV-1 infection is usually asymptomatic or leads to mild symptoms (e.g., cold sores). However, it can also lead to severe or even life-threatening outcomes (e.g., encephalitis) (Whitley 2002, Terni et al. 1971, Binder 1977, Whitley et al. 1984, Olson et al. 1967). Following primary infection and replication within epithelial cells, the virus is transported to the trigeminal ganglia of infected hosts where it establishes a life-long latent infection. Periodic viral reactivation causes episodes of recurrent disease and transmission to new hosts (Spruance 1992, Ship et al. 1977, Segal et al. 1974). The frequency and severity of reactivation vary between individuals. Efficient antiviral drugs (e.g., acyclovir, famciclovir, and valacyclovir) are currently available (Coen 1990). However, HSV-1 drug-resistant strains have been reported (Frobert et al. 2014). Therefore, there is a need for novel anti-viral drugs or effective vaccines.

1.2. Herpesviridae family

HSV-1 belongs to the *herpesviridae* family that comprises more than 200 members. Only nine of them can cause disease in humans (grouped as human herpesviruses; HHV). They are classified based on the genome structure, site of latent infection, pathogenesis and clinical manifestations into three subfamilies: (i) *Alphaherpesvirinae* which includes HHV-1, -2, and -3 (HSV-1, HSV-2, and varicella-zoster virus (VZV), respectively). (ii) *Betaherpesvirinae* which includes HHV-5 (cytomegalovirus (CMV)), HHV-6A, HHV-6B, and HHV-7. (iii) *gammaherpesvirinae* which includes HHV-4 and HHV-8 (Epstein-Barr virus (EBV) and Kaposi sarcoma-associated herpesvirus, respectively) (Fields et al. 2013).

1.3. HSV-1 virion structure

The HSV-1 virion is a spherical particle with an average diameter of 186 nm (Figure 1) (Grunewald et al. 2003). It comprises four components: the core, capsid, tegument, and envelope. The core contains a linear double-strand (ds) DNA genome packaged as a toroid or spool (Furlong et al. 1972, Zhou et al. 1999). However, this linear DNA is circularized rapidly after nuclear entry in the absence of protein synthesis (Poffenberger and Roizman 1985). Complete genome sequencing revealed that the HSV-1 strain 17 genome is 152,260 bp with 68.3% guanine and cytosine and little variations between different strains. The viral genome consists of two elements: unique long (U_L) and unique short (U_S) bracketed by inverted repeats ab and b'a', and ac and c'a', respectively (Wadsworth et al. 1975). The core is surrounded by an icosahedral (T=16) capsid which is composed of 162 capsomers (Schrag et al. 1989).The polyamines spermidine and spermine in the core neutralize the negative charge on viral DNA (vDNA) which allows proper folding of vDNA within the inner surface of the capsid (Gibson and Roizman 1971). Capsid assembly requires VP5, VP19C, VP21, pre-VP22a, VP23, VP24, and VP26 (Trus et al. 1996, Newcomb et al. 1996, Newcomb et al. 1999). Self-interaction of VP5-pre-VP22 complexes forms two types of capsomeres: pentons and hexons (Newcomb et al. 1993). VP26 forms a ring-like structure around the top of hexons (Trus et al. 1995, Zhou et al. 1995). The triplexes (1 copy of VP19C and two copies of VP23) link adjacent capsomeres generating a procapsid with a portal comprised of pUL6 through which vDNA enters and exists the capsid. Maturation of the procapsid is achieved by cleavage of pre-Vp22a by the VP24 viral protease (Desai et al. 1994, Gao et al. 1994). The area between the outer surface of the capsid and the undersurface of the envelope is called tegument. It is a highly unstructured element that forms in the cytoplasm as nuclear capsids are devoid of tegument. Newly assembled capsids undergo primary envelopment at the inner nuclear membrane, de-envelopment at the outer nuclear membrane, and secondary envelopment at the trans-Golgi network and tubular membranes in order to acquire the tegument and envelope proteins (Ibiricu et al. 2011, Ibiricu et al. 2013, Owen et al. 2015, Duffy et al. 2006, Hollinshead et al. 2012). The tegument comprises more than

20 viral proteins identified by biochemical assays and proteomics analysis (Zhou et al. 1999, Roller and Roizman 1992, Loret et al. 2008). Tegument proteins regulate many aspects of viral infection, including entry into target cells, delivery of viral genome to the nucleus, transactivation and repression of viral genes, assembly and egress of progeny virions, and host immune evasion (Table 1). The tegument is enclosed in the viral envelope which consists of a lipid bilayer with spike-like projections embedded in it. Thirteen glycosylated (gB-E, and gG-N) and, at least, two non-glycosylated (U_L20 and U_s9) envelope proteins have been identified. Glycoprotein projections embedded on the surface are particularly crucial for HSV-1 attachment to target cells.
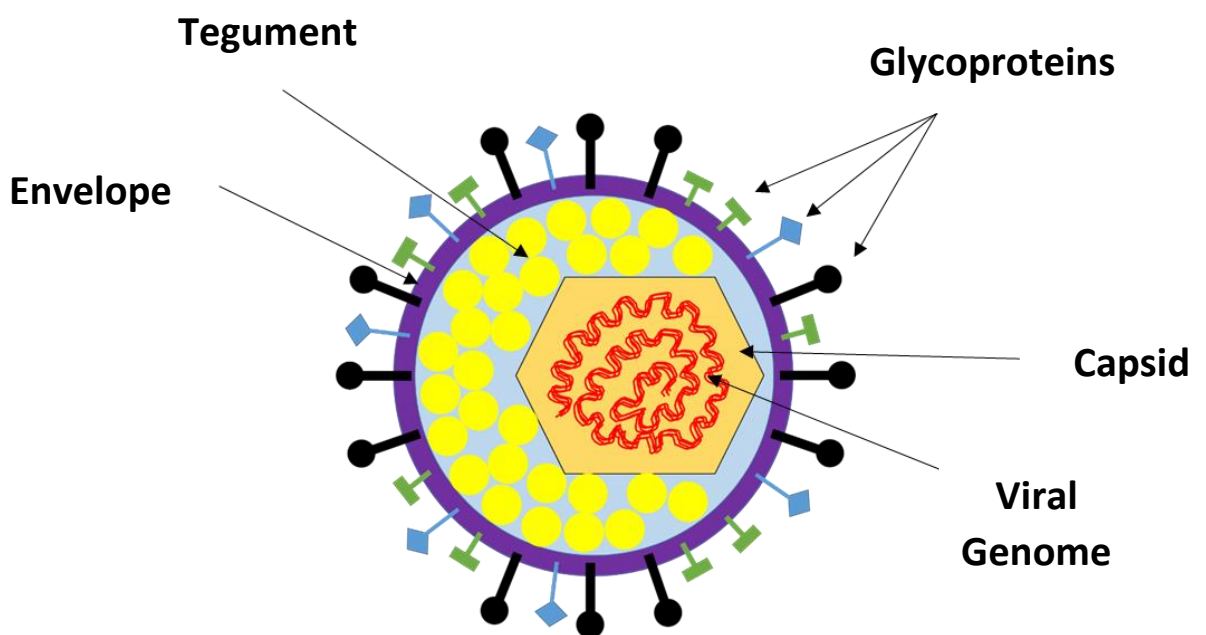
Figure 1. HSV-1 virion structure.

The virion is composed of viral genome, capsid, tegument, and envelope. The viral genome is a linear dsDNA enclosed in the capsid. The tegument represents the area between the capsid and the envelope. The envelope is a lipid bilayer membrane with glycoprotein projections embedded in it (Fields et al. 2013).

Table 1. HSV-1 tegument proteins and their key functions during the viral replication cycle.

Reviewed in (Kelly et al. 2009).

Tegument protein	Functions
RL2 (ICP0)	Transactivation of viral gene transcription and evasion of intracellular immunity
RS1 (ICP4)	Transactivation of viral gene transcription
RL1 (ICP34.5)	Neuro-virulence factor, evasion of intracellular immunity, and stimulation of host translation and vDNA replication
U_s2	Unknown
U_s3	Stimulation of gB-mediated fusion, phosphorylation and dissociation of the tegument proteins from the nucleocapsid, promotion of anti-apoptotic activity, and regulation of nuclear egress and budding
U_s10	Unknown
U_s11 (US11)	Packaging viral and cellular RNA into virions, and stimulation of host translation
U_L7	Regulation of mitochondrial function
U_L11	maturation and envelopment of capsids
U_L13	Phosphorylation and dissociation of the tegument from the nucleocapsid, promotion of apoptosis, evasion of IFN-dependent immunity, and regulation of nuclear egress and budding
U_L14	Delivery of viral genome into the nucleus, enhancement of VP16 nuclear localization, and promotion of anti-apoptotic activity
U_L16	maturation and envelopment of capsids
U_L21	maturation and envelopment of capsids
U_L23 (Thymidine kinase)	Regulation of nucleotide metabolism and vDNA replication
U_L36 (VP1-2)	Promotion of capsid motility along microtubules, delivery of viral genome into the nucleus, regulation of cellular posttranslational ubiquitination, and maturation and envelopment of capsids

U$_L$37	Regulation of immediate early (IE) gene transcription, promotion of capsid motility along microtubules, and maturation of capsids into enveloped virions
U$_L$41 (vhs)	Suppression of host cell and viral protein synthesis, and evasion of intracellular immunity
U$_L$46 (VP11-12)	Enhancement of VP16 transcriptional activity, and maturation and envelopment of capsids
U$_L$47 (VP13-14)	Enhancement of VP16 transcriptional activity, packaging viral and cellular RNA into virions, and maturation and envelopment of capsids
U$_L$48 (VP16)	Initiation of IE gene expression, and maturation and envelopment of capsids
U$_L$49 (VP22)	Packaging viral and cellular RNA into virions, binding to histones and inhibition of nucleosome formation, and maturation and envelopment of capsids
U$_L$50	Regulation of nucleotide metabolism and vDNA replication
U$_L$51	Assembly of virions
U$_L$55	Unknown

1.4. HSV-1 replication cycle

1.4.1. Attachment, fusion, and nuclear delivery of viral genomes

To start replication, the virus needs to first attach to cellular receptors. Several viral-host interactions have been identified during viral attachment: (i) the initial interaction between viral glycoprotein (gB and gC) and heparan sulfate glycosaminoglycans (Spear et al. 1992), and (ii) the interaction between HSV-1 gD and cellular nectin, herpesvirus entry mediator, or 3-O-sulfated heparin sulfate (Shukla et al. 1999, Warner et al. 1998, Geraghty et al. 1998). It is believed that the interaction between gD and its receptors leads to conformational changes of gH and gL, and activation of gB. These processes allow the fusion of the viral envelope with the cellular plasma membrane which mediates viral entry (Avitabile et al. 2007, Gianni et al. 2009, Satoh et al. 2008). In addition to direct fusion with the plasma membrane, endocytosis is another

pathway utilized by HSV-1 to enter into target cells (Lycke et al. 1988, Wittels and Spear 1991, Nicola et al. 2003, Nicola et al. 2005, Nicola and Straus 2004). Following viral entry into the cell, the de-enveloped nucleocapsid is transported to the nuclear pore through the microtubular network (Kristensson et al. 1986, Sodeik et al. 1997, Wolfstein et al. 2006, Radtke et al. 2010). The vDNA is released into the nucleus through nuclear pores without capsid dissociation (Miyamoto and Morgan 1971). The viral protein UL25 and host nuclear protein importin B play central roles in capsid interaction with nuclear pore complex and delivery of vDNA into the nucleus (Pasdeloup et al. 2009, Rode et al. 2011, Copeland et al. 2009). The viral proteins VP1-2, encoded by U$_L$36, must also be cleaved to allow proper uncoating (Jovasevic et al. 2008).

1.4.2.   Viral gene expression and DNA replication

The viral gene products are expressed in a temporal manner. They are classified as immediate-early (IE encoded by α genes), early (E encoded by ß1 and ß2 genes), and late (L encoded by γ1 and γ2 genes) proteins (Honess and Roizman 1974, Honess and Roizman 1975). IE protein (ICP0, ICP4, ICP22, ICP27, and ICP47) expression is turned on by the virion-associated protein VP16, a tegument protein which dissociates from the capsid and localizes to the nucleus upon ejection of vDNA through the nuclear pores (Triezenberg et al. 1988). VP16 forms a transcription complex containing host cell factor (HCF-1) and the octamer-binding protein (Oct-1) which, in turn, recruits Lysine-specific histone demethylase 1A (LSD1) to enable the transcription of the α gene promoters (Gerster and Roeder 1988, Herr 1998, Stern et al. 1989, Wysocka and Herr 2003, Liang et al. 2009). Additional binding between VP16 and other host transcriptional factors (e.g., TATA-binding protein (TBP) and TBP-associated factors) induces the formation of RNA polymerase II preinitiation complex at α gene promoters to stimulate their expression (Sampath and Deluca 2008).

De novo Synthesis of α gene products promotes the expression of E and L viral genes. The IE protein ICP4 is an essential regulator for this process. ICP4 is

a vDNA-binding protein, and it serves as both a transactivator and repressor of viral gene expression depending on the target promoter (O'Hare and Hayward 1985b, DeLuca and Schaffer 1985, Gelman and Silverstein 1985, O'Hare and Hayward 1985a). ICP4 mutants that failed to bind to vDNA stimulated a lower level of E and L protein expression (Shepard et al. 1989), but retained some transactivation activity, suggesting that ICP4 vDNA binding is not solely responsible for its transactivation properties (Shepard and DeLuca 1991). ICP4 interacts with cellular transcription factors (e.g., TBP, transcription factor II B (TFIIB), TFIID, and the Mediator complex) which are required for RNA polymerase II-dependent viral gene transcription. These protein-protein interactions have significant effects on the ability of ICP4 to regulate viral gene expression (Smith et al. 1993, Lester and DeLuca 2011, Sampath and Deluca 2008).

ICP27 is essential for viral replication, and the stimulation of E and L gene expression. ICP27 directly interacts with RNA polymerase II in the absence of vDNA synthesis (Zhou and Knipe 2002). Given that ICP27 binds to vDNA-binding proteins ICP4 and ICP8, it has been proposed that ICP27 recruits RNA polymerase II to vDNA to transactivate gene expression (Panagiotidis et al. 1997, Olesky et al. 2005). ICP27 also enhances the nuclear export of viral mRNA, and promotes their expression (Sandri-Goldin 1998, Fontaine-Rodriguez and Knipe 2008).

ICP0 plays an important role in promoting the expression of E and L genes. ICP0 is not essential for this process but promotes the efficient onset of viral gene expression under low multiplicity of infection (MOI) conditions in a cell-type dependent manner (Cai et al. 1993, Sacks and Schaffer 1987, Yao and Schaffer 1995). The importance of ICP0 in promoting viral gene expression and host immune evasion is discussed below (section 1.7.1.).

The accumulation of E proteins provides the necessary components for triggering vDNA replication. Seven viral gene products have been shown to be essential for vDNA replication: the origin-binding protein U_L9, vDNA polymerase catalytic subunit U_L30 and its processivity factor U_L42, the multifunctional

single-strand (ss) DNA-binding protein ICP8, and the helicase-primase complex (U_L5, U_L8, and U_L52). vDNA replication starts at "prereplicative sites" adjacent to PML-NBs, and then forms larger vDNA replication compartments (Uprichard and Knipe 1997). vDNA replication involves two modes: (i) theta replication starts by binding of U_L9 to one of the three replication origins (two OriS and an OriL) which begins unwinding and separation of dsDNA. This process is followed by the recruitment of ICP8 and the formation of replication complex (Weir et al. 1989, Rabkin and Hanlon 1991, Olivo et al. 1988). dsDNA is further separated, and primers are synthesized by the helicase-primase complex (U_L5, U_L8, and U_L52). Then, vDNA polymerase (U_L30- U_L42) is recruited to perform leading- and lagging-strand synthesis (Wu et al. 1988, Purifoy et al. 1977). (ii) theta replication then switches to a rolling circle mechanism generating long concatemers that are cleaved into unit-length monomers by the terminase complex (U_L15, U_L28, and U_L33) during packaging into progeny virions (Rabkin and Hanlon 1990, Wilkinson and Weller 2003). vDNA replication in cooperation with IE protein ICP22 stimulates the expression of L proteins (Long et al. 1999, Rice et al. 1995, Advani et al. 2000, Advani et al. 2003). Following synthesis of L proteins, the nucleocapsid assembly and vDNA packaging are initiated.

1.4.3.   Nucleocapsid assembly and viral egress

Capsid assembly requires VP5, VP19C, VP21, pre-VP22a, VP23, VP24, and VP26 (Trus et al. 1996, Newcomb et al. 1996, Newcomb et al. 1999). Some of these capsid proteins cannot directly localize to the nucleus. They form complexes in the cytoplasm in order to enter the nucleus. VP5, the major capsid protein, is carried into the nucleus by scaffolding protein pre-VP22a. In the nucleus, VP5-pre-VP22 complexes undergo self-interaction forming two types of capsomeres (pentons and hexons) (Newcomb et al. 1993). VP26, the smallest capsid protein, forms a ring-like structure around the top of hexons (Trus et al. 1995, Zhou et al. 1995). The triplexes (1 copy of VP19C and two copies of VP23) link adjacent capsomeres generating a procapsid with a portal comprised of pU_L6. Maturation of the procapsid is achieved by cleavage of the scaffolding

protein (pre-Vp22a) by the VP24 viral protease (Desai et al. 1994, Gao et al. 1994). Empty capsids containing scaffolding structures are formed at sites in proximity to vDNA replication compartment. This is followed by insertion of progeny DNA through the pU_L6 portal into the capsids, cleavage of concatemers into unit-length monomers, and packaging of these monomers into the capsids (Newcomb et al. 2001, Yang et al. 2011, Yang and Baines 2006, Beard and Baines 2004).

Viral egress is a complicated process because mature nucleocapsids are required to bud through nuclear membrane, transport through the cytoplasm, and fuse with the plasma membrane to release infectious progeny virions (Mettenleiter et al. 2009). The most widely accepted model for viral egress is the envelopment/de-envelopment/re-envelopment model (Mettenleiter et al. 2013). Newly synthesized nucleocapsids bud at the inner nuclear membrane forming primary enveloped particles within the lumen of the nuclear envelope (primary envelopment). The nuclear egress is mediated by the nuclear egress complex which is composed of the phosphoprotein pUL31 and the integral membrane protein pUL34 (Chang and Roizman 1993, Roller et al. 2000, Reynolds et al. 2001, Newcomb et al. 2017, Bigalke et al. 2014). The pUL31 and pUL34 is associated with primary but not mature virions (Reynolds et al. 2002, Loret et al. 2008). Following primary envelopment, primary enveloped particles fuse with the outer nuclear membrane releasing nascent capsids into the cytoplasm (de-envelopment). In the cytoplasm, capsids acquire inner tegument proteins followed by a secondary envelopment in which outer tegument proteins and envelope glycoproteins are acquired via budding into the trans-Golgi network and tubular membranes (Ibiricu et al. 2011, Ibiricu et al. 2013, Owen et al. 2015, Duffy et al. 2006, Hollinshead et al. 2012). Mature virions are then released from the cell by exocytosis ready to attach to cellular receptors on non-infected neighbor cells, and the cycle continues. An overview of HSV-1 replication cycle is shown in Figure 2.
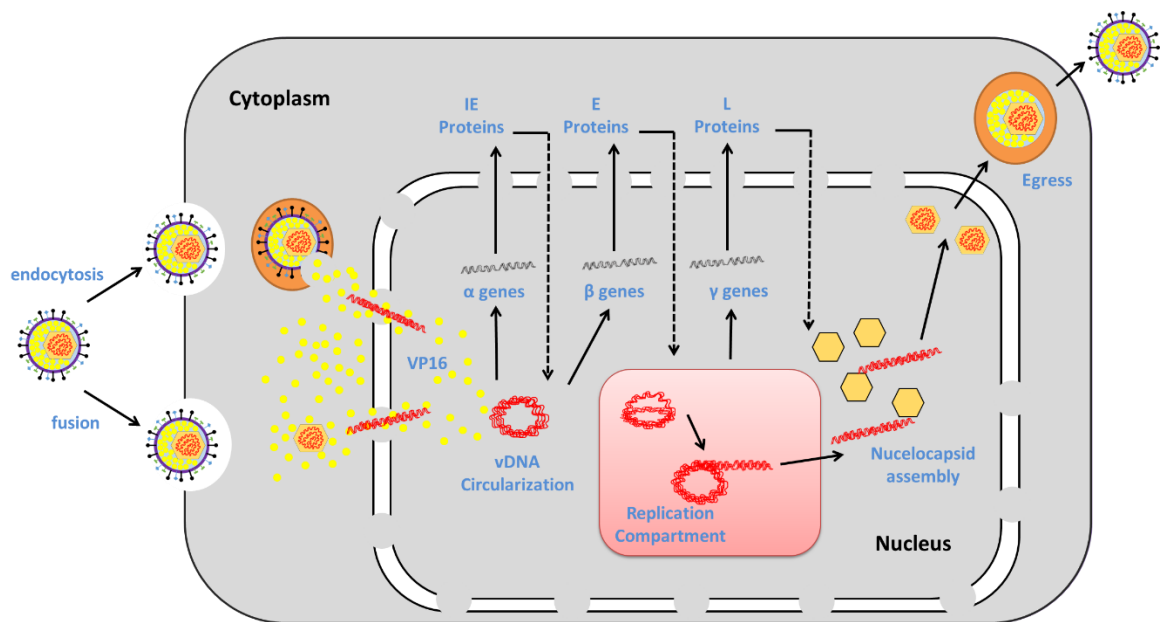
Figure 2. HSV-1 replication cycle.

The virus attaches via glycoproteins to cellular receptors. It enters the cells via fusion of viral envelope with the plasma membrane or endocytosis. The de-enveloped nucleocapsid is transported to the nuclear pores, and the vDNA is ejected into the nucleus. The viral genes are transcribed in a temporal cascade: immediate early (IE), early (E), and late (L) proteins. IE protein expression is turned on by the virion-associated protein VP16. E proteins require IE protein synthesis for their expression and play critical roles in triggering vDNA replication. Theta replication and rolling circle are two suggested mechanisms for vDNA replication. L protein expression is dependent on vDNA replication. The capsid is assembled at sites adjacent to vDNA replication compartments permitting the insertion of vDNA into the capsid. The nucleocapsid buds through nuclear membrane, transports through the cytoplasm, and fuses with the plasma membrane. During this journey, the nucleocapsid acquires tegument and envelope proteins. The release of mature progeny virions promotes attachment to new cells, and the cycle continues (Fields et al. 2013).

1.5. Viral latency

Epithelial cells are the primary sites of HSV-1 lytic replication. The virus then gains access to the sensory neurons at the axonal termini followed by retrograde axonal transport of nucleocapsid to the neuronal nucleus where viral latency is established (Arthur et al. 2001, Camarena et al. 2010). The vDNA is circularized and associated with nucleosomal chromatin, leading to viral gene silencing with the exception of latency-associated transcripts (LATs) (Rock and Fraser 1983, Rock and Fraser 1985, Deshmane and Fraser 1989). Indeed, most of the lytic gene promoters are associated with heterochromatic marks (e.g., H3K27me3 and H3K9me3) during viral latency, rendering them transcriptionally inactive (Kwiatkowski et al. 2009). In contrast, LAT promoters are associated with acetylated histones during viral latency (Kubat et al. 2004). The expressions of LATs in addition to microRNAs have been shown to promote the loading of heterochromatin on lytic gene promoters required for lytic replication; demonstrating a pivotal role for LATS and microRNAs in the establishment of viral latency (Umbach et al. 2008, Mador et al. 1998, Cliffe et al. 2009, Wang et al. 2005). Host immunity also promotes the establishment and maintenance of viral latency. Prolonged and persistent cytokines and chemokines expression, and continued activation of CD8+ T cell have been reported in the latently-infected neurons (Cantin et al. 1995, Cook et al. 2004, Halford et al. 1996, Khanna et al. 2003). HSV-1 can reactivate from latency in response to different stimuli including stress, exposure to UV irradiation, hyperthermia, and injuries and trauma (Sawtell and Thompson 1992, Laycock et al. 1991, Hill et al. 1978). During reactivation, LAT-associated histones are deacetylated while histones associated with viral lytic genes (e.g., ICP0) are acetylated promoting the onset of lytic replication (Du et al. 2011, Amelio et al. 2006). Reactivated virus travels, via anterograde axonal transport, to peripheral tissues at or near sites of primary infection (Penfold et al. 1994). The severity of reactivation ranges from shedding viruses in the absence of symptoms to severe and serious lesions.

1.6. Host immunity to HSV-1 infection

Host cells possess many antiviral factors. Some of them are activated as soon as the virus attaches to the target cell, while others are triggered at different stages of infection. They can act directly and immediately to control the onset of infection, or confer antiviral activities indirectly by inducing signaling cascades and activating effector proteins. The molecular basis of this multifaceted system has been extensively studied during HSV-1 infection. In this section, the current understanding of all three branches of host immunity (intrinsic, innate, and adaptive) to HSV-1 infection is discussed. The ubiquitination and SUMOylation pathways are introduced first given the importance of these post-translational modifications in maintaining the integrity, localization, and functions of host immune factors as well as the fact that HSV-1 employs these modifications to counteract the effect of these factors.

Ubiquitination:

Ubiquitination involves a three-step enzymatic cascade leading to covalent attachment of a ubiquitin (Ub) molecule to a lysine residue of the target substrate (Figure 3). Ubiquitin is a small protein (8.6 kDa) that is translated as an inactive polyprotein which is then cleaved into monomers by the action of deubiquitinating enzymes (Ciechanover et al. 1980). Ubiquitin monomer is activated at its C-terminal glycine by E1-Ub activating enzyme forming E1-Ub thioester which is, then, transferred to E2-Ub conjugating enzyme (Ciechanover et al. 1981). In the third enzymatic step, E3-Ub ligase facilities and promotes the transfer of the E2-conjugated Ub to the substrate (Hershko et al. 1983, Hershko et al. 1986). The conjugated Ub itself can be ubiquitinated at one of its seven lysine residues or N-terminal methionine forming a poly-ubiquitin chain on the target protein (Hershko and Heller 1985). Deubiquitinating enzymes can detach Ub from its substrate and, thereby, reverse the effect of ubiquitination (Hershko et al. 1980). Ubiquitination and deubiquitination are

widely utilized by hosts and viruses in order to modulate the stability, integrity, and function of their proteins including key intrinsic and innate immune regulators (Table 2).
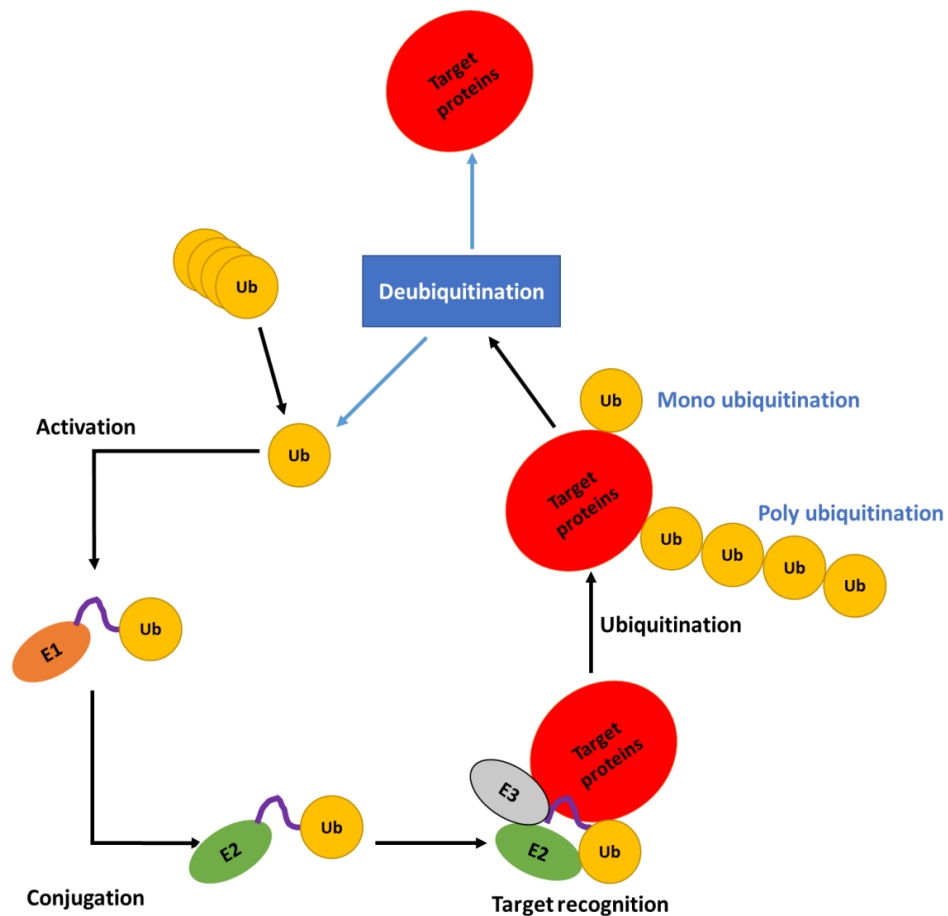
Figure 3. Ubiquitination pathway.

Ubiquitination involves a three-step enzymatic cascade leading to covalent attachment of a ubiquitin (Ub) molecule to a lysine residue of the target substrate. Ubiquitin is a small protein (8.6 kDa) that is translated as an inactive polyprotein which is then cleaved into monomers by the action of deubiquitinating enzymes (Ciechanover et al. 1980). Ubiquitin monomer is activated at its C-terminal glycine by E1-Ub activating enzyme forming E1-Ub thioester, which is then transferred to E2-Ub conjugating enzymes (Ciechanover et al. 1981). In the third enzymatic step, E3-Ub ligases promote the transfer of the E2-conjugated Ub to the substrate (Hershko et al. 1983, Hershko et al. 1986). Of note, Ub itself can be ubiquitinated at one of its seven lysine residues or N-terminal methionine forming a poly-ubiquitin chain on the target protein (Hershko and Heller 1985). Deubiquitinating enzymes can detach Ub from its substrate, thereby reverse the effect of ubiquitination (Hershko et al. 1980). Hosts and viruses widely utilize ubiquitination and deubiquitination to modulate the stability, integrity, and function of many immune regulators (Heaton et al. 2016, Davis and Gack 2015).

SUMOylation:

SUMOylation is the process of attaching a mature SUMO molecule to the target protein via a three-step enzymatic pathway (Figure 4). SUMO is a small protein (12 kDa) that is produced normally as an immature precursor (Mahajan et al. 1997, Matunis et al. 1996, Boddy et al. 1996, Shen et al. 1996, Okura et al. 1996). SUMO maturation upon truncation of the last four amino acids of its C-terminus by SUMO-specific proteases (SENP) (Li and Hochstrasser 1999). This process reveals a diglycine motif required for efficient binding of SUMO to E1 SUMO activating enzyme (SAE) (Desterro et al. 1999). SAE induces adenylation and processing of mature SUMO forming an E1-SUMO thioester which is, then, passed to the SUMO E2 conjugating enzyme Ubc9. UBC9 can directly and independently pass SUMO to the substrate (Lee et al. 1998, Schwarz et al. 1998). However, the contribution of E3 SUMO ligases to this pathway promotes specificity and enhances conjugation between the C-terminal glycine residue of SUMO and a lysine residue on the target protein (Kagey et al. 2003). SUMOylation can be reversed by the action of SENP which disrupts the isopeptide bond between SUMO and its target substrate leading to SUMO deconjugation (Li and Hochstrasser 1999).

In human, 5 SUMO isoforms (designed as SUMO 1–5) have been identified. Mature forms of SUMO2 and SUMO3 demonstrate a great level (97%) of homology in amino acid sequence, and the current antibodies available cannot distinguish between these two isoforms. SUMO2/3 covalently attached to the target protein can be further SUMOylated leading to the formation of poly-SUMO chains (Tatham et al. 2001). SUMO1 shares only about 46% amino acid identity with SUMO2/3, and lack the ability to be SUMOylated (Kamitani et al. 1998a). Hence, it can only promote mono-SUMOylation, or alternatively terminates a poly-SUMO2/3 chain. SUMO4 shares 86% sequence identity with SUMO 2/3 (Bohren et al. 2004). Unlike SUMO1 and SUMO2/3, SUMO4 and SUMO5 are expressed exclusively in specific types of human cells (Guo et al. 2004). SUMOylation plays

a key role in regulating the function and activity of many intrinsic and innate immune factors (Table 2). Moreover, some viruses including HSV-1 have been shown to manipulate some aspects of this pathway in order to evade host intracellular immunity and promotes viral replication.
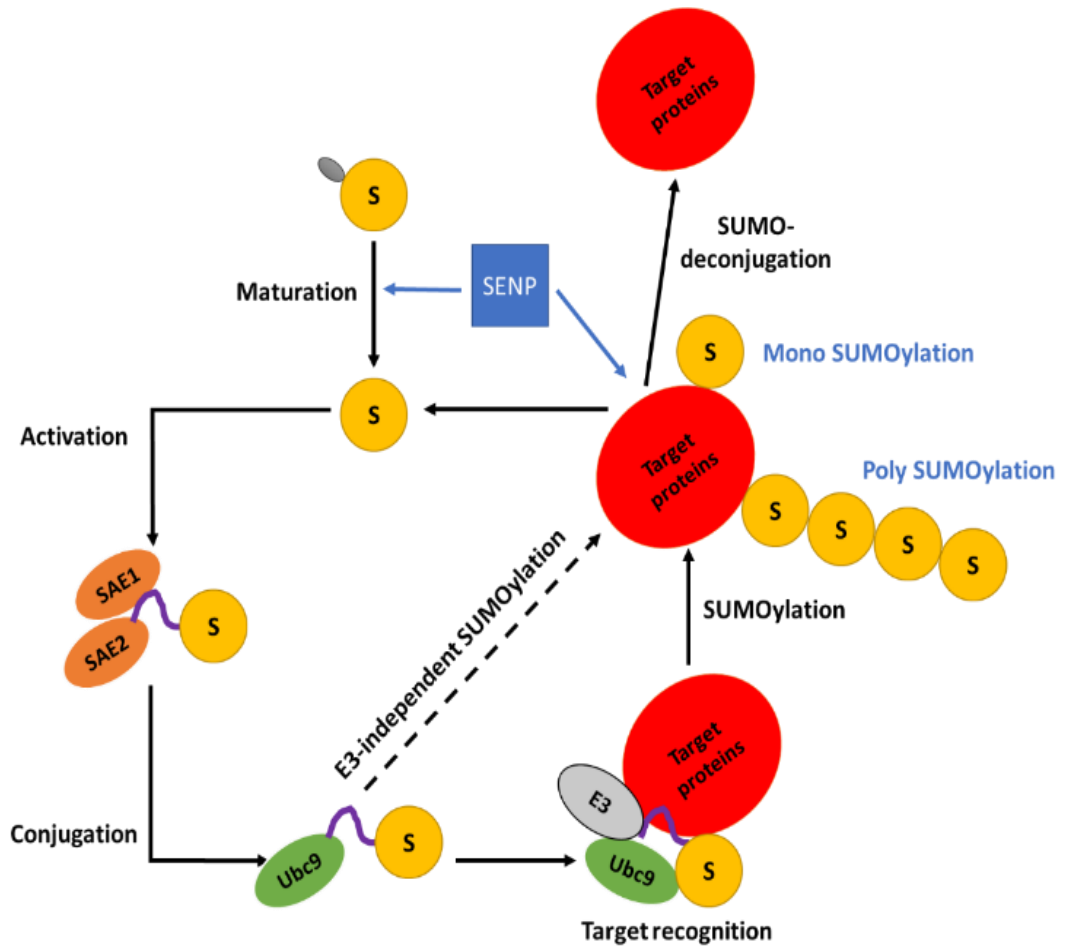
Figure 4. SUMOylation pathway.

Small ubiquitin-like modifiers (SUMO) are activated by SUMO-activating enzymes (SAE1/2) (Desterro et al. 1999). Activated SUMO molecule is transferred to the SUMO E2 conjugating enzyme Ubc9 which directly, or with the support of E3 SUMO ligases, conjugates SUMO onto the target substrate (mono-SUMOylation) (Lee et al. 1998, Schwarz et al. 1998, Kagey et al. 2003). The conjugated SUMO can also be SUMOylated to form poly-SUMO chains (poly-SUMOylation). SUMO specific protease (SENP) breaks the bond between SUMO and its target substrate leading to deSUMOylation (Li and Hochstrasser 1999).

Table 2. The role of post-translational modifications in regulating host immunity:

Target	PTM	effect	References
IRF1	SUMOylation	Represses its transcriptional activity	(Nakagawa and Yokosawa 2002, Kim et al. 2008)
IRF2	SUMOylation	Represses its transcriptional activity	(Han et al. 2008)
IRF3	SUMOylation	Enhances its antiviral role	(Ran et al. 2011)
IRF7	SUMOylation	Negatively regulates IFN type I	(Kubota et al. 2008)
RIG-I and MDA5	SUMOylation	Positively regulates IFN type I	(Mi et al. 2010, Fu et al. 2011)
PML, PKR, ad P35	SUMOylation	Required for their antiviral activity	(de la Cruz-Herrera et al. 2014, Marcos-Villar et al. 2013, Cuchet-Lourenco et al. 2011)
TRAF6	Ubiquitination	TLR signaling, T cell tolerance, and B cell development	(Deng et al. 2000, King et al. 2006, Rowland et al. 2007)
TRIM25	Ubiquitination	RIG-I signaling, and IFN type I production	(Gack et al. 2007)
TRAF2 and 3	Ubiquitination	B cell development	(Vallabhapurapu et al. 2008)
LUBAC	Ubiquitination	IL-1β signaling	(Tokunaga et al. 2009)

1.6.1. Intrinsic immunity

Intrinsic immunity is the first line of intracellular defense against viral pathogens. This arm of immunity is mediated by constitutively expressed host cell restriction factors that can directly and immediately act to control viral replication. In the case of HSV-1 infection, the use of HSV-1 ICP0-null mutants (ΔICP0) has been extremely valuable for defining many aspects related to the regulation of intrinsic antiviral immunity. Compared to wild type (WT) HSV-1, ΔICP0 HSV-1 grows poorly under low MOI conditions (Stow and Stow 1986, Sacks and Schaffer 1987). This phenotype is both cell type- and MOI-dependent. Indeed, the replication defect of ΔICP0 HSV-1 ranges from severe (e.g., ~1000 fold in fibroblast and keratinocytes) to intermediate (e.g., 30-100 fold in BHK and Vero cells) to almost absent (e.g., U2OS and SAOS) when compared to the replication of WT HSV-1 in these cells (Yao and Schaffer 1995, Everett et al. 2004a). This has led to cells being described as restrictive or permissive based on their ability to support ΔICP0 HSV-1 replication. Given that U2OS cells fully complement the growth defect of ΔICP0 HSV-1, these cells are used to determine both WT and ΔICP0 HSV-1 titers (Yao and Schaffer 1995, Everett et al. 2004a).

Importantly, the intrinsic antiviral immunity in restrictive cell lines can be saturated at increased MOI (Everett et al. 2004a). A study conducted on human fibroblasts demonstrated that ΔICP0 HSV-1 under low MOI conditions (e.g., 0.2 to 1 PFU/cell based on viral titer in U2OS) was able to initiate plaque formation only in a minor population of infected cells, with the majority of cells containing quiescent viral genomes (Everett et al. 2004a). Correspondingly, at equivalent genome input levels, gene expression of ΔICP0 HSV-1 were severely restricted in comparison to WT virus. However, at higher MOI (5 to 10 PFU/cell), the extent of ΔICP0 HSV-1 replication defect was reduced leading to WT level of replication (Everett et al. 2004a).

Collectively, these data demonstrate that intrinsic immunity renders some cell types non-permissive to HSV-1 infection in the absence of ICP0 and under low MOI conditions. Several intrinsic antiviral factors have been identified including PML-NB constituent proteins (PML, Sp100, Daxx, ATRX, and MORC3), E3 SUMO ligases (PIAS1 and PIAS4), and interferon gamma inducible protein 16 (IFI16) (Everett et al. 2006, Everett et al. 2008, Lukashchuk and Everett 2010, Conn et al. 2016, Brown et al. 2016, Sloan et al. 2016, Orzalli et al. 2013).

1.6.1.1.   PML-NB constituent proteins

PML-NB constituent proteins (e.g., PML, SP100, Daxx, ATRX, and MORC3) are involved in many cellular processes, including the cell cycle, DNA damage response, DNA repair, apoptosis, and metabolism. In addition, they play vital roles in the regulation of intrinsic host immunity against several viruses (e.g., herpes-, retro-, papilloma-, adeno-, and parvoviruses (Dutrieux et al. 2015, Kahle et al. 2015, Mitchell et al. 2014, Reichelt et al. 2011, Stepp et al. 2013, Tavalai and Stamminger 2009).

Over two decades ago, a disappearance of PML-NBs following HSV-1 infection was observed; a process that was linked to the expression of the viral IE protein ICP0 and the functional activity of its really interesting new gene (RING) finger domain (section 1.7.1.) (Maul and Everett 1994). Fluorescent *in situ* hybridization (FISH) experiments demonstrated that infecting HSV-1 genomes localized adjacent to PML-NBs upon nuclear entry; suggesting a role for these bodies during viral infection (Maul et al. 1996). This phenotype was prominent in newly infected cells at the edge of developing plaques where an accumulation of dot-like complexes of ICP4 was observed in close proximity to PML-NBs (Everett et al. 2004b). These viral-induced complexes contained incoming viral genomes (Everett and Murray 2005). PML-NB constituent proteins (PML, SP100, Daxx, and ATRX) rapidly associated with these complexes and demonstrated a distinct asymmetric distribution from that observed in non-infected cells (Everett et al. 2004b, Everett and Murray 2005). Although it was

initially unclear whether this phenotype reflected a beneficial or inimical effect on viral infection, it is now evident that PML-NB proteins play fundamental roles in the regulation of intrinsic antiviral defense to HSV-1 infection.

1.6.1.1.1.   PML (Promyelocytic leukemia protein)

PML is the major scaffolding protein of PML-NBs. It belongs to the tripartite motif (TRIM) family of proteins that share conserved structural features, including an amino-terminal RING finger, one or two B boxes, and a coiled-coil domain (Duprez et al. 1999, Tao et al. 2008, Kastner et al. 1992) (Figure 5). There are several PML isoforms in humans which have common N-terminal 418 amino acids but vary in carboxy-terminal domains as a consequence of alternative splicing (Jensen et al. 2001). PML isoforms are predominantly nuclear but can be cytoplasmic depending on the presence of nuclear localization signal (NLS). Different isoforms confer distinct functions (Jensen et al. 2001). All PML isoforms are highly modified by SUMO family of proteins. Studies identified several PML SUMOylation sites (K65, K160, K490, and K616), which are known to play key roles in modulating its function (Kamitani et al. 1998b, Cuchet-Lourenco et al. 2011, Vertegaal et al. 2006, Galisson et al. 2011). SUMOylation of PML is also essential for maintaining the structural integrity of PML-NBs (Zhong et al. 2000). In response to stimuli, PML is also subjected to other forms of post-translational modification (e.g., phosphorylation and ubiquitination) which influences PML-NB stability and function (Cheng and Kao 2012).
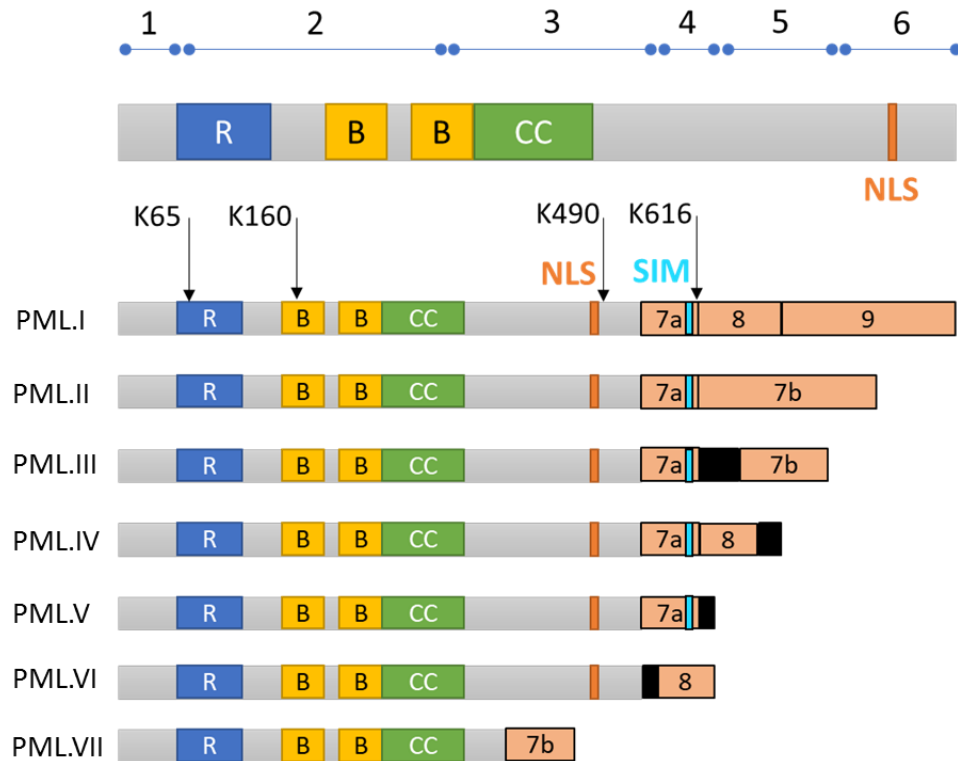
Figure 5. PML structure and isoforms.

PML exists in different isoforms due to alternative splicing of its C-terminus. All isoforms contain a RING finger domain (R), two B-boxes (B), and a coiled-coil domain (CC) that are encoded by the first three exons. PML isoforms are mostly nuclear (PML.I-VI), but can be cytoplasmic (PML.VII), depending on the presence or absence of the nuclear localization signal (NLS) (Jensen et al. 2001). Several SUMOylation sites (K65, K160, K490, and K616) have been identified (Kamitani et al. 1998b, Cuchet-Lourenco et al. 2011, Vertegaal et al. 2006, Galisson et al. 2011). All nuclear PML isoforms (with the exception of PML.IV) include exon 7a that encodes a SUMO-interacting motif (SIM) (Cuchet-Lourenco et al. 2011, Jensen et al. 2001). PML.I and PML.II are the most abundantly expressed among PML isoforms (Condemine et al. 2006).

During HSV-1 infection, PML and other PML-NB proteins relocalize to sites that are associated with viral genomes. This recruitment occurs rapidly as a consequence of viral genome entry into the nucleus, and independently of *de novo* viral protein expression (Everett and Murray 2005, Everett et al. 2007). Although recruitment could be detected during WT HSV-1 infection, it was more evident during ΔICP0 HSV-1 infection. Importantly, PML recruitment to ΔICP0 HSV-1 genomes correlates with a repressive activity that impedes lytic replication (Everett et al. 2006). Depletion of PML from human fibroblasts by short-hairpin (sh) RNA has been shown to enhance plaque formation and viral protein expression of ΔICP0, but not WT, HSV-1. This study provided the first conclusive evidence that PML confers intrinsic antiviral immunity to HSV-1 infection that is countered by the activity of ICP0 (Everett et al. 2006).

PML recruitment to the infecting viral genomes is dependent on the SUMOylation pathway (Cuchet-Lourenco et al. 2011). PML isoforms (PML.I-V) associate with ICP4 foci, a proxy for viral genome localization, in a SUMO-interacting motif (SIM)-dependent manner. Notably, PML.VI failed to associate with viral-induced foci due to a lack of exon 7a that contains the PML.SIM. Mutations of SIMs in PML.I and PML.IV influenced their recruitment to viral-induced foci. Consistent with the correlation between PML recruitment to viral genomes and repressive activity, the relief of restriction of ΔICP0 HSV-1 in PML-depleted cells was reversed following reconstitution of WT PML.I, but not PML.I SIM mutants (Cuchet-Lourenco et al. 2011). Similar to PML SIM mutants, PML.I and PML.IV carrying a single or multiple mutation(s) at major SUMOylation sites (K65, K160, K490, and K616) were less efficiently recruited to viral genome foci (Cuchet-Lourenco et al. 2011). Correspondingly, depletion of Ubc9, the sole SUMO E2 conjugating enzyme, impaired the recruitment of PML (and other PML-NB restriction factors) to ΔICP0 HSV-1 genomes and enhanced plaque formation (Boutell et al. 2011). These studies collectively demonstrated a key role for host SUMOylation in the regulation of PML-NB mediated intrinsic antiviral immunity. Of note, the TRIM domains (B-box 1, the coiled-coil domain, and to lesser extent the RING finger domain) of PML also play important roles during PML recruitment

to infecting ΔICP0 HSV-1 genomes (Cuchet-Lourenco et al. 2011, Cuchet et al. 2011).

1.6.1.1.2.   SP100 (Speckled protein of 100 kDa)

SP100 shares many features with PML. For instance, SP100 is covalently SUMO-modified and highly localized at PML-NBs (Sternsdorf et al. 1997). It also contains A SIM (residues 323-326) and a major SUMOylation acceptor site (K297). SP100 exists in different isoforms due to alternative splicing which influences their functions (Kim et al. 2009, Sternsdorf et al. 1999, Guldner et al. 1999, Negorev et al. 2006).

During HSV-1 infection, SP100 is rapidly recruited to sites associated with infecting viral genomes in a PML-independent manner (Everett et al. 2008, Everett et al. 2006). The presence of SIM, but not the major SUMO modification site, is required for the recruitment of SP100A (the most abundant isoform) to viral genomes (Cuchet-Lourenco et al. 2011). The recruitment phenotype of SP100 correlates with repression of viral gene expression (Everett et al. 2008). Indeed, SP100 depletion enhanced the plaque formation of ΔICP0, but not WT, HSV-1. Moreover, double depletion of PML and SP100 additively enhanced the plaque formation and gene expression of ΔICP0, demonstrating that each protein independently contributes to the repression of HSV-1 in the absence of ICP0 (Everett et al. 2008). Importantly, simultaneous depletion of PML and SP100 was not sufficient to complement the plaque forming defect of ΔICP0 HSV-1 to WT levels; indicative of the presence of other cellular restriction factors (Everett et al. 2008).

1.6.1.1.3. Daxx (Human death-domain associated protein) and ATRX (Alpha-thalassemia mental retardation X-linked)

Daxx is a transcriptional repressor that physically interacts with several nuclear proteins. Daxx interacts with PML and localizes to PML-NBs. The presence of SUMO-modified PML is important for maintaining Daxx localization at PML-NBs (Li et al. 2000, Ishov et al. 1999). Daxx interacts with ATRX via its paired amphipathic helices (PAH1) domain forming an ATP chromatin-remodeling complex (Tang et al. 2004). Daxx-ATRX association mediates histone H3 variant (H3.3) loading at specific genomic locations (Xue et al. 2003, Goldberg et al. 2010). Daxx, like other PML-NB constituent proteins, is subjected to post-translational modifications that modulate its function (Hollenbach et al. 2002).

Similar to PML and SP100, Daxx is recruited to sites associated with infecting viral genomes in a SIM-dependent manner (Lukashchuk and Everett 2010, Glass and Everett 2013, Cuchet-Lourenco et al. 2011). Depletion of Daxx enhanced the plaque formation of ΔICP0, but not WT, HSV-1 (Lukashchuk and Everett 2010). The relief of restriction of ΔICP0 HSV-1 in Daxx-depleted cells was reversed following reconstitution of WT Daxx, but not Daxx SIM mutant, again highlighting a crucial role of host SUMOylation in mediating intrinsic immunity in response to HSV-1 infection (Cuchet-Lourenco et al. 2011).

Daxx recruitment to viral genome foci occurs independently of PML and SP100 (Everett et al. 2006). Correspondingly, triple depletion of PML, SP100, and Daxx substantially enhanced the PFE of ΔICP0 HSV-1 (~100 fold) in comparison to single or double depleted cells (Glass and Everett 2013). These data suggested that PML-NB proteins act cooperatively, but independently, to impair viral infection. However, the additive effect of triple depletion was not enough to fully complement the lack of ICP0 (Glass and Everett 2013), again highlighting that additional restriction factors contribute to the repression of ΔICP0 HSV-1.

ATRX has also been identified as a PML-NB restriction factor (Lukashchuk and Everett 2010). However, the recruitment phenotype and repression activity of ATRX on ΔICP0 HSV-1 is dependent on its interaction with Daxx. Indeed, ATRX failed to localize to viral genome foci in Daxx-depleted cells. Reintroduction of WT Daxx, but not Daxx PAH1 mutant, in Daxx-depleted cells restored the recruitment phenotype and the efficient restriction of ΔICP0 HSV-1 (Lukashchuk and Everett 2010). These findings demonstrated that the interaction between ATRX and Daxx is essential for ATRX-mediated restriction of ΔICP0 HSV-1 replication (Lukashchuk and Everett 2010).

1.6.1.1.4.   MORC3 (Microrchidia family CW-type zinc finger 3)

MORC3 has been recently shown to restrict ΔICP0 HSV-1 replication. MORC3 is a nuclear matrix protein that belongs to the MORC family (Iyer et al. 2008). Among the four family members (MORC1-4), MORC3 is considered as a PML-NB component protein. Indeed, MORC3 interacts with PML isoform I in a SUMO-SIM dependent manner (Mimura et al. 2010).

During WT HSV-1 infection, the level of MORC3 is reduced by approximately 5.6 fold due to ICP0-mediated degradation of both SUMO-modified and unmodified forms (Sloan et al. 2015, Sloan et al. 2016). During ΔICP0 infection, MORC3 was found to asymmetrically distribute and associate with the incoming vDNA in newly infected cells at the edge of developing plaques. These data raised the hypothesis that MORC3 mediates an intrinsic antiviral role against HSV-1. Depletion of MORC3 influenced the recruitment of PML-NB proteins (PML, SP100, and Daxx) to incoming viral genomes, and enhanced the plaque formation of ΔICP0 (~10-15 fold) in comparison to control cell lines (Sloan et al. 2016). This study demonstrated that MORC3 also confers intrinsic antiviral immunity to HSV-1; a process that is counteracted by ICP0 (Sloan et al. 2016).

1.6.1.2. Protein Inhibitor of Activated STAT (PIAS) 1 and 4

SUMOylation plays a key role in the rapid recruitment of host cell restriction factors to infecting viral genomes. *De novo* SUMO conjugates accumulate at sites of infecting ΔICP0 HSV-1 genomes, a process that stimulates the recruitment of PML-NB associated restriction factors (PML, SP100, and Daxx) in a SUMO-SIM dependent manner (Boutell et al. 2011, Cuchet-Lourenco et al. 2011). Recently, SUMO E3 ligases belonging to the PIAS family have been shown to confer intrinsic immunity during HSV-1 infection (Conn et al. 2016, Brown et al. 2016). There are five types of PIAS (termed PIAS1, 2α, 2ß, 3, and 4) which share several conserved domains and motifs, including SIM (Rytinki et al. 2009, Jackson 2001). PIAS1 is the only family member to be a constituent PML-NB protein (Brown et al. 2016). However, both PIAS1 and PIAS4 play critical roles in mediating the intrinsic antiviral response to HSV-1 infection (Brown et al. 2016, Conn et al. 2016). Plaque edge assays demonstrated that both PIAS1 and PIAS4 were recruited to the infecting ΔICP0 HSV-1 genomes at the nuclear periphery of newly infected cells. As in the case of PML-NB restriction factors (PML, SP100, and Daxx), the recruitment of PIAS1 and PIAS4 to viral genomes occurs in a SIM-dependent manner (Brown et al. 2016, Conn et al. 2016). Depletion of either PIAS1 or PIAS4 enhanced the plaque formation of ΔICP0, but not WT, HSV-1. Simultaneous co-depletion of both proteins (PIAS1 and PIAS4) further enhanced the plaque formation of ΔICP0 HSV-1 to a greater level than achieved by a single depletion. Moreover, co-depletion of PML and either PIAS1 or PIAS4 also additively enhanced the plaque formation of ΔICP0 HSV-1, demonstrating that each protein acts independently to restrict the replication of ΔICP0 HSV-1 (Brown et al. 2016, Conn et al. 2016).

1.6.1.3. Interferon Gamma Inducible Protein 16 (IFI16)

IFI16 is a member of the PYHIN (Pyrin domain and two DNA-binding hematopoietic interferon-inducible nuclear proteins with 200-amino acids repeat

(HIN-200) domains) family of proteins (Johnstone et al. 1998). Similar to PML-NB associated restriction factors, IFI16 puncta were localized to the viral-induced foci that contain ΔICP0 HSV-1 genomes at the nuclear periphery of newly infected cells in a pyrin domain-dependent manner (Cuchet-Lourenco et al. 2013). The plaque formation efficiency, viral yields, and levels of gene expression of HSV-1 ICP0 mutants were enhanced in the absence of IFI16 (Cuchet-Lourenco et al. 2013, Diner et al. 2016, Orzalli et al. 2013). Overexpression of IFI16 in U2OS or HEK293 cells reduced viral gene expression and replication. Importantly, this process occurred independently of IFN-regulatory factor 3 (IRF3) and activation of interferon (IFN) production (Orzalli et al. 2013, Deschamps and Kalamvoki 2017b).

Some mechanisms for IFI16-mediated intrinsic immunity have been proposed. IFI16 depletion negatively influenced the recruitment of PML and Daxx to incoming viral genomes; which may explain the relief of ΔICP0 HSV-1 restriction in IFI16-depleted cells (Cuchet-Lourenco et al. 2013). It has also been proposed that IFI16 mediates viral genome silencing through heterochromatin formation, leading to the accumulation of repressive histone H3K9me3 and reduction of active H3K4me3 association on viral genomes (Orzalli et al. 2013, Johnson et al. 2014). Chromatin immune-precipitation (ChIP) analysis indicated that IFI16 also prevents the accumulation of cellular transcriptional factors (e.g., RNA polymerase II, TBP, and Oct) at HSV-1 promoters; a process that interferes with the initiation of viral transcription and the onset of lytic replication. (Johnson et al. 2014). Collectively, these data demonstrate that in addition to its key role in the induction of host innate immune response (as described below), IFI16 confers intrinsic antiviral defenses to HSV-1 infection.

1.6.2. Innate immunity

Innate immunity, unlike intrinsic immunity, is induced and upregulated in response to viral infection. IFN, a family of proinflammatory cytokines, plays a central role in the regulation of innate immunity during HSV-1 infection. IFNs are classified into three main types (type I, II, and III) depending on the type of receptor utilized for signaling (Kotenko et al. 2003) (Table 3). Many cell types can produce more than one type of IFN. However, studies showed that some cells are predominantly responsible for specific types of IFN expression and secretion. For example, (i) leucocytes, macrophages, and dendritic cells (DCs) for IFNα, (ii) fibroblast and epithelial cells for IFNß, and (iii) natural killer cells and activated CD8$^+$ T-lymphocytes for IFNγ. In this section, the antiviral roles of different types of IFNs, sensing and detection of viral components, IFN signaling cascades, and induction of interferon-stimulated genes (ISGs) during HSV-1 infection are reviewed.

Table 3. IFN types and receptors

Type of IFN	Members	Receptors
Type I	IFNα, ß, ε, κ, and ω	IFNα receptor 1 and 2 (IFNAR1/2)
Type II	IFNγ	IFNγ receptor (IFNGR)
Type III	IFNλ1, λ2, λ3 (IL-28A, IL28B, and IL29)	IL 28 receptor α (IL-28Rα) and IL-10 receptor ß (IL-10Rß)

1.6.2.1. Type I IFN response

Type I IFN plays a critical antiviral role against HSV-1 infection. Historically, the resistance and susceptibility of different mouse strains to HSV-1

infection were linked to their abilities to induce type I IFN response (Lopez 1975, Gresser et al. 1976, Ellermann-Eriksen et al. 1986, Halford et al. 2004). Increased viral replication, severe pathogenesis, and reduced survival rates have been observed in mice lacking type I IFN receptors in comparison to WT controls (Leib et al. 1999, Luker et al. 2003). Several *in vitro* studies also highlighted the important role of type I IFN in controlling the replication, spread, and cytopathic effect of HSV-1 infection (Sainz and Halford 2002, Domke-Opitz et al. 1986, Rosato and Leib 2014). The induction of IFN response involves two phases: (i) Sensing of viral particles or viral replication products by pattern recognition receptors (PRRs) that leads to the production of IFN. (ii) Binding of the secreted IFN to its cognate receptors and subsequent activation of IFN-signaling cascades leading to the induction of ISGs that establish an antiviral state to control the spread of infection.

1.6.2.2. Sensing and detection of HSV-1 by PRRs

The activation of phase I of the IFN response is dependent on the ability of PRRs to recognize pathogen-associated molecular patterns (PAMPs) during viral infection. Numerous PRRs have been identified (Table 4) (Paludan et al. 2011, Knipe 2015, Orzalli and Knipe 2014). Many of them share the same signaling cascades and play redundant roles to mediate a robust antiviral response. Studies conducted on various herpesviruses have proposed that PRRs can recognize and sense virion components (e.g., viral glycoprotein and vDNA) as well as structures shown to be accumulated during viral replication (e.g., cytosolic dsRNA) (Paludan et al. 2011). The interaction between PRRs and their viral ligands leads to activation of TANK-binding kinase 1 (TBK-1) in fibroblasts or inhibitor of NFκB epsilon (IKKε) in immune cells (Fitzgerald et al. 2003, Sharma et al. 2003). These protein kinases induce the phosphorylation and activation of IRF3 and IRF7, which in cooperation with other transcription factors (e.g., NFκB), bind to IFN gene promoters and stimulate the secretion of type I IFN (Honda and Taniguchi 2006) (Figure 6).

Table 4. PRRs and proposed PAMPs in HSV-1 induced innate immunity

PRR	Proposed PAMP	Reference
cGAS	Cytosolic vDNA	(Almine et al. 2017, Sun et al. 2013, Wu et al. 2013)
DAI	Cytosolic vDNA	(Takaoka et al. 2007)
DHX9/36	Cytosolic vDNA	(Kim et al. 2010)
IFI16	Cytosolic and nuclear vDNA	(Almine et al. 2017, Ansari et al. 2015, Bowie et al. 2017, Diner et al. 2015, Orzalli et al. 2012, Unterholzner et al. 2010, Horan et al. 2013)
MDA5	dsRNA and cytosolic vDNA	(Melchjorsen et al. 2010, Melchjorsen et al. 2006, Yoneyama et al. 2005, Choi et al. 2009)
Pol III / RIG-I	Cytosolic vDNA	(Chiu et al. 2009)
TLR2	Glycoprotein	(Kurt-Jones et al. 2004)
TLR3	dsRNA	(Alexopoulou et al. 2001, Weber et al. 2006, Zhang et al. 2007)
TLR9	vDNA in endosome	(Lund et al. 2003, Krug et al. 2004, Ahmad-Nejad et al. 2002)

cGAS, Cyclic guanosine monophosphate–adenosine monophosphate (cGAMP) synthase; DAI, DNA-dependent activator of interferon regulatory factors; DHX, DExD/H-box helicase; IFI16, interferon gamma inducible-16; MDA, melanoma differentiation-associated gene 5; Pol III, RNA polymerase III; RIG, Retinoic acid inducible gene; TLR, Toll-like receptor.
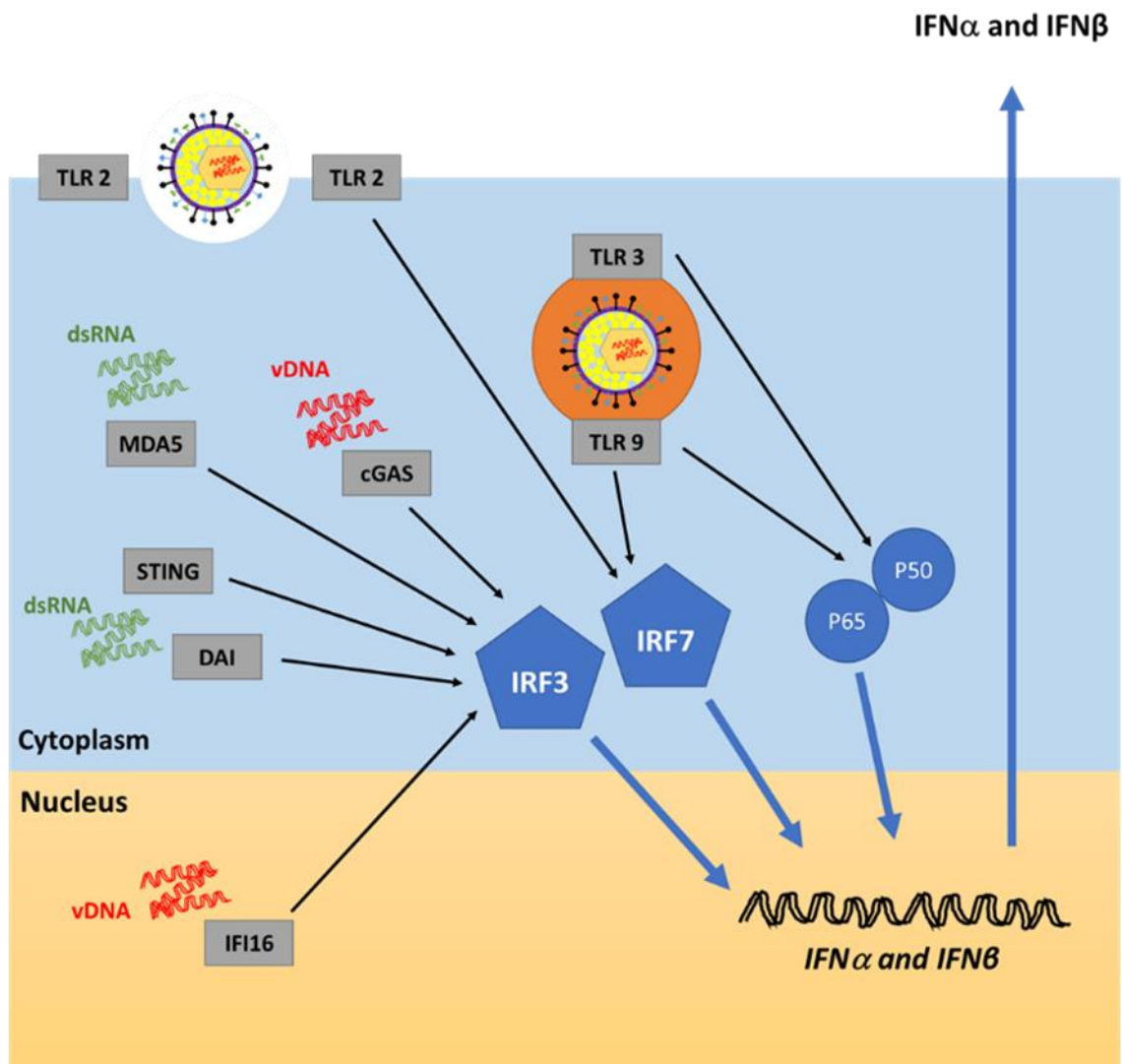
Figure 6. The first phase of IFN response.

Host cells are equipped with several pattern recognition receptors (PRRs) that can recognize virion components (e.g., glycoprotein and vDNA) and structures accumulated during vDNA replication (e.g., dsRNA). PRRs signal through different pathways (e.g., IRF3, IRF7, and NF-κB) to induce cytokine (IFNα and β) and chemokine expression.

1.6.2.2.1. IFI16 is a key regulator of host innate immunity

vDNA is one of the most potent inducers of host innate immunity. Following viral entry into the target cell, HSV-1 is exposed to a number of cytosolic DNA sensors (e.g., cGAS, DAI, DHX9/36, and MDA5). However, vDNA is protected by the capsid during cytoplasmic transport to the nuclear pore where vDNA is ejected into the nucleus. Hence, cytosolic DNA sensors have only a limited access to vDNA (Miyamoto and Morgan 1971, Pasdeloup et al. 2009, Komatsu et al. 2016). Thus, IFI16 has attracted significant attention due its ability to act as both a cytosolic and nuclear vDNA sensor during HSV-1 infection (Diner et al. 2015, Orzalli et al. 2012, Unterholzner et al. 2010, Horan et al. 2013).

1.6.2.2.2. IFI16 as a cytosolic vDNA sensor

IFI16 was initially reported as a cytosolic DNA sensor in human monocytes (Unterholzner et al. 2010). It was directly associated with transfected DNA derived from HSV-1 genome leading to IFNß production; a process that occurred in a stimulator of interferon genes (STING)-, TBK1-, and IRF3-depndent manner. Short-hairpin mediated depletion of IFI16, or its mouse ortholog p204, significantly inhibited IFNß production in response to DNA transfection. Notably, stimulation of IFI16-mediated sensing was dependent on foreign DNA length and structure, but occurred independently of nucleotide content (Unterholzner et al. 2010). During HSV-1 infection, colocalization between IFI16 and vDNA has been observed in the cytoplasm of human macrophages; a process that led to IFN production (Horan et al. 2013). It was proposed in this study that HSV-1 capsid proteins are targeted for degradation in the cytoplasm exposing the vDNA to IFI16-mediated sensing and subsequent IFN production (Horan et al. 2013).

1.6.2.2.3.   IFI16 as a nuclear vDNA sensor

Although IFI16 can be cytoplasmic in some cell types, it is predominantly localized to the nucleus of fibroblast, endothelial, and epithelial cells (Veeranki and Choubey 2012). A bipartite NLS that includes two motifs, termed motif 1 (residues 96–100) and motif 2 (residues 128–131), have been identified as essential for IFI16 nuclear distribution (Li et al. 2012). Deletion of either motif leads to cytoplasmic localization of IFI16 (Li et al. 2012).

In HSV-1 infected fibroblasts (MOI of $\geq$10 PFU/cell), a dynamic subnuclear redistribution of IFI16 has been observed (Everett 2015, Diner et al. 2016, Cuchet-Lourenco et al. 2013, Diner et al. 2015). As early as 30 minutes to 1 hpi, IFI16 puncta are transiently formed on the nuclear periphery in a pyrin-dependent manner (Everett 2015, Diner et al. 2016). As infection progresses (approximately 3-4 hpi), IFI16 puncta were observed to assemble in the nucleoplasm of the infected cells. Soon after, these IFI16 signals were lost in WT HSV-1 infected cells but remained stable during ΔICP0 and ICP0 RING mutant infections (Diner et al. 2015, Cuchet-Lourenco et al. 2013). Correspondingly, infection of human fibroblasts with HSV-1 ICP0 mutants led to the induction of IFNß production and ISG expression in an IFI16-dependent manner (Diner et al. 2015, Diner et al. 2016, Orzalli et al. 2012). Importantly, blocking of vDNA release into the nucleus using tosyl phenylalanyl chloromethyl ketone (TPCK), a serine-cysteine protease inhibitor which blocks U_L36 cleavage that is required for vDNA release, substantially inhibited the induction of IFNß and ISG54 following infection; demonstrating that accumulation of vDNA in the nucleus of fibroblasts is required for IFI16-mediated induction of host innate immunity (Horan et al. 2013, Orzalli et al. 2012).

1.6.2.2.4.   Mechanism of action of IFI16

IFI16 undergoes conformational changes after binding to the vDNA. IFI16, through its positively charged HIN domain, interacts with the sugar-phosphate backbone of dsDNA which primes the pyrin domain for activation. Subsequently, activated IFI16 translocates to the cytoplasm to activate the STING pathway and inflammasome formation (Jin et al. 2012). Re-localization of IFI16 to the cytoplasm after vDNA sensing has been proposed to occur through acetylation of the NLS of IFI16 by the acetyltransferase activity of p300 (Li et al. 2012, Ansari et al. 2015, Dutta et al. 2015).

Recent studies have also proposed an interplay and cooperation between IFI16 and cGAS during vDNA sensing and induction of innate immunity (Almine et al. 2017, Bowie et al. 2017, Orzalli et al. 2015). cGAS has been shown to promote IFI16-mediated vDNA sensing by interacting with and mediating the stability of IFI16 (Orzalli et al. 2015). IFI16 in cooperation with cGAS also plays a crucial role in the phosphorylation of TBK-1 and IRF-3, recruitment of TBK-1 to STING complex, cGAMP production, and cGAMP-induced STING activation (Almine et al. 2017, Bowie et al. 2017).   Activated STING translocates from the endoplasmic reticulum (ER) to ER-Golgi intermediate compartments. STING then associates with TBK1 promoting IRF3 phosphorylation and nuclear translocation leading to IFNß production and secretion.

1.6.2.3.   Type I IFN signaling

In the second phase of the IFN response, binding of secreted IFN to its cognate receptors (IFNAR) activates Janus-associated kinase 1 (JAK-1) and tyrosine kinase 2 (TYK-2) that induce the phosphorylation and activation of signal transducers and activators of transcription 1 (STAT-1) and STAT-2 (Watling et al. 1993, Shuai et al. 1993b, Silvennoinen et al. 1993). The interaction between STAT1, STAT2, and IRF9 leads to the formation of IFN-stimulated gene

factor 3 (ISGF3) complex at ISG promoters that induces the expression of ISGs products (Figure 6) (Kessler et al. 1990, Fu et al. 1990). This process functions in both an autocrine and paracrine fashion to inhibit viral replication and to protect neighboring cells from infection (Figure 7).

1.6.2.4.   ISG-mediated antiviral response

Relatively few ISG products have been identified to confer an antiviral response to HSV-1. An *in vivo* study suggested that the presence of ISG15, a ubiquitin-like molecule, is crucial for an efficient IFN-mediated host response to HSV-1 infection (Lenschow et al. 2007). Compared to WT mice, ISG15–deficient mice showed increased susceptibility to WT HSV-1 infection and decreased survival rates. However, the underlying mechanism for ISG15-mediated immunity remains to be determined (Lenschow et al. 2007). Other ISG products (e.g., viperin, tetherin, and zinc finger antiviral protein (ZAP)) have been shown to restrict HSV-1 infection, a process that is counteracted by vhs protein encoded by UL41 (Shen et al. 2014, Su et al. 2015, Zenner et al. 2013). Viperin and tetherin inhibit the release of virions from the plasma membrane, while ZAP targets viral mRNA for degradation. Ectopic expression or depletion of these proteins reduced or enhanced, respectively, the viral yield of UL41-null mutant but not WT HSV-1. UL41 encodes vhs protein, a viral protein that targets cellular mRNAs for degradation and thereby inhibits ISG expression (Shen et al. 2014, Su et al. 2015, Zenner et al. 2013). 2-5 Oligoadenylate synthetase (OAS) was also shown to confer antiviral immunity to HSV-1 infection, a process that is counteracted by the viral protein Us11 (Sanchez and Mohr 2007). Although these studies identified effector ISG products during HSV-1 infection, this area of research remains understudied and requires further investigations.
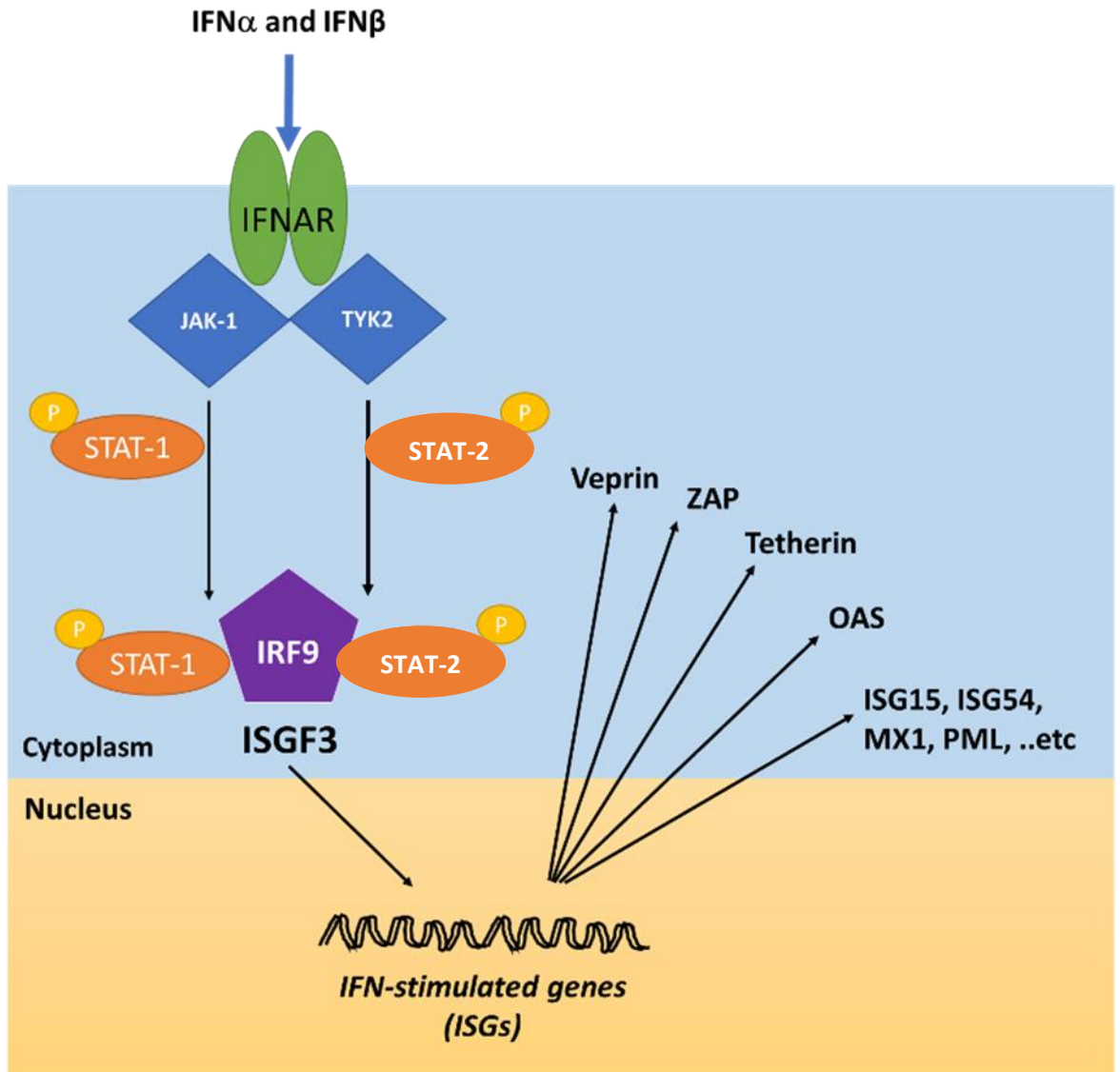
Figure 7. The second phase of IFN response.

IFNα and IFNß bind to their receptors (IFNAR) on the cell surface leading to the activation of the JAK-STAT pathway. Phosphorylated STAT1 and STAT2 bind to IRF9 to form ISGF3 which translocates to the nucleus to induce the expression of ISGs (e.g., viperin, tetherin, ZAP, OAS, ISG15, ISG54, and Mx1.

1.6.2.5.   Other types of IFNs

The production of IFNα and IFNß upon initial infection of peripheral epithelial cells upregulates ISG expression and activates several types of immune cells (e.g., macrophages, natural killer (NK) cells, and DCs). Activated NK cells in addition to CD8+ T cells are predominantly responsible for IFNγ production (Djeu et al. 1982, Pasternack et al. 1984). Many lymphoid and non-lymphoid cells express IFNGR (Anderson et al. 1982, Orchansky et al. 1984). The type II IFN signaling cascade is triggered when IFNγ binds to IFNGR followed by the assembly of IFNγ-IFNGR-JAK1-JAK2 complex (Silvennoinen et al. 1993, Igarashi et al. 1994). Activation of JAK1 and JAK2 induce IFNGR phosphorylation and STAT1 docking site formation (Greenlund et al. 1995). STAT1 molecules are first recruited to the complex, phosphorylated, dissociated, and translocated to the nucleus where they act as gene transactivators (Shuai et al. 1993a).

Several studies highlighted the importance of IFNγ signaling pathway in controlling and minimizing the pathogenesis of HSV-1 infection during both lytic and latent infection. Mice lacking IFNGR were more susceptible to HSV-1 infection and showed higher mortality rate than WT mice (Cantin et al. 1995). IFNγ itself can independently induce an antiviral state through ISG induction. Moreover, IFNγ synergizes with type I IFN during HSV-1 infection leading to a dramatic reduction in viral replication (Vollstedt et al. 2004, Sainz and Halford 2002, Zerial et al. 1982). Mice lacking both IFNAR and IFNGR showed increased susceptibility to HSV-1 infection in comparison to mice lacking either one of the receptors individually (Luker et al. 2003). IFNγ is also known to link host innate and adaptive immune responses. It stimulates the expression of major histocompatibility complex (MHC) class I to enhance antigen presentation to CD8+ T cells, and thereby playing a key role in the maintenance of viral latency (Shaw et al. 1985). Mice lacking IFNGR have higher levels of viral gene expression during reactivation than WT mice (Cantin et al. 1999). Collectively, these studies have demonstrated that IFNγ plays crucial roles against HSV-1 infection during both lytic and latent stages of infection.

Type III IFN (IFNλ1-3), the most recently discovered member of the IFN family, has unique receptors but shares the same signaling cascade with type I IFN (Kotenko et al. 2003). Few studies have investigated the role of IFNλ during HSV-1 infection. Patients with recurrent herpes labialis are associated with marked decrease in IFNλ levels in their peripheral blood mononuclear cells (Pica et al. 2010). Exogenous treatment of primary human astrocytes and neurons with IFNλ inhibited viral gene expression and viral protein synthesis by stimulating the induction of endogenous type I IFN production and ISG expression (Li et al. 2011). In support of this hypothesis, it has been shown that the subset of plasmacytoid dendritic cells (pDCs) that can produce IFN-λ in response to HSV-1 infection is associated with higher levels of IFN-α production in comparison to cells that do not produce IFN-λ (Yin et al. 2012). Overall, the underlying mechanism of IFN-λ-mediated antiviral immunity is far from being understood.

1.6.3.   Adaptive (humoral and cellular) immunity

Humoral and cellular immunity also play key roles in controlling HSV-1 infection. An early study demonstrated that transfer of serum containing anti-HSV antibody protects susceptible mice from viral-induced stromal keratitis (Raizman and Foster 1988). An independent study showed that transfer of anti-HSV serum to pharmacologically immunosuppressed mice subjected to lethal HSV-1 footpad inoculation fully protects them from mortality (Mitchell and Stevens 1996). B cell-deficient mice also showed enhanced vulnerability to develop encephalitis and keratitis following ocular inoculation with HSV-1 (Deshpande et al. 2000). This phenotype can be a direct consequence of B cell deficiency but can also be linked to lack of efficient Th2 response as observed by impaired production of IL-4 and IL-10 in these mice. In contrast to these studies, another study supported the hypothesis that humoral immunity does not play an important role in immune protection against HSV-1 infection (Kuklin et al. 1998). Immunized mice that are genetically incapable of producing anti-HSV-1 antibodies could survive and resist the infection to the same extent as WT mice,

while immunized mice deficient in CD4+ T cell demonstrated increased susceptibility to the infection (Kuklin et al. 1998). These apparent contradictions between studies can be due to experimental design, viral dose, route of infection, or mice strains used for experimentation.

The antiviral role of T cells during HSV-1 infection is evident. Following antigen presentation mediated by MHC and DCs, naïve T cells are activated and differentiated. CD8+ T cells produce IFNγ to induce IL-12 to promote differentiation (Yoshida et al. 1994). CD8+ T cells exhibit cytolytic activity on cells lytically-infected with HSV-1 (Lawman et al. 1980, Rouse and Lawman 1980). In the absence of CD8+ T cells, effector CD4+ T cells are sufficient to clear the infection from neuronal tissues of infected mice (Johnson et al. 2008a). Establishment and maintenance of latency is another major antiviral role for CD8+ T cells (Liu et al. 2000). Indeed, IFNγ-producing CD8+ T cells persist during viral latency to reduce viral dissemination (Sheridan et al. 2009).

Together, these studies demonstrate how the host employs a multifaceted approach to control HSV-1 infection. These antiviral mechanisms closely interact with each other in order to efficiently restrict HSV-1 replication and maintain viral latency.

1.7. HSV-1 strategies to counteract host immunity

HSV-1 has evolved multiple strategies to antagonize several aspects of host immunity, including evasion of PRR detection, modulation or blocking of immune signaling cascades, and interference with effector protein functions (Table 5). In this section, the central role of HSV-1 ICP0 in counteracting PML-NB mediated intrinsic immunity and innate immunity signaling is discussed.

Table 5. HSV-1 proteins that counteract host innate immune response.

Viral proteins	Function	Reference
ICP0	Interferes with intrinsic and innate antiviral immunity	(Boutell and Everett 2013, Lanfranca et al. 2014)
vhs	Induces vDNA sensors (IFI16 and cGAS) and ISGs (viperin, tetherin, and ZAP) degradation.	(Orzalli et al. 2016, Shen et al. 2014, Zenner et al. 2013, Su et al. 2015, Su and Zheng 2017)
Us3	Reduces the expression of TLR3, impedes TLR2 signaling, hyper-phosphorylates IRF3 and inhibits its activation, prevent p65 nuclear translocation and NF-κB activity	(Peri et al. 2008, Sen et al. 2013, Wang et al. 2013b)
Us11	binds to MDA5 and interferes with its downstream signaling, blocks ISG 2.5 oligoadenylate synthetase (OAS) activation	(Xing et al. 2012, Sanchez and Mohr 2007)
ICP34.5	Binds to TBK1 and disrupts its interaction with IRF3	(Verpooten et al. 2009)
VP16	Blocks the recruitment of IRF3 trans-activator CREB binding protein (CBP)	(Xing et al. 2013)
gM	Interferes with tetherin antiviral activity	(Blondeau et al. 2013)
UL24	Inhibits cGAS-STING signaling pathway	(Zhang et al. 2016, Xue et al. 2003)
ICP27	Interacts with TBK1 and STING, and interferes with cGAS-STING signaling pathway	(Christensen et al. 2016)
UL46	interferes with cGAMP-dependent immune signaling pathway	(Deschamps and Kalamvoki 2017a)

1.7.1. An overview of ICP0

ICP0 is a multifunctional IE protein that plays a key role to enhance HSV-1 lytic infection and reactivation from latency. It is encoded by *IE-0* gene (also called α) that is located within the inverted repeats sequence *ab* and *b'a'* (Wadsworth et al. 1975). Several functional domains and interacting motifs have been identified within ICP0 (Figure 8). The most important functional domain for ICP0 is the zinc-binding RING finger domain located in the N-terminal third between amino acids 116 to 156 within exon 2. Indeed, HSV-1 mutants that express catalytically inactive RING domain have equivalent replication defects to that of ΔICP0 HSV-1 (section 1.6.1.) (Everett 1989, Lium and Silverstein 1997, Everett et al. 2004a, Boutell et al. 2002, Vanni et al. 2012). The RING finger domain confers E3 ubiquitin ligase activity (Boutell et al. 2002, Vanni et al. 2012, Diao et al. 2005, Parkinson and Everett 2001). ICP0 interacts with components of the ubiquitin pathway to conjugate ubiquitin onto the lysine residues of target proteins, promoting their 26S proteasome-dependent degradation. Importantly, many ICP0-targeted proteins are key regulators of host intrinsic and innate immunity (Figure 9). Targeting these immune factors by ICP0, directly or indirectly, provides a favorable environment for viral replication.
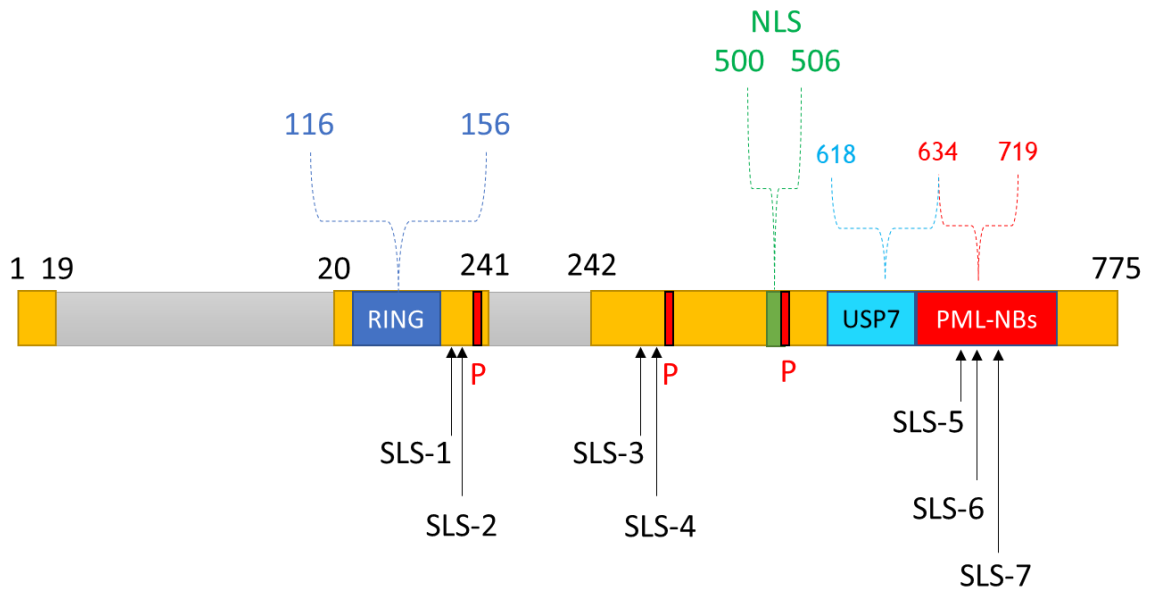
Figure 8. ICP0 structure and functional domains.

ICP0 is 775 amino acids in size, and is encoded by *IE-0* gene that is located within the inverted repeats sequence *ab* and *b'a'* (Wadsworth et al. 1975). *ICP0* is composed of three exons (1-19, 20-241, and 242-775 amino acids) (yellow), and two introns (765 and 136 nucleotides) (grey) (Perry et al. 1986). Several functional domains and interacting motifs have been identified within ICP0. A zinc-binding RING finger domain (RING) is located within the N-terminal third of ICP0 (residues 116-156) (Barlow et al. 1994, Everett et al. 1993a). The C-terminal third contains a nuclear localization signal (NLS; residues 500-506), a ubiquitin-specific protease 7 (USP7)-binding motif (residues 618-634), and sequences required for localization at PML-NBs (residues 634-719) (Everett 1988, Mullen et al. 1994, Meredith et al. 1995, Maul and Everett 1994). Three major phosphorylation sites (P; 224-234, 365- 371 and 508-518) of ICP0 have been identified (Davido et al. 2005). ICP0 contains several SUMO Interaction Motif (SIM)-like sequences (SLS-1 to SLS-7) (Boutell et al. 2011).
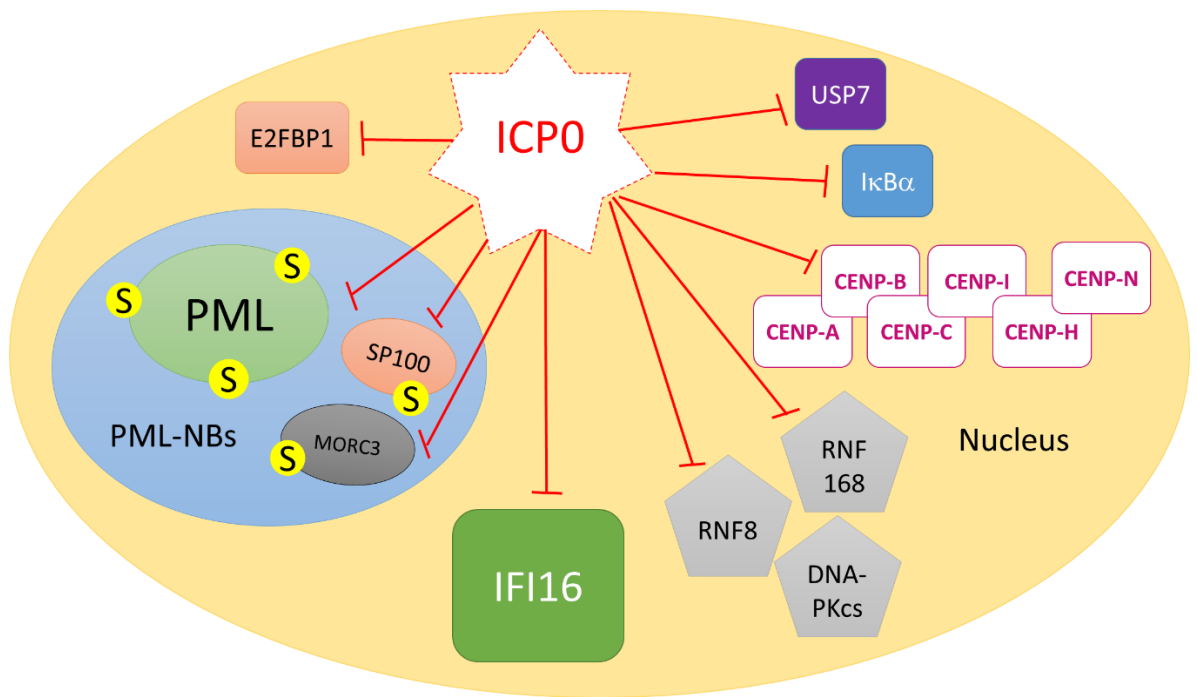
Figure 9. Cellular proteins known to be targeted directly or indirectly by HSV-1 ubiquitin ligase ICP0 for proteasome-dependent degradation.

ICP0 employs multiple mechanisms to induce the degradation of host proteins during HSV-1 infection, including high molecular weight SUMO-conjugated proteins, PML-NB constituent proteins (PML.I, and SUMO-modified forms of PML and SP100), DNA repair proteins (RNF8, RNF168, and DNA-PKcs), centromere and kinetochore proteins (CENP-A, B, C, I, H, and N), de-ubiquitinating enzyme (USP7), transcriptional factors (IκBα, and E2FBP1). Reviewed in (Boutell and Everett 2013).

1.7.1.1.   ICP0 counteracts PML-NB mediated intrinsic immunity

Several PML-NB constituent proteins (e.g., PML, SP100, Daxx, ATRX, MORC3, and PIAS-1) have been shown to restrict ΔICP0 HSV-1 replication (section 1.6.2.). However, they failed to do so during WT HSV-1 infection due to the presence of ICP0. During the initial stages of infection, ICP0 localizes to PML-NBs prior to mediating their disruption (Everett and Maul 1994, Everett et al. 1998, Chelbi-Alix and de The 1999). PML and SP100, core constituent proteins of PML-NBs, are among the first proteins identified as substrates for ICP0-mediated degradation (Chelbi-Alix and de The 1999, Everett et al. 1998). Recently, MORC3 was also shown to be subjected to ICP0-mediated degradation. Other PML-NB restriction factors (e.g., Daxx, ATRX, and PIAS-1) are not degraded during WT HSV-1 infection, although the presence of ICP0 blocks their recruitment to infecting viral genomes and efficiently counteracts their repressive antiviral activity (Lukashchuk and Everett 2010, Brown et al. 2016). ICP0 employs multiple mechanisms to counteract the intrinsic repression mediated by PML-NB restriction factors.

1.7.1.1.1.   Mechanisms of PML-NB proteins targeting by ICP0

Proteomics have identified 124 proteins that showed reduction (≥ 3 fold) in levels of their SUMO-modified forms during HSV-1 infection, some of which are target substrates of ICP0 (e.g., PML and SP100) (Sloan et al. 2015). During the initial stages of infection, ICP0 localizes to SUMO1 and SUMO2/3 conjugates (including SUMO-modified PML and SP100) and preferentially targets them for proteasomal degradation in a RING finger-dependent manner (Boutell et al. 2011). Indeed, ICP0 shares many features with SUMO-targeted ubiquitin ligases (STUbL); a family of enzymes that contain SIMs which mediates the interaction with SUMO-modified proteins (Boutell et al. 2011, Perry et al. 2008). Seven SIM-like sequences (SLS1-7) have been identified within the ICP0 open reading frame

(Figure 7). SLS-4 has been shown to be necessary for the ICP0 interaction with SUMO2/3 and targeting of SUMO-modified forms of PML for degradation (Boutell et al. 2011, Everett et al. 2014). Moreover, multiple mutations within ICP0 SLSs (4-7) rescued SUMO-conjugated proteins from degradation and influenced ICP0 ability to complement the plaque formation of ΔICP0 HSV-1, highlighting a key role for ICP0 STUbL-like activity in counteracting host intrinsic immunity (Boutell et al. 2011).

ICP0 also employs a SUMO-independent mechanism for PML targeting (Cuchet-Lourenco et al. 2012). It directly interacts with PML.I and induces its degradation. This process occurs independently of PML.I SIM and TRIM domains (the RING finger, B-Boxes and coiled-coil), and does not require ICP0 SLS4-7. Instead, ICP0-PML.I interaction is dependent on PML.I-specific exon 9 the N-terminal half of ICP0 (Cuchet et al. 2011, Zheng et al. 2016). Recently, MORC3 was identified as a target substrate for ICP0 (Sloan et al. 2016, Sloan et al. 2015). During WT HSV-1 infection, a high degree of colocalization between ICP0 and MORC3 was observed during the initial stages of infection prior to the degradation of SUMO-modified and unmodified MORC3. This process occurred in an ICP0 RING finger-dependent manner, but independently of SLS4-7. Whether ICP0 directly interacts with MORC3 remains to be determined. ICP0-mediated degradation of MORC3 not only counteracts MORC3-mediated intrinsic restriction, but also interfere with the recruitment of other PML-NB restriction factors (PML, SP100, and Daxx) to viral genomes (Sloan et al. 2016).

Collectively, HSV-1 efficiently counteracts PML-NB mediated silencing of the viral genomes. The viral E3 ubiquitin ligase ICP0 employs SUMO-dependent and independent targeting to mediate the degradation and dispersal of host restriction factors away from viral genomes to promote the onset of lytic infection.

1.7.1.2. ICP0 interferes with the induction of host innate immunity

Several lines of evidence demonstrated an important role for ICP0 to inhibit innate immune signaling. Compared to WT virus, ΔICP0 HSV-1 exhibits hypersensitivity to IFN pre-treatment (Mossman et al. 2000). The presence of ICP0 has been shown to inhibit both IFN-induced and viral-induced ISG expression (Eidson et al. 2002, Mossman and Smiley 2002). Indeed, robust induction of ISGs was only observed during infection with HSV-1 mutants that failed to express ICP0 (Eidson et al. 2002). Multiple mechanisms for ICP0-mediated inhibition of innate immunity have been proposed, although it remains controversial whether ICP0 is directly required and sufficient for this process (Lanfranca et al. 2014, Cuchet-Lourenco et al. 2013, Everett and Orr 2009). ICP0 has been shown to induce the degradation of the vDNA sensor IFI16 in a RING-dependent manner (Orzalli et al. 2016, Orzalli et al. 2012). It has also been proposed that cytoplasmic ICP0 binds to IRF3 and its-binding partner CBP leading to the formation of the ICP0/IRF3/CBP nuclear complex. This interaction inhibits the dimerization and activation of IRF3, accelerates turnover of IRF3, and prevents ISG expression (Melroe et al. 2007, Paladino et al. 2010). ICP0 also interferes with NF-κB signaling pathway by different mechanisms (e.g., degradation of TLR2, degradation of p50, and blocking of p65 nuclear import) (van Lint et al. 2010, Zhang et al. 2013). Collectively, these studies demonstrate that ICP0 impedes the induction of host innate immunity during HSV-1 infection in addition to its key role in antagonizing intrinsic antiviral immunity.
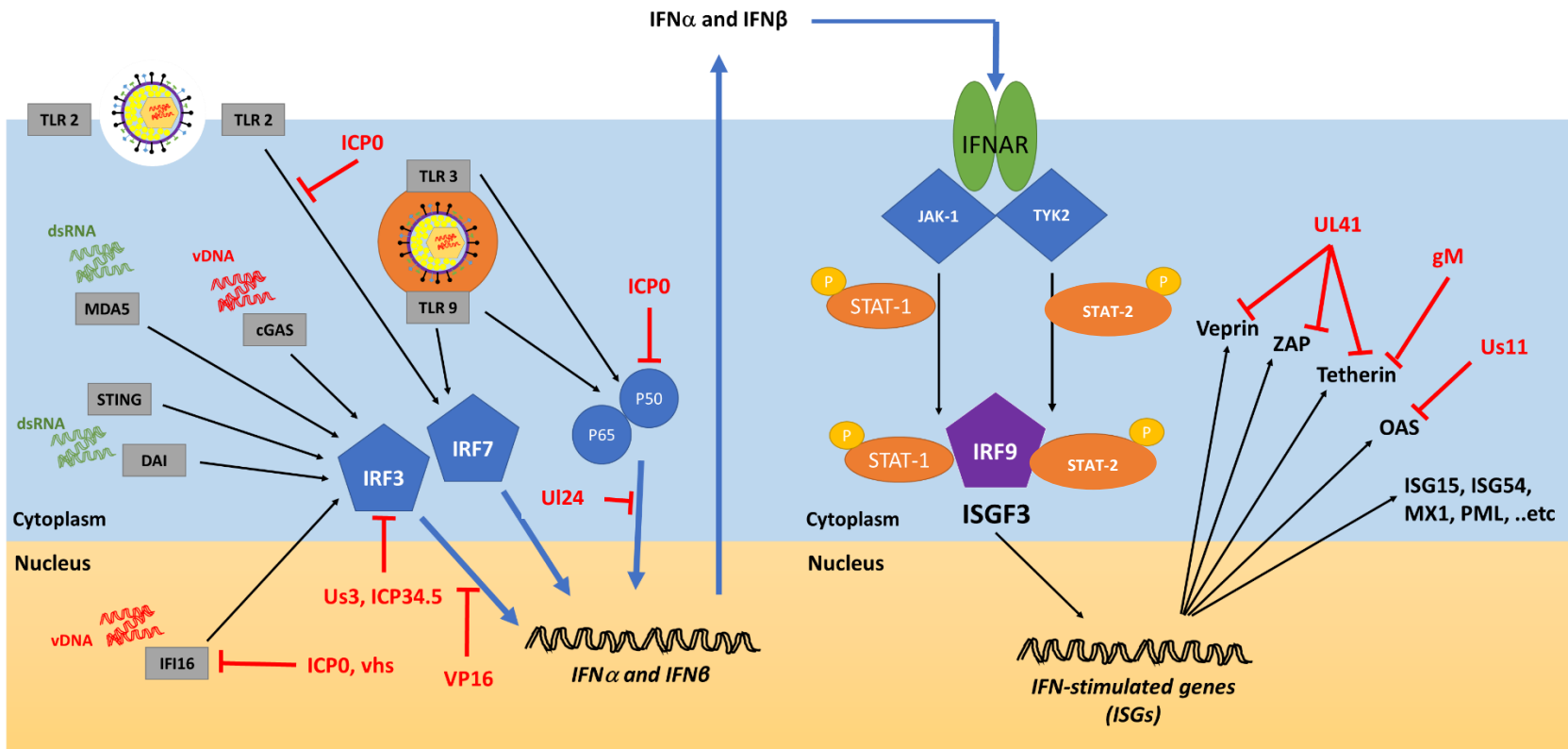
Figure 10. HSV-1 evasion of host IFN response.

The virus employs several proteins and interferes with IFN pathway at multiple stages. The expression of ICP0, vhs, Us3, ICP34.5, UL24, and VP16 directly or indirectly antagonize the function of PRRs, block the activation of downstream signaling cascades (IRF3, IRF7, and NF-κB), and inhibits the secretion of IFNα and IFNß. The expression of UL41, gM, and Us11 counteract the antiviral effects of IFN-stimulated genes (ISGs) such as Veprin, ZAP, Tetherin, and OAS.

1.8. Rationale and aim of this project

Intrinsic (constitutive) and innate (inducible) antiviral responses play key roles during the intracellular restriction of HSV-1 infection. The viral protein ICP0 efficiently antagonizes these immune responses. Hence, ΔICP0 HSV-1 has been an important tool for defining many aspects related to the regulation of intracellular antiviral immunity. However, several questions remain unanswered with regards to how intrinsic and innate immune responses are regulated. For example, (1) are they simultaneously or temporally induced in response to infection, (2) do they impair viral infection at distinct stages of replication, and (3) does the permissiveness of certain cell types to ΔICP0 HSV-1 infection correlate with the lack of ability to mount efficient intrinsic or innate immune response in these cells?

One of the main reasons why the temporal regulation of these two branches of immunity remains poorly defined is that most microscopy-based studies utilized to examine interactions between host immune factors and HSV-1 have used indirect methods to detect vDNA (e.g., immuno-staining or fluorescent-tagging of vDNA binding proteins) (Everett 2013, Komatsu et al. 2016). As this approach necessitates the onset of viral gene expression, it limits our understanding of the viral-host interactions that occur immediately upon nuclear entry prior to the expression of viral proteins which may displace host factors recruited or bound to viral genomes. Some studies have utilized direct methods for vDNA detection (e.g., FISH and Bromodeoxyuridine (BrdU)-labeling of vDNA). However, these experiments were conducted under high MOI conditions due to the technical difficulties associated with low genome copy-number detection (Everett et al. 2007, Glauser et al. 2007, Jensen 2014). These experimental settings are suboptimal to study the regulation between intrinsic and innate immunity given that intrinsic immunity has a threshold of MOI above which this arm of immunity is saturated and no longer effective (section 1.6.1.) (Everett et al. 2004a). FISH and BrdU-labeling also require harsh denaturation

conditions and substantial sample processing which can be incompatible with IF staining of host factors.

Hence, the main objectives of this project were as follows:

(1) Develop and optimize a minimally invasive protocol to directly visualize vDNA under low MOI conditions that do not saturate intrinsic host defenses.

(2) Investigate the temporal recruitment of intrinsic (PML-NB associated restriction factors) and innate immune (IFI16) factors to infecting viral genomes.

(3) Evaluate the consequence of intrinsic and innate immunity induction on viral replication.

(4) Assess whether intrinsic and innate antiviral responses to ΔICP0 HSV-1 infection occurs in a cell type-dependent manner, rendering certain cell types more permissive to ΔICP0 HSV-1 infection.

2. Materials

Table 6. Types of cells used in the study.

Name	Type	Growth and maintenance media	Growth and maintenance condition
BHK	Baby hamster kidney cells	Glasgow modified Eagle's medium (GMEM) supplemented with 10% fetal calf serum (FCS), 10% tryptose phosphate broth, 100 units/ml penicillin, and 100 µg/ml streptomycin	All cell lines were maintained at 37°C with 5% CO_2.
HaCaT	A spontaneously transformed aneuploid immortal keratinocyte cell line from adult human skin	Dulbecco's Modified Eagle Medium (DMEM) supplemented with 10% FCS, 100 units/ml penicillin, and 100 µg/ml streptomycin	
U2OS	Human bone osteosarcoma epithelial cells		
SAOS	Human bone osteosarcoma epithelial cells		
HEK-293t	Human embryonic kidney cells immortalized by insertion of human telomerase reverse transcriptase (hTERT)	Dulbecco's modified Eagle's medium supplemented with 10% FCS, 0.5 µg/ml hygromycin, 100 units/ml penicillin, and 100 µg/ml streptomycin	
HFt	Human foreskin fibroblasts immortalized hTERT		
RPE	Retinal pigmented epithelial cells immortalized hTERT		

Table 7. Cell culture media and chemicals commonly used throughout the study.

Reagents name and abbreviations	Provider	Catalog or reference
Bovine serum albumin (BSA)	Sigma-Aldrich	A3294
Dimethyl sulfoxide (DMSO)	Sigma-Aldrich	D2650
Dulbecco's Modified Eagle Medium (DMEM)	Life Technologies	41966-029
Ethylene glycol-bis(β-aminoethyl ether)-N,N,N',N'-tetraacetic acid(EGTA)	BDH	28672
Fetal Calf serum (FCS)	Life Technologies	10270-106
Formaldehyde	Sigma-Aldrich	f8775
Giemsa	VWR	350864X
Glasgow's MEM (GMEM)	Life Technologies	11710035
DAPI	Sigma-Aldrich	D9542
DL-Dithiothreitol (DTT)	Sigma-Aldrich	D0632
Dulbecco's Phosphate Buffered Saline (PBS)	Sigma-Aldrich	D1408
Glycine	VWR	101196X
HEPES	Sigma-Aldrich	H3375
Human serum (HS)	MP Biomedicals	2931149
Lipofectamine® LTX with Plus™ Reagent	Invitrogen	15338100
Magnesium chloride (MgCl2)	Sigma-Aldrich	M8266

NP-40	Sigma-Aldrich	9016-45-9
NuPAGE™ MES SDS Running Buffer	ThermoFisher	NP0002
NuPAGE™ MOPS SDS Running Buffer	ThermoFisher	NP0001
NuPAGE™ Transfer Buffer	ThermoFisher	NP0006-1
Polybrene	Sigma-Aldrich	H9268
Sodium Chloride (NaCl)	VWR	27810.295
Sodium dodecyl sulfate (SDS)	VWR	442444H
Sucrose	Sigma-Aldrich	S7903
Triton X-100	Promega	H5142
True blue HRP substrate	KPL	50-78-02
Trypsin	Life Technologies	15090-046
Tryptose Phosphate Broth (TPB)	Life Technologies	18050-039
Tween 20	Bio-Rad	170-6513
Urea	Sigma-Aldrich	U0631
Versene	E and O laboratories	BM0400
5-Ethynyl-2'-deoxyuridine, (EdU)	Sigma-Aldrich	T511285

Table 8. Commonly used drugs, preparation, and storage.

Name and abbreviation	Provider and Catalog number	Preparation
Acycloguanosine (ACG)	Sigma-Aldrich A4669	• Suspended in Milli-Q H2O • Aliquoted and store at -20° C
Hygromycin	Invitrogen 10687-010	• Stored at 4° C
Interferon alpha (IFNα)	CALBIOCHEM 407294	• Aliquoted and store at -70° C
Interferon beta (IFNß)	CALBIOCHEM 407318	• Suspended in Milli-Q H2O • Aliquoted and store at -70° C
Interferon gamma (IFNγ)	CALBIOCHEM 407306	• Aliquoted and store at -70° C
Interferon lambda (IFNλ)	SIGMA-ALDRICH 284270	• Suspended in 0.1% BSA • Aliquoted and store at -70° C
Penicillin/streptomycin (P/S) solution	Life Technologies 15140122	• Aliquoted and store at -20° C
Phosphonoacetic acid (PAA)	SIGMA-ALDRICH 284270	• Suspended in Milli-Q H2O • Aliquoted and store at -20° C
Puromycin	Sigma-Aldrich P8833	• Suspended in Milli-Q H2O • Aliquoted and store at -20° C • Stock concentration: 5 µg/ml
Ruxolitinib (Rux)	Sellechchem S1378	• Suspended in DMSO • Aliquoted and store at -20° C

Table 9. Plasmids.

Plasmid	Description	Source
pVSV-G	Vector used for expression of vesicular stomatitis virus envelope protein	BD Biosciences
pCMV delta R.8.91	Lentivirus helper vector that contains reverse transcriptase polymerase (pol), capsid protein (gag), regulatory proteins (Rev), and CMV promoter	A gift from Didier Trono (Addgene plasmid # 12263)
shCtrl	Plasmids encoding short hairpin RNA against a non-targeted control sequence (5'-TTATCGCGCATATCACGCG-3')	
pLKO-shPML	Plasmids encoding short hairpin RNA against PML (5'-AGATGCAGCTGTATCCAAG-3')	(Everett et al. 2006)
pLKO-shIFI16	Plasmids encoding short hairpin RNA against IFI16 (5'-CCACAATCTACGAAATTCA-3')	(Cuchet-Lourenco et al. 2013)

Table 10. List of primary antibodies.

Antibody	Species	Provider	Dil. used in WB*	Dil. used in IF*
Actin	Rabbit	Sigma, A5060	1:1000	N/A
Daxx	Rabbit	Upstate, 04-445	1:500	1:500
ICP0 (11060)	Mouse	(Everett et al. 1993b)	1:10000	1:1000
ICP4 (58S)	Mouse	(Showalter et al. 1981)	1:500	N/A
ICP4	Mouse	Abcam, ab6514	N/A	1:1000
IFI16	Mouse	Abcam, ab55328	N/A	1:1000
IFI16	Mouse	Santa Cruze, sc-8023	1:250	N/A
ISG15	Rabbit	ProteinTech, 15981-1-AP	1:1000	1:500
ISG54	Rabbit	ProtienTech, 12604-1-AP	1:1000	N/A
Mx1	Rabbit	Santa Cruze, sc-50509	1:300	N/A
Mx1	Rabbit	ProteinTech, 13750-1-AP	N/A	1:500
PML	Rabbit	Bethyl Laboratories, A301-167A	1:2000	1:1000
PML	Mouse	Abcam, ab96055	N/A	1:1000
SP100	Mouse	GeneTex, GTX131569	N/A	1:500
VP5 (DM165)	Mouse	(McClelland et al. 2002)	1:500	N/A

* dil (dilution), WB (western blot), IF (immune-fluorescence staining).

Table 11. List of secondary antibodies used.

Antibody	Origin	Provider, Catalog Number	Assay and dilution
Rabbit IgG (H+L) Alexa-Flour 488	Donkey	Life Technologies, A21206	Immuno-fluorescence (IF) staining (1/1000)
Rabbit IgG (H+L) Alexa-Flour 647	Donkey	Life Technologies, A31573	
Mouse IgG (H+L) Alexa-Flour 488	Donkey	Life Technologies, A21202	
Mouse IgG (H+L) Alexa-Flour 647	Donkey	Life Technologies, A31571	
Rabbit IgG (H+L) DyLight 680	Goat	Thermo Scientific, 35568	Western blot (1/5000)
Rabbit IgG (H+L) DyLight 800	Goat	Thermo Scientific, SA5-35571	
Mouse IgG (H+L) DyLight 680	Goat	Thermo Scientific, 35518	
Mouse IgG (H+L) DyLight 800	Goat	Thermo Scientific, SA5-35521	
Anti-Mouse IgG-Peroxidase antibody	Goat	Sigma-Aldrich, A4416	Immuno-staining plaque assay (1/1000)

Table 12. List of primers/probes used.

Primer/Probe	Catalog number (assay ID)	Provider
GAPDH	4333764F	ThermoFisher
PML	(4331182) HS00231241_m1	
ISG15	(4331182) HS01921425_s1	
Mx1	4331182 (HS00895608_m1)	
ISG54	4331182 (Hs01922738_s1)	
IFI16	4331182 (Hs00986757_m1)	

3. Methods

3.1. Cell culture

3.1.1. Maintenance, growth, and passaging of cells

Unless stated otherwise, cell lines were maintained and grown on T75 cell culture flasks (Nunc Fisher Scientific UK Ltd) in the appropriate media described in (Table 6) at 37ºC with 5% CO_2. When cells were 80-90% confluent, they were washed twice with 2.5 ml versene, followed by incubation with 1.5 ml of trypsin-versene until the cells were detached from the flasks. Detached cells were re-suspended in 8.5 ml of the appropriate medium before reseeding in new flasks for maintenance, or plating for experimentation.

3.1.2. Seeding of cells

The number of cells in the suspension was determined using Neubauer hemocytometer counting chamber under a light microscope. Cells were seeded in 12 or 24 well plates in a total volume of 0.5-1 ml of culture medium. For confocal microscopy analysis, cells were seeded onto 13 mm glass coverslips in 24 well plates. The seeding density was dependent on the cell type, with typical seeding density ranging from 1×10^5 to 2×10^5 cells per well. Cells were incubated overnight before further manipulation.

3.2. Lentiviral vector-based short hairpin RNA methods for generating PML- or IFI16-depleted cells

3.2.1. Generation of lentivirus stocks

Transformation of competent bacteria and propagation of plasmid DNA were conducted by Steven McFarlane. For generation of lentivirus stocks, HEK-293T cells (2×10^6 cells) were seeded onto 60 mm dishes and incubated overnight at 37°C in 5% CO_2. pLKO plasmid (3 µg) expressing a non-targeting control, PML-targeting, or IFI16-targeting short hairpin RNA (shCtrl, shPML, and shIFI16, respectively) plus pVSV-G (3 µg) plasmid and pCMV-DR8.91 helper plasmid (3 µg) were added to 250 µl of serum-free DMEM. PLUS reagent (8 µl) was added to the plasmid mixture and incubated for 15 minutes at room temperature. After incubation, serum-free DMEM (250 µl) and lipofectamine (12 µl) were added to the plasmid-reagent plus mixture and allowed to incubate for 15 minutes at room temperature.

The culture medium of HEK-293T cells was removed and saved as "conditioned medium". Serum-free medium (850 µl) was added to the prepared plasmid-PLUS reagent-lipofectamine mixture prior to adding the entire volume to the cells and incubating at 37°C for 3 hours. Then, 3 ml conditioned medium were added, and incubated at 37°C for 4 hours. Following incubation, the medium was replaced by 4 ml of fresh DMEM supplemented with 30% FCS. Lentivirus stocks were harvested when cells showed severe cytopathic effect, typically 48 hrs post-transfection. Lentivirus stocks were filtered using 0.45 µm filter and used immediately.

3.2.2. Lentiviral transduction of cells

HFt cells were seeded at 1 X 10^6 cells in 60 mm dishes and incubated overnight at 37°C in 5% CO$_2$. Cells were infected four times with lentivirus supernatants. For each infection, 1 ml of lentivirus supernatant containing 1 µl of polybrene was added to the cell monolayer. The infected plates were kept at 37°C in 5% CO$_2$ incubator for 1 hour with rocking every 5-10 minutes. Following the third round of infection, 4 ml of lentivirus supernatant containing 4 µl of polybrene were added to the cells and incubated overnight at 37°C in 5% CO2. On the following day, the lentivirus-containing medium was discarded and replaced by antibiotic selection medium (HFt media containing puromycin at 1 µg/ml) and then passaged with continuous puromycin selection. The level of mRNA and protein expression was monitored by qPCR, IF and Western blotting. All experiments were repeated on independent batches of depleted cells.

3.3. Viruses:

3.3.1. Standard protocol for growing HSV-1 stocks

BHK cells were seeded at 1 X 10^6 cells per 60 mm dish and incubated overnight at 37°C with 5% CO2. Cells were infected with WT HSV-1 (*17syn+*) at an MOI of 0.001 PFU/cell, or its corresponding ΔICP0 (*dl1403*) at an MOI of 0.5 PFU/cell in 500 µl of serum-free DMEM (Stow and Stow 1986). During viral absorption, the plates were rocked every 5-10 minutes for one hour to ensure equal distribution of the virus across the cell monolayer. Following the absorption, cells were overlaid with complete medium and incubated at 37°C with 5% CO2. Infected cells were checked regularly (every 24 hrs) for cytopathic effect. Virus suspension was collected when a severe cytopathic effect was observed, typically 3 to 4 days post-infection. The cell-released virus was clarified by low-speed centrifugation at 1500 rpm for 10 minutes to remove cell

debris. Virus stocks were aliquoted, snap frozen on dry ice, and stored at - 70 °C.

3.3.2. Growing EdU-labeled viruses

EdU-labeled viruses were grown on RPE cells. Cells were infected with either WT HSV-1 at an MOI of 0.001 PFU/cell or ΔICP0 HSV-1 at an MOI of 0.5 PFU/cell in a total volume of 2.5 ml DMEM containing 0.2% FCS at 33°C with 5% CO2. The flasks were rocked every 5-10 minutes for one hour. Following viral absorption, 2.5 ml of DMEM containing 0.2% FCS were added to each flask making a total of 5 ml per flask. At 4 hrs post-infection, EdU was added to a final concentration of 0.5 µM per flask. Then, a fresh pulse of EdU (0.5 µM) was added every 24 hrs for three days. When cells showed an extensive cytopathic effect, the yields were collected and combined in a 50 ml corning tubes. In order to remove cell debris, the tubes were centrifuged at 1500 RPM for 10 minutes. Supernatants containing labeled cell-released virus were filtered through 0.45 µm filter to remove small debris. The filtered suspensions were transferred into 5 ml Beckman Coulter ultra-clear centrifuge tubes (Catalog number 344057). Tubes were loaded into Beckman TLA100.3 rotor and ultra-centrifuged at 25000 for 3 hrs at 4°C. Supernatants were discarded, and the virus pellets were resuspended in 500 µl of complete DMEM medium. The viral suspensions were combined and titrated in U2OS cells (described below).

3.3.3. Virus stock titration

All virus stocks (WT HSV-1, ΔICP0, HSV-1^{EdU}, and ΔICP0^{EdU}) were titrated in U2OS cells. Cells were seeded overnight at 2×10^5 cells per well in 24-well plate. The virus stocks were serially diluted (dilution factor of 10). Cells were infected in a total volume of 100 µl of serum-free DMEM. During viral absorption, the plates were rocked every 5-10 minutes for one hour to ensure equal distribution of the virus across the cell monolayer. Then, cells were overlaid

with DMEM supplemented with 10% FCS and 2% human serum (HS), and incubated at 37ºC with 5% CO2. The infected cells were checked regularly for viral plaques which were observed typically 2 to 3 days post-infection. The plates were Giemsa stained (described below), and the plaques were counted under a plate microscope. Then, viral titers were calculated using the following formula:

$$PFU/ml = Number\ of\ plaque * dilution\ factor * 10\ (used\ 100\mu l\ inoculum)$$

MOI (PFU/cell) was estimated based on the virus titer and the number of cells. Irrespective of the cell types to be infected, the MOI was estimated based on the virus titer determined on U2OS cells. This is particularly important for ΔICP0 HSV-1 as U2OS is known to supplement for ICP0 function (Yao and Schaffer 1995, Everett et al. 2004a).

3.4. Assays

3.4.1. Giemsa staining.

Cells were washed twice with PBS, before adding 500 µl of Giemsa solution to each well. After incubation for 10 minutes at room temperature, Giemsa solution was removed, and the cells were washed thoroughly with water. The number of plaques was counted under a plate microscope.

3.4.2. Immuno-staining plaque assay

Cells were seeded in 24-well plates and incubated at 37˚C in 5% CO2 overnight before further manipulations. Cells were inoculated with either a serial dilution or fixed MOI (PFU/cell as indicated) of WT or ΔICP0 HSV-1 in a total volume of 100 µl serum-free DMEM. Plates were rocked every 10 min for 1 h prior to overlay with complete medium containing 2% HS. At the indicated

time post-infection, the media were removed, and the cells were washed three times with PBS. Cells were simultaneously fixed and permeabilized in PBS containing 1.8% formaldehyde and 0.5% NP40, followed by blocking in PBS-tween (PBST) containing 5% skimmed milk for 30 minutes at room temperature. Cells were sequentially incubated for 60 minutes at room temperature with primary anti-VP5, followed by anti-Mouse IgG–peroxidase secondary antibody. Three washes with PBST were performed following each antibody incubation. Finally, True Blue Peroxidase stain was added and incubated until the color was developed. Plates were then washed three times with PBST, PBS, and distilled water. The number of plaques was counted under a plate microscope.

3.4.3. Viral release assay

Cells were seeded in 24-well plates and incubated at 37°C in 5% CO2 overnight. Cells were inoculated with WT (MOI of 0.001 PFU/cell) or ΔICP0 HSV-1 (MOI of 1 PFU/cell) in a total volume of 100 µl serum-free DMEM. Plates were rocked every 10 minutes for 1 h prior to overlay with complete medium containing either DMSO or 5 µM ruxolitinib (RUX). Supernatants are collected at the indicated time points post-infection (shown in the figures). Viral yields were titrated on U2OS cells (section 3.4.3.).

3.4.4. Sodium dodecyl sulfate-polyacrylamide gel electrophoresis (SDS-PAGE) and Western blotting

Cells were washed twice with PBS before whole cell lysates were harvested in a 1.5X boiling mix (SDS-PAGE loading buffer containing 4 M urea and 50 mM DTT). Harvested lysates were either used immediately or snap frozen and stored at - 20° C. Samples were boiled for 10 minutes in a water bath prior to loading. Wells were loaded with 15-20 µl of whole cell lysates. PageRuler pre-stained NIR protein ladder was used as a reference marker for molecular mass.

Proteins were resolved by SDS-PAGE on Novex 4-12% Bis-Tris gel (Invitrogen NP0322BOX) using either NuPAGE MOPs (1X) or NuPAGE MES (1X) running buffer. Gels were run at 120 volts until the dye front reached the bottom of the gel.

Separated proteins were electro-transferred for 1 hr at 30 volts onto Hybond-ECL 0.2 µm nitrocellulose membranes for western blotting. Protein transfer was conducted using Novex NuPAGE transfer buffer (1X) containing 10% methanol. Membranes were blocked for 1 hour at room temperature in filtered PBS supplemented with 5% FCS (PBS-FCS). Primary and secondary antibody incubations were performed in filtered PBST–FCS (PBS-FCS supplemented with 0.1% Tween-20) at the desired antibody dilution (Table 10 and 11). Membranes were washed three times in PBS supplemented with 0.1% Tween-20 (PBST) for 10 min following each antibody incubation. Prior to scanning, membranes were washed two times in PBS and two times in distilled water. Membranes were imaged on an Odyssey Infrared Imager (LiCor) and analyzed with Odyssey Image Studio Lite software.

3.4.5. Click chemistry, indirect IF staining, and confocal microscopy

3.4.5.1. Fixation and permeabilization

Coverslips were washed twice in cytoskeleton (CSK) buffer (10 mM HEPES (pH 7.0), 100 mM NaCl, 300 mM sucrose, 3 mM MgCl2, 5 mM EGTA) prior to fixation and permeabilization in CSK buffer containing 1.8% formaldehyde and 0.5% Triton-X100 for 10 minutes at room temperature. Cells were washed twice in CSK buffer, and coverslips were blocked in PBS containing 2% HS (PBS-HS) for at least 10 minutes at 4 ℃.

3.4.5.2.   CLICK chemistry and detection of EdU signals

Detection of the EdU-labeled virus was conducted using Click-iT® Plus EdU Alexa Fluor 555 Imaging Kit (ThermoFisher Scientific, C10638) according to the manufacturers' instructions. Each ml of reaction solution contained 880 µl of 1X Click-iT® reaction buffer, 20 µl of copper protectant, 2.5 µl of Alexa Fluor® picolyl azide, and 100 µl of reaction buffer additive. Click chemistry was always conducted prior to indirect IF staining.

3.4.5.3.   Indirect IF staining protocol

Primary and secondary antibody incubations were performed at room temperature. Following a 60-minute incubation with primary antibody at the desired dilution (Table 10), coverslips were washed three times with PBS prior to a 60-minute incubation with the secondary antibody and DAPI. The secondary antibodies used were Alexa 488, 555, and 647 conjugated donkey anti-rabbit, and anti-mouse IgG (Table 11). Coverslips were washed three times with PBS followed by three washes with distilled water. Coverslips were allowed to air dry prior to mounting on glass slides using Citifluor AF1 mounting medium. Clear nail varnish was used to seal the edge of coverslips to the slides.

3.4.5.4.   Confocal microscopy, image analysis, and three-dimensional (3D) image reconstitution

The samples were examined using a Zeiss LSM 710 or LSM880 confocal microscope using the 63x Plan-Apochromat oil immersion lens with 408, 488 nm, 543 nm and 633 nm laser lines. Zen black software (Zeiss) was used for capturing Z-series images, generating cut mask channels, exporting the maximum intensity projection images, and determining the weighted (w.) colocalization coefficient. Imaris (Bitplane) software was used to generate 3D images.

3.4.6.   Quantitative reverse-transcriptase polymerase chain reaction (qRT-PCR)

3.4.6.1.   RNA preparation

RNA extraction was conducted using RNeasy Plus Mini Kit (Qiagen) according to manufacturer's instructions. Cells were washed twice with PBS, harvested in 200 µl Buffer RLT Plus, snap frozen, and either used immediately or stored at -20 °C. The cell lysate was vortexed for 30 seconds, and centrifuged for 3 minutes at the maximum speed (17000 X g). The supernatant was carefully removed, transferred to a gDNA Eliminator spin column, and centrifuged for 30 seconds at 8000 X g. The column was discarded, and 180 µl of 70% ethanol were added to the flow-through. The entire volume was transferred to an RNeasy spin column and centrifuged for 15 seconds at 8000 X g. The flow-through was discarded, and 700 µl of Buffer RW1 were added to the column, followed by centrifugation for 15 seconds at 8000 X g. The flow-through was discarded, and 500 µl of Buffer RPE were added to the column, followed by centrifugation for 15 seconds at 8000 X g. The last step was repeated. In order to dry the membrane, the RNeasy column was placed in a new 2 ml collection tube and centrifuged at 17000 X g for 1 minute. Finally, 30 µl of RNase-free water were added, and the column was centrifuged for 1 minute at 8000 X g to elute RNA. Extracted RNA was used immediately for complementary DNA (cDNA) synthesis or stored at -20 °C.

3.4.6.2.   cDNA synthesis

Reverse transcription (RT) of cellular RNA to cDNA was performed using TaqMan Reverse Transcription Reagent Kit (Life Technologies, catalog number N808-0234). Purified RNA was reverse transcribed in a total volume of 20 µl of reaction mix containing 2 µl of RT buffer (1x), 4.4 µl of $MgCl_2$ (5.5 mM), 4 µl of dNTPs (2mM), 1 µl of Oligo dT, 0.4 µl of RNase inhibitor (8 U), 0.5 µl of

multiscribe reverse transcriptase (25 U), and 6.7 μl of RNase-free water. RNA template was sequentially incubated at 25 °C for 10 minutes for primer annealing, at 37 °C for 60 minutes for extension, and at 95 °C for 5 minutes for RT inactivation.

3.4.6.3.   Quantitative real-time PCR

cDNA was amplified using target and control-specific primer/probe mixes (Table 12). Each sample was run in duplicate or triplicate as a singleplex reaction in a total volume of 20 μl per reaction. Each reaction contained 1 μl of primer/probe mix, 10 μl of TaqMan fast universal mix (ThermoFisher Scientific, catalog number 4352042), 7 μl of RNase-free of H2O, and 2 μl of cDNA. RT-PCR cycling condition as follows: a cycle of denaturation at 95 ℃ for 20 seconds, and 40 cycles of annealing at 95 ℃ for 3 seconds, and extension at 60 ℃ for 30 seconds.

3.4.6.4.   Analysis of qPCR data

Data were analyzed using applied biosystems 7500 fast real-time PCR system software. The level of mRNA for host gene under investigation was normalized to GAPDH mRNA level, internal control, using the threshold cycle (ΔΔCT) method. Normalized values were expressed relative to the normalized level of mRNA in a control sample (as indicated in the figure legends).

3.5.   Data plotting and statistical analysis

GraphPad Prism 7.02 was used for blotting the data and calculating P values. T-test or Mann-Whitney U-test was used to determine statistical significance (as indicated in the figure legends).

4. Host intrinsic and innate immune factors are sequentially recruited to viral genomes

4.1. Overview

HSV-1, like other nuclear-replicating DNA viruses, needs to reach the nucleus in order to replicate. During the journey from the cell surface to the nucleus, the infected cell employs several mechanisms to control HSV-1 infection. Different parts of host cells (cell surface, cytoplasm, and nucleus) are equipped with immune factors which can recognize various PAMPs including virion components and viral replication products. vDNA is one of the most potent inducers of host intracellular immunity. Rapid recognition of viral nucleic acid is key for suppression of viral replication (Pandey et al. 2014, Orzalli and Knipe 2014, Komatsu et al. 2016).

Given that non-nuclear immune factors have limited access to vDNA due to the presence of the viral capsid, nuclear antiviral factors have historically attracted significant attention (Komatsu et al. 2016). The recruitment of host cell restriction factors to viral genomes and the sensing of vDNA by PRRs are very early cellular responses to infection. Host cell restriction factors immediately and directly induce viral genome silencing (intrinsic immune response). On the other hand, PRRs activate downstream signaling cascades leading to the induction of ISGs (innate immune response) (Yan and Chen 2012, Hannoun et al. 2016, Tavalai and Stamminger 2009, Scherer and Stamminger 2016). Whether host cells employ recruitment of host cell restriction factors and PRRs simultaneously or sequentially remains unknown.

Microscopy-based techniques have been widely utilized to investigate the relationship between nuclear immune factors and the infecting viral genomes. However, these studies offered limited conclusions with respect to the temporal regulation of intrinsic and innate immune responses. Studies, that have utilized

direct vDNA detection methods such as FISH or BrdU-labeling, have relied on high MOI conditions due to the technical challenges associated with vDNA detection at low MOI conditions (Everett et al. 2007, Glauser et al. 2007, Jensen 2014). Giving that the antiviral effect of host cell restriction factors has a threshold of MOI above which this system is saturated (Section 1.6.1.) (Everett et al. 2004a), this approach has limitations for understanding the regulatory mechanisms between intrinsic and innate immune responses. Moreover, FISH and BrdU-labeling protocols require harsh denaturation conditions (e.g., heat and HCl treatment) and can be cytotoxic and incompatible with IF staining of host factors. Other studies used IF staining or fluorescent tagging of vDNA-binding proteins (e.g., ICP4 and ICP8) to indirectly determine the localization of viral genome foci. A strong colocalization has been observed between vDNA and ICP4 detected by FISH and IF staining, respectively (Everett and Murray 2005). This finding validated the use of ICP4 as a proxy for viral genome localization. However, a subset of vDNA foci was not associated with ICP4 signals indicative of viral genomes that are yet to establish a productive infection (Everett and Murray 2005). While informative, this approach necessitates the onset of viral gene expression and limits our understanding of the very early viral-host interactions that occur immediately upon nuclear entry of vDNA prior to the expression of viral proteins. Recently, ethenyl-modified nucleoside labeling in combination with click chemistry has been utilized to directly visualize the vDNA of adenoviruses, herpesviruses, papillomaviruses, and retroviruses (Wang et al. 2013a, Dembowski and DeLuca 2015, Broniarczyk et al. 2015, Peng et al. 2014, Johnson et al. 2014). Labeling of vDNA replication compartments with ethenyl-modified nucleosides showed similar patterns to that observed in samples processed by FISH technique. Unlike FISH and BrdU, this technique is minimally invasive and compatible with IF staining protocols (Salic and Mitchison 2008, Chehrehasa et al. 2009). Click chemistry-mediated detection of DNA is based on the incorporation of nucleoside analogs into newly synthesized DNA followed by copper (I)-catalyzed reaction between alkynes on the labeled DNA and azides on the fluorescent dyes. Due to the small size of azide, this method does not involve denaturation or substantial sample processing (Salic and Mitchison 2008, Chehrehasa et al. 2009). Moreover, using bio-orthogonal moieties in click reaction enhances the specificity and sensitivity to detect the labeled DNA in

comparison with antibody-based detection methods. Wang et al. 2013 were first to label HSV-1 replication compartments with EdU, 5-Ethynyl-2'-deoxycytidine (EdC), or 5-Ethynyl-2'-deoxyadenosine (EdA). Although there was variation in the incorporation efficiency, all nucleoside analogs were successfully incorporated into vDNA replication compartments as demonstrated by colocalization between click and vDNA-binding protein ICP8 signals (Wang et al. 2013a). An independent study showed a similar colocalization pattern between EdU-labeled vDNA replication centers and vDNA-binding protein ICP4 signals (Dembowski and DeLuca 2015). This study also attempted to grow and purify EdU-labeled virus stocks in Vero cells. EdU ($\leq$ 2.5 µM) was poorly incorporated into WT virus, but UL2/UL50 mutant was successfully labeled. In our lab, protocols for EdU-labeling of HSV-1 genomes and purification of high titer stocks of labeled WT virus (HSV-1[EdU]) and ICP0-nulll mutant (ΔICP0[EdU]) have been optimized. This was achieved by infecting RPE cells with either WT (MOI of 0.001 PFU/cell) or ΔICP0 HSV-1 (MOI of 0.5 PFU/cell) in combination with EdU pulse labeling (0.5 µM) into infected cultures at 24h intervals. When cells showed extensive cytopathic effect, the labeled viral stocks (HSV-1[EdU] and ΔICP0[EdU]) were collected, purified, and titrated (section 3.3.2.). The cell type, EdU concentration, and the MOIs used were crucial for this protocol. It is still unclear why RPE cells were most permissive to viral propagation in the presence of EdU, an observation that requires further investigation (Alandijany et al. 2018).

In this chapter, click chemistry-mediated detection of HSV-1[EdU] and ΔICP0[EdU] DNA in combination with indirect IF staining protocol were used to examine the recruitment of PML-NB associated restriction factors and PRR IFI16 to infecting viral genomes during the initial stages of nuclear infection (within 30-90 minutes post-addition of virus; 30-90 mpi). Importantly, these experiments were conducted under low MOI conditions (MOI 0.1-3 PFU/cell) providing temporal resolution for this study. Our microscopy observations demonstrate that the recruitment of PML-NB constituent proteins occurs rapidly upon genome delivery into the nucleus. These recruitment events correlated with induction of viral genome silencing. Sensing of vDNA by IFI16 and subsequent induction of ISG expression only occur when infecting genomes escape from PML-NB mediated

silencing and initiate a productive infection. These findings, for the first time, put a clear temporal context in the sequential induction of intrinsic and innate immune responses during HSV-1 infection. However, HSV-1 counteracts these host antiviral defenses by expressing ICP0 which targets PML and IFI16 for proteasome-dependent degradation.

4.2. Results

4.2.1. Direct visualization of infecting EdU-labeled HSV-1 genomes and quantitation of their nuclear entry

EdU-labeled viruses in combination with click chemistry enabled the detection of input viral genomes at the early stages of infection prior to the expression of viral proteins. HFt cells were seeded onto coverslips and infected with HSV-1^{EdU} or ΔICP0^{EdU} at an MOI of 3 PFU/cell. Coverslips were fixed at different time points after addition of the virus (30, 60 and 120 mpi), and click chemistry was utilized to detect the viral genomes. To examine the specificity of the click signals detected, HFt cells were mock or infected with unlabeled HSV-1 as negative controls.

The detection of click signals was specific for EdU vDNA labeling as they were not detected in mock or unlabeled HSV-1 infected samples (figure 11A). Viral genome foci could be detected in the nuclei of HSV-1^{EdU} and ΔICP0^{EdU}-infected cells within 30 mpi with a gradual increase over time in the number of nuclei containing vDNA. Viral genome foci could be detected in more than 60% of the infected cells by 120 mpi. The number of nuclei containing vDNA during ΔICP0^{EdU} infection was slightly lower in comparison with HSV-1^{EdU} infection (figure 1B). The reason for this is not clear, but it might be linked to variations in the labeling efficiency of vDNA in RPE cells that are restrictive for ΔICP0 HSV-1 replication (Alandijany et al. 2018). Of note, encapsidated viral genomes in the cytoplasm could not be detected.

(A)
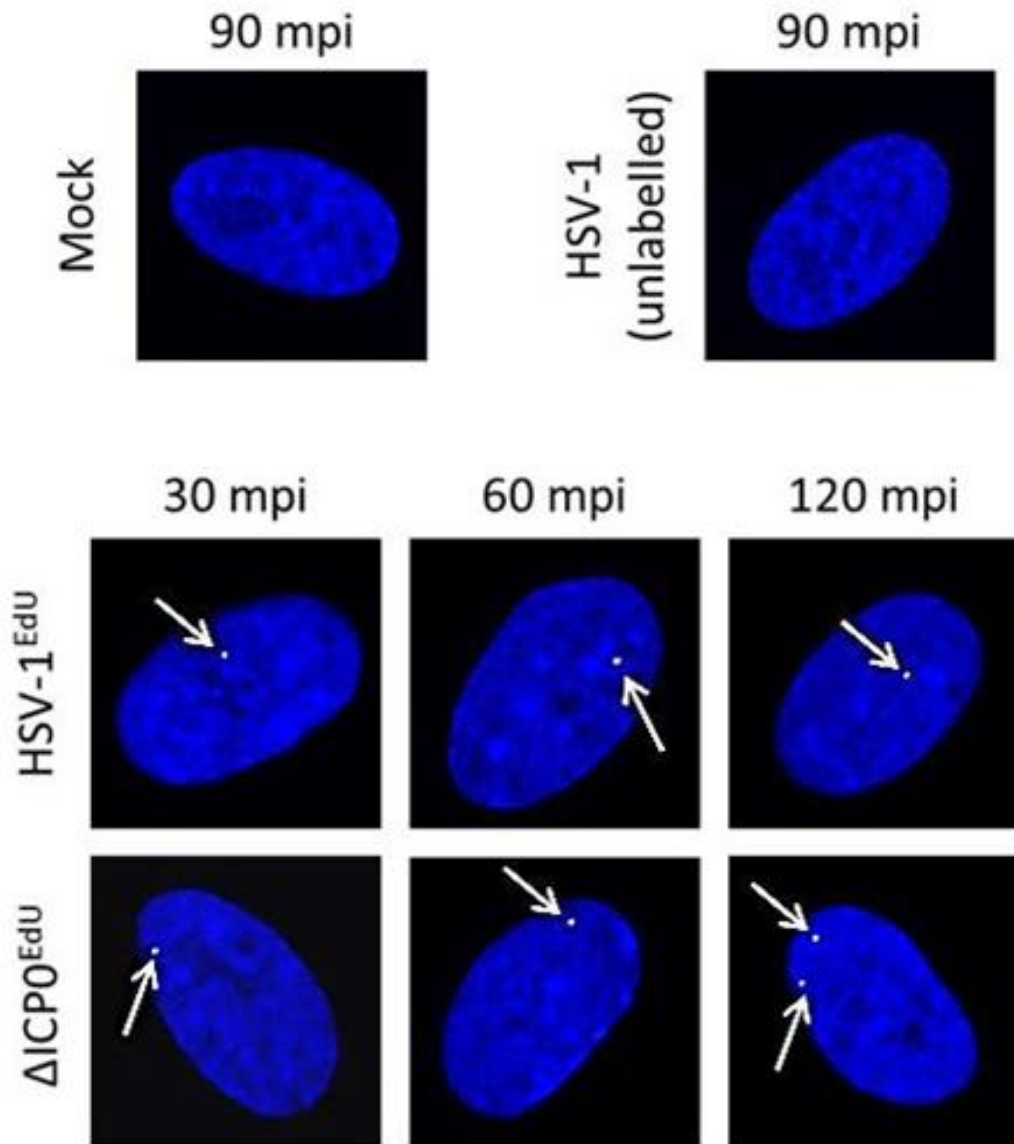
(B) Next page

(B)
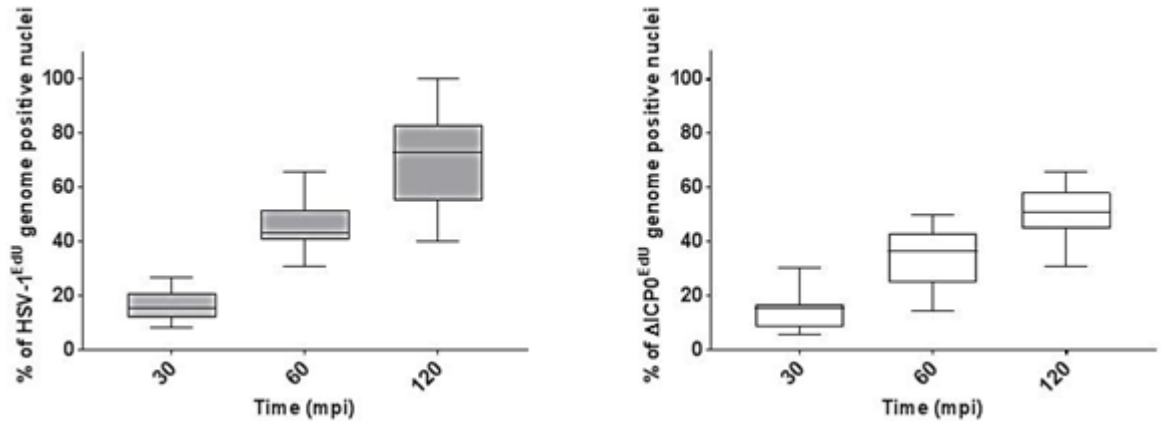
Figure 11. Sensitive visualization of infecting viral genomes using EdU-labeling of vDNA in combination with click chemistry.

HFt cells were mock, or infected with either unlabeled WT HSV-1, EdU-labeled WT virus (HSV-1^{EdU}) or EdU-labeled ICP0-null mutant (ΔICP0^{EdU}) at an MOI of 3 PFU/cell. Cell monolayers were fixed and permeabilized at the indicated minutes after addition of the virus (mpi). vDNA (white; highlighted by white arrows) was detected by click chemistry, and nuclei (blue) were visualized by DAPI. **(A)** Representative confocal microscopy images showing nuclei containing viral genomes over a time course of infection. Click signals were specific for infection with HSV-1^{EdU} and ΔICP0^{EdU}, as they were not observed in mock or unlabeled HSV-1 infected samples. **(B)** Quantitation of nuclei containing viral genomes over a time course of infection. Boxes represent 25th to 75th percentile range; black lines represent medians; whiskers represent Min to Max range of samples. n $\geq$ 300 genomes. Results derived from 3 independent experiments.

4.2.1. PML-NB associated restriction factors are rapidly recruited to vDNA immdetialy upon nuclear entry

One of the main advantages of click chemistry detection of EdU-labeled vDNA is its compatibility with indirect IF staining protocols. It allowed investigation of the recruitment of host restriction factors and PRRs to vDNA over a very short time-course of infection (30-90 mpi) under low MOI conditions (MOI of ≤ 3 PFU/cell). The use of Zen software allowed measurement of the weighted (w.) colocalization coefficient between these host immune regulators and vDNA. The results are presented on a scale of 0 (no localization) to 1 (perfect localization). The use of this software offered quantitative analyses for our microscopy observations. The focus of this work was to assess and characterize the recruitment of PML-NB constituent proteins and IFI16 to vDNA because of their well-reported roles in conferring intrinsic and innate antiviral responses, respectively (Everett et al. 2006, Everett et al. 2008, Veeranki and Choubey 2012, Orzalli et al. 2012, Diner et al. 2016).

HFt cells were mock or infected with HSV-1[EdU] or ΔICP0[EdU] at an MOI of 3 PFU/cell. Coverslips were fixed and processed at 90 mpi. Click and IF labeling were utilized to detect vDNA and host immune factors (PML and Daxx), respectively. In mock-infected cells, click signal was not detected. These cells exhibited a high degree of colocalization efficiency (> 0.7) between PML and Daxx (Figure 12A). In HSV-1[EdU] and ΔICP0[EdU]-infected cells, both PML and Daxx showed a high degree of colocalization to the viral genome foci (Figure 12B, and 12C). 3D Z-series image analysis revealed that viral genome was entrapped within PML-NBs (Figure 12D). Quantitative analysis of these microscopy observations demonstrated that PML-NB associated restriction factors were efficiently recruited to the viral genome foci rapidly upon genome delivery to the nucleus and independently of ICP0 (Figure 12E). Moreover, the nuclear distribution of PML-NBs and the high colocalization efficiency between PML and Daxx was not affected at these time points post-infection; demonstrating that PML-NBs that contained vDNA were relatively equivalent in compositions and

post-translational modification to PML-NBs which did not contain vDNA (Figure 12E).
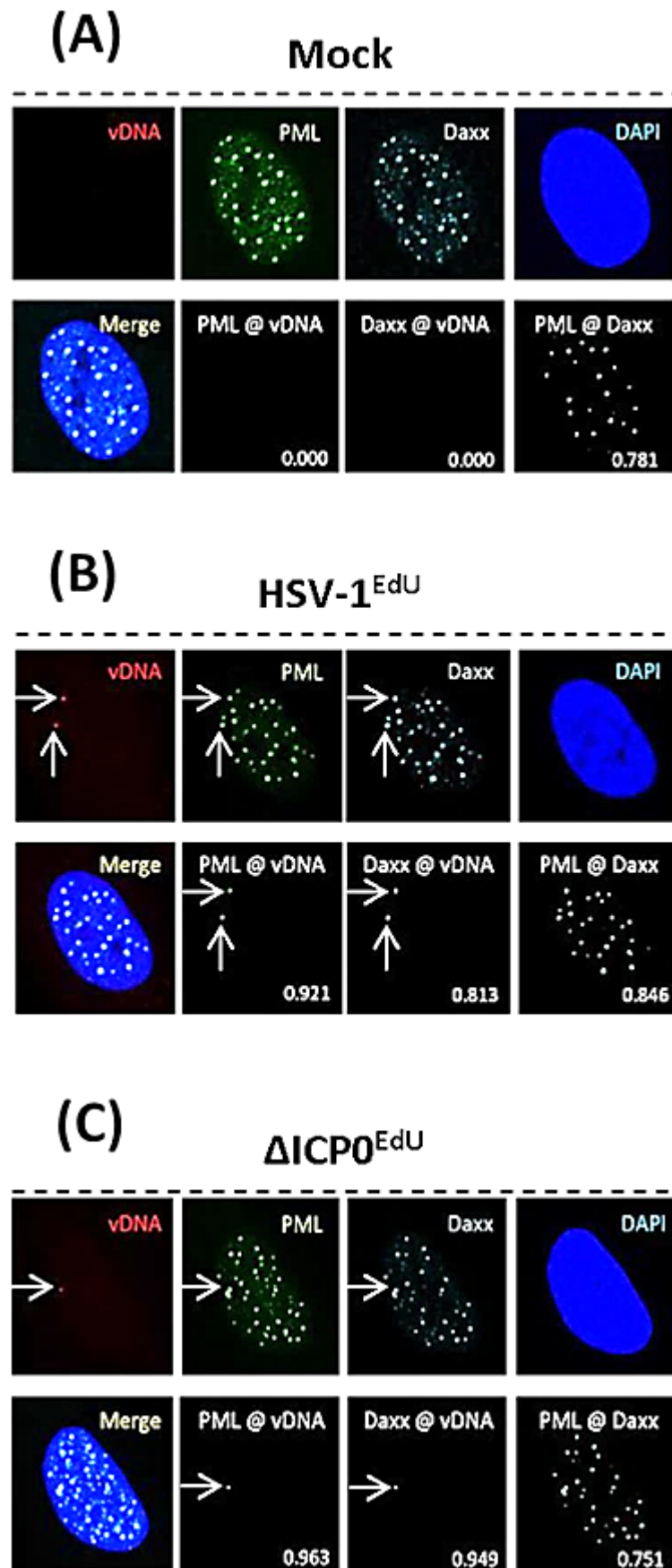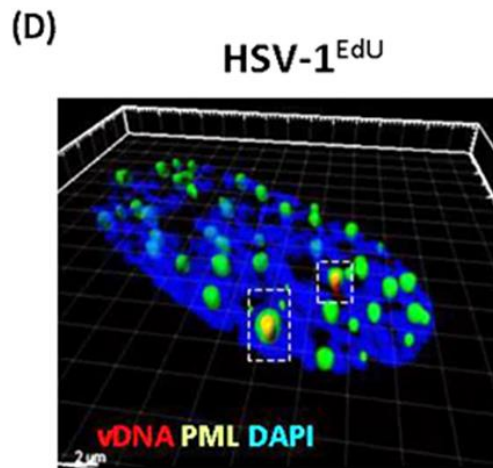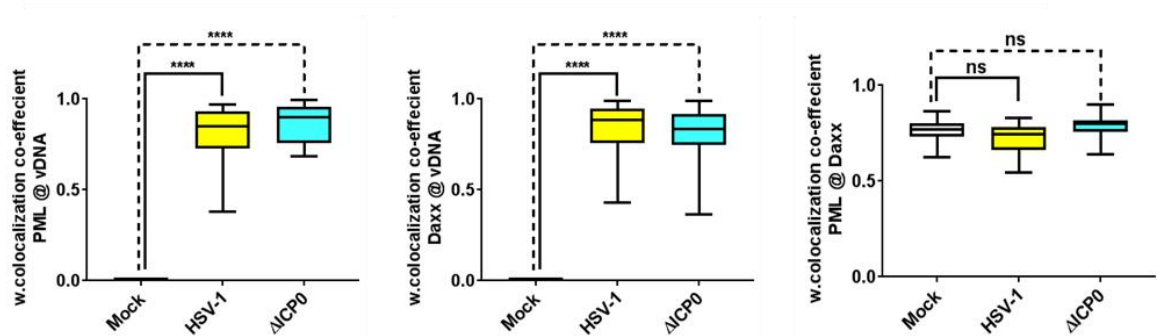
Figure 12. PML and Daxx are efficiently recruited to infecting viral genomes.

HFt cells were mock or infected with HSV-1^{EdU} or ΔICP0^{EdU} at an MOI of 3 PFU/cell. Monolayers fixed and permeabilized at 90 mpi. Viral genomes and host factors were labeled by click chemistry and indirect IF staining protocols, respectively. (A-C) Representative confocal microscopy images showing the nuclear localization of PML (green) and Daxx (cyan) to viral genomes (red; highlighted by white arrows). Cut mask highlights regions of colocalization between PML, Daxx, and vDNA (as indicated). Weighted (w.) colocalization coefficients are shown. (D) 3D image generated by imaris software. Insets show regions of interest (dashed boxes) highlighting infecting HSV-1^{EdU} genomes entrapped within PML-NBs at 90 mpi. (E) Quantitation of host factor colocalization with each other and with infecting viral genomes. Boxes: 25th to 75th percentile range of samples; black line: median weighted colocalization coefficient; whiskers: Min and Max range. n $\geq$ 25 viral genomes from two independent experiments. *** P = < 0.0001, and ns= non-significant; Mann-Whitney U-test.

4.2.2. The presence of PML is required for the stable recruitment of Daxx to vDNA

PML is the major scaffolding protein of PML-NBs (Ishov et al. 1999). Previous plaque-edge recruitment studies have demonstrated that Daxx recruitment to incoming ΔICP0 genomes in newly infected cells occurs in a PML-independent manner (Everett et al. 2006). Herein the importance of PML for the early recruitment of Daxx (within first 90 mpi) to vDNA under low MOI condition was assessed.

PML was depleted in HFt cells using lentivirus vectors expressing PML-targeting short hairpin RNA (shPML) (Everett et al. 2006). To exclude any non-specific effect of lentivirus transduction, parallel HFt cells were transduced with lentivirus vectors expressing non-targeting control short-hairpin RNA (shCtrl). The level of PML depletion was evaluated by IF confocal microscopy, WB, and qPCR. The mRNA and protein expression levels of Daxx and IFI16 were also assessed to evaluate the effect of PML depletion on their expression and ensure the specificity of shRNA. PML was successfully depleted in shPML-transduced cells without affecting Daxx or IFI16 expression (Figure 13). Consistent with previous reports, PML depletion did not affect the nuclear distribution of IFI16 (Figure 14A) (Everett 2015). However, localization of Daxx to PML-NBs was abolished in PML-depleted cells. Daxx staining in the absence of PML showed a diffuse nuclear signal concentrated into distinct speckles (Figure 14B) (Everett et al. 2006, Ishov et al. 1999). Next, the recruitment efficiency of Daxx to HSV-1^{EdU} vDNA was assessed. PML and Daxx were efficiently recruited to vDNA in shCtrl-transduced cells, which recapitulated the data obtained from parental HFt cells. In PML-depleted cells, however, there was a high degree of variation in the recruitment efficiency of Daxx to vDNA (Figure 15A). Quantitative analysis indicated that the colocalization coefficient of Daxx recruitment to vDNA was significantly reduced in the absence of PML (Figure 15B). To exclude any effect ICP0 may have on Daxx localization, a similar experiment was conducted on ΔICP0^{EdU}-infected cells and similar results were obtained (C. Boutell; (Alandijany

et al. 2018)). These data demonstrate that stable Daxx recruitment to vDNA under low MOI conditions occurs in a PML-dependent and ICP0-independent manner.
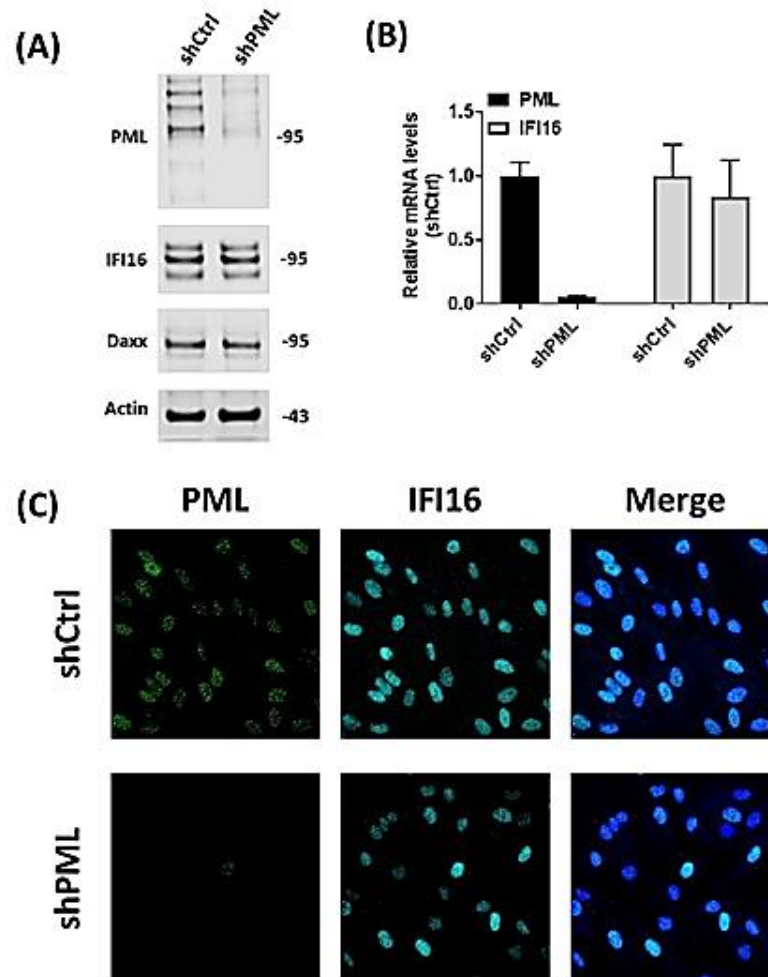
Figure 13. Successful knock-down of PML.

HFT cells were transduced using lentivirus vectors expressing non-targeting control short-hairpin RNA (shCtrl) or PML-targeting short hairpin RNA (shPML). (A) Western blots show the levels of PML, IFI16, Daxx, and actin in whole cell lysates. Membranes were probed for PML to determine the level of knock-down, IFI16 and Daxx to investigate the influence of PML depletion on their expression and to assess shRNA off-target effects, or actin (loading control). (B) Bar graphs show the mRNA levels of PML and IFI16 in shCtrl and shPML cells. The levels of mRNA were determined using the TaqMan system of quantitative RT-PCR. Values were normalized to GAPDH mRNA levels, internal control, using the threshold cycle ($\Delta\Delta CT$) method, and expressed relative to the normalized level of mRNA in shCtrl sample. Results represent relative quantitation (RQ) of three RTs. (C) Confocal images demonstrate the level of PML depletion. PML and IFI16 were labeled by indirect IF staining protocol. Nuclei were visualized by DAPI.
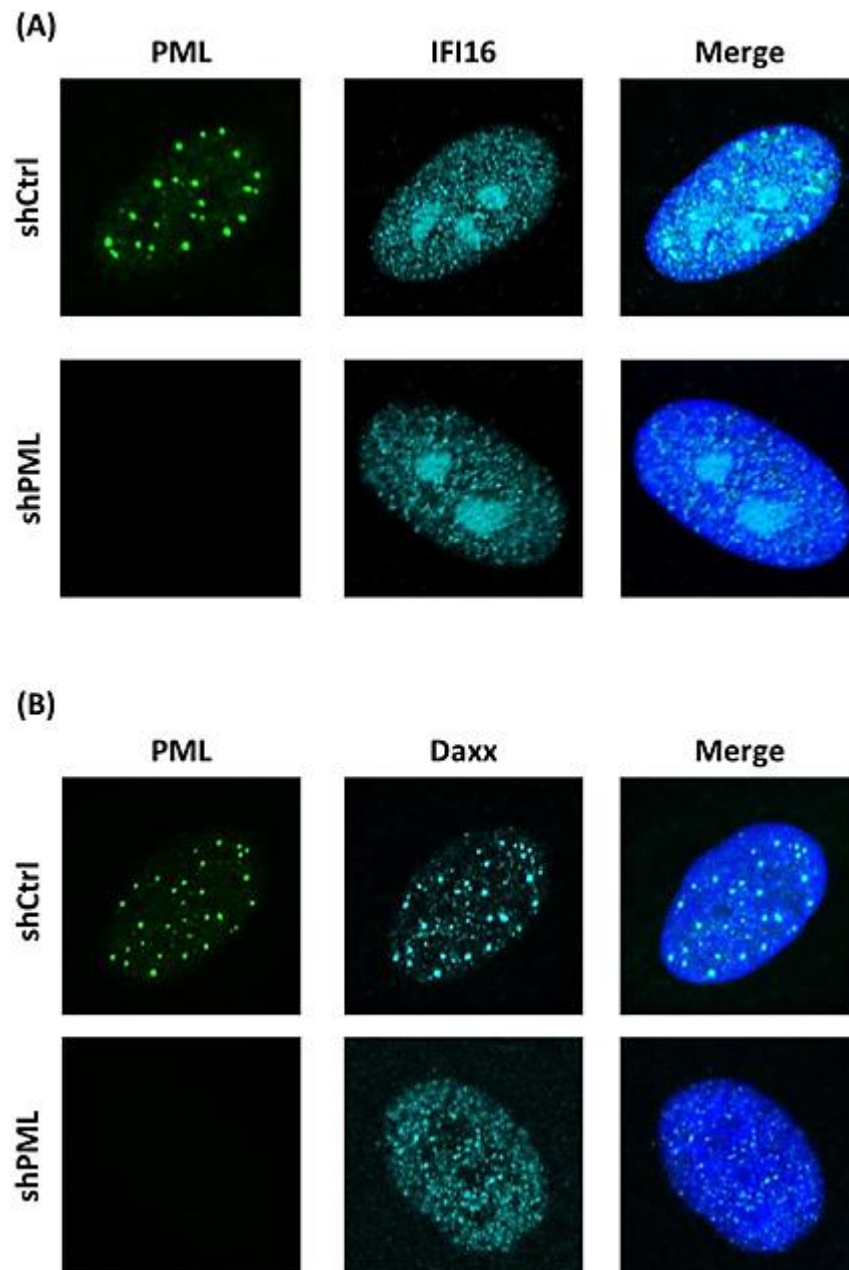
Figure 14. PML depletion influences the nuclear distribution of Daxx, but not IFI16.

HFT Cells were transduced using lentivirus vectors expressing non-targeting control short-hairpin RNA (shCtrl) or PML-targeting short hairpin RNA (shPML). The effect of PML depletion on the nuclear distribution of IFI16 and Daxx was assessed by confocal microscopy. PML, IFI16, and Daxx were labeled by indirect IF staining protocol. Nuclei were visualized by DAPI. (A and B) Representative images show that PML depletion did not affect the nuclear distribution of IFI16, but abolished the localization of Daxx to PML-NBs. Daxx exhibited nuclear diffuse signal in shPML-transduced cells.
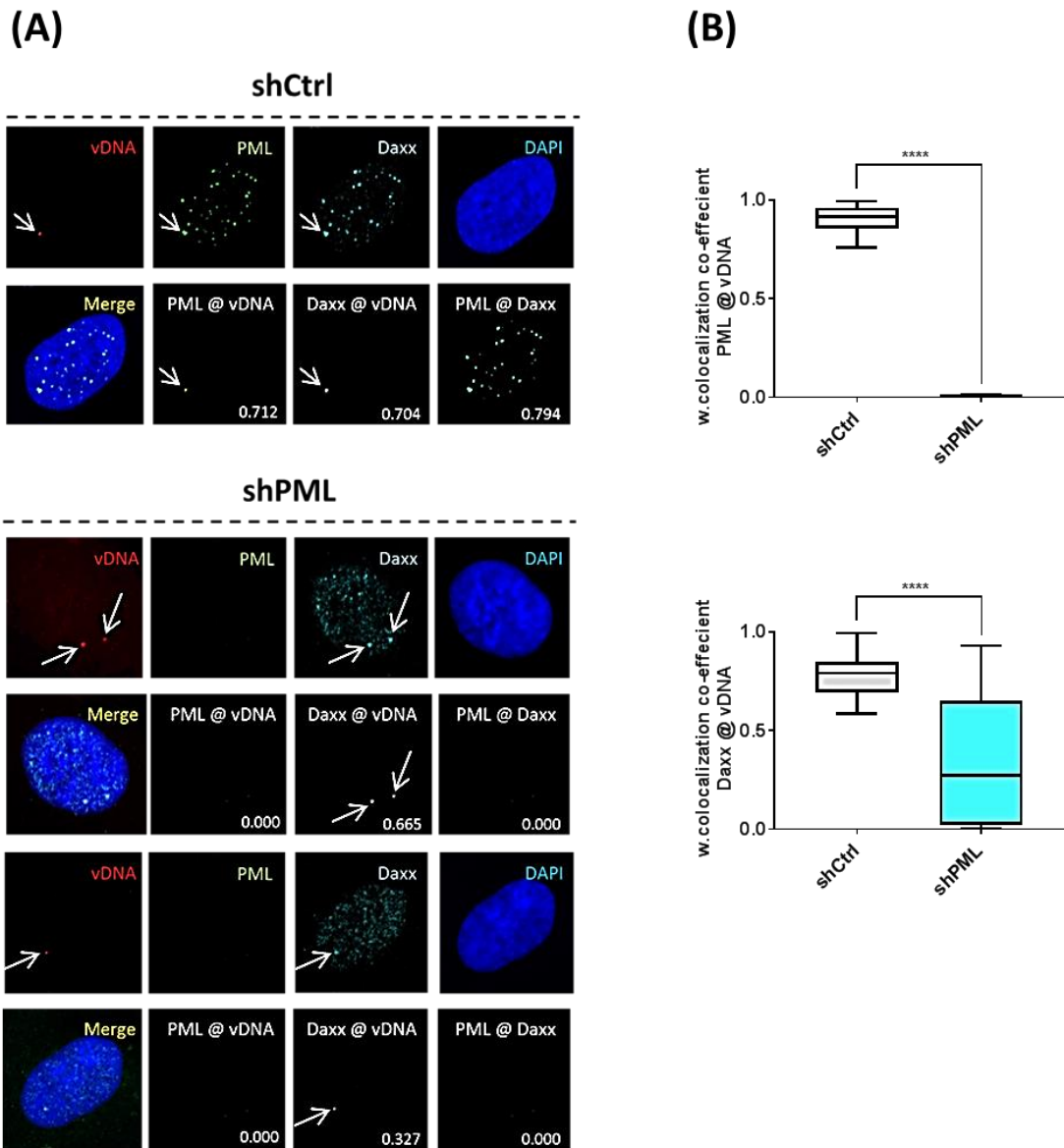
Figure 15. Stable Daxx recruitment to infecting viral genomes occurs in a PML-dependent manner.

shCtrl and shPML cells were mock or infected with HSV-1^{EdU} at an MOI 3 PFU/cell. Monolayers were fixed and permeabilized at 90 mpi. Viral genomes were labeled by click chemistry. Host factors were labeled by indirect IF staining protocol. Nuclei were visualized by DAPI. (A) Confocal microscopy images showing the nuclear localization of PML (green) and Daxx (cyan) to vDNA (red, highlighted by white arrows). Cut mask highlights regions of colocalization between host factors and vDNA (as indicated). Weighted (w.) colocalization coefficients are shown. (B) Quantitation of host factor recruitment to infecting viral genomes. Boxes: 25th to 75th percentile range; black line: median weighted colocalization coefficient; whiskers: Min and Max range of samples. n ≥ 25 viral genomes from two independent experiments. *** P = < 0.0001; Mann-Whitney U-test.

4.2.3. Recruitment of PML to vDNA induces viral genome silencing; a process that is counteracted by ICP0

It is well reported that PML confers intrinsic antiviral immunity against HSV-1 infection. However, HSV-1 expresses ICP0 to counteract this process by targeting PML for proteasome-dependent degradation (Everett et al. 2006, Everett et al. 2008, Chelbi-Alix and de The 1999, Maul and Everett 1994). ICP0 was observed to initially localize to PML-NBs prior to PML degradation (figure 16A and 16B). This process should release vDNA from PML-NBs to permit the onset of viral gene expression and replication. In order to demonstrate the importance of ICP0 to de-repress viral genomes, the plaque-forming efficiency (PFE) of both WT virus and ΔICP0 was determined in HFt cells. Cells were seeded and infected with the same input MOI, and immuno-staining plaque assay was conducted at 24 hrs post-infection (as described in 3.5.2. Immuno-staining plaque assay). Of note, virus input doses were calculated based on viral titers determined on U2OS cells, which complements the growth defect of ΔICP0 HSV-1 (Yao and Schaffer 1995, Everett et al. 2004a). Clearly, the PFE of WT HSV-1 was greater than that of ΔICP0 HSV-1 in HFt cells (figure 17) (Everett et al. 2004a, Sacks and Schaffer 1987). PML depletion significantly enhanced the PFE of ΔICP0 mutant, but not that of WT virus (Everett et al. 2006) (figure 18). The relief of restriction of ΔICP0 HSV-1 in PML-depleted cells was not sufficient to complement the plaque formation of ΔICP0 to WT HSV-1 level; indicative of the presence of other cellular restriction factors (e.g., Sp100, Daxx, PIAS1, and PIAS4) that act independently of PML (Lukashchuk and Everett 2010, Everett et al. 2008, Brown et al. 2016). Collectively, PML-NB associated restriction factors are rapidly recruited to viral genome upon delivery to the nucleus. Entrapment of vDNA within PML-NBs induces viral genome silencing. Expression of HSV-1 protein ICP0 is necessary to release the viral genomes entrapped within PML-NBs and initiate viral replication.
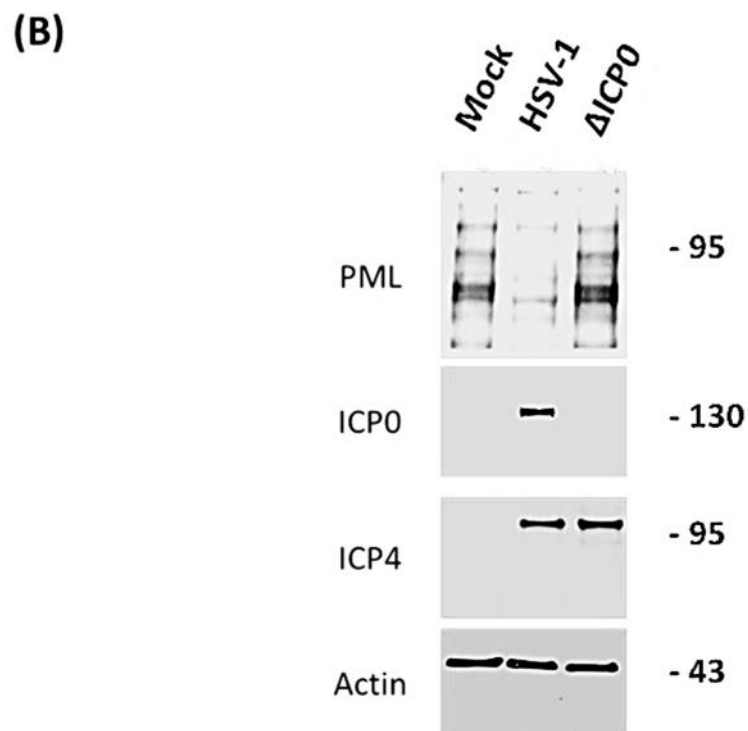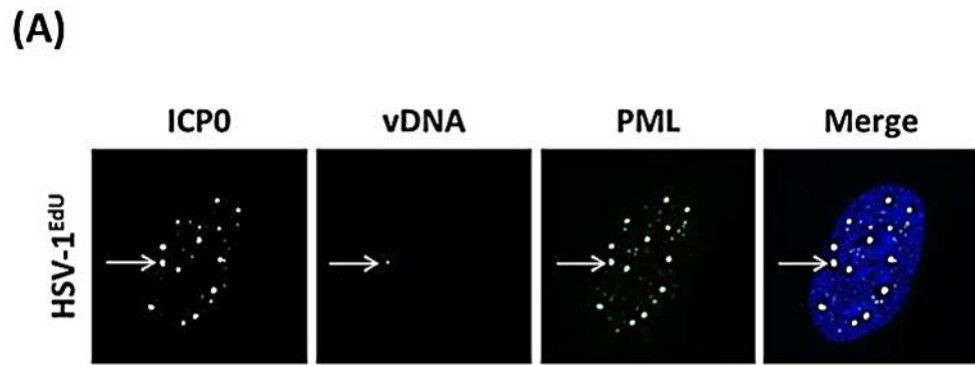
Figure 16. ICP0 colocalizes with PML-NBs and induces PML degradation.

**(A)** Confocal microscopy images showing the nuclear localization of ICP0 (white) to PML (green) in a vDNA (red)-positive cell. HFt cells were mock, or infected with HSV-1^{EdU} at an MOI of 3 PFU/cell. Monolayers fixed and permeabilized at 90 mpi. Viral genomes were labeled by click chemistry. ICP0 and PML were labeled by indirect IF staining protocol. Nuclei were visualized by DAPI. **(B)** Western blot demonstrates the induction of PML degradation during WT, but not ΔICP0, HSV-1 infection. HFt cells were mock, or infected with WT (MOI of 1 PFU/cell) or ΔICP0 HSV-1 (MOI of 10 PFU/cell). Whole cell lysates were harvested at 6 hrs post-infection. Membranes were probed for viral proteins (ICP0 and ICP4) to monitor the progress of infection, PML to monitor the effect of viral infections, and actin (loading control).
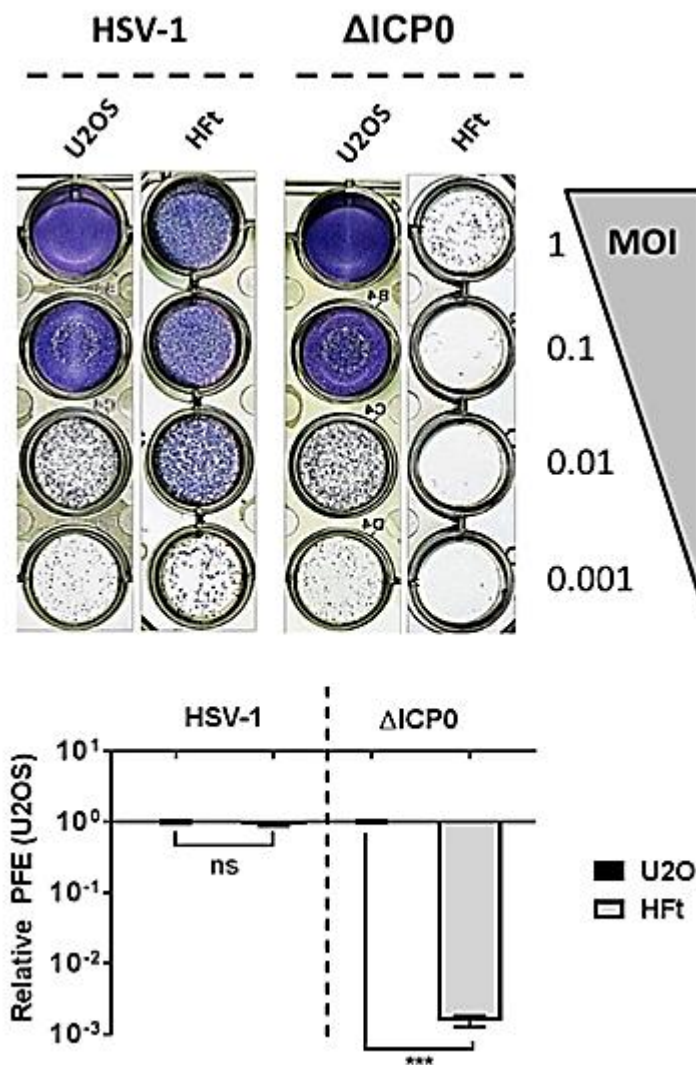
Figure 17. The presence of ICP0 is crucial for efficient plaque formation of HSV-1 infection in HFt cells.

HFt and U2OS cells were seeded overnight before infected with either WT or ΔICP0 HSV-1 at the indicated MOIs. Virus input doses were calculated based on viral titers determined on U2OS cells which complement ICP0 function. After an hour of viral adsorption, cells were overlaid with media containing 2% HS. At 24 hours post-infection, cells were fixed and permeabilized, and immunostaining plaque assay was conducted. The number of plaques (blue) was counted manually under a plate microscope. Bar graphs show the defect of PFE in HFt cells relative to U2OS cells. Results represent relative mean ± SD; n = 3. ns= non-significant, *** P = < 0.001; unpaired T-test.
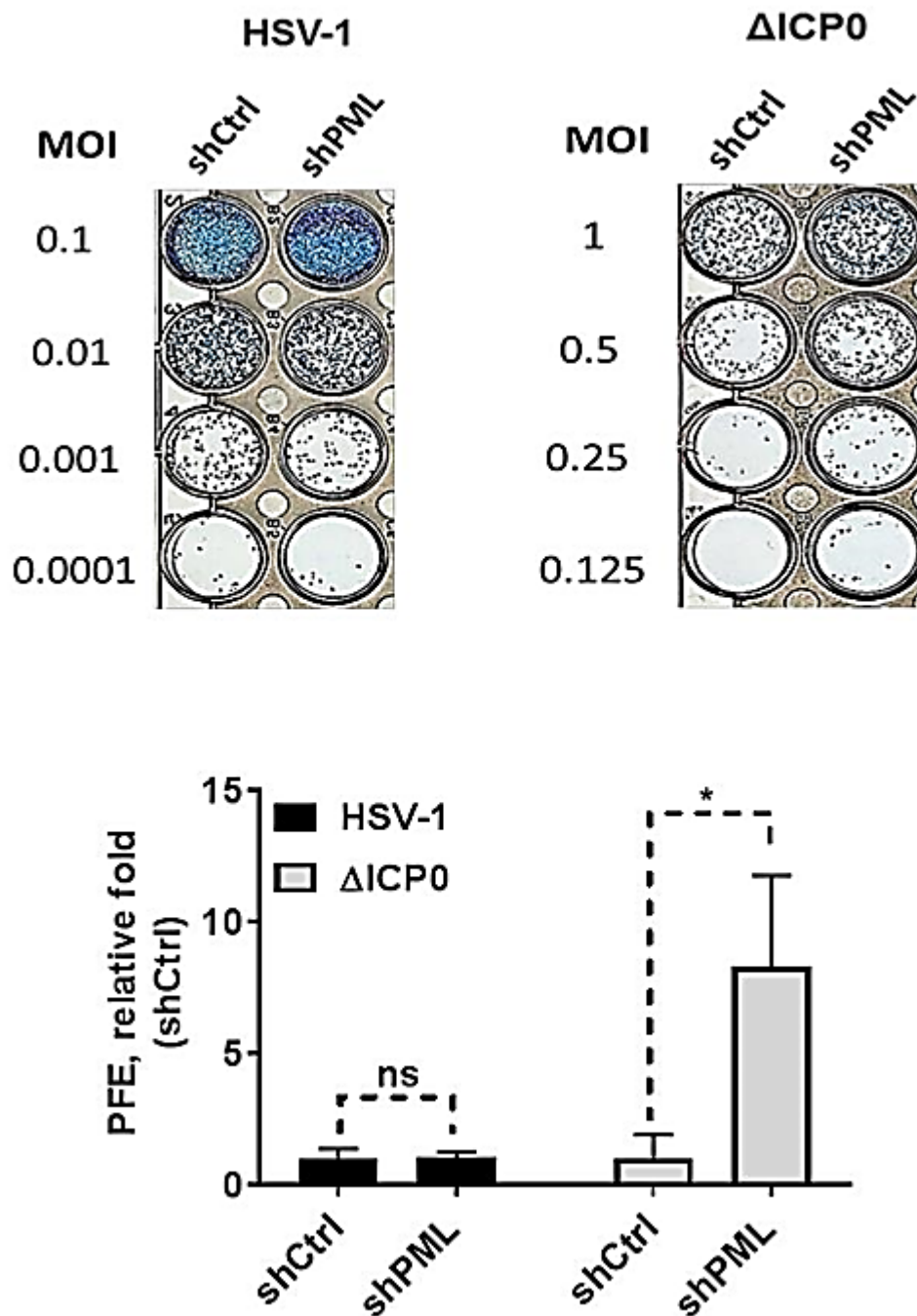
Figure 18. PML depletion enhances the PFE of ΔICP0, but not WT HSV-1.

shCtrl and shPML cells were seeded overnight and infected with either WT or ΔICP0 HSV-1 at the indicated MOIs. After an hour of viral adsorption, cells were overlaid with media containing 2% HS. At 24 hours post-infection, cells were fixed and permeabilized, and immunostaining plaque assay was conducted. The number of plaques was counted manually under a plate microscope. Bar graphs represent the fold increase in plaque number in infected shPML relative to infected shCtrl cells (as indicated). Results represent relative mean + SD; (n= 3). Similar results were obtained from independent batches of depleted cells. * P= < 0.05, and ns= non-significant; paired T-test.

4.2.4. PRR IFI16, unlike PML-NB proteins, does not stably localize to vDNA upon nuclear entry

PRR IFI16 is a vDNA sensor and key regulator of the host innate immune response. Upon recognition of vDNA, IFI16 signals through STING/TBK1/IRF3 pathway leading to the induction of ISG expression (Unterholzner et al. 2010, Orzalli et al. 2012, Diner et al. 2016). Live-cell microscopy-based studies have proposed a transient localization between IFI16 and viral genome foci under high MOI condition (MOI of ≥10 PFU/cell) upon nuclear infection (within 60 minutes of infection) (Everett 2015, Diner et al. 2016). Importantly, however, neither direct nor indirect detection of vDNA was applied in these studies. Instead, it was based on the observation that IFI16 puncta were detected at the nuclear rim of infected samples, but not in the uninfected controls. Herein, a direct comparison between the recruitment efficiency of PML-NB constituent proteins (PML, SP100, and Daxx) and PRR IFI16 to vDNA was conducted in HSV-1^{EdU}-infected cells. Unlike previous studies, our experiments utilized direct detection of vDNA to investigate the recruitment efficiency of host factors under low MOI conditions (MOI of ≤ 3 PFU/cell). Interestingly, the colocalization between IFI16 and vDNA was completely absent at 90 mpi. This was in direct contrast to PML-NB-associated restriction factors (PML, Daxx, and SP100), which showed almost perfect localization to vDNA (figure 19). Given that ICP0 has been shown to induce IFI6 degradation, the same experiment was conducted on ΔICP0^{EdU}-infected cells to exclude any potential effect ICP0 may have on IFI16 recruitment (Orzalli et al. 2012). The same conclusion was drawn that IFI16 does not stably localize to vDNA at 90 mpi. Moreover, PML depletion did not enhance the colocalization between IFI16 and vDNA, demonstrating that entrapment of vDNA within PML-NBs does not eliminate IFI16 recruitment to vDNA (Alandijany et al. 2018). However, we cannot rule out the potential of transient interaction between IFI16 and vDNA because our data were obtained at fixed time points post-infection. Collectively, we concluded that PML-NB restriction factors, but not IFI16, stably localize to HSV-1 genomes rapidly upon genome delivery to the nucleus.
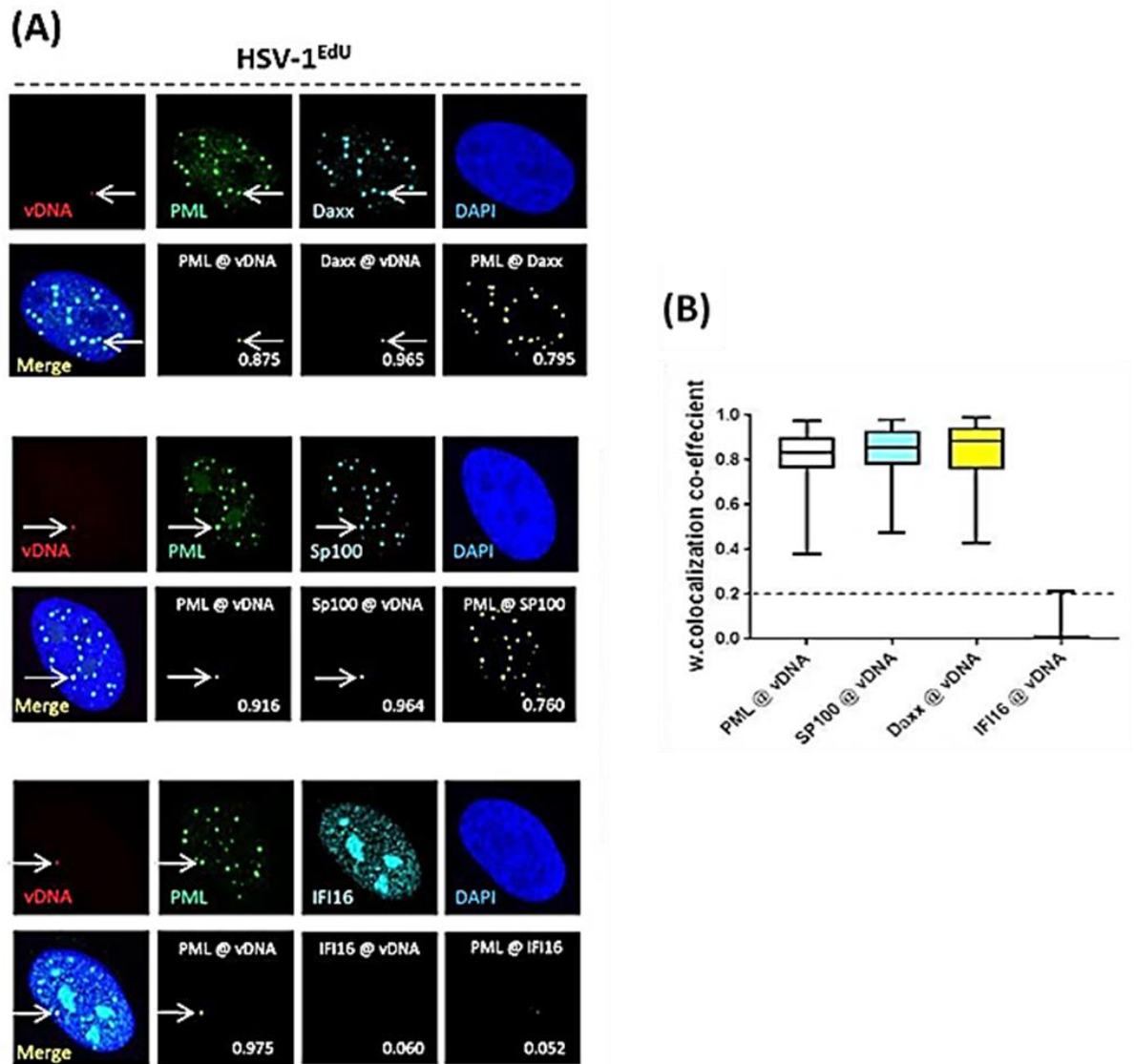
Figure 19. PML-NB constituent proteins, but not IFI16, are efficiently recruited to infecting viral genomes.

HFt cells were mock or infected with HSV-1^{EdU} at an MOI of 3 PFU/cell. Monolayers were fixed and permeabilized at 90 mpi. Viral genomes and host factors were labeled by click chemistry and IF staining protocols, respectively. Nuclei were visualized by DAPI. **(A)** Confocal microscopy images showing the nuclear localization of PML (green) and either Daxx, SP100, or IFI16 (cyan) to viral genomes (red; highlighted by white arrows). Cut mask highlights regions of colocalization between host factors and vDNA (as indicated. Weighted (w.) colocalization coefficients are shown. **(B)** Quantitation of host factor recruitment to infecting viral genomes. Boxes: 25th to 75th percentile range; black line: median weighted colocalization coefficient; whiskers: Min and Max range of samples. n ≥ 25 viral genomes from a minimum of two independent experiments.

4.2.5. The presence of IFI16 is not necessary for PML recruitment to vDNA

Previous plaque-edge recruitment studies have shown that IFI16, similar to PML-NB constituent proteins, is recruited to incoming viral genomes in newly infected cells (Cuchet-Lourenco et al. 2013, Orzalli et al. 2013). Depletion of IFI16 negatively influenced the frequency of PML and Daxx recruitment to vDNA, although this issue remains to be controversial (Cuchet-Lourenco et al. 2013, Orzalli et al. 2013). We did not observe any stable localization between IFI16 and EdU-labeled vDNA at 90 mpi under low MOI conditions (Figure 19). However, we cannot rule out the possibility of transient IFI16-vDNA interactions that may occur prior to PML-NB entrapment. We sought to assess whether the presence of IFI16 is crucial for PML-NB-mediated entrapment of vDNA. IFI16 was depleted in HFt cells using lentivirus vectors expressing IFI16-targeting shRNA (shIFI16). Parallel HFt cells were transduced with lentivirus vectors expressing non-targeting control short-hairpin RNA (shCtrl). The level of IFI16 depletion was evaluated by IF confocal microscopy, WB, and qPCR. The mRNA and protein expression levels of PML and Daxx were also assessed in order to evaluate the effect of IFI16 depletion on their expression and ensure the specificity of shIFI16. IFI16 was successfully depleted in shIFI16-transduced cells without affecting PML or Daxx expression (Figure 20). Depletion of IFI16 also did not affect the nuclear distribution and localization of PML to PML-NBs (Figure 21). PML was efficiently recruited to HSV-1^{EdU} genome foci in both shCtrl and shIFI16-transduced cells (Figure 22). A similar conclusion was drawn when the recruitment of Daxx to vDNA was examined (Alandijany et al. 2018). These data demonstrate that IFI16 is not necessary for entrapment of vDNA within PML-NBs.
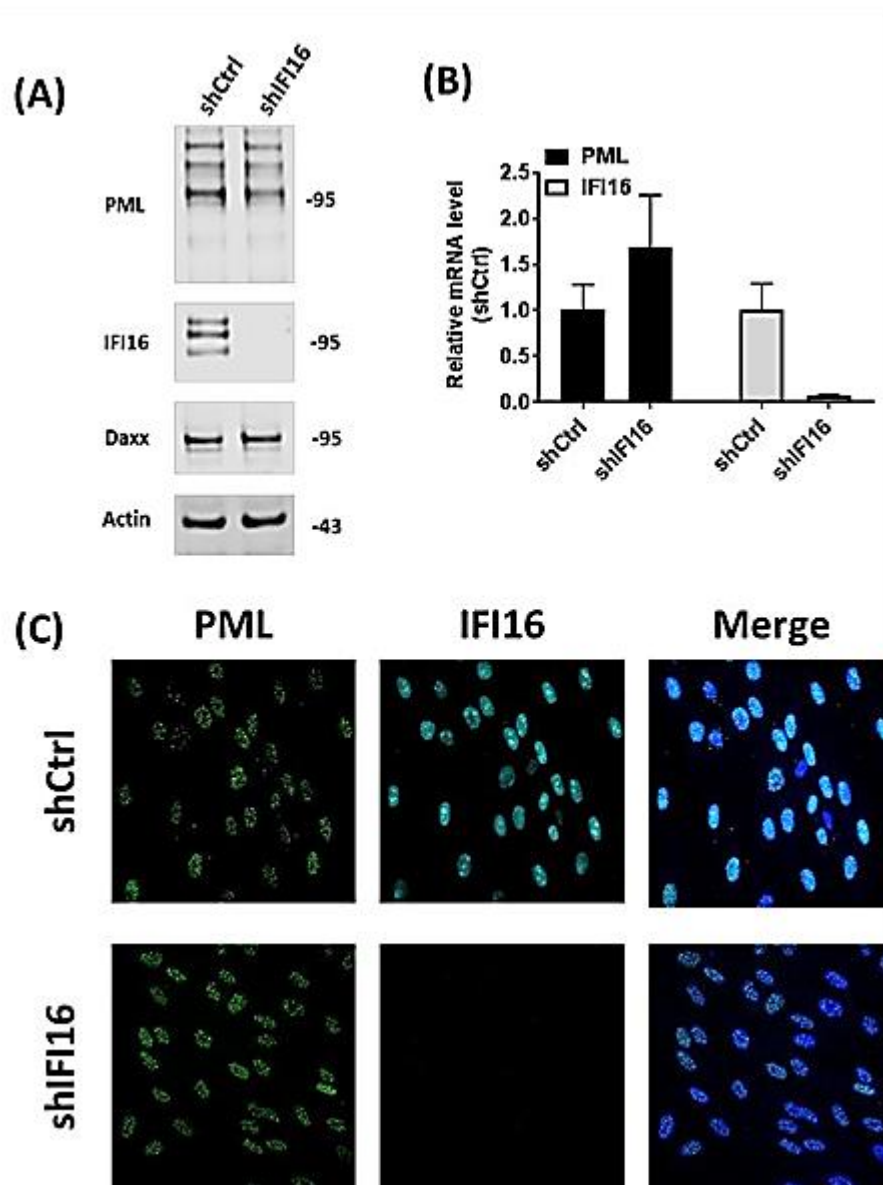
Figure 20. Successful knock-down of IFI16.

HFt cells were transduced using lentivirus vectors expressing non-targeting control short-hairpin RNA (shCtrl) or IFI16-targeting short-hairpin RNA (shIFI16). **(A)** Western blots show the levels of PML, IFI16, Daxx, and actin in whole cell lysates. Membranes were probed for IFI16 to determine the level of knock-down, PML and Daxx to evaluate the influence of IFI16 depletion on their expression and assess shRNA off-target effects, or actin (loading control). **(B)** Bar graphs show the mRNA levels of PML and IFI16 in shCtrl and shIFI16 cells. The levels of mRNA were determined using the TaqMan system of quantitative RT-PCR. Values were normalized to GAPDH mRNA levels, internal control, using the threshold cycle ($\Delta\Delta CT$) method, and expressed relative to the normalized level of mRNA in shCtrl sample. Results represent relative quantitation (RQ) of three RTs. **(C)** Confocal images show the level of IFI16 depletion. PML and IFI16 were visualized by indirect IF staining protocol. Nuclei were visualized by DAPI.
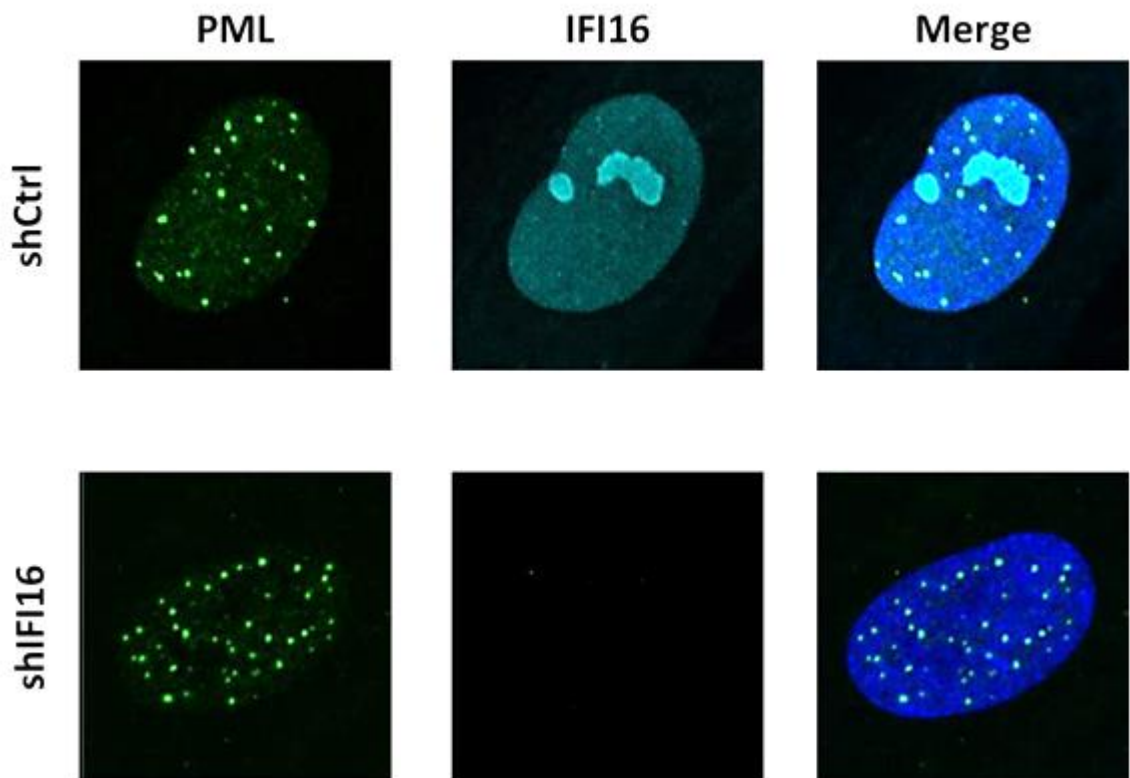
Figure 21.IFI16 depletion did not affect the nuclear distribution of PML.

HFT Cells were transduced using lentivirus vectors expressing non-targeting control short-hairpin RNA (shCtrl) or IFI16-targeting short-hairpin RNA (shIFI16). The effect of IFI16 depletion on PML was assessed by confocal microscopy. PML and IFI16 were visualized by IF staining protocol. Nuclei were visualized by DAPI. Representative confocal microscopy images show that IFI16 depletion did not affect the localization of PML to PML-NBs.
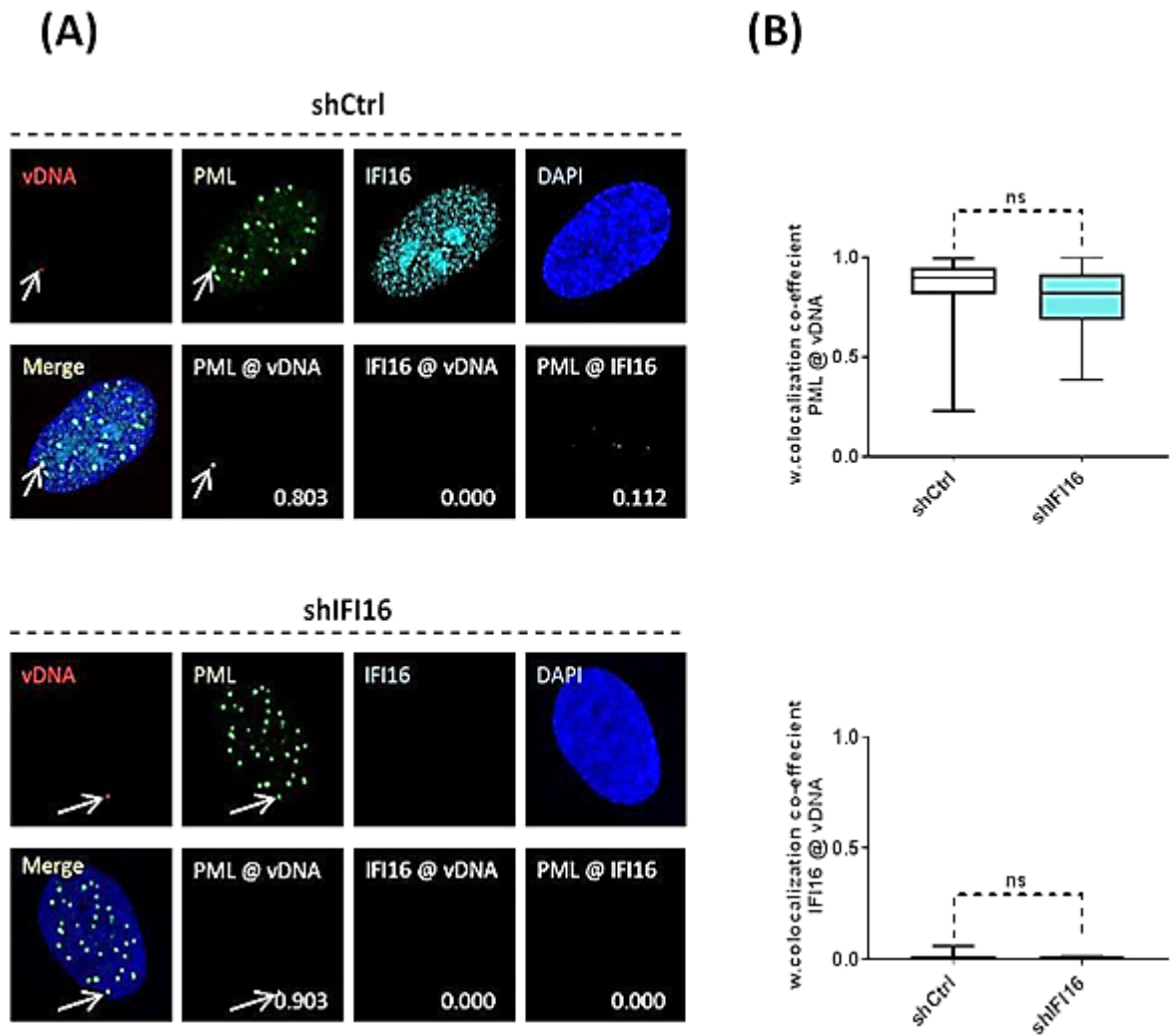
Figure 22. PML is efficiently recruited to infecting viral genomes independently of the presence of IFI16.

shCtrl and shIFI16 cells were mock or infected with HSV-1^{EdU} at an MOI of 3 PFU/cell. Monolayers were fixed and permeabilized at 90 mpi. Viral genomes were labeled by click chemistry. Host factors were labeled by indirect IF staining protocol. Nuclei were visualized by DAPI. **(A)** Confocal microscopy images showing the nuclear localization of PML (green) and IFI16 (cyan) to vDNA (red; highlighted by white arrows). Cut mask highlights regions of colocalization between host factors and vDNA (as indicated). Weighted (w.) colocalization coefficients are shown. **(B)** Quantitation of host factor recruitment to infecting viral genomes. Boxes: 25th to 75th percentile range; black line: median weighted (w.) colocalization coefficient; whiskers: Min and Max range of samples. n ≥ 25 viral genomes from a minimum of two independent experiments. ns= non-significant; Mann-Whitney U-test.

4.2.6. IFI16 is stably localized to vDNA expressing viral proteins

In previous plaque-edge recruitment studies which have suggested that IFI16 is recruited to incoming viral genomes at the nuclear periphery of newly infected cells, ICP4 was used as a proxy for genome localization (Diner et al. 2016, Everett 2015). Although it was previously shown that ICP4 dot-like complexes contain viral genomes, some viral genome foci detected by FISH were not associated with ICP4 signals (Everett and Murray 2005). Hence, the use of ICP4 signal to determine the viral genome localization by proxy is valid but suboptimal for reproducible genome detection (Everett and Murray 2005). These findings together with the absence of localization between IFI16 and vDNA at 90 mpi raised the hypothesis that IFI16 only localizes to the viral genomes that establish productive infection and express viral proteins. To test this hypothesis, a modified plaque-edge recruitment assay was conducted (Data obtained by C. Boutell). Cells were infected with ΔICP0 expressing eYFP-tagged ICP4 at an MOI of 2. At 24 h post-infection, 1 µM of EdU was added for 6 hours to label vDNA. This experimental condition allowed visualization of the following: (1) EdU-labeled vDNA replication compartments within the body of developing plaques; and (2) EdU-positive viral genomes in newly infected cells, with many of them detected prior to the expression of ICP4. The recruitment of PML and IFI16 to EdU-positive ΔICP0 genomes in newly infected cells was assessed. PML was efficiently recruited to vDNA irrespective of ICP4 expression, whereas IFI16 was only localized to vDNA in cells containing genomes actively expressing the viral protein (Figure 23) (Alandijany et al. 2018). These data put a clear temporal context in the recruitment of PML and IFI16 to infecting HSV-1 genomes that are dependent on nuclear entry of the viral genomes and the onset of lytic gene expression, respectively.
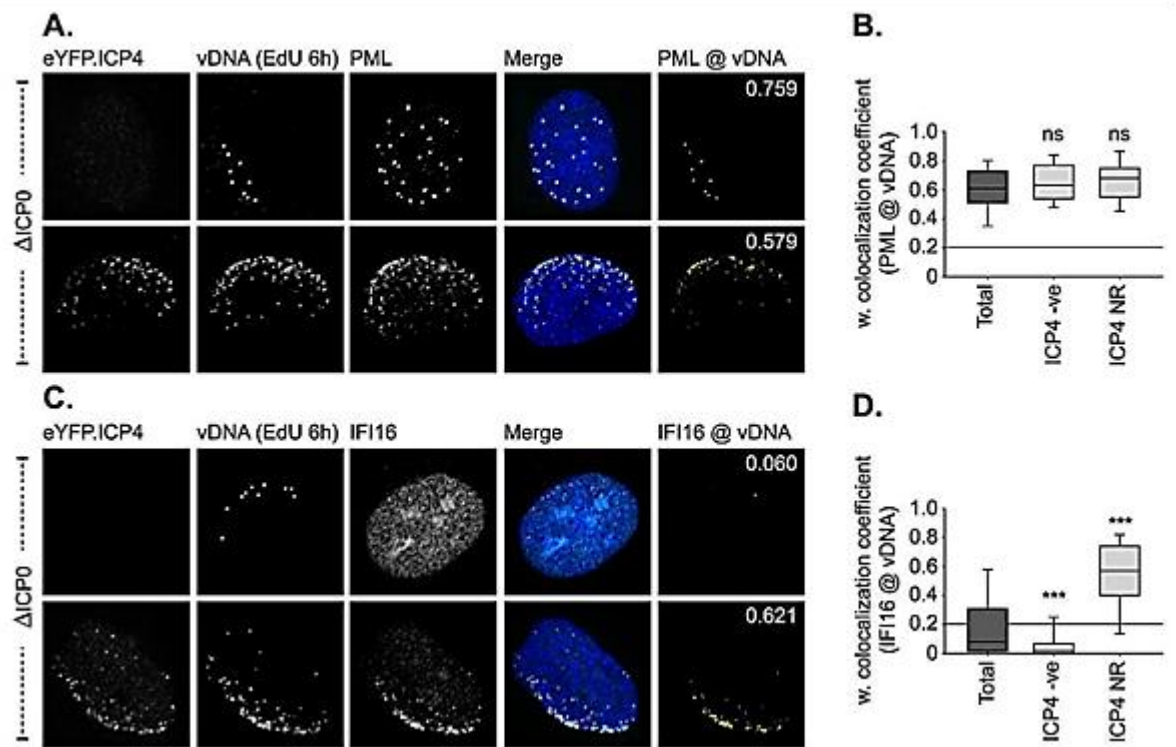
Figure 23. Initiation of productive infection is required for IFI16-mediated sensing of viral genomes.

Plaque-edge recruitment assays of HFt cells that were infected with ΔICP0 expressing eYFP-tagged ICP4. At 24 h post-infection, 1 µM of EdU was added for 6 hours to label the vDNA. The recruitment efficiency of eYFP.ICP4 (green) and PML or IFI16 (cyan; as indicated) to vDNA (red) in newly infected cells at the edge of developing plaque was assessed. Viral genomes were labeled by click chemistry. Host factors were labeled by indirect IF staining protocol. Nuclei were visualized by DAPI. (A, C) Confocal microscopy images showing the nuclear localization of host factors to vDNA. Cut mask highlights regions of colocalization between host factors and vDNA (as indicated). Weighted (w.) colocalization coefficients are shown. (B, D) Quantitation of host factor recruitment to vDNA that express or do not express eYFP.ICP4 (ICP4 nuclear rim (ICP4 NR) and ICP4 -ve, respectively). Boxes: 25th to 75th percentile range; black line: median; whiskers: 5th to 95th percentile range. n = 100 plaque-edge cells positive for DNA per sample population. Results were obtained from 4 independent experiments. *** $P < 0.001$, ns = not significant; Mann-Whitney U-test. (Alandijany et al. 2018).

4.2.7. Viral genome nuclear entry alone is not sufficient to induce host innate immunity

The lack of localization between vDNA sensor IFI16 and HSV-1 vDNA prior to the onset of viral gene expression raised the question of whether induction of innate immunity occurs directly following the nuclear entry of viral genomes. To address this question, the input MOI of ΔICP0 HSV-1 which either restricts or permits the initiation of plaque formation was determined, and the induction of ISG expression under these MOI conditions was investigated. HFt cells were infected with ΔICP0 HSV-1 across a range of MOI and assessed for plaque formation efficiency at 24 hrs post-infection. At low MOI condition (MOI of 0.1 PFU/cell; genome copy/cell ≈ 2.6), the plaque formation of ΔICP0 HSV-1 was fully blocked due to the intrinsic repression of viral genomes and the lack of viral countermeasure ICP0. However, increasing the input MOI level (MOI of 1 PFU/cell; genome copy/cell ≈ 26) overcame intrinsic repression and permitted the initiation of plaque formation (Figure 24).The induction of innate immunity following ICP0-null^{EdU} infection was assessed under these two MOI conditions. Cells were infected with ΔICP0^{EdU} either at an MOI of 1 or MOI of 0.1 for 24 h, and the stimulation of ISG product Mx1 expression was assessed by confocal microscopy. Mock-treated and IFNß-treated cells were included as a negative and positive control, respectively. Cells infected with ΔICP0^{EdU} at an MOI of 1.0, but not those infected at an MOI of 0.1, induced the expression of Mx1 (Figure 25A and 25B). In cells infected at MOI of 0.1, viral genomes were stably entrapped within PML-NBs even after 24 h post-infection without induction of MX1 expression (Figure 25A and 25B). These data demonstrate that under low MOI conditions, the nuclear entry of viral genome alone is not enough to induce innate immunity. Escape or saturation of intrinsic immunity is a prerequisite for innate immunity induction during HSV-1 infection. The number of viral genomes detected within the nuclei of cells infected at MOI of 0.1 PFU/cell correlated with the input multiplicity (1-2 genomes/cell; Figure 15C). However, the number of gnomes detected in cells infected at an MOI of 1 was lower (1-5 genomes/cell) than the expected ≈20 genomes/cell. This is due to the ≈60% labeling efficiency of our viral stocks as demonstrated by *in vitro* viral genome

release (Alandijany et al., 2018). It also indicates that $\Delta ICP0^{EdU}$ genome signal is lost under infection conditions that permit the initiation of vDNA replication.
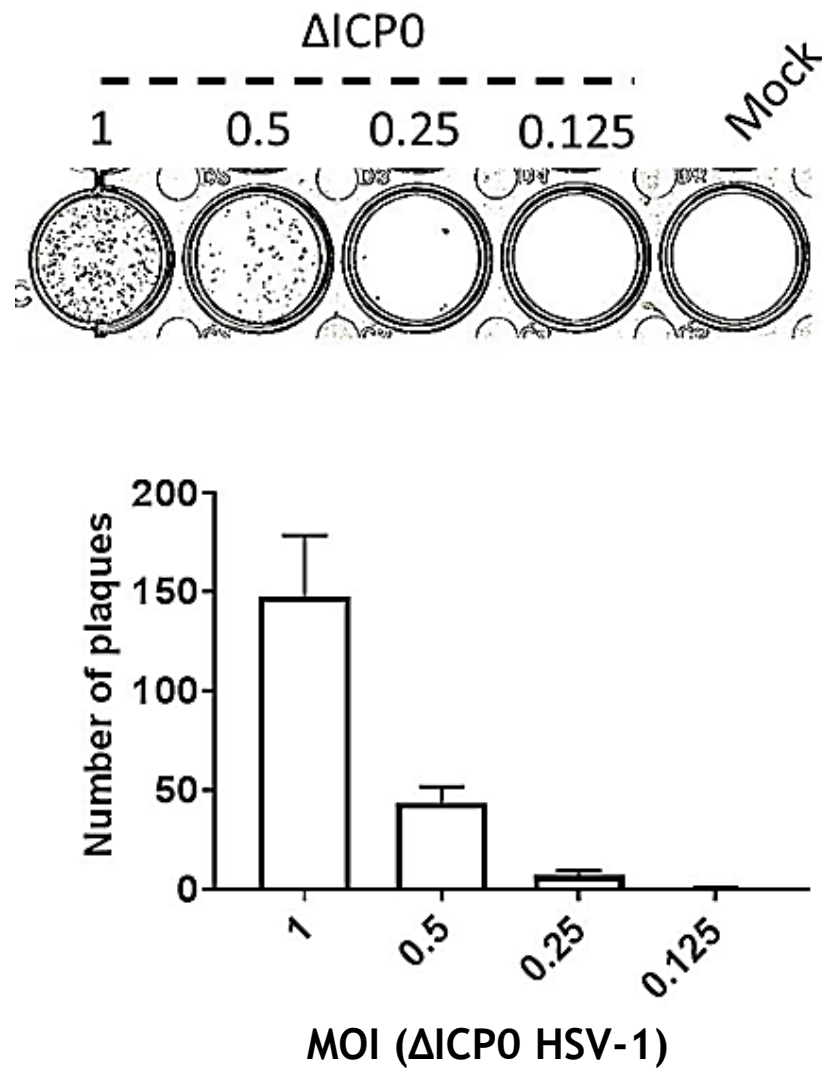
Figure 24. ΔICP0 HSV-1 overcomes intrinsic repression and initiates plaque formation at increased input multiplicities.

HFt cells were mock or infected with ΔICP0 HSV-1 at the indicated MOIs. Immuno-staining plaque assay was conducted at 24 hrs post-infection. The numbers of plaques were counted manually under a plate microscope. Results represent the means of plaque number + SD; (n=3).
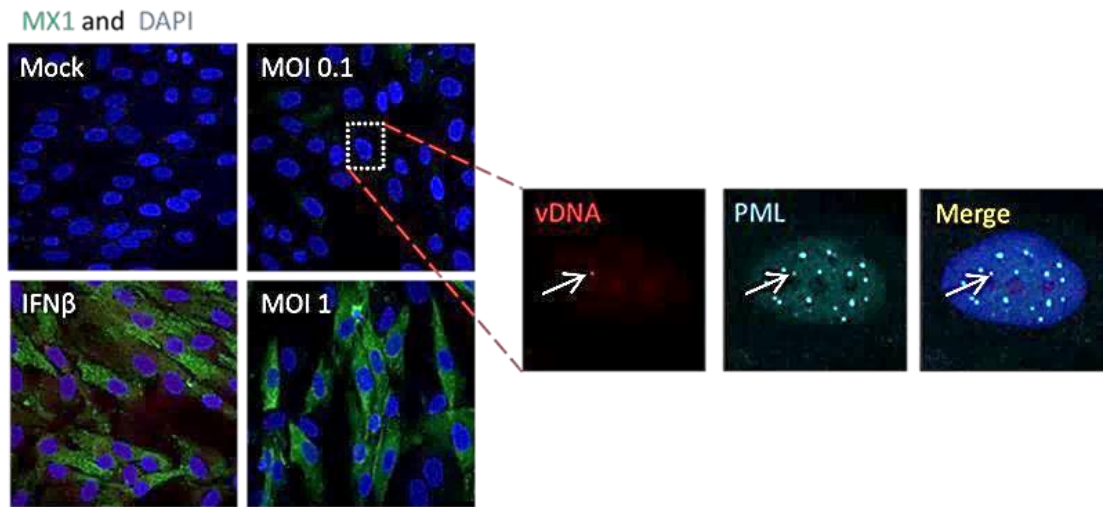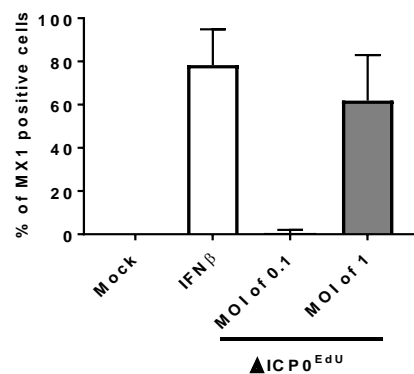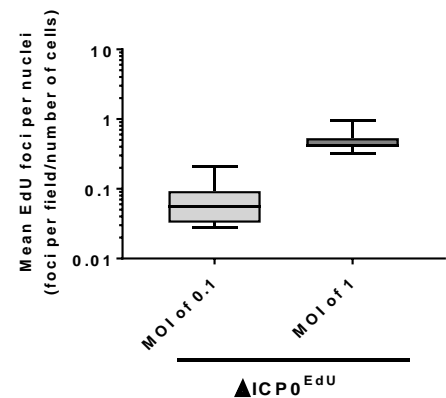
Figure 25. Viral genome entry into the nucleus alone is not sufficient to induce MX1 expression.

HFt cells were mock, treated with IFNß (100 IU/ml), or infected with ΔICP0^{EdU} at an MOI of 0.1 or 1 PFU/cell. The induction of MX1 expression was assessed by confocal microscopy at 24 hrs post-infection. MX1 (green) and PML (cyan) were labeled by indirect IF staining protocol. vDNA (red; highlighted by white arrows) was labeled by click chemistry. Nuclei (blue) were visualized by DAPI. **(A)** Representative images show MX1 expression. Insets show regions of interest (dashed boxes) highlighting the recruitment of PML to infecting ΔICP0^{EdU} genome under an MOI of 0.1. **(B)** Bar graph shows the percentage of the number of Mx1 positive cells relative to the total number of cells. n ≥ 250 cells derived from 3 independent experiments. **(C)** Quantitation of nuclear ΔICP0^{EdU} foci. Boxes: 25th to 75th percentile range; black line: median; whiskers: Min and Max range of samples.

4.3. Summary

Rapid recruitment of host immune regulators to vDNA upon nuclear entry is crucial for the efficient induction of host immunity and suppression of viral replication. Pre-existing restriction factors, as part of the intrinsic immune response, directly induce viral genome silencing (Yan and Chen 2012, Tavalai and Stamminger 2009). PRRs, as part of the innate immune response, activate IFN-signaling cascades leading to the expression of ISGs (Orzalli and Knipe 2014, Hannoun et al. 2016). It remains unclear whether recruitment of the intrinsic and innate immune factors to vDNA occurs simultaneously or sequentially because of the technical difficulties associated with viral genome detection under low MOI conditions. Utilizing click chemistry (Salic and Mitchison 2008, Chehrehasa et al. 2009), we provided a non-invasive assay to quantitatively assess the recruitment efficiency of host immune factors to EdU-labeled vDNA under low MOI conditions (MOI of ≤ 3 PFU/cell within 90 mpi). This protocol allowed direct visualization of vDNA (Figure 11) and enabled detailed investigation into the temporal recruitment of intrinsic and innate immune factors to infecting viral genomes.

PML-NB constituent proteins (PML, SP100, Daxx, ATRX, PIAS-1, and MORC3) are the most prominent examples of host cell restriction factors (Everett et al. 2008, Everett et al. 2006, Lukashchuk and Everett 2010, Brown et al. 2016, Sloan et al. 2016). It was initially reported that PML-NBs disappear during HSV-1 infection as a consequence of ICP0 expression (Maul and Everett 1994). ΔICP0 HSV-1 was very valuable to understand the relationship between PML-NBs and HSV-1 during lytic and latent infections (Stow and Stow 1986, Sacks and Schaffer 1987). Plaque-edge recruitment assays have shown that PML-NB proteins are recruited to sites associated with incoming viral genomes (Everett et al. 2004a). These recruitment phenotypes correlated with suppression of viral gene transcription. The presence of PML, the major scaffolding protein of PML-NBs, is not necessary for recruitment of other PML-NB proteins (e.g., SP100 and Daxx) to vDNA. Consistently, PML-NB proteins (SP100 and Daxx) independently and additively promote transcriptional repression of viral genes as demonstrated by

co-depletion and triple-depletion studies (Lukashchuk and Everett 2010, Everett et al. 2006, Everett et al. 2008, Brown et al. 2016, Glass and Everett 2013). The antiviral role of PML-NBs against HSV-1 extends to latent infection. Indeed, the viral genomes were shown to be stably entrapped within PML-NBs in latently-infected mouse neurons and quiescently-infected cell culture (Catez et al. 2012, Maroui et al. 2016, Everett et al. 2007). The microscopy observations in this study demonstrated for the first time that the viral genomes are rapidly and stably entrapped within PML-NBs immediately upon genome delivery to the nucleus during lytic infection (Figure 12). HSV-1 expresses ICP0 which localizes to PML-NBs to induce PML degradation leading to the dispersal of PML-NBs. This process disrupts the spatial recruitment of PML-NB restriction factors to vDNA, and allows the virus to counteract PML-NB mediated viral genome silencing and initiate lytic replication (Figure 15, 16, 17, and 18) (Maul and Everett 1994, Chelbi-Alix and de The 1999, Boutell et al. 2002, Boutell et al. 2011). In the absence of ICP0 and under MOI conditions that do not saturate intrinsic immunity, the viral genomes remained stably silenced and entrapped within PML-NBs. Importantly, this process occurred in the absence of ISG expression, demonstrating that vDNA entry into the nucleus alone is not sufficient for induction of innate immune response (Figure 24 and 25). In support of this conclusion, no stable localization between PRR IFI16 (a key regulator of host innate immunity) and vDNA was observed prior to the expression of viral genes (Figure 19) (Unterholzner et al. 2010, Orzalli et al. 2012). Live cell microscopy demonstrated that IFI16 puncta were transiently formed on the nuclear periphery of infected cells (Everett 2015, Diner et al. 2016). This observation raised the speculation that IFI16 is rapidly recruited to vDNA upon nuclear entry leading to the induction of ISG expression (Orzalli et al. 2012, Orzalli et al. 2016). Yet, no direct or indirect detection of vDNA was demonstrated in these studies (Everett 2015, Diner et al. 2016). Moreover, the number of IFI16 puncta observed did not correlate with the viral genome copy number expected to be delivered to the nucleus at high MOI (MOI of ≥ 10 PFU/cell) (Everett 2015, Diner et al. 2016). Although the interaction between IFI16 and vDNA have been previously demonstrated by ChIP (Johnson et al. 2014), direct detection of EdU-labeled vDNA did not reveal any significant colocalization between IFI16 and vDNA under low MOI conditions (Figure 19). However, this experiment was

conducted at fixed time points post-infection and does not exclude the possibility of transient interactions between IFI16 and vDNA.

Previous plaque-edge recruitment studies suggested that IFI16, similar to PML-NB proteins, is stably recruited to infecting ICP4 dot-like complexes that contain vDNA (Cuchet-Lourenco et al. 2013, Orzalli et al. 2013). Although controversial, IFI16 depletion has been shown to negatively influence the frequency of PML-NB protein recruitment to incoming viral genomes (Orzalli et al. 2013, Cuchet-Lourenco et al. 2013). Importantly, these studies have relied on the use of ICP4 signals as a proxy for viral genome localization; a suboptimal approach giving that ICP4 signals are only localized to a subset of transcriptionally active viral genome foci (Everett and Murray 2005). Consistence with these reports, we observed stable recruitment of IFI16 and PML to vDNA in newly infected cells next to developing plaques. However, IFI16 recruitment was observed only at the viral genomes expressing ICP4 while PML was recruited to vDNA irrespective of ICP4 expression (Figure 23) (Alandijany et al. 2018). These data demonstrate that the onset of viral gene expression or initiation of vDNA replication is required for IFI16-mediated sensing of HSV-1 DNA. Collectively, our data put a clear temporal context for the stable recruitment of PML and IFI16 to vDNA which correlates with the nuclear delivery of viral genome and expression of viral proteins, respectively.

In summary, the data presented in this chapter shed light on the temporal regulation of intrinsic and innate immune responses during intracellular restriction of HSV-1 infection. PML-NB associated restriction factors are rapidly recruited to vDNA upon nuclear entry leading to viral genome silencing. Saturation of or escape from this intrinsic immune response is required to induce innate immunity. Induction of viral gene transcription and/or initiation of vDNA replication triggers the stable recruitment of PRR IFI16 to viral genome foci and robust induction of ISG expression. However, HSV-1 expresses ICP0 which counteracts both intrinsic and innate immune responses by targeting PML and IFI16 for proteasome-dependent degradation.

5. Intrinsic and innate antiviral responses are temporally and functionally distinct arms of host intracellular immunity

5.1. Overview

Innate immunity plays a pivotal role in restricting HSV-1 infection both *in vivo* and *in vitro* (Gresser et al. 1976, Zawatzky et al. 1982, Pedersen et al. 1983). Central to this arm of immunity is IFN type I, that signals through the JAK/STAT/IRF pathway leading to the induction of ISGs (Stark et al. 1998). Induction of IFN production is dependent on the ability of host PRRs (table 4) to recognize virion components (e.g., viral proteins or nucleic acids) or structures accumulated during vDNA replication (e.g., dsRNA) (Paludan et al. 2011). However, HSV-1 evolved multiple strategies (e.g., including expression of ICP0) to interfere with the induction of innate immunity (table 5 and section 1.7.1.2.). Indeed, ICP0 has been shown to induce the degradation of IFI16, inhibits the activation of IRF3, and impedes NF-κB signaling (Melroe et al. 2007, Paladino et al. 2010, Orzalli et al. 2012, Zhang et al. 2013).

Hence, ΔICP0 HSV-1 was very valuable for advancing our understanding of host innate immunity during HSV-1 infection. Previous reports demonstrated that the induction of ISGs in the absence of ICP0 occurred in a dose-dependent manner with the most pronounced effect detected at high MOI of ≥10 PFU/cell between 6 and 24 h post-infection (Eidson et al. 2002, Orzalli et al. 2012, Diner et al. 2015). Utilizing such high MOI conditions, while informative, provides a limited characterization of the regulation of innate immunity during HSV-1 infection. In this chapter, we used ΔICP0 HSV-1 infected HFt cells (MOI of ≤ 1 PFU/cell) as a model to (i) explore the kinetics of viral replication that leads to the induction of host innate immunity; (ii) explore the effect of innate immunity induction on viral infection; and (iii) assess whether PML plays a key role in the regulation of this arm of immunity.

Our microscopy observations, presented in the previous chapter, demonstrated ISG expression during ΔICP0 HSV-1 infection to be induced only at MOIs that enable plaque formation (MOI of ≥ 1 PFU/cell). We concluded that the escape from intrinsic immunity and initiation of productive infection are required for innate immunity induction. In this chapter, we show that ΔICP0 HSV-1 infection induces ISG expression in a time-, dose-, and JAK-dependent manner. Treatment of the infected monolayers with a vDNA polymerase inhibitor phosphonoacetic acid (PAA) could block ISG induction in a dose-dependent manner, demonstrating that the initiation of vDNA replication is required for the induction of innate immunity. Unlike depletion of intrinsic restriction factors, blocking of ISG induction by ruxolitinib (a JAK pathway inhibitor) did not enhance the PFE of ΔICP0 HSV-1. Instead, it enhanced viral yields in a PML- and IFI16-dependent manner. Similar to IFI16 depletion, depletion of PML significantly inhibited ISG induction, identifying a key role for PML in regulating innate immunity to HSV-1 infection. These findings, along with the data presented on the first chapter, demonstrate that intrinsic and innate antiviral responses are temporally and functionally distinct arms of intracellular host immunity during HSV-1 infection.

5.2. Results

5.2.1. Induction of ISG expression during ΔICP0 HSV-1 infection occurs in a time-, and dose-dependent manner

Several reports have demonstrated that HSV-1 infection induces ISG expression. However, this process is antagonized by the expression of ICP0 (Eidson et al. 2002, Orzalli et al. 2012, Diner et al. 2015). We, therefore, assessed the induction of ISG expression during HSV-1 infection. HFt cells were seeded overnight before infection with either WT (MOI of 1 PFU/cell) or ΔICP0 HSV-1 (MOI of 0.1 to 1 PFU/cell). Samples were collected at the indicated time points post-infection (1 to 16 hours post-infection), and the induction of ISG was assessed by western blotting and qPCR. Consistent with the previous reports (Eidson et al. 2002, Orzalli et al. 2012, Diner et al. 2015), ΔICP0 but not WT HSV-1 markedly upregulated mRNA and protein expression levels of ISGs in a time- and MOI-dependent manner (figure 26 and 27). Robust induction of innate immunity during ΔICP0 was observed at increased MOI (≥ 1 PFU/cell) and only at a late stage post-infection (8–9 hours post-infection for mRNA levels and 16 hours post-infection for protein expression). These findings correlate with our microscopy observations which suggested that viral genome delivery to the nucleus alone was not sufficient to induce Mx1 ISG expression under low MOI conditions that failed to initiate plaque formation (figure 25).
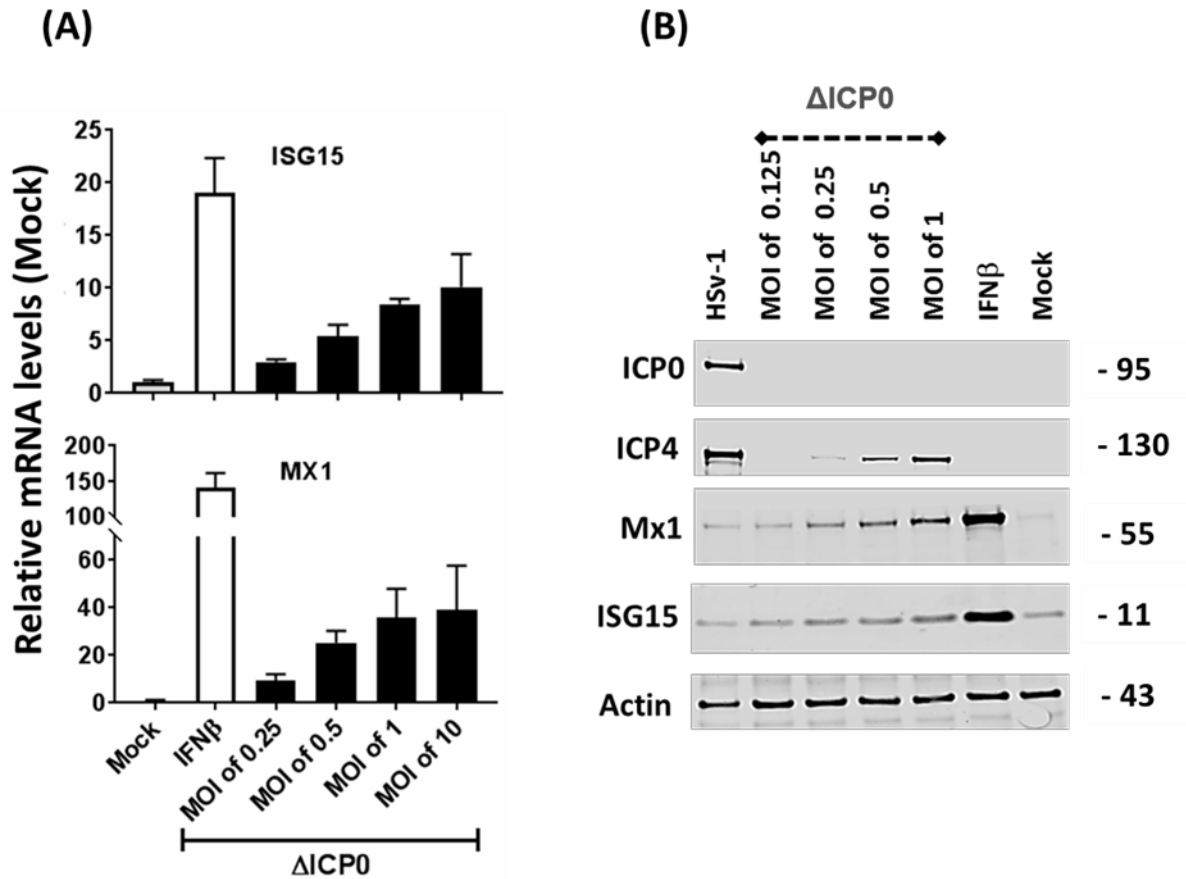
Figure 26. ΔICP0 HSV-1 infection induced ISG mRNA and protein levels in an MOI-dependent manner.

HFt cells were infected with WT (MOI of 1 PFU/cell) or ΔICP0 HSV-1 (at the indicated MOIs). Mock or IFNβ (100 IU/ml)-treated cells were included as a negative and positive control for ISG induction, respectively. Samples were collected at 9 hrs post-infection for qPCR and 16 hrs post-infection for western blotting. **(A)** Bar graphs show the mRNA levels of ISG15 and Mx1. The levels of mRNA were determined using the TaqMan system of quantitative RT-PCR. Values were normalized to GAPDH mRNA level, internal control, using the threshold cycle (ΔΔCT) method and expressed relative to the normalized level of mRNA in mock samples. Results represent means of relative quantitation (RQ) and RQ max; n=2. **(B)** Western blot membranes were probed for the viral proteins (ICP0, and ICP4) to track the progress of viral infection, the ISG products (MX1 and ISG15) to monitor the effect of the infection on the induction of ISGs, or actin (as a loading control). Molecular mass markers are shown.
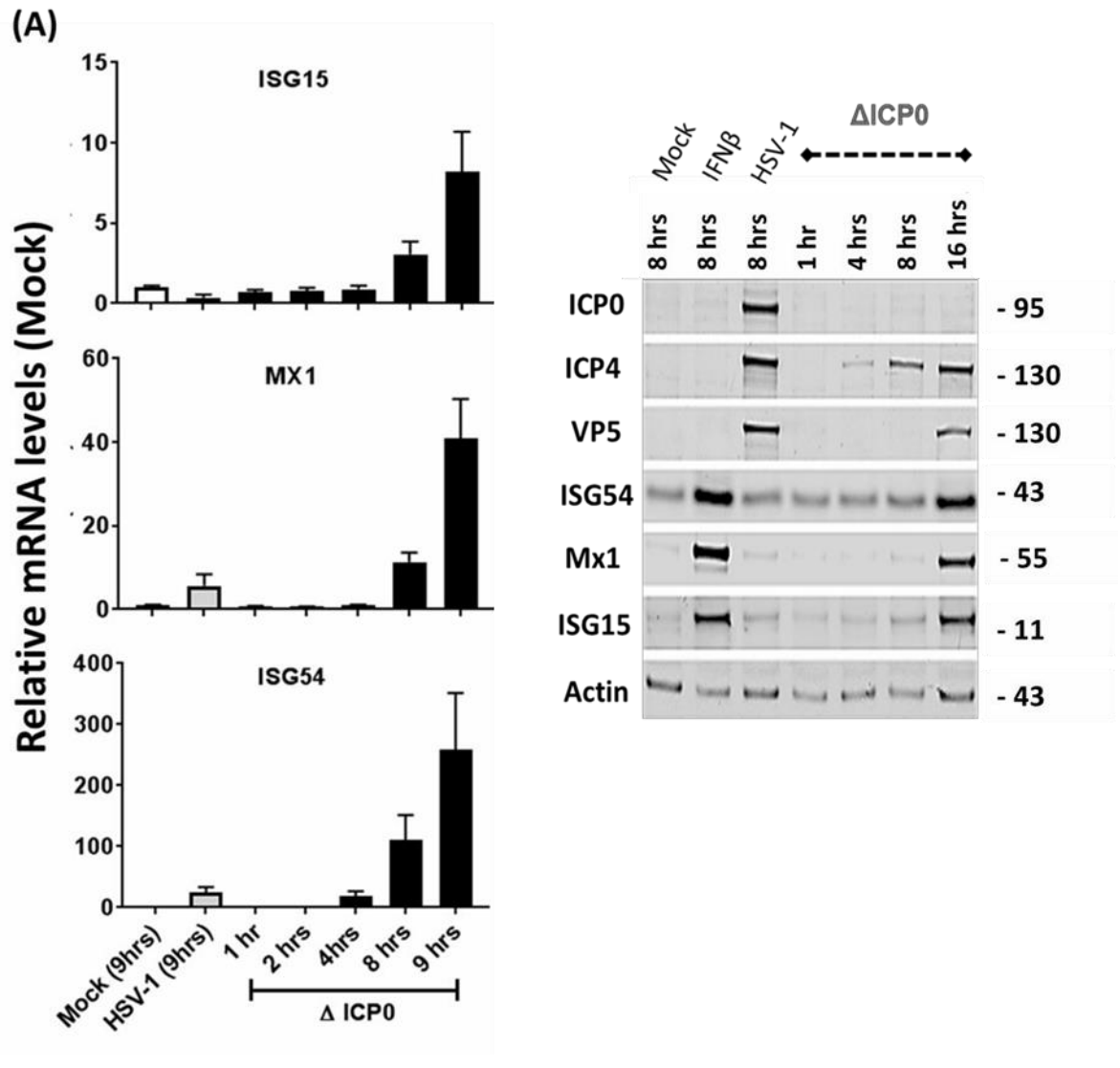
Figure 27. ΔICP0 HSV-1 infection induced ISG mRNA and protein levels in a time-dependent manner.

HFt cells were infected with WT or ΔICP0 HSV-1 at an MOI of 1 PFU/cell. Mock or IFNβ (100 IU/ml)-treated cells were included as a negative and positive control for ISG induction, respectively. Samples were collected at the indicated time point post-infection. **(A)** Bar graphs show the mRNA levels of ISG15, Mx1, and ISG54. The levels of mRNA were determined using the TaqMan system of quantitative RT-PCR. Values were normalized to GAPDH mRNA level, internal control, using the threshold cycle (ΔΔCT) method and expressed relative to the normalized level of mRNA in mock samples. Results represent means of relative quantitation (RQ) and RQ max; n=2. **(B)** Western blot membranes were probed for the viral proteins (ICP0, ICP4, and VP5) to track the progress of viral infection, the ISG products (ISG15, Mx1, and ISG54) to monitor the effect of infection on the induction of ISGs, or actin (as a loading control). Molecular mass markers are shown.

5.2.2. Initiation of vDNA replication is required for ISG induction.

Robust induction of ISG mRNA and protein levels was detected only at MOI conditions that enable plaque formation. Our microscopy observations also indicated that PRR IFI16 is only localized to vDNA in cells expressing ICP4 (Figure 23). Reports suggested that IFI16 preferably binds to higher order DNA structures (e.g., G quadruplex), which are shown to be accumulated during vDNA replication (Artusi et al. 2016, Haronikova et al. 2016). These findings suggest that the initiation of vDNA replication may play an important role in the induction of host innate immune response.

We assessed whether ISG induction during HSV-1 infection is linked to vDNA replication by monitoring ISG transcription in the presence of vDNA replication inhibitors acyclovir (ACG) and PAA (Schang et al. 2000, Honess and Watson 1977, Elion et al. 1977, Crumpacker et al. 1979). All qPCR experiments were conducted at an MOI of 1 PFU/cell, and samples were collected at 9 h post-infection. Following an hour of viral absorption, cells were overlaid with treatment-free media or media containing ACG or PAA (Figure 28). The concentrations of ACG and PAA used in this study are known to effectively block viral replication (Alandijany et al., 2018). ISG induction was inhibited in PAA-treated samples in a dose-dependent manner while only a moderate decrease was observed in ACG-treated cells (Figure 28). The differences in the inhibitory effect between PAA and ACG on ISG induction might be linked to their distinct mechanisms of action. The differential effects of these two vDNA replication inhibitors can be linked to their distinct mechanisms of action. PAA specifically targets the vDNA polymerase and inhibits the initiation of vDNA replication, whereas ACG is a synthetic purine nucleoside analog that acts as a premature DNA chain terminator and interferes with nascent vDNA synthesis (Honess and Watson 1977, Schang et al. 2000, Crumpacker et al. 1979, Elion et al. 1977). Hence, ACG treatment likely leads to the accumulation of prematurely terminated vDNA replication intermediates that still can be sensed by IFI16 which may account for the inefficient inhibition of ISG induction in ACG-treated cells. Importantly, the inhibitory effect of PAA was specific to the viral-mediated induction of ISGs, as PAA had no effect on Mx1 and ISG15 induction in

IFNβ-treated cells (Figure 29). Collectively, these data demonstrate that initiation of vDNA replication is a prerequisite for induction of host innate immune response to HSV-1 infection.
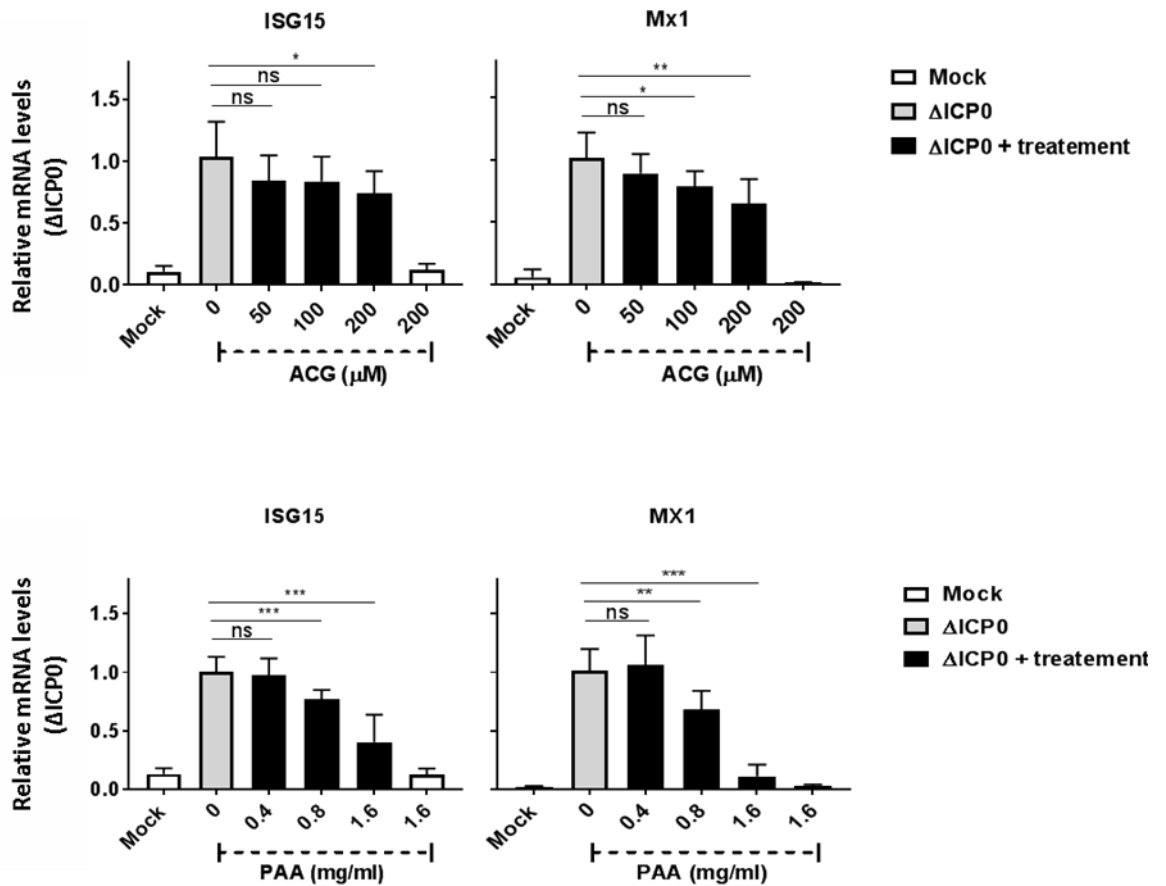
Figure 28. Initiation of vDNA replication is required for ISG induction during ΔICP0 HSV-1 infection.

HFt cells were mock or infected with ΔICP0 at an MOI of 1. Following an hour of viral absorption, cells were overlaid with treatment-free media or media containing acyclovir (ACG) or phosphonoacetic acid (PAA) at the indicated concentrations. Samples were collected at 9 hrs post-infection. Bar graphs show the mRNA levels of MX1 and ISG15. The levels of mRNA were determined using the TaqMan system of quantitative RT-PCR. Values were normalized to GAPDH mRNA level, internal control, using the threshold cycle (ΔΔCT) method and expressed relative to the normalized level of mRNA in ΔICP0-infected samples with no treatment. Results represent means of relative quantitation (RQ) and standard deviation; n=3. * P < 0.05, ** P < 0.01, *** p < 0.001, and ns= non-significant; paired T-test.
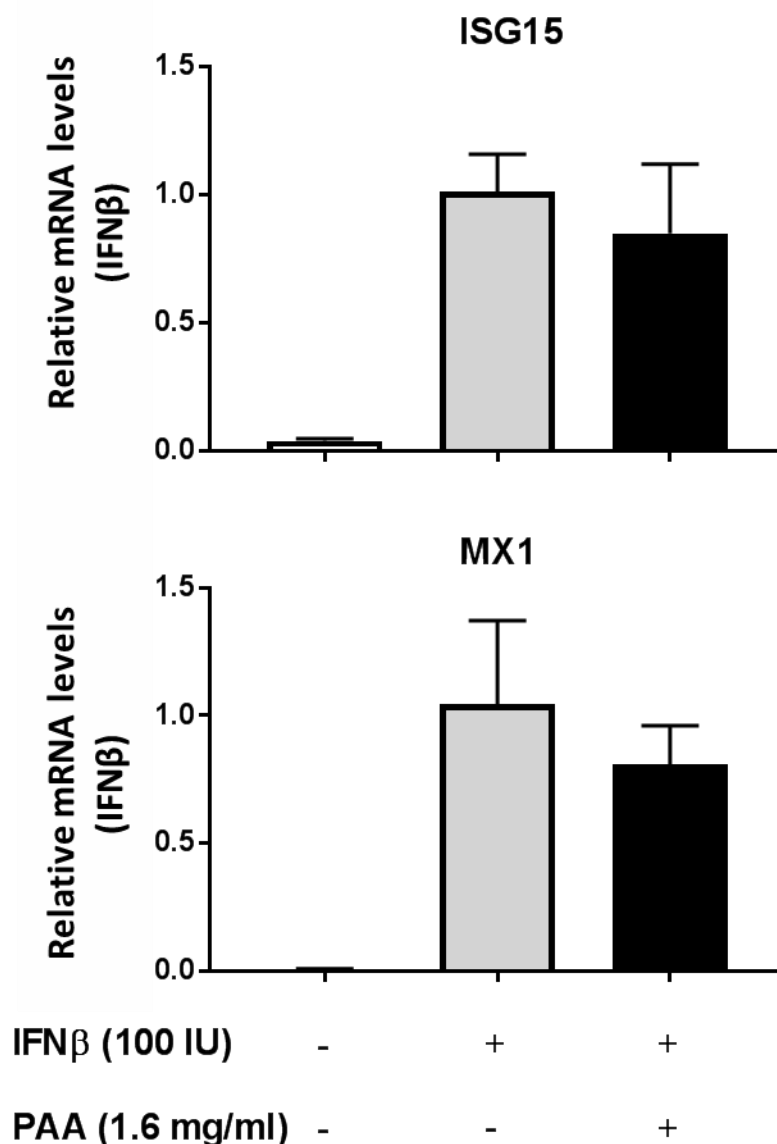
Figure 29. PAA does not affect ISG induction in IFNß-treated cells.

HFt cells were untreated or treated with IFNß (100 IU/ml) and PAA (1.6 mg/ml) as indicated. Samples were collected at 9 hrs post-treatment. Bar graphs show the mRNA levels of MX1 and ISG15. The levels of mRNA were determined using the TaqMan system of quantitative RT-PCR. Values were normalized to GAPDH mRNA level, internal control, using the threshold cycle ($\Delta\Delta$CT) method and expressed relative to the normalized level of mRNA in IFNß-treated samples. Results represent means of relative quantitation (RQ) and SD; n=2.

5.2.3. JAK signaling plays a key role in the induction of ISGs during HSV-1 infection

JAK1 and TYK2 play a central role in the IFN signaling cascade. Interactions between secreted IFNs and their receptors activate JAK-1 and TYK2 that induce the phosphorylation of STAT1 and STAT2. Phosphorylated STAT1/2 associates with IRF9 leading to ISGF3 complex formation. Upon nuclear translocation of ISGF3, the expression of ISGs is upregulated (Stark et al. 1998). Consistent with the key role of JAK in the IFN signaling pathway, we found that JAK1/2 inhibitor ruxolitinib (Rux) blocked the induction of Mx1 and ISG15 in IFNβ-treated cells (Figure 30) (Shuai et al. 1993b, Quintas-Cardama et al. 2010). Ruxolitinib also blocked ISG expression in ΔICP0 HSV-1 infected cells, demonstrating that JAK activity is key for innate immunity induction during HSV-1 infection (Figure 31) (Yokota et al. 2001, Johnson et al. 2008b). Then, we asked whether JAK is required for ISG induction during the initial cycle of vDNA replication, or it requires multiple cycles of viral replication to be activated. ACG at 50 µM did not affect ISG induction during ΔICP0 infection, but completely blocked the plaque formation and stalled the infection at the first cycle of replication (Alandijany et al. 2018). Combined ACG and ruxolitinib efficiently blocked ISG induction, demonstrating that JAK activity is specifically required during the initial cycles of ΔICP0 infection to stimulate ISG induction (Figure 32).
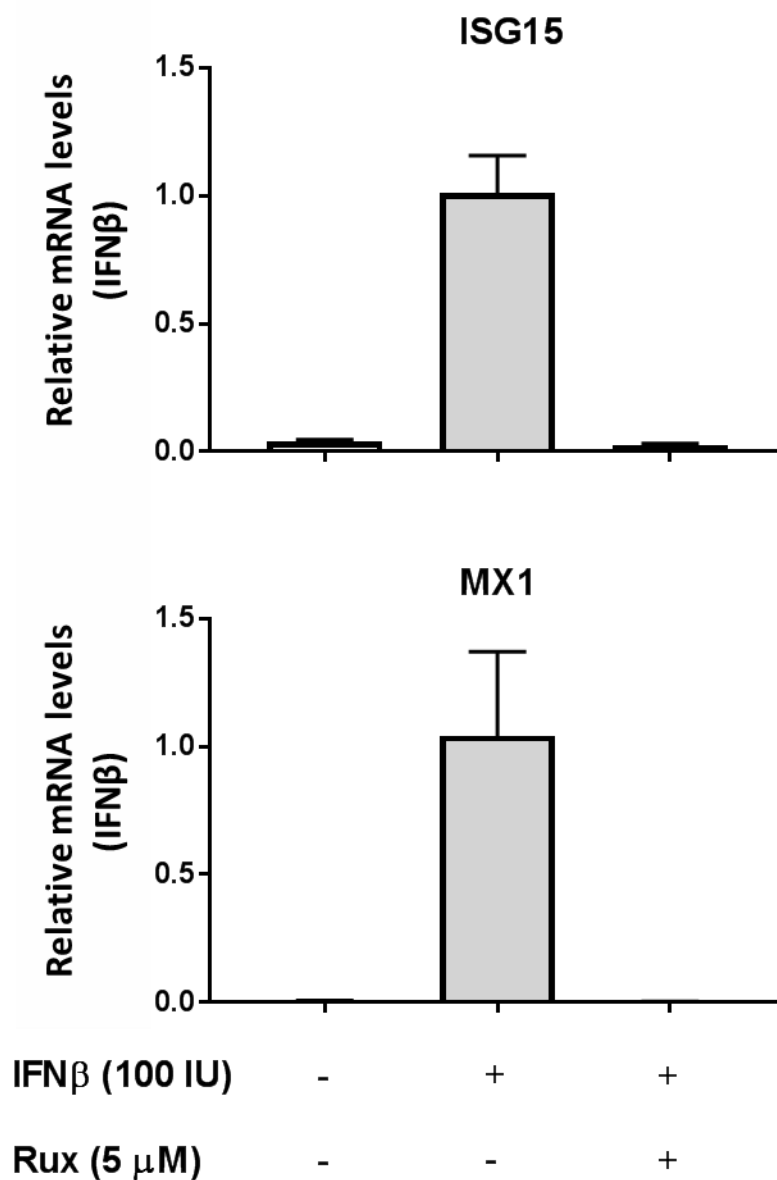
Figure 30. Ruxolitinib, a JAK1/2 inhibitor, blocked ISG induction in IFNß-treated cells.

HFt cells were untreated or treated with IFNß (100 IU/ml) and Ruxolitinib (Rux; 5 μM) as indicated. Samples were collected at 9 hrs post-treatment. Bar graphs show the mRNA levels of MX1 and ISG15. The levels of mRNA were determined using the TaqMan system of quantitative RT-PCR. Values were normalized to GAPDH mRNA level, internal control, using the threshold cycle (ΔΔCT) method and expressed relative to the normalized level of mRNA in IFNß-treated samples. Results represent means of relative quantitation (RQ) and SD; n=2.
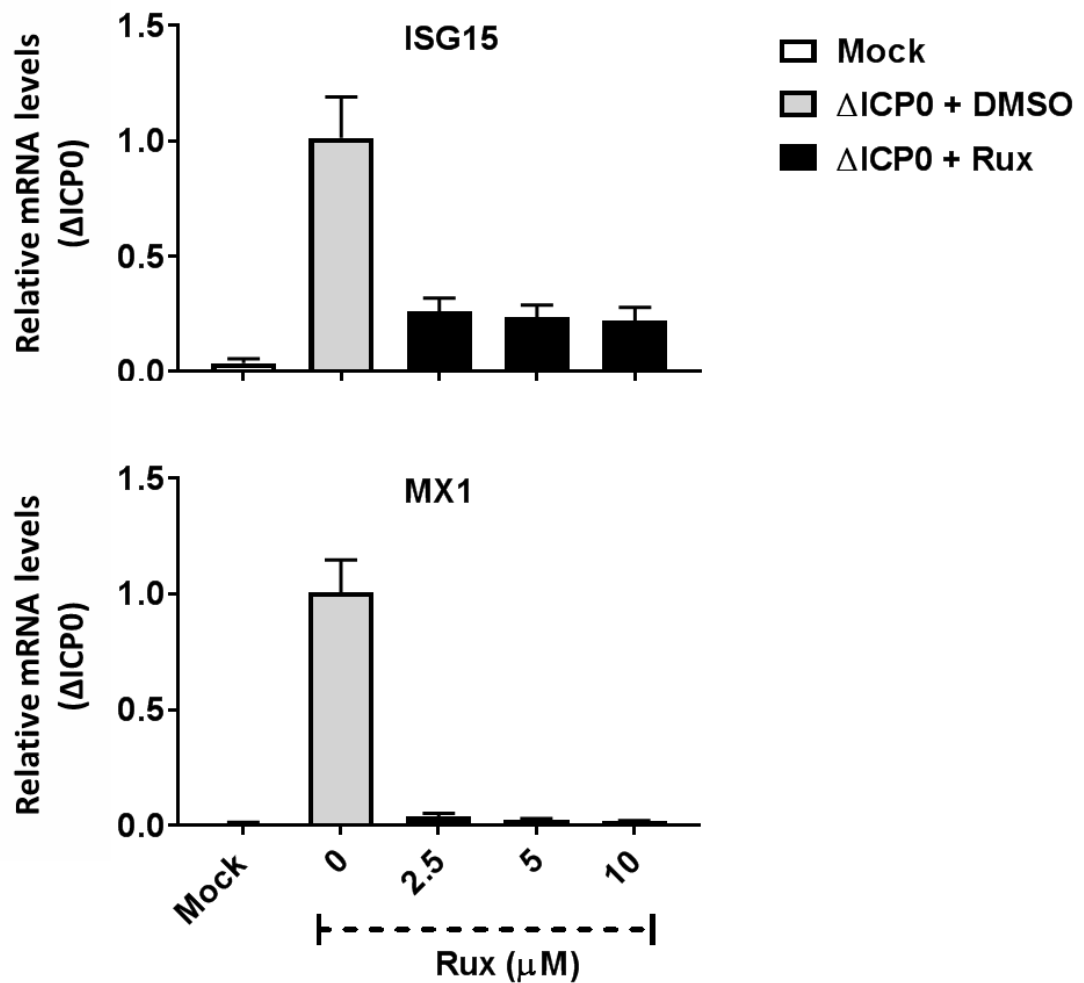
Figure 31. Ruxolitinib inhibited the induction of ISGs during ΔICP0 HSV-1 infection.

HFt cells were mock or infected with ΔICP0 at an MOI of 1 PFU/cell. Following an hour of viral absorption, cells were overlaid with media containing either DMSO or Rux (at the indicated concentrations). Samples were collected at 9 hrs post-infection. Bar graphs show the mRNA levels of MX1, and ISG15. The levels of mRNA were determined using the TaqMan system of quantitative RT-PCR. Values were normalized to GAPDH mRNA, internal control, using the threshold cycle (ΔΔCT) method, and expressed relative to the normalized level of mRNA in ΔICP0 HSV-1 infected samples with DMSO treatment. Results represent means of relative quantitation (RQ) and SD; n=2.
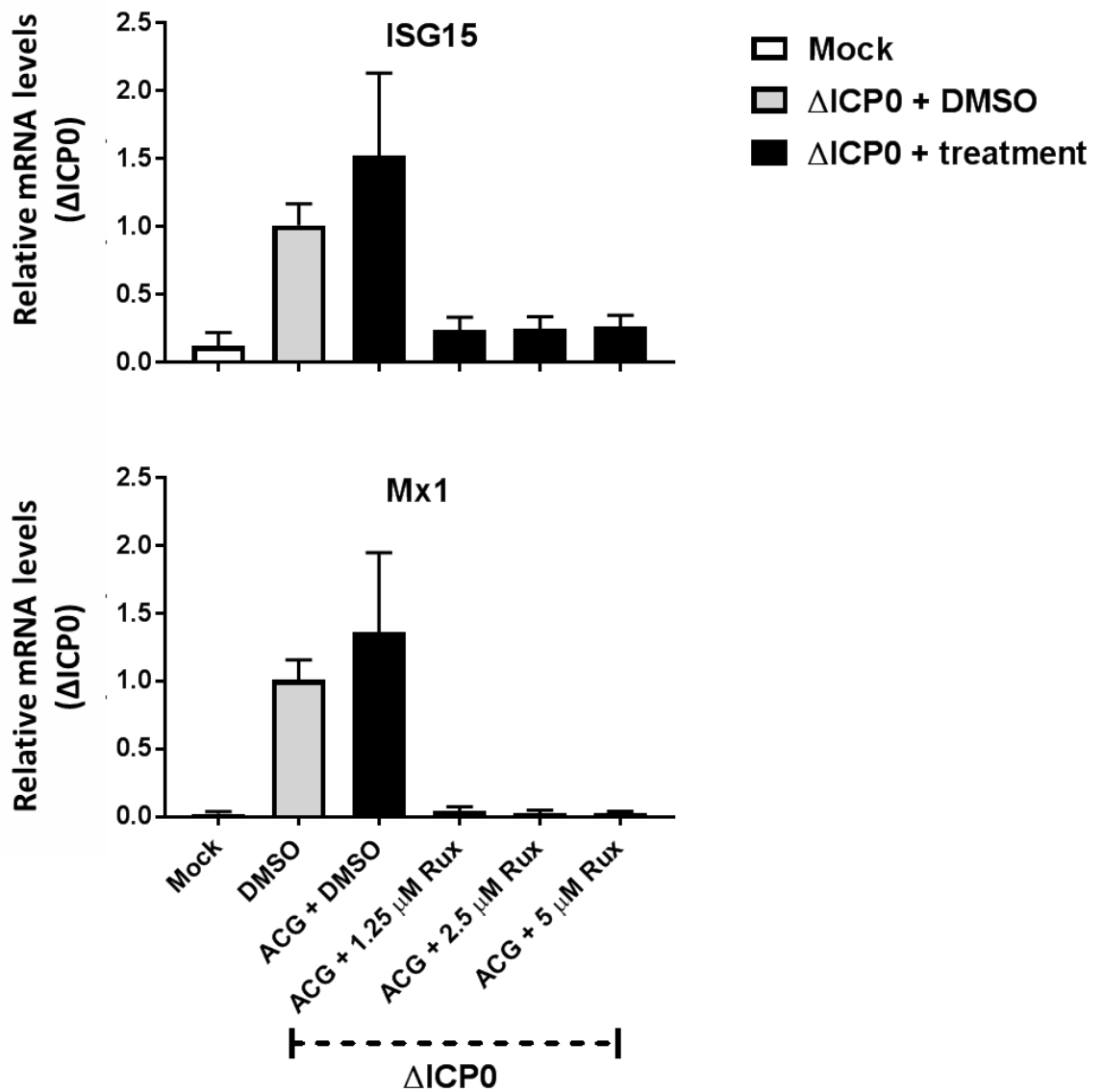
Figure 32. JAK activity is required for ISG induction during the initiating cycle of ΔICP0 HSV-1 infection.

HFt cells were mock or infected with ΔICP0 at an MOI of 1 PFU/cell. Following an hour of viral absorption, cells were overlaid with media containing DMSO, ACG (50 μM), and Rux (at the indicated concentration). Samples were collected at 9 hrs post-treatment. Bar graphs show the mRNA levels of MX1 and ISG15. The levels of mRNA were determined using the TaqMan system of quantitative RT-PCR. Values were normalized to GAPDH mRNA level, internal control, using the threshold cycle (ΔΔCT) method and expressed relative to the normalized level of mRNA in ΔICP0 HSV-1 infected samples with DMSO treatment. Results represent means of relative quantitation (RQ) and SD; n=2.

5.2.4. Innate immunity constricts viral propagation over multiple cycles of replication

As the inhibition of JAK pathway effectively blocked ISG induction in ΔICP0 HSV-1 infected cells, we investigated the effect of ruxolitinib on WT and ΔICP0 HSV-1 replication. First, PFE of both WT and ΔICP0 HSV-1 in HFt cells was assessed at 24 h post-infection in the presence of either ruxolitinib (5 μM) or DMSO (a carrier control). Given that WT virus did not robustly induce ISG expression, it was unsurprising that JAK inhibition did not affect the PFE of WT HSV-1 (Figure 33). Interestingly, the PFE of ΔICP0 HSV-1 was also not significantly influenced by ruxolitinib treatment, indicating that ISG induction does not significantly contribute to the plaque-formation defect of ΔICP0 HSV-1 observed in HFt cells (figure 33 and 17). However, a substantial increase in the size of ΔICP0 plaques in ruxolitinib-treated cells versus DMSO-treated cells was observed when PFE was assessed at 48 h post-infection (Figure 34). These findings encouraged us to assess the effect of blocking ISG induction on viral propagation. HFt cells were seeded and infected with either WT (MOI of 0.001 PFU/cell) or ΔICP0 HSV-1 (MOI of 1 PFU/cell). Following an hour of viral absorption, infected cells were overlaid with media containing either ruxolitinib (5 μM) or DMSO. Supernatants were collected at 24 hours intervals for three days (24, 48, and 72 hours post-infection), and viral yields were determined in U2OS cells. The viral yields of ΔICP0, but not WT, HSV-1 were substantially increased in ruxolitinib-treated cells in comparison to DMSO-treated controls (Figure 35). Collectively, these findings suggested that innate immunity does not restrict the initiation of viral infection, but rather constricts viral propagation over multiple cycles of replication. These results demonstrate that intrinsic and innate immunity are functionally distinct arms of host response that impair viral replication at different stages of infection.
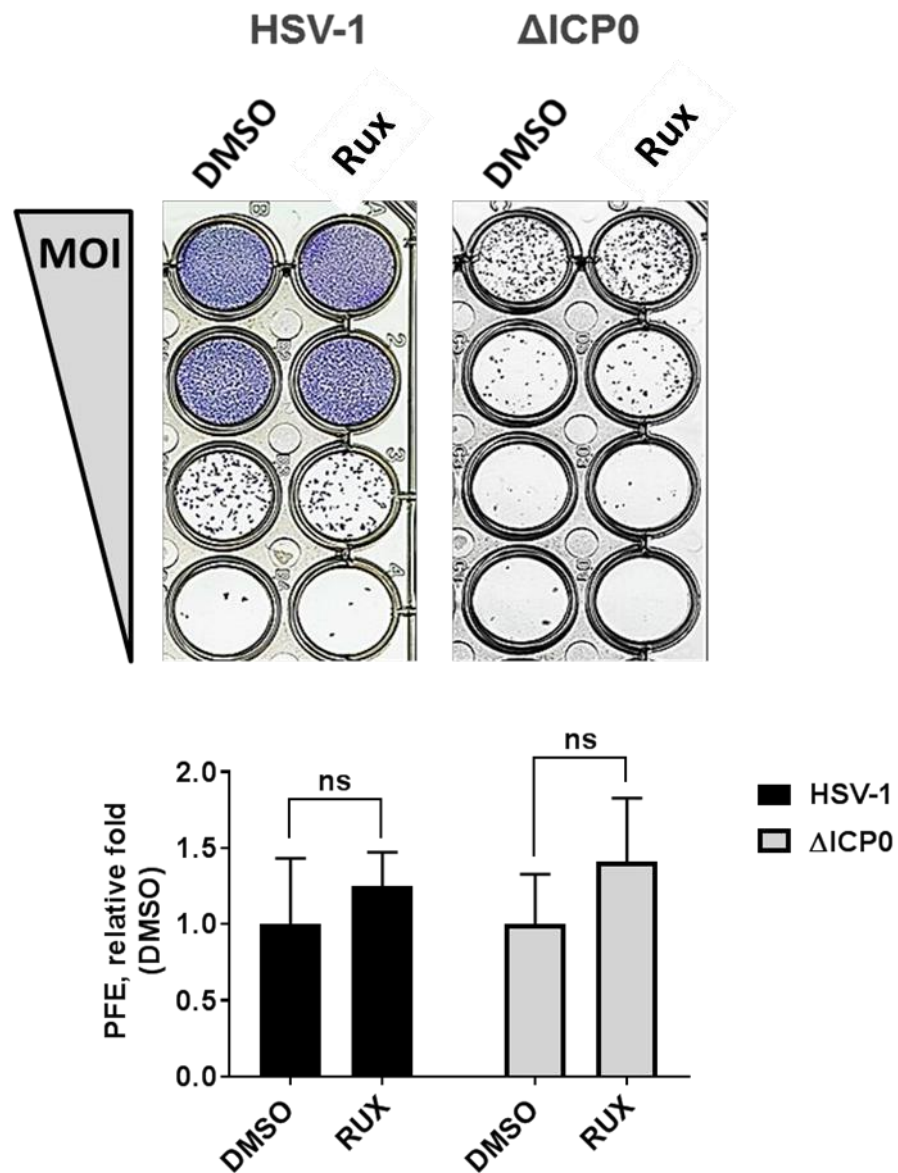
Figure 33. Inhibition of JAK signaling does not enhance PFE of HSV-1 at 24 hours post-infection.

HFt cells were infected with serial dilutions of either WT (dilution factor of 10) or ΔICP0 HSV-1 (dilution factor of 2). Following an hour viral absorption, cells were overlaid with media containing 2% HS and either DMSO or ruxolitinib (Rux; 5 µM). At 24 hrs post-infection, plaques were visualized by immune-staining plaque assay. Bar graphs show the number of plaques in Rux-treated cells relative to DMSO-treated cells. Results represent mean + SD; n=3. ns=non-significant; paired T-test.
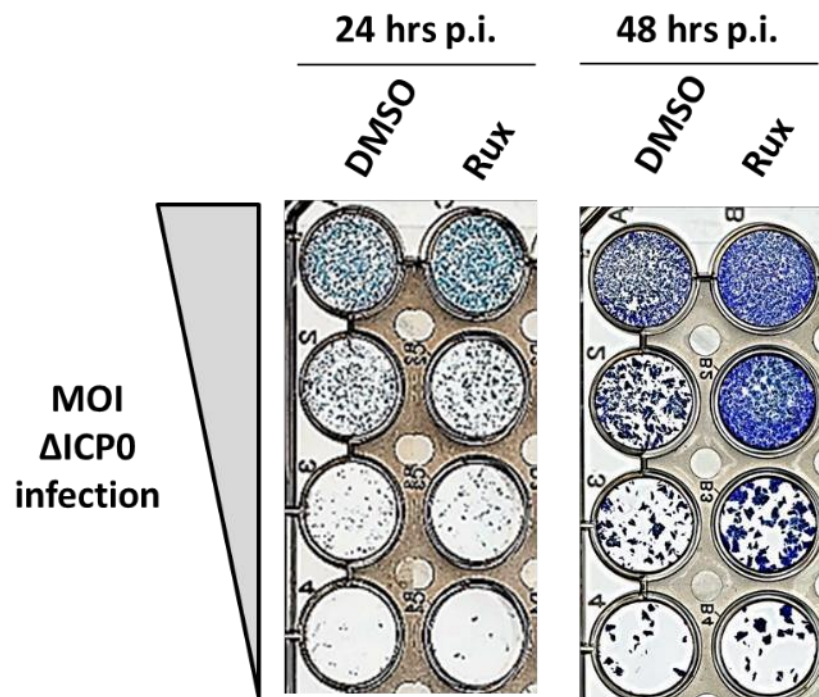
Figure 34. Inhibition of JAK signaling enhanced the plaque size of ΔICP0 at 48 hours post-infection.

HFt cells were infected with serial dilutions of ΔICP0 HSV-1. Following an hour viral absorption, cells were overlaid with media containing 2% HS and either DMSO or ruxolitinib (Rux; 5 µM). Plaques were visualized by immune-staining plaque assay at 24 and 48 hrs post-infection.
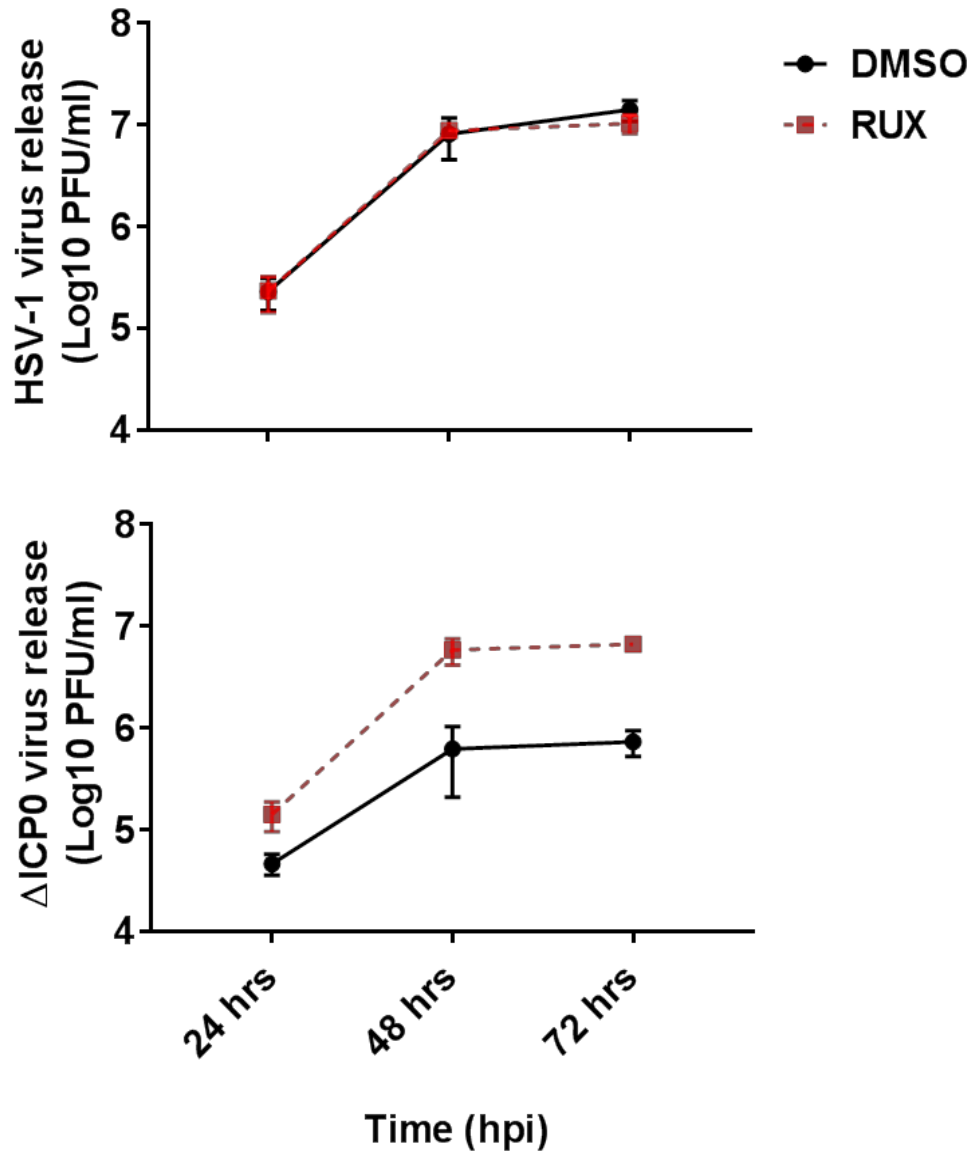
Figure 35. Inhibition of JAK signaling enhanced the viral yields of ΔICP0, but not, HSV-1.

HFt cells were infected with either WT (MOI of 0.001 PFU/cell) or ΔICP0 HSV-1 (MOI of 1 PFU/cell). Following an hour viral absorption, cells were overlaid with media containing either DMSO or ruxolitinib (Rux; 5 µM). Supernatants were collected at 24, 48, and 72 hrs post-infection, and viral yields were determined on U2OS cells. Results represent mean ± SD; n=3.

5.2.5. IFI16 and PML play key roles in the induction of innate immunity during ΔICP0 HSV-1 infection

Unlike JAK inhibition, a single depletion of PML or IFI16 enhanced the PFE and viral yields of ΔICP0, but not WT, HSV-1 (Figure 18, 36 and 37). These data correlate with the intrinsic antiviral roles of PML and IFI16 that are antagonized by the viral protein ICP0 (Everett et al. 2006, Cuchet-Lourenco et al. 2013, Orzalli et al. 2013). Importantly, ruxolitinib treatment did not lead to any further increase of ΔICP0 HSV-1 yields in IFI16- or PML-depleted cells (Figure 37). These findings were unsurprising in IFI16-depleted cells, as IFI16 is known to play a key role in the induction of innate immunity during HSV-1 infection (Diner et al. 2015, Orzalli et al. 2012, Unterholzner et al. 2010). However, they raised the hypothesis that PML is crucial for efficient induction of ISGs. The mRNA levels of ISGs during ΔICP0 HSV-1 infection in IFI16-, PML-depleted cells and their relative controls were assessed. Consistent with previous reports (Diner et al. 2015, Orzalli et al. 2012, Unterholzner et al. 2010), the induction of ISGs in IFI16-depleted cells was significantly reduced in comparison to the control cell lines (Figure 38). Interestingly, the induction of ISGs in PML-depleted was also significantly impaired, demonstrating a key role for PML in innate immunity induction during ΔICP0 HSV-1 infection (Figure 39).
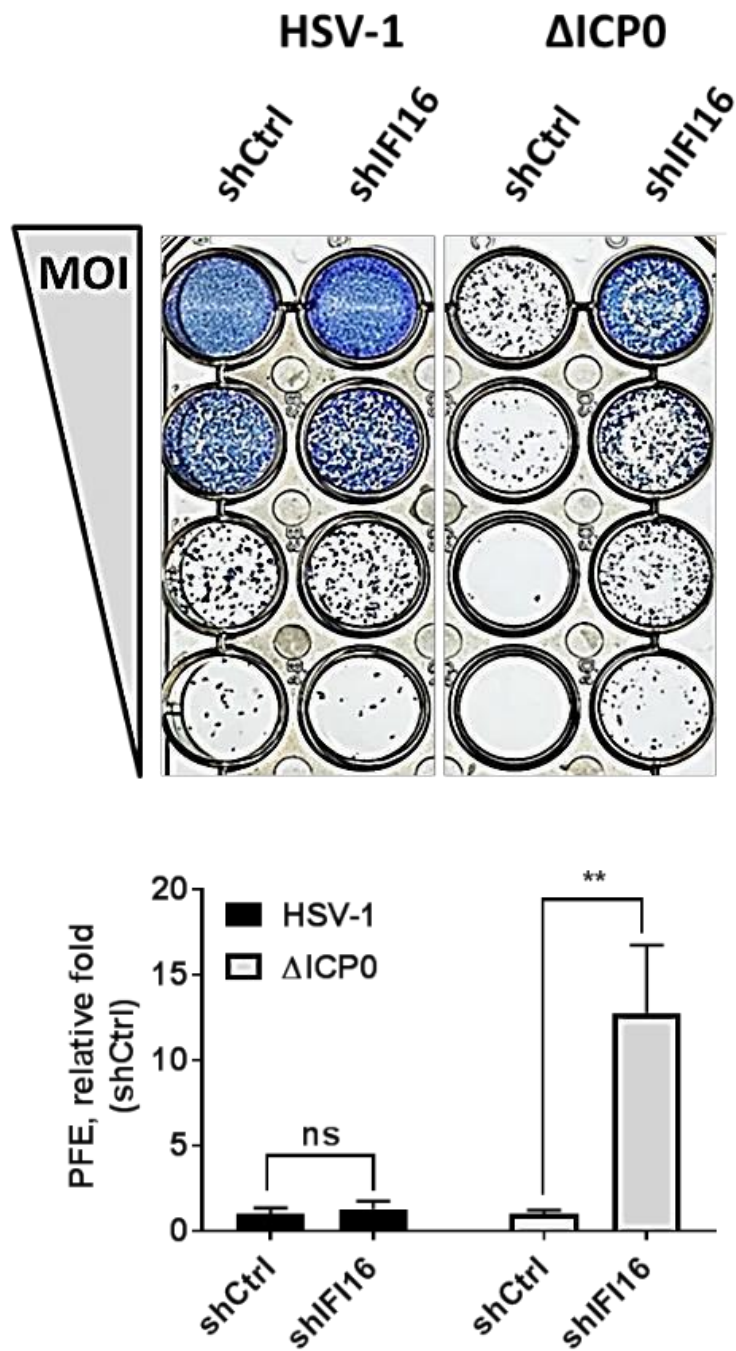
Figure 36. IFI16 depletion enhances the PFE of ΔICP0, but not, HSV-1.

shCtrl and shIFI16 cells were seeded overnight and infected with serial dilutions of either WT (dilution factor of 10) or ΔICP0 HSV-1 (dilution factor of 2). Plaques were visualized at 24 hrs by immuno-staining plaque assay. Bar graphs represent the fold increase in plaque number in the infected shIFI16 relative to infected shCtrl cells (as indicated). Results represent relative mean + SD; (n= 3). Similar results were obtained from independent batches of depleted cells. ** P= < 0.01, and ns= non-significant; paired T-test.
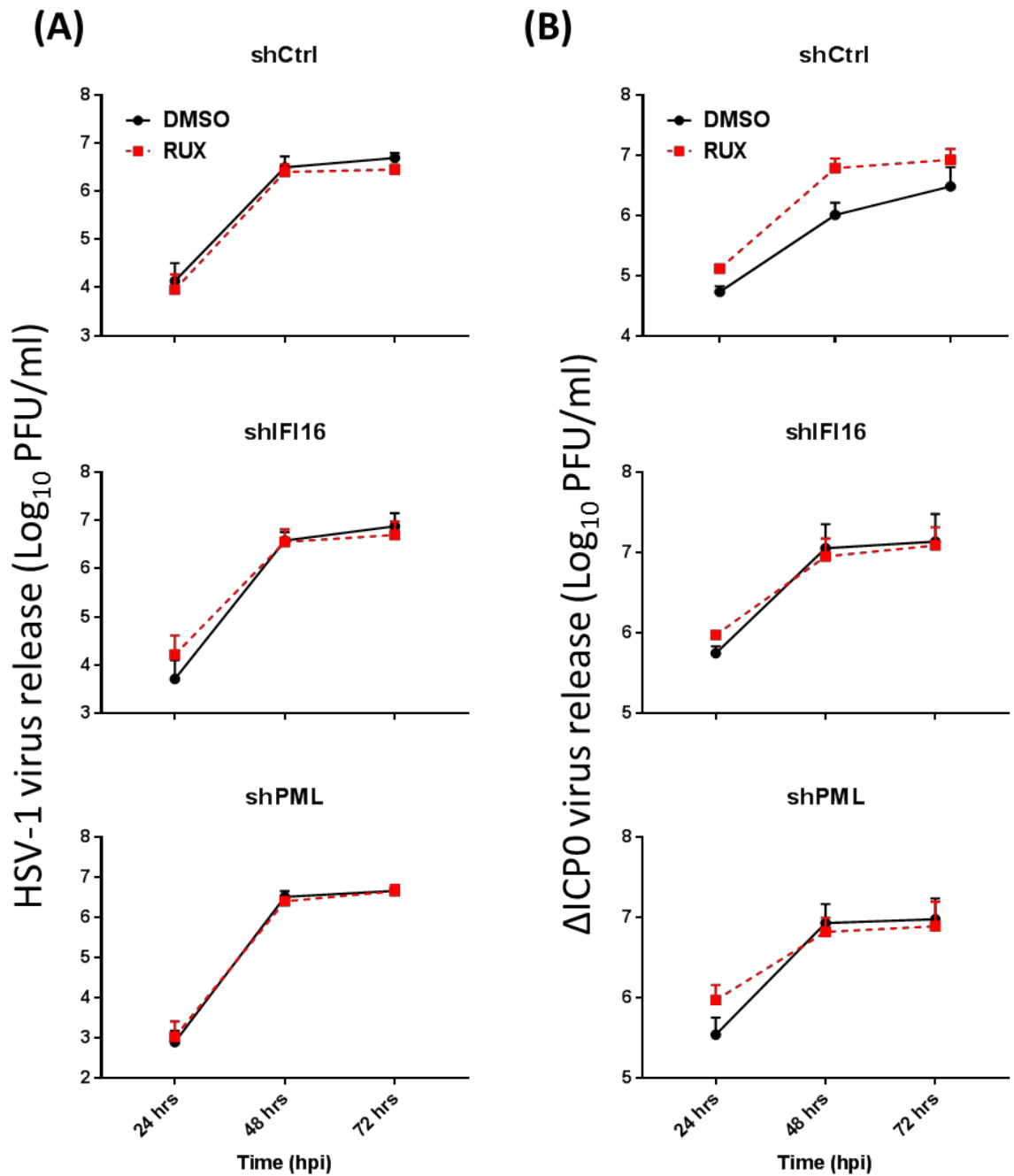
Figure 37. Inhibition of JAK signaling failed to enhance the viral yields of WT and ΔICP0 HSV-1 in IFI16- and PML-depleted cells.

Cells were seeded overnight and infected with either WT (MOI of 0.001 PFU/cell) or ΔICP0 HSV-1 (MOI of 1 PFU/cell) (A and B, respectively). Cells were overlaid with media containing either DMSO or ruxolitinib (Rux; 5 μM). Supernatants were collected at 24, 48, and 72 hours post-infection (hpi), and viral yields were determined on U2OS cells. Results represent mean and SD; n=3.
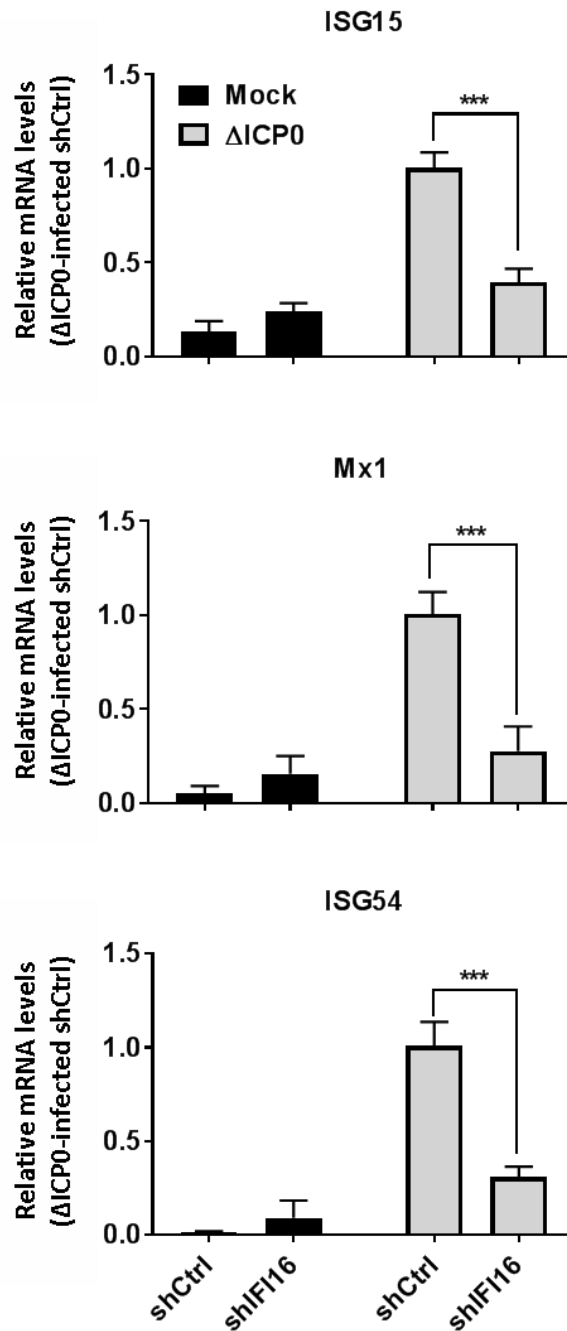
Figure 38. ΔICP0 HSV-1 infection induced ISG transcription in an IFI16-dependent manner.

shCtrl or shIFI16 cells were mock or infected with ΔICP0 HSV-1 at an MOI of 1 PFU/cell. Samples were collected at 9 hours post-infection. Bar graphs show the mRNA levels of MX1, ISG15, and ISG54. The levels of mRNA were determined using the TaqMan system of quantitative RT-PCR. Values were normalized to GAPDH mRNA level, internal control, using the threshold cycle (ΔΔCT) method and expressed relative to the normalized level of mRNA in ΔICP0 HSV-1 infected shCtrl samples. Results represent means of relative quantitation (RQ) and SD; n=3. *** P < 0.001; paired T-test.
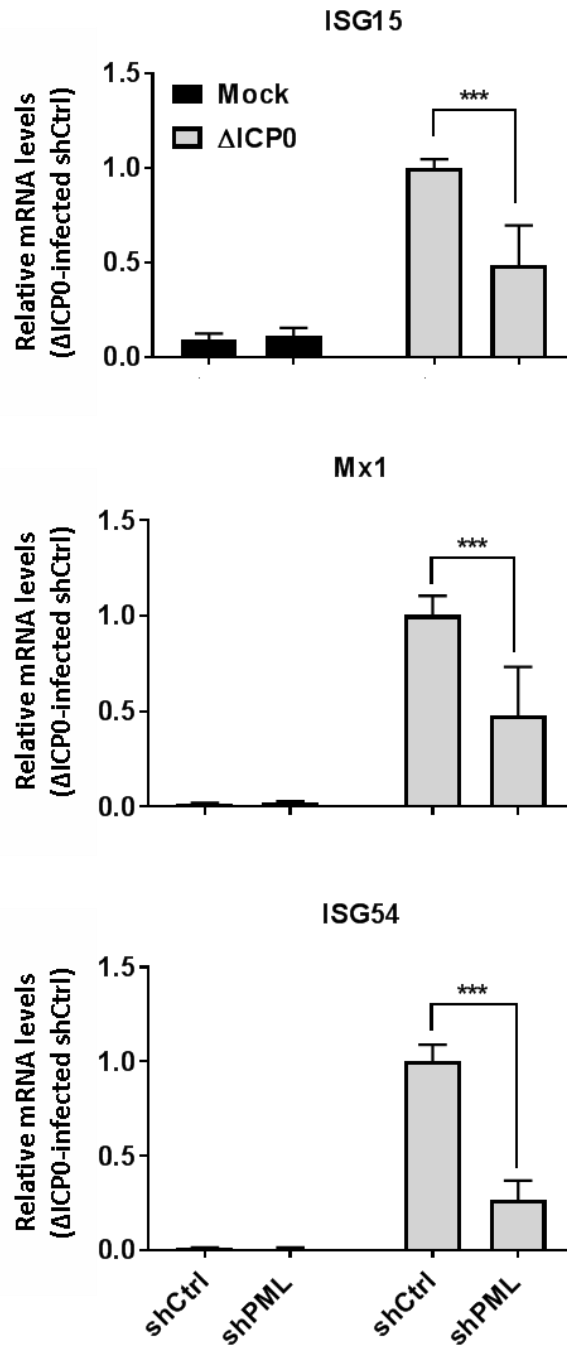
Figure 39. ΔICP0 infection induced ISG transcription in a PML-dependent manner.

shCtrl or shPML cells were mock or infected with ΔICP0 HSV-1 at an MOI of 1 PFU/cell. Samples were collected at 9 hours post-infection. Bar graphs show the mRNA levels of MX1, ISG15, and ISG54. The levels of mRNA were determined using the TaqMan system of quantitative RT-PCR. Values were normalized to GAPDH mRNA level, internal control, using the threshold cycle (ΔΔCT) method and expressed relative to the normalized level of mRNA in ΔICP0 HSV-1 infected shCtrl samples. Results represent means of relative quantitation (RQ) and SD; n=3. *** P < 0.001; paired T-test.

5.3. Summary

Intrinsic and innate immunity play key roles in the intracellular restriction of HSV-1 infection. However, the regulation of these two arms of immunity remains unclear. We showed in the previous chapter that induction of intrinsic and innate immune responses are temporally distinct processes. Entry of vDNA into the nucleus of infected cells triggers intrinsic antiviral response which leads to viral genome silencing. Escape from silencing is required to induce host innate immune response. In this chapter, further investigations were carried out to assess the kinetics of viral infection that leads to the induction of host innate immunity as well as exploring the consequences of this induction on viral replication.

It is well reported that HSV-1 infection induces ISG expression. However, HSV-1 expresses ICP0 which impairs several cellular pathways to interfere with the induction of innate immunity (Chew et al. 2009, Lanfranca et al. 2014, Orzalli and Knipe 2014). Although controversial, ICP0 has been shown to induce proteasome-dependent degradation of PRR IFI16 (Orzalli et al. 2012, Diner et al. 2015, Orzalli et al. 2016, Cuchet-Lourenco et al. 2013). ICP0 is, then, translocated to the cytoplasm of infected cells where it binds to IRF3 and sequesters it away from ISG promoters (Melroe et al. 2007, Paladino et al. 2010). Consistent with these reports, ΔICP0 but not WT HSV-1 induced ISG mRNA and protein levels (Figure 26 and 27). Importantly, robust induction of ISGs during ΔICP0 HSV-1 infection was observed only at MOI conditions that enabled plaque formation (MOI of ≥1,~26 genome copies/nuclei) to occur (Figure 24 and 25) (Alandijnay et al., 2018), and at a late stage of viral infection (≥ 8h post-infection for mRNA level and ≥16 hrs post-infection for protein level) (Figure 26, and 27). Our microscopy observations indicate that PRR IFI16 is recruited only to viral genomes in cells that successfully established the onset of viral gene expression (Figure 24). IFI16 has a high affinity to bind to higher-order DNA structures (e.g., G quadruplex DNA), which are predominantly accumulated during vDNA replication (Haronikova et al. 2016, Artusi et al. 2016). These findings suggested that vDNA replication is required for robust induction of

innate immunity. Correspondingly, PAA inhibited the induction of ISGs in a dose-dependent manner, although ACG only moderately influenced this host response (Figure 28). The differential effects of these two vDNA replication inhibitors can be linked to their distinct mechanisms of action. PAA specifically targets the vDNA polymerase and inhibits the initiation of vDNA replication, whereas ACG is a synthetic purine nucleoside analog that acts as a premature DNA chain terminator and interferes with nascent vDNA synthesis (Honess and Watson 1977, Schang et al. 2000, Crumpacker et al. 1979, Elion et al. 1977). Hence, ACG treatment likely leads to the accumulation of prematurely terminated vDNA replication intermediates that still can be sensed by IFI16 which may account for the inefficient inhibition of ISG induction in ACG-treated cells. Collectively, these data demonstrate that the onset of vDNA replication plays a critical role in stimulating ISG induction during HSV-1 infection. In agreement with our findings, previous reports demonstrated that HSV-1 induced cytokine expression is dependent on viral replication, as UV-inactivated virus failed to induce this immune response (Melchjorsen et al. 2006, Rasmussen et al. 2007). Nevertheless, other reports suggested that ISGs induction requires viral particle entry but not viral replication (Collins et al. 2004, Eidson et al. 2002). The discrepancies in findings can be due to differences between studies in terms of experimental design, cell types, virus strain or mutants, particle to PFU ratio of viral stocks, and MOI used. Here we provided evidence that nuclear entry of viral genomes alone is not sufficient to induce host innate immunity but requires the initiation of vDNA replication. Our data put a clear temporal context for the induction of intrinsic and innate immunity during HSV-1 infection; likely to be relevant for other viral systems.

JAK inhibition studies demonstrated that intrinsic and innate antiviral responses are functionally distinct from one another. A previous report showed that depletion of STAT, unlike depletion of PML-NB associated restriction factor, did not enhance the PFE of ΔICP0 HSV-1 (Everett et al. 2008) (Figure 18). Consistent with this report (Everett et al. 2008, the viral plaque numbers were not affected upon inhibition of JAK activity with ruxolitinib (Figure 33). However, a substantial increase in the plaque size and virus yield of ΔICP0 HSV-1

was observed in the presence of ruxolitinib, phenotypes not observed during WT HSV-1 infection (Figure 34 and 35). Our data demonstrate that induction of ISG expression does not repress the onset of viral replication, but instead constricts viral propagation. Collectively, our data demonstrate that intrinsic and innate immunity are temporally and functionally distinct arms of intracellular immunity during HSV-1 infection.

It is clear that IFI16 is one of the key innate immune regulators and its action is antagonized by ICP0 expression (Diner et al. 2015, Orzalli et al. 2016, Orzalli et al. 2012, Unterholzner et al. 2010). Consistent with these reports, the presence of IFI16 was crucial for efficient induction of ISGs during ΔICP0 HSV-1 infection (Figure 38). Hence, ruxolitinib treatment failed to enhance ΔICP0 HSV-1 yields in the absence of IFI16 (Figure 37). Our microscopy observations demonstrated that IFI16 and PML are recruited to vDNA expressing ICP4 in a similar fashion (Figure 23). Moreover, ISG induction in ΔICP0 HSV-1 infected cells was impaired in the absence of PML (Figure 39). Correspondingly, the yield of ΔICP0 HSV-1 was not enhanced upon JAK inhibition in PML-depleted cells (Figure 37). These findings identify PML as a key innate immune regulator during HSV-1 infection. PML-mediated ISG induction during DNA virus infections (e.g., HCMV and VSV) and exogenous IFN treatment has been previously reported (Kim and Ahn 2015, Scherer et al. 2015, El Asmi et al. 2014, Chee et al. 2003, El Bougrini et al. 2011). Although the underlying mechanism for this process remains to be fully established, some mechanisms have been proposed (section 7.2.). The current knowledge supports a conserved role for PML in the regulation of innate immunity to viral infection.

Temporal regulation of intracellular Immunity to HSV-1 Infection

Intrinsic immunity (constitutive) ⊢ **HSV-1 ICP0** ⊣ **Innate immunity (inducible)**

- ✓ **Acts immediately upon genome delivery to the nucleus (minutes p.i.)**
- ✓ **Activation is dependent on the initiation of productive infection (hours p.i.)**

- ✓ **Induces viral genome silencing and represses the onset of replication**
- ✓ **Constricts viral propagation and limits the spread of infection**

✓ **PML is key for both aspects of immunity**

In summary, our data identify dual and temporal roles for PML in the sequential induction of intrinsic and innate immunity to HSV-1 infection. PML acts immediately upon viral genome delivery to the nucleus in order to suppress the onset of viral gene expression. Escape from this intrinsic immune defense and initiation of vDNA replication trigger the induction of innate immunity which constricts the viral propagation and limits the spread of infection in a PML-dependent manner. However, both arms of host defense are counteracted by the viral ubiquitin ligase ICP0 which targets PML and other immune factors for proteasome-dependent degradation during the course of HSV-1 infection

6. Defects in intrinsic and innate immunity correlate with the cell line permissiveness to ΔICP0 HSV-1 replication

6.1. Overview

Although ICP0 is not essential for HSV-1 replication, the growth of ΔICP0 is impaired in a cell type-dependent manner (Stow and Stow 1986, Yao and Schaffer 1995, Everett et al. 2004a). Cells have been described as either permissive (e.g., U2OS and SAOS-2) or restrictive (e.g., fibroblasts) based on their ability to support ΔICP0 HSV-1 replication. In HFt cells, the PFE defect of ΔICP0 HSV-1 was about 1000-fold in comparison to that in U2OS cells (Figure 17). The data presented in the first two result chapters demonstrate that HFt cells possess functional and effective intrinsic and immune responses to ΔICP0 HSV-1 infection that account for the replication defects in these cells. However, both arms of host intracellular immunity are efficiently counteracted by ICP0. These findings raised the question of whether permissive cell lines are unable to mount efficient immune responses to ΔICP0 HSV-1 infection which renders them more susceptible to infection. Alternatively, permissive cell lines may exhibit a cellular ICP0-like activity that complements the lack of ICP0. In this study, the first hypothesis was considered. The ability of restrictive (RPE and HaCaT) and permissive (U2OS and SAOS-2) cells to confer efficient intrinsic and innate immune responses during HSV-1 infection were assessed. HFt cells were included as a positive control for these studies. We mainly focused on the following: (i) comparing the viral replication efficiency in these cells; (ii) assessing the ability of these cells to recruit PML-NB associated restriction factors to infecting viral genomes upon nuclear entry; and (iii) investigating the efficiency of ISG induction in response to infection.

Consistent with the previous reports (Everett et al. 2004a, Stow and Stow 1986), our data demonstrated that HFt, RPE, and HaCaT cells restrict the onset of plaque formation of ΔICP0 but not WT HSV-1. U2OS cells fully complement ΔICP0 HSV-1 while SAOS-2 cells partially do so (Yao and Schaffer 1995). The

recruitment efficiency of PML-NB constituent proteins to vDNA was significantly impaired in permissive cell lines in comparison to restrictive cell types, demonstrating that entrapment of vDNA by PML-NBs correlates with the ability of infected cells to induce genome silencing. In agreement with a very recent report, U2OS and SAOS cells failed to induce robust ISG response to ΔICP0 HSV-1 infection (Deschamps and Kalamvoki 2017b). Interestingly, restrictive RPE and HaCaT cells also failed to robustly induce the expression of ISGs in response to ΔICP0 HSV-1 infection. These findings may explain the significant increase in ΔICP0 HSV-1 yields in RPE and HaCaT cells in comparison to HFt cells, although all three cell lines exhibited similar PFE. Importantly, the data highlight that nuclear entry of vDNA and its entrapment within PML-NBs is not enough to induce host innate immune response. The inability of RPE and HaCaT cells to induce ISG expression was not due to a defect in IFN-signaling, as they efficiently responded to different types of exogenous IFN treatment. More investigations are required to reveal the defects in RPE, HaCaT, U2OS, and SAOS cells that prevent them from inducing robust ISG expression in response to ΔICP0 HSV-1 infection. Collectively, these data demonstrate that the inability to mount efficient intrinsic or innate responses correlates with the cell line permissiveness to ΔICP0 HSV-1 infection.

6.2. Results

6.2.1. Host cells restrict ΔICP0 HSV-1 replication in a cell type-dependent manner

The PFE of both WT and ΔICP0 HSV-1 was assessed in five cell lines (HFt, RPE, HaCaT, U2OS, and SAOS). Of these, U2OS and SAOS-2 cells have been described historically as permissive to ΔICP0 HSV-1 infection (Yao and Schaffer 1995, Everett et al. 2004a). Cells were seeded overnight and infected with either WT or ΔICP0 HSV-1. Following an hour of viral absorption, cells were overlaid with the appropriate media containing 2% HS (Table 6). Infected cells were fixed and permeabilized at 24 hours post-infection, and immune-staining plaque assay was conducted. WT HSV-1 showed relatively equivalent PFE in the different cell types (Figure 40). However, the plaque formation of ΔICP0 HSV-1 was significantly restricted in HFt, RPE, and HaCaT cells versus U2OS and SAOS (Figure 40). Although the PFE of ΔICP0 HSV-1 was comparable in restrictive cell lines (approximately 1000-fold less than U2OS cells), the viral yields at 48 hours post-infection were significantly higher in RPE and HaCaT cells in comparison to HFt cells (Figure 41). These results raised the hypothesis that some cell types may not confer equally effective intrinsic and innate immune responses to ΔICP0 HSV-1 infection that render them more permissive to infection.
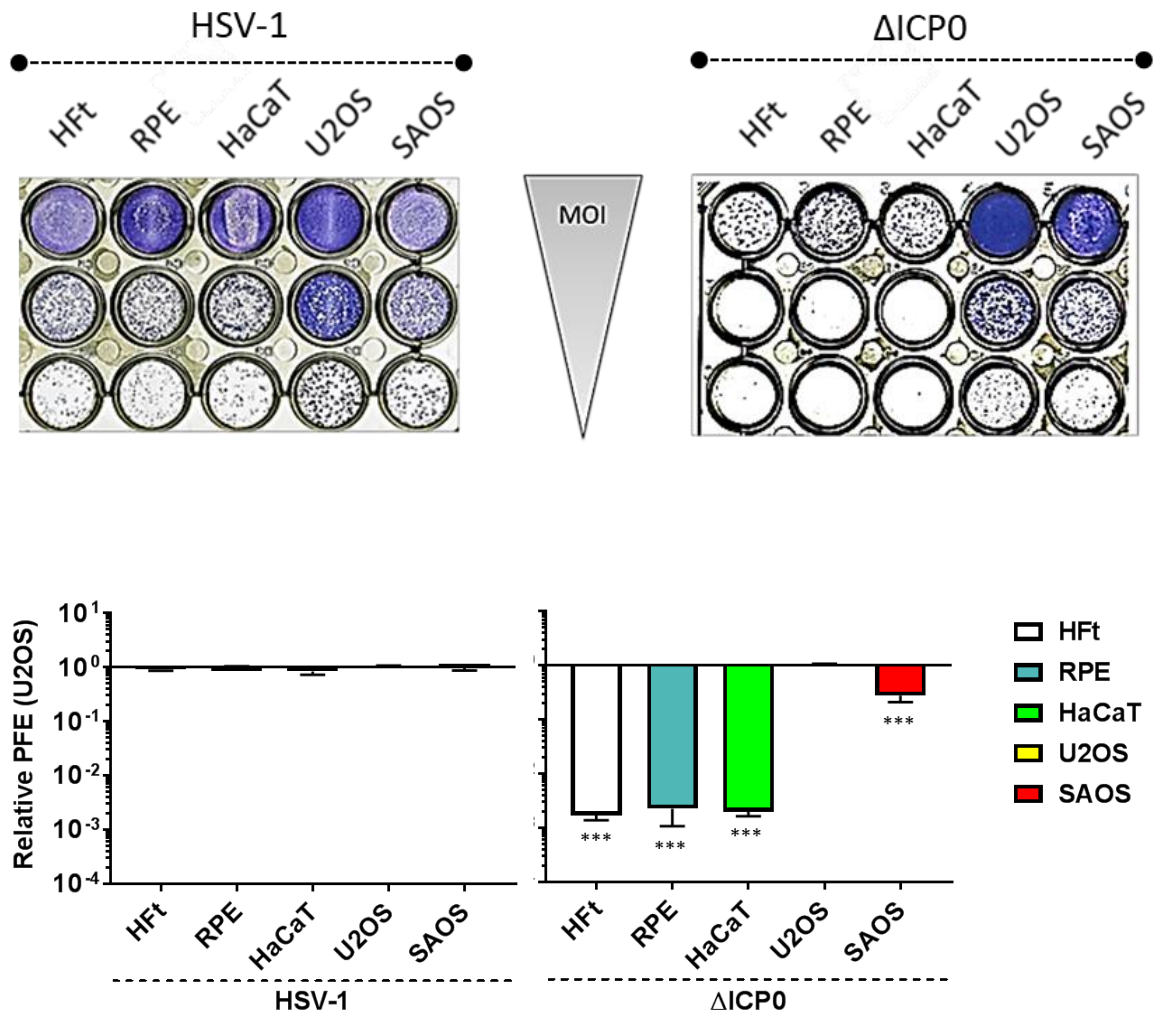
Figure 40. Host cells restrict the PFE of ΔICP0 HSV-1 infection in a cell type-dependent manner.

Cells were seeded overnight and infected with serial dilutions of either WT or ΔICP0 HSV-1. Following an hour of viral absorption, cells were overlaid with complete media containing 2% HS. At 24 hrs post-infection, cells were fixed and permeabilized and immune-staining plaque assay was conducted. Plaque numbers were counted under a plate microscope. Bar graphs show the numbers of plaques relative to U2OS cells. Results represent relative mean and SD (n=3). *** P = < 0.001; unpaired T-test.
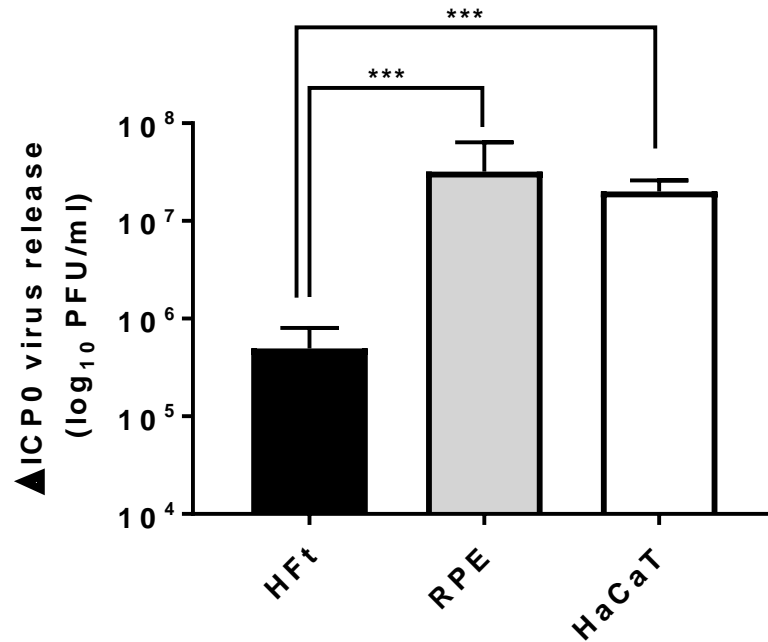
Figure 41. Enhanced viral yields of ΔICP0 HSV-1 in RPE and HaCaT cells in comparison to HFt cells.

Cells were seeded overnight and infected with ΔICP0 HSV-1 at MOI of 1 PFU/cell. Following an hour of viral absorption, cells were overlaid with complete media. Supernatants were collected at 48 hrs post-infection, and viral titers were determined on U2OS cells. Bar graphs represent mean and SD; n=3. *** P = < 0.001; unpaired T-test.

6.2.2. The efficient recruitment of PML-NB associated restriction factors to vDNA occur in a cell type-dependent manner

In order to investigate the ability of restrictive and permissive cell types to confer efficient intrinsic immunity to HSV-1 infection, the recruitment of PML and Daxx to EdU-labeled vDNA was assessed. Cells were seeded overnight onto coverslips and infected with HSV-1^{EdU} at an MOI of 3 PFU/cell. The coverslips were fixed and permeabilized at 90 mpi. vDNA was detected by click chemistry, host factors (PML and Daxx) were detected by indirect IF staining, and nuclei were visualized by DAPI. Both PML and Daxx were efficiently recruited to vDNA in HFt cells demonstrated by high weighted colocalization coefficient (> 0.7) between host factors and vDNA. Similarly, RPE and HaCaT cells exhibited a strong colocalization coefficient between host factors (PML and Daxx) and vDNA. However, the recruitment efficiency of PML and Daxx to vDNA was significantly impaired in U2OS and SAOS cells. We also noted that the weighted colocalization coefficient between PML and Daxx was significantly lower in permissive cell lines in comparison to restrictive cell types (Figure 42). These data identify a correlation between recruitment PML-NB proteins to vDNA and the ability of infected cells to restrict ΔICP0 HSV-1 plaque formation.

It was previously reported that both U2OS and SAOS lack ATRX, a PML-NB associated restriction factor (Lovejoy et al. 2012, McFarlane and Preston 2011). To determine the importance of ATRX in the entrapment of vDNA within PML-NBs, the recruitment of PML to vDNA was investigated in ATRX-depleted HFt cells and their relative controls. ATRX depletion significantly influenced the recruitment of PML to vDNA, demonstrating a key role for ATRX in the entrapment of vDNA within PML-NBs (Alandijany et al. 2018).

(A)
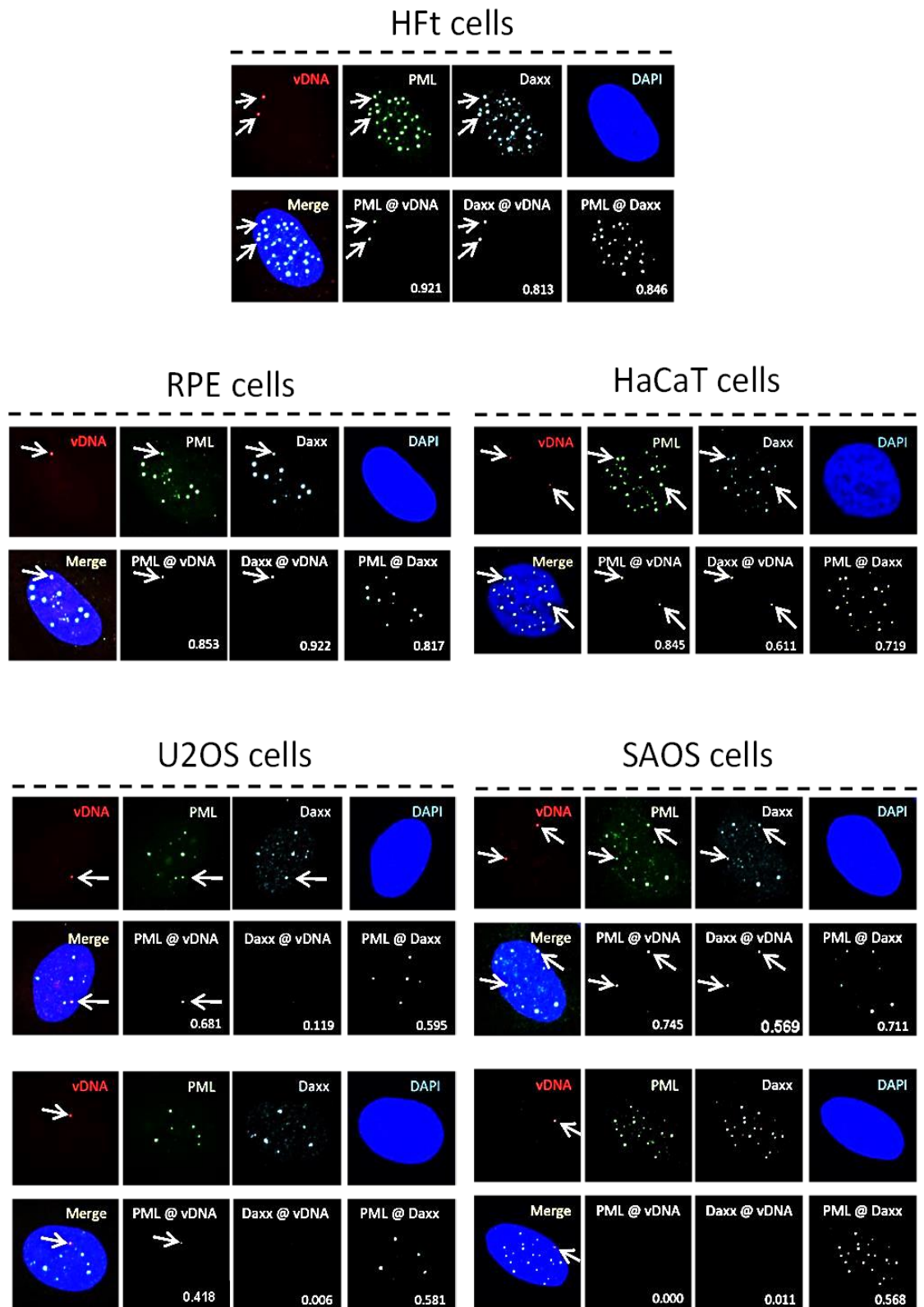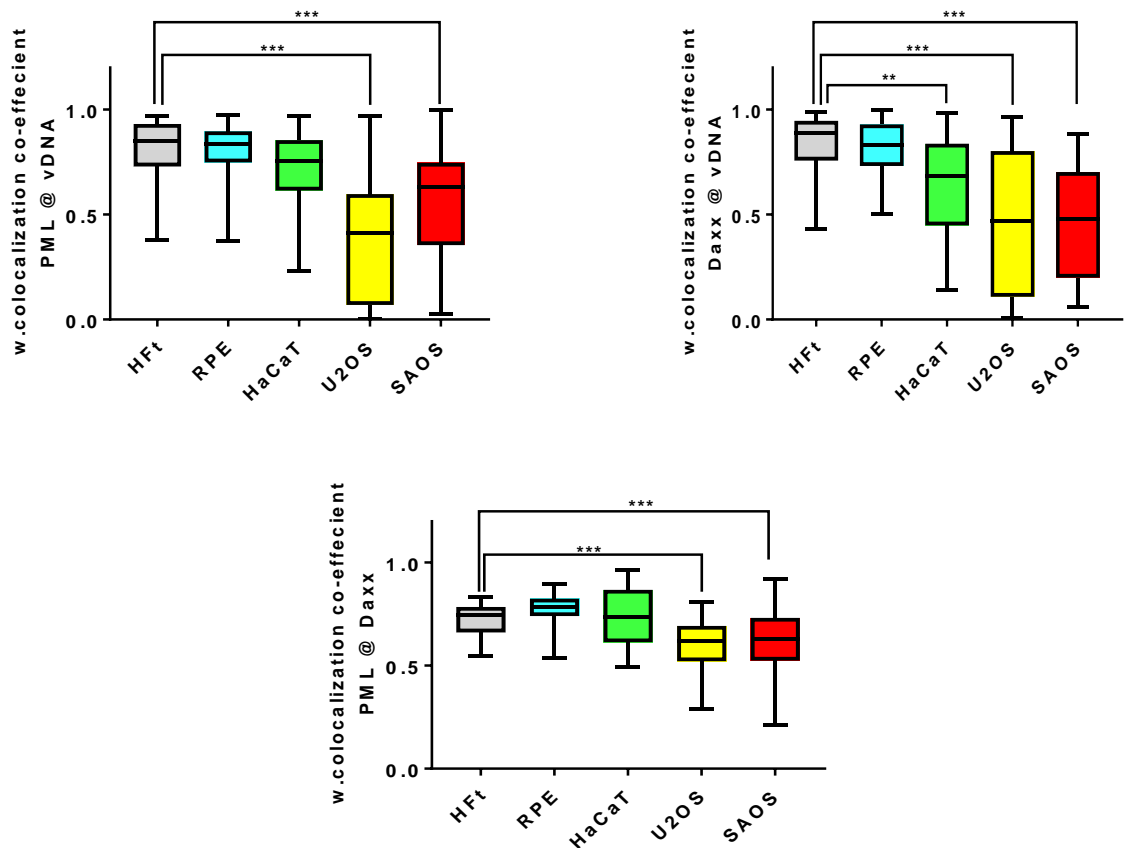
Figure 42. PML-NB constituent proteins (PML and Daxx) are efficiently recruited to infecting viral genomes in a cell type-dependent manner.

Cells were infected with HSV-1^{EdU} at an MOI 3 of PFU/cell. Infected monolayers were fixed and permeabilized at 90 mpi. Viral genomes and host factors were labeled by click chemistry and indirect IF staining protocols, respectively. Nuclei were visualized by DAPI. (A) Representative confocal microscopy images showing the nuclear localization of PML (green) and Daxx (cyan) to vDNA (red; highlighted by the white arrows). The cut mask highlights regions of colocalization between host factors and vDNA (as indicated). Weighted (w.) colocalization coefficients are shown. (B) Quantitation of host factor colocalization with each other and with infecting viral genomes. Boxes: 25th to 75th percentile range of sample; black line: median; whiskers: Min and Max range of samples. n ≥ 25 viral genomes from two independent experiments. *** P = < 0.0001; Mann-Whitney U-test.

6.2.3. The induction of ISG expression in response to ΔICP0 HSV-1 infection occurs in a cell type-dependent manner

ΔICP0 HSV-1 infection leads to robust induction of ISGs in HFt cells (Figure 26 and 27). This induction of innate immune response subsequently constricts the viral propagation (Figure 35). Previous reports demonstrated enhanced viral yields of ΔICP0 HSV-1 in U2OS and SAOS cells in comparison to Vero cells (Yao and Schaffer 1995, Deschamps and Kalamvoki 2017b). In this study, the viral yields of ΔICP0 HSV-1 in RPE and HaCaT cells were significantly greater than HFt cells (Figure 41). Thus, we asked whether permissive (U2OS and SAOS) and other restrictive (RPE and HaCaT) cell lines can or cannot stimulate efficient ISG induction in response to ΔICP0 HSV-1 infection.

Cells were seeded overnight and infected with either WT or ΔICP0 HSV-1 at an MOI of 1 PFU/cell. Mock and IFNß (100 IU/ml)-treated cells were included as a negative and positive control for ISG induction, respectively. The induction of ISG mRNA and protein levels was assessed at 9 hrs and 16 hrs post-infection, respectively. ΔICP0 HSV-1 stimulated robust induction of ISG mRNA and protein levels in HFt cells while WT HSV-1 impaired this host response. Interestingly, all other cell lines (RPE, HaCaT, U2OS, and SAOS) failed to prompt the induction of ISGs in response to both WT and ΔICP0 HSV-1 infection, although responded to exogenous IFNß treatment (Figure 43 and 44). Correspondingly, ruxolitinib treatment of the infected cell monolayers enhanced the viral yields of ΔICP0 HSV-1 in HFt cells, but failed to do so in the other cell types (Figure 45).

Collectively, these data demonstrate that although RPE and HaCaT cells efficiently recruited PML-NB associated restriction factors to vDNA and restricted the onset of ΔICP0 HSV-1 replication, they fail to induce ISG expression in response to ΔICP0 HSV-1 infection under MOI conditions that saturate host intrinsic immunity. U2OS and SAOS cells are defective in both intrinsic and innate arms of host immunity which renders them highly permissive to ΔICP0 HSV-1 infection.

(A)

(B)

(C)
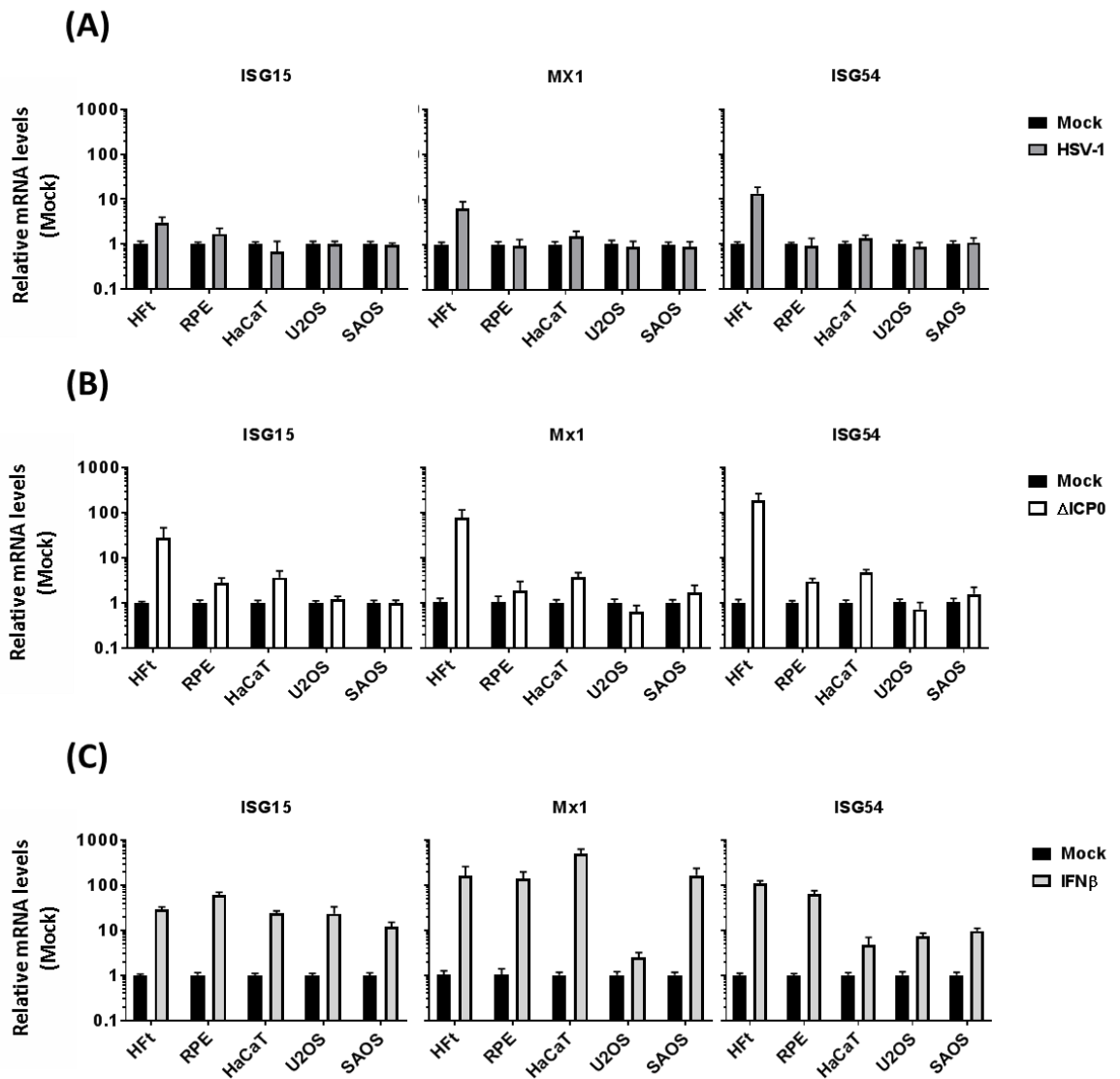
Figure 43. ΔICP0 but not WT HSV-1 infection induces ISG transcription in a cell type-dependent manner.

Cells were mock, treated with IFNβ (100 IU/ml), or infected with either WT or ΔICP0 HSV-1 (MOI of 1 PFU/cell). Samples were collected at 9 hrs post-infection. Bar graphs show the mRNA levels of MX1, ISG15, and ISG54. The levels of mRNA were determined using the TaqMan system of quantitative RT-PCR. Values were normalized to GAPDH mRNA level, internal control, using the threshold cycle (ΔΔCT) method and expressed relative to the normalized level of mRNA in the mock sample. Results represent means of relative quantitation (RQ) and SD; n ≥ 2.
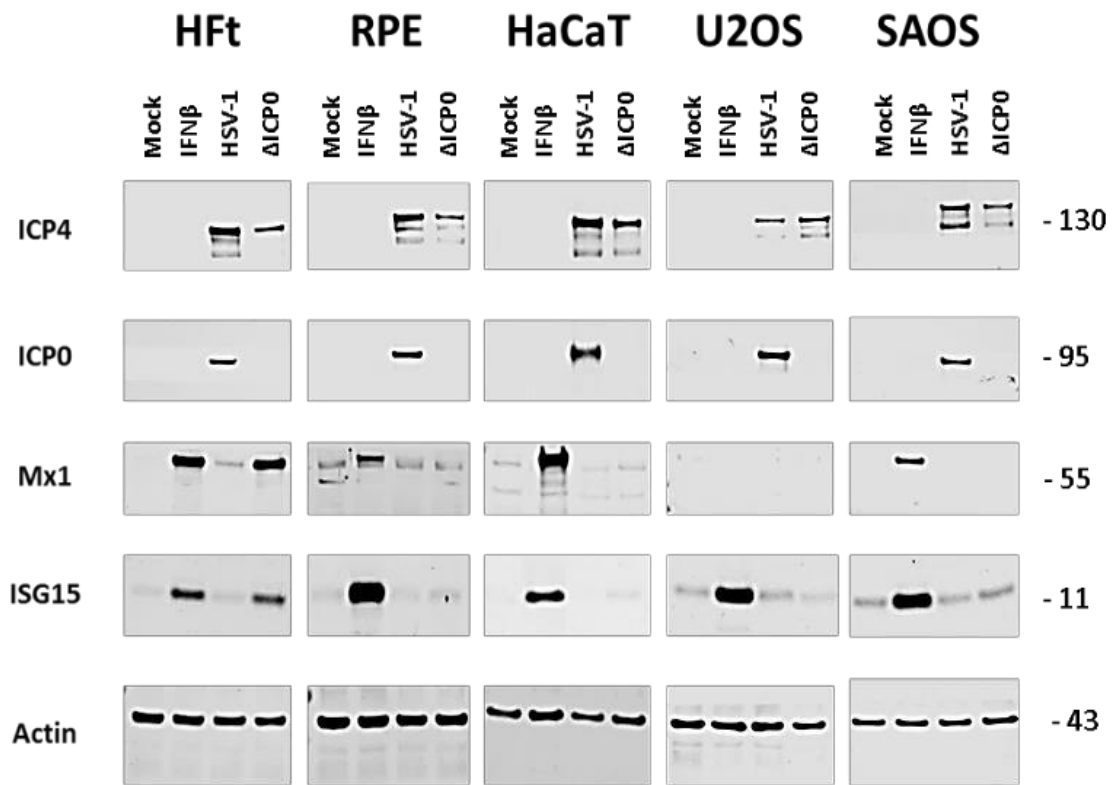
Figure 44. ΔICP0 but not WT HSV-1 infection induces ISG protein levels in a cell type-dependent manner.

Cells were infected with WT or ΔICP0 HSV-1 (MOI of 1 PFU/cell). Mock cells and IFNβ (100 IU/ml)-treated cells were included as a negative and positive control, respectively. Samples were collected at 16 hrs post-infection. Membranes were probed for the viral proteins (ICP0 and ICP4) to track the progress of infection, MX1 and ISG15 were used to monitor the effect of infection on ISG induction, or actin (as a loading control). Molecular mass markers are shown.
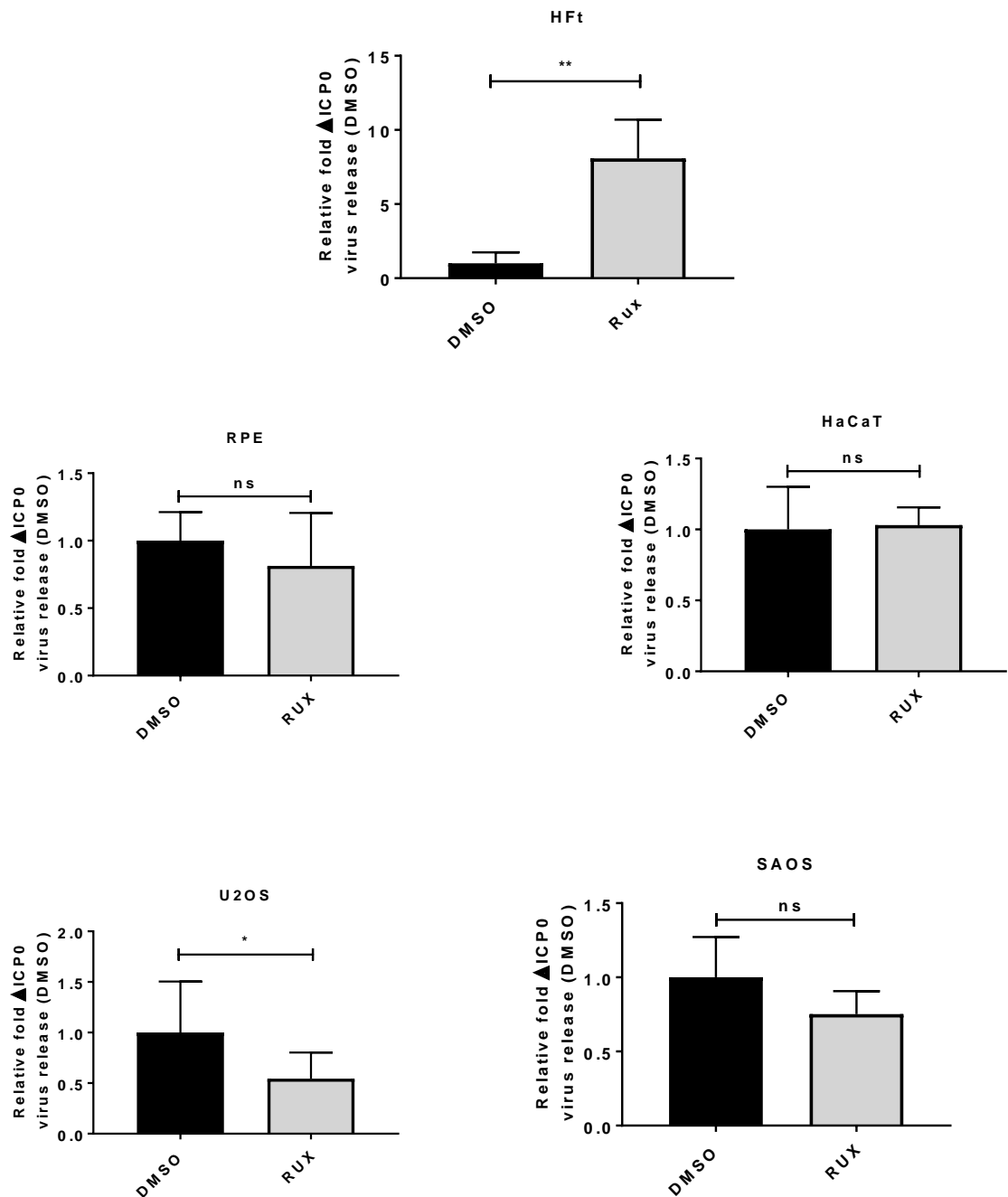
Figure 45. Inhibition of JAK signaling, using ruxolitinib, enhanced ΔICP0 HSV-1 yields in a cell type-dependent manner.

Cells were seeded overnight and infected with ΔICP0 HSV-1 (MOI of 1 PFU/cell). Following an hour of viral absorption, cells were overlaid with media containing either DMSO or ruxolitinib (Rux; 5 μM). Supernatants were collected at 48 hrs post-infection, and viral titers were determined on U2OS cells. Results represent relative mean and SD; n=3. * $P \leq 0.05$, ** $P \leq 0.01$, ns = non-significant; paired T-test.

6.2.4. The inability of RPE and HaCaT to induce ISGs expression was not due to a defect in IFN signaling pathway

The induction of innate immunity during HSV-1 infection occurred in an ICP0- and cell type-dependent manner. Although HFt, RPE, and HaCaT cells were restrictive to ΔICP0 HSV-1 infection, only HFt cells were capable of inducing ISG expression in response to ΔICP0 HSV-1 infection. All three cell types, however, responded to the exogenous IFNß treatment indicating that these cells are not defective in IFN signaling pathway. It is known that IFN functions in both autocrine and paracrine fashions. Hence, cells that are unable to induce innate immunity themselves might still be protected and armed against infection via cytokine secretion mediated by adjacent cells. To test this hypothesis, we assessed the effect of pre-immune stimulation by exogenous IFN (type I, type II, or type III) treatment on the viral PFE in all three cell lines (HFt, RPE, and HaCaT). Cells were seeded and treated with different types and concentrations of IFN for 24 hours before infection with WT (MOI of 0.002 PFU/cell) or ΔICP0 HSV-1 (MOI of 1 PFU/cell). Following an hour of viral absorption, cells were overlaid with media containing IFN and 2% HS. Immuno-staining plaque assay was conducted at 24 hrs post-infection.

In HFt cells, both WT and ΔICP0 HSV-1 were sensitive to IFN type I (IFNα and IFNß) treatment. Consistent with the previous reports (Eidson et al. 2002, Mossman et al. 2000), ΔICP0 was more sensitive than WT HSV-1 to IFN-mediated restriction at equivalent concentrations of IFN treatment (Figure 46 and 47). Indeed, the PFE of ΔICP0 HSV-1 was substantially reduced in response to both type I and type II IFN treatments, even at very low concentrations (0.003 and 0.05 ng/ml, respectively). WT HSV-1 was sensitive to type I IFN but only at higher concentration (≥ 0.3 ng/ml). The PFE of WT virus was only moderately inhibited in IFNγ-treated cells even at very high concentration (50 ng/ml). These data support previous findings (Harle et al. 2002, Klotzbucher et al. 1990, Mossman and Smiley 2002), and suggest that HSV-1 directly or indirectly antagonizes IFNγ- and, to a lesser extent, IFNα- and ß-mediated antiviral

responses through the expression of ICP0. Notably, neither WT nor ΔICP0 HSV-1 was influenced by IFNλ pre-treatment (Figure 46 and 47).

Next, we assessed the PFE of WT HSV-1 in IFN-treated RPE and HaCaT cells. RPE cells recapitulated the data obtained from HFt cells (Figure 48). IFNα and IFNß reduced the plaque numbers in a dose-dependent manner. IFNγ moderately inhibited HSV-1 plaque formation. IFNλ also failed to induce an effective antiviral response in RPE cells.

In HaCaT cells, a dose-dependent reduction in plaque numbers was observed in response to all types of IFN treatment (IFNα, ß, γ, and λ) (Figure 49). WT HSV-1 was remarkably sensitive to IFNγ treatment in HaCaT cells even at a very low concentration (0.005 ng/ml), a phenotype that was not observed in HFt and RPE cells. However, as previously reported, substantial cell death in HaCaT cells treated with IFNγ at a concentration of > 0.5 ng/ml was observed (Henseleit et al. 1996). This phenotype was not observed with other IFN treatments or cell types. Interestingly, HaCaT cells were responsive to IFNλ treatment, and the PFE of HSV-1 was inhibited in a dose-dependent manner.

Collectively, these data demonstrate that cells which lack the ability to induce innate immunity in response to infection (HaCaT and RPE cells) are not defective in IFN signaling in response to exogenous IFN stimulation. Hence, these cells can be armed against HSV-1 infection via cytokine secretion mediated by neighboring immune cells.
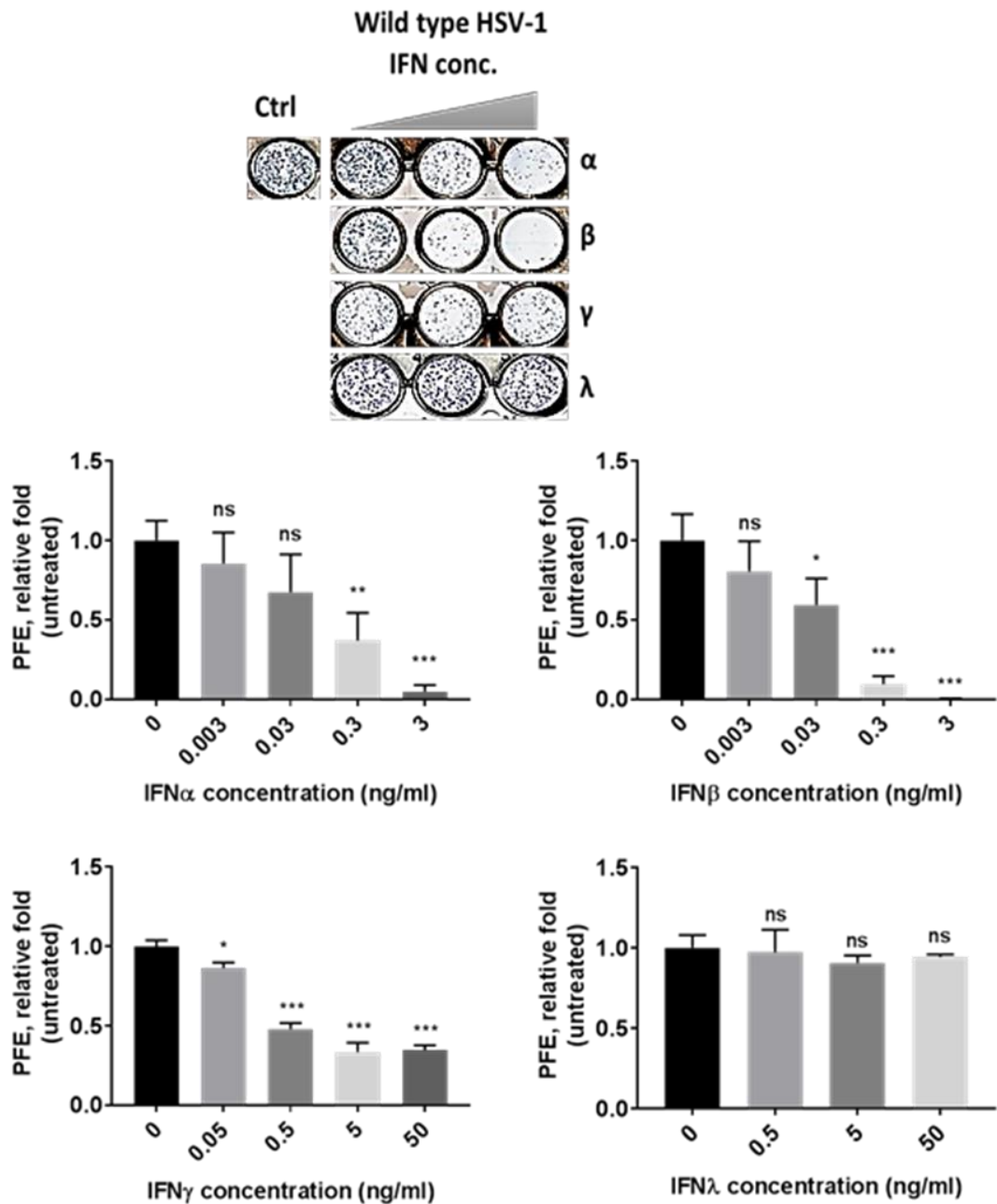
Figure 46. IFN type I and type II, but not type III, inhibited the PFE of WT HSV-1 in HFt cells.

Cells were untreated or treated with the indicated concentrations of IFNα, IFNß, IFNγ, or IFNλ for 24 hrs. The following day, treated cells were infected with WT HSV-1 (MOI of 0.002 PFU/cell). After an hour of viral adsorption, cells were overlaid with media containing IFN and 2% HS. At 24 hours post-infection, cells were fixed and permeabilized, and immune-staining plaque assay was conducted. Bar graph shows fold inhibition in plaque numbers in IFN-treated cells relative to untreated control. Results represent mean + SD; n= 3. * P ≤ 0.05, ** P ≤ 0.01, *** P ≤ 0.001, ns = non-significant; paired T-test.

Figure 47. IFN type I and type II, but not type III, inhibited the PFE of ΔICP0 HSV-1 in HFt cells.

Cells were untreated or treated overnight with the indicated concentrations of IFNα, IFNß, IFNγ, or IFNλ for 24 hrs. The following day, treated cells were infected with ΔICP0 HSV-1 (MOI of 1 PFU/cell). After an hour of viral adsorption, cells were overlaid with media containing IFN and 2% HS. At 24 hours post-infection, cells were fixed and permeabilized, and immune-staining plaque assay was conducted. Bar graph shows fold inhibition in plaque numbers in IFN-treated cells relative to untreated control. Results represent mean + SD; n= 3. * P ≤ 0.05, ** P ≤ 0.01, *** P ≤ 0.001, ns = non-significant; paired T-test.
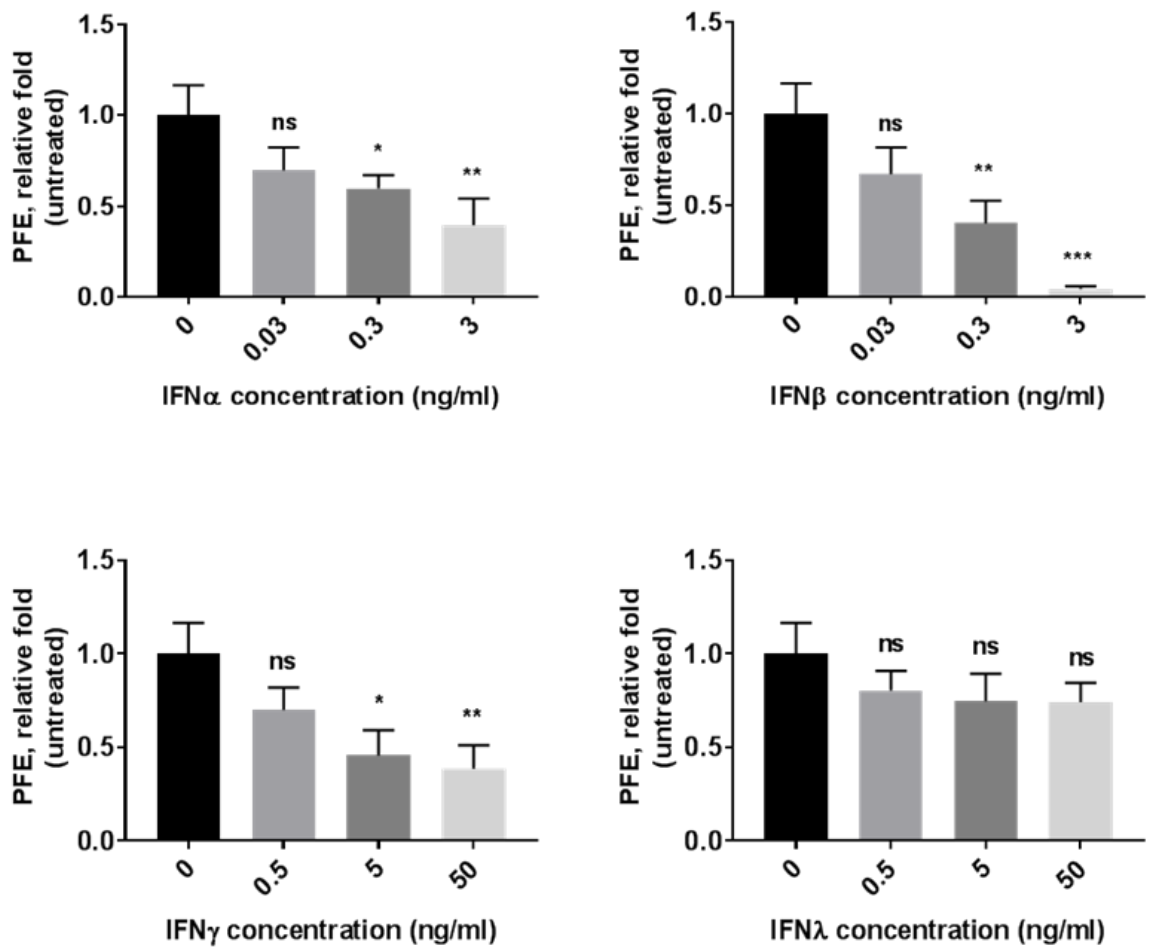
Figure 48.IFN type I and type II, but not type III, inhibited the PFE of WT HSV-1 in RPE cells.

Cells were untreated or treated with the indicated concentrations of IFNα, IFNß, IFNγ, or IFNλ for 24 hrs. The following day, treated cells were infected with WT HSV-1 (MOI of 0.002 PFU/cell). After an hour of viral adsorption, cells were overlaid with media containing IFN and 2% HS. At 24 hours post-infection, cells were fixed and permeabilized, and immune-staining plaque assay was conducted. Bar graph shows fold inhibition in plaque numbers in IFN-treated cells relative to untreated control. Results represent mean + SD; n= 3. * P ≤ 0.05, ** P ≤ 0.01, *** P ≤ 0.001, ns = non-significant; paired T-test.
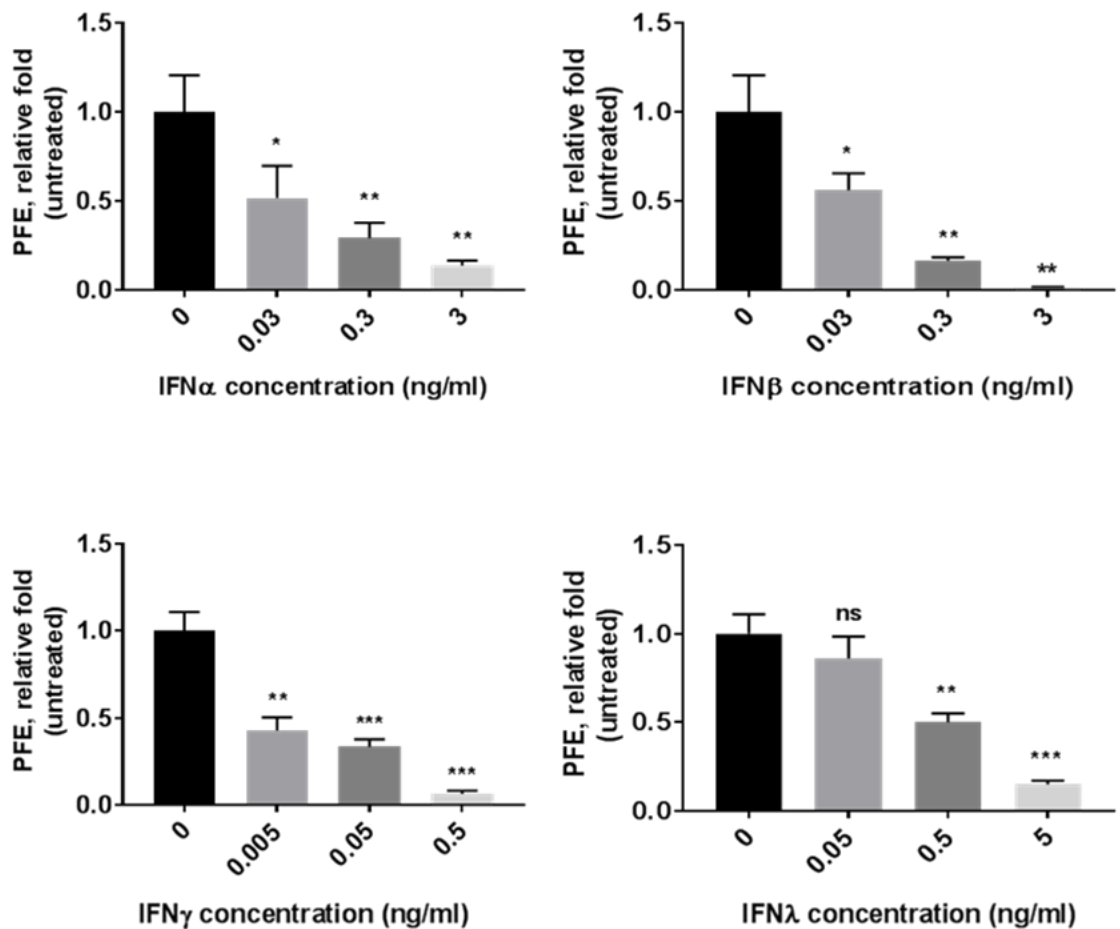
Figure 49. IFN type I, type II, and type III inhibited the PFE of WT HSV-1 in HaCaT cells.

Cells were untreated or treated with the indicated concentrations of IFNα, IFNß, IFNγ, or IFNλ for 24 hrs. The following day, treated cells were infected with WT HSV-1 (MOI of 0.002 PFU/cell). After an hour of viral adsorption, cells were overlaid with media containing IFN and 2% HS. At 24 hours post-infection, cells were fixed and permeabilized, and immune-staining plaque assay was conducted. Bar graph shows fold inhibition in plaque numbers in IFN-treated cells relative to untreated control. Results represent relative mean + SD; n= 3. * P ≤ 0.05, ** P ≤ 0.01, *** P ≤ 0.001, ns = non-significant; paired T-test.

6.3. Summary

Intrinsic and innate immunity play key roles in the intracellular restriction of HSV-1 infection. These two arms of host immunity confer temporally and functionally distinct responses, but both are required to effectively control infection. As shown in the previous chapters, host cell restriction factors are recruited to vDNA upon nuclear entry leading to viral genome silencing. Following saturation of these intrinsic host factors, the innate immune response is triggered by the initiation of vDNA replication. ISG expression constricts viral propagation and limits the spread of infection. However, HSV-1 expresses ICP0 which counteracts both aspects of host antiviral immunity (Boutell and Everett 2013, Lanfranca et al. 2014, Gu 2016). Importantly, these conclusions were derived from works carried out on HFt cells, a cell type that is known to be highly restrictive to ΔICP0 HSV-1 infection (Everett et al. 2004a). Over two decades ago, it was shown that human osteosarcoma cells (U2OS and SAOS) are highly permissive to ΔICP0 HSV-1 infection. However, the mechanism(s) of how these cells support ΔICP0 HSV-1 infection has remained unclear (Yao and Schaffer 1995). Given that ICP0 is a major host immunity antagonist, we proposed that permissive cells might be defective in aspects related to intracellular immunity rendering them permissive to HSV-1 infection in the absence of ICP0.

We tested this hypothesis and found that permissive cells were defective in both intrinsic and innate antiviral responses (Figure 42-44). In comparison with restrictive cell lines (HFt, RPE and HaCaT), both U2OS and SAOS cells failed to efficiently recruit PML and Daxx to infecting vDNA (Figure 42). These observations were not due to defects in PML and Daxx expression, as all cell lines expressed similar protein levels (Alandijany et al. 2018). However, we visually noted that U2OS and SAOS cells might possess irregular PML-NBs, demonstrated by the poor colocalization between PML and Daxx (Figure 42). Moreover, permissive U2OS and SAOS cells lack ATRX, a chromatin-remodeling protein and a PML-NB associated restriction factor (Lukashchuk and Everett

2010). Depletion of ATRX in HFt cells not only enhanced the PFE of ΔICP0 HSV-1, but also significantly influenced the recruitment of PML to vDNA (Alandijany et al. 2018, Lukashchuk and Everett 2010). These findings demonstrated that efficient recruitment of PML is dependent on ATRX, and partially explained the defect in PML recruitment in permissive cell lines. The effect of ATRX ectopic expression on PML recruitment to vDNA in permissive cells was not investigated due to time constraints, but it remains an attractive experiment to consider.

U2OS and SAOS were not only defective in recruiting restriction factors to the viral genome foci, but also unable to efficiently induce innate immunity in response to ΔICP0 HSV-1 infection. Neither U2OS nor SAOS could induce ISG expression during ΔICP0 HSV-1 infection, although both cell lines responded to IFNβ treatment (Figure 43 and 44). During our study, a research article was published supporting these findings that U2OS and SAOS cells fail to induce ISG expression in response to ΔICP0 HSV-1 infection (Deschamps and Kalamvoki 2017b). This process was linked to the low expression level of STING in these cells. Ectopic expression of STING partially restored innate immunity in U2OS cells. On the other hand, overexpression of IFI16 failed to so, although it conferred intrinsic repression to viral infection (Deschamps and Kalamvoki 2017b). It is likely that permissive cell lines are defective in multiple aspects related to host immunity and further investigations are required to reveal them.

Interestingly, our data identified cell types to be restrictive for ΔICP0 HSV-1 plaque formation but defective in inducing ISG expression in response to infection. Both RPE and HaCaT cells efficiently recruited restriction factors (PML and Daxx) to the infecting viral genomes, and this recruitment correlated with restriction in plaque formation of ΔICP0 HSV-1 (Figure 40 and 42). Unlike HFt cells, they failed to substantially induce ISGs expression in response to ΔICP0 HSV-1 infection (Figure 43 and 44). These observations may explain the enhanced viral yields in these cells in comparison to HFt cells, although all three cell lines exhibit similar PFE (Figure 40 and 41). The entrapment of vDNA within PML-NBs and restriction of plaque formation without induction of ISG expression

demonstrates that intrinsic and innate immune responses are distinct from one another.

Although RPE and HaCaT cells were unable to induce ISG expression in response to ΔICP0 HSV-1 infection, they exhibited a strong response to IFNß treatment (Figure 43 and 44). Moreover, exogenous IFN treatment established effective antiviral responses in RPE and HaCaT cells similar to that observed in IFN-treated HFt cells (Figure 46-49). These findings demonstrate that cells unable to induce innate immunity themselves might still be protected and armed against viral infection via cytokine secretion mediated by neighboring immune cells (e.g., macrophages, NK cells, neutrophils, and DCs). Although RPE and HaCaT cells are not defective in IFN signaling pathways, they are still defective in aspects related to inducing innate immunity in response to infection. Failure of these cells to recognize PAMPs, or the inability to produce IFN are some hypotheses to consider for future research.

Host cells differentially express different types of IFN receptors. HFt, RPE, and HaCaT responded to IFN type I (α and β) and type II (γ) treatment, as demonstrated by the significant inhibition of viral PFE in comparison to untreated controls (Figure 46-49). Fibroblast cells do not express IFNλ receptors which explains the lack of IFNλ-mediated antiviral effect in HFt cells (Figure 46 and 47) (Sommereyns et al. 2008, Palma-Ocampo et al. 2015). Epithelial cells derived from different organs (e.g., lung and gastrointestinal tracts) were previously shown to strongly respond to IFN-λ treatment (Sommereyns et al. 2008, Palma-Ocampo et al. 2015, Pott et al. 2011, Mordstein et al. 2010). Although we did not directly assess the ISG induction in RPE cells following IFNλ treatment, these epithelial cells failed to confer effective IFNλ-mediated antiviral response (Figure 48). This can be due to lack of IFNλ receptors or failure to induce the expression of effective ISG products. Unlike HFt and RPE, HaCaT cells were responsive to all types of IFN treatment, including IFNλ which provides an attractive model to directly compare the biological properties of different types of IFN (Figure 49). We noted cell death upon IFNγ treatment of HaCaT cells at concentration of ≥ 0.5 ng/ml. This is believed to be due to IFNγ-

induced DNA cleavage at the linker regions leading to apoptotic cell death (Henseleit et al. 1996, Maher et al. 2008). The effect of exogenous IFN treatment on viral PFE in U2OS and SAOS was not assessed due to time constraints. However, previous reports suggest that IFNα treatment substantially reduced ΔICP0 HSV-1 plaque formation in Vero cells but not U2OS cells. These findings demonstrated that U2OS lack the IFN-mediated antiviral effector(s) (Eidson et al. 2002). We noted that U2OS failed to induce Mx1 expression following IFNβ treatment (Figure 43 and 44). Mx1 is a well-established ISG product that is shown to confer antiviral response to many viral infections (Arnheiter and Haller 1988, Fernandez et al. 1997, Frese et al. 1996, Haller et al. 1995, Schneider-Schaulies et al. 1994, Staeheli et al. 1988). Mx1 is also one of the most highly upregulated ISG products in response to HSV-1 infection (Eidson et al. 2002). Hence, it is plausible to explore the role of Mx1 during HSV-1 infection and the effect of ICP0 expression on Mx1 function.

The fact that ΔICP0 HSV-1 was sensitive to exogenous IFN treatment was not surprising as this mutant lacks a major host immunity antagonist. However, WT HSV-1 was also sensitive to increased concentration of IFNs. Although these observations are not novel and have been reported a long time ago, this area of research is understudied (Gloger and Panet 1984, Oberman and Panet 1988). It remains unknown which ISG products are responsible for mediating antiviral response in the presence of ICP0 during WT HSV-1 infection. It is also unclear whether these effective ISG products are novel to HSV-1 or previously identified for other viruses. An alternative hypothesis is that IFN treatment possibly influences the biochemical activity of ICP0 directly, rendering WT HSV-1 sensitive to cellular immune factors that are usually targeted by ICP0. Considering these hypotheses should advance our understanding of the role of IFN and innate immunity during WT HSV-1 infection.

Collectively, these findings support our conclusions that intrinsic and innate immunity are separate branches of host intracellular immunity. The infected host requires intrinsic and innate immunity to efficiently restrict the onset of viral replication and limit the spread of the viral infection, respectively.

Cells that lack one or both aspects of these host antiviral responses are more permissive to infection. The expression of ICP0 can antagonize both aspects of host immunity. However, an IFN-mediated pre-induced antiviral state can protect host cells from WT HSV-1 infection. The underlying mechanism for this process is not clear, and requires further investigation.

7. Discussion

Host immunity plays a crucial role in controlling HSV-1 replication at primary sites of infection and in blocking genome reactivation from latency (Egan et al. 2013). During lytic infection, intrinsic and innate antiviral responses represent the first lines of host defense to infection (Komatsu et al. 2016, Lanfranca et al. 2014). The key finding of this study is that intrinsic and innate immune responses are separable by virtue of temporal induction at different stages of infection, and kinetically distinct effects on viral replication. The intrinsic response is mediated by pre-existing host cell restriction factors (e.g., PML-NB constituent proteins) which immediately recognize vDNA upon nuclear entry, and directly repress the onset of viral replication through the suppression of viral gene expression (Tavalai and Stamminger 2009, Boutell and Everett 2013, Geoffroy and Chelbi-Alix 2011). On the other hand, the induction of innate immune response (PRR-mediated IFN production and ISG expression) is triggered following the escape of viral genome from intrinsic silencing, and initiation of vDNA replication. The induction of ISG expression in the infected and neighboring uninfected cells inhibits viral propagation and limits the spread of infection (Paludan et al. 2011, Knipe 2015, Chew et al. 2009). The secretion of type I IFN is also known to activate and recruit immune cells (e.g., macrophages, NK cells, neutrophils, and DCs) to the site of infection (Pollara et al. 2004). Activated immune cells can directly restrict viral replication, induce apoptosis of infected cells, phagocytose apoptotic infected cells, produce type II IFN, and stimulate the adaptive immune response (Djeu et al. 1982, Cheng et al. 2000, Bosnjak et al. 2005, Kassim et al. 2006, Grubor-Bauk et al. 2008). Indeed, one of the main functions of DCs is to present viral antigens to CD4+ and CD8+ T cells which play a central role in maintaining the viral genomes in a latent state (Liu et al. 2000, Knickelbein et al. 2008, Pereira et al. 2000).

Our study advanced our understanding of the very early events in cellular response to HSV-1 infection prior to the initiation of viral gene expression (Alandijany et al. 2018). This sequential regulation of intracellular immunity

likely applies to other viral systems, particularly other herpesviruses susceptible to PML-NB repression, and worthy of investigation.

7.1. Click chemistry-mediated detection of vDNA as a tool to investigate key aspects and early events of viral replication

Microscopy and vDNA detection assays have had a great impact on advancing our understanding of many aspects related to viral infections (e.g., viral entry into host cells, host antiviral responses, and viral immune-evasion strategies). These methods provide analysis, dissection, and elucidation of virus-cell interaction pathways at a single-cell resolution. However, direct detection of vDNA under low MOI conditions with FISH and BrdU-labeling is technically challenging (Jensen 2014). Additionally, these assays can be incompatible with IF staining due to substantial sample processing and harsh treatment conditions (Greber et al. 1997, Nguyen et al. 2010, Wang et al. 2013a). These problems left many questions unanswered, particularly with regards to the temporal regulation of intrinsic and innate immune responses to infection. Click chemistry-mediated detection of ethynyl-tagged deoxynucleotide-labeled vDNA has solved this issue. This protocol allowed specific detection of EdU-labeled vDNA under low MOI and as early as 30 minutes post-addition of virus (Figure 11). Importantly, the protocol described in this study was associated with high labeling efficiency (more than 60% of genomes were labeled), and was not detrimental for viral infection (Alandijany et al. 2018). Moreover, it was compatible with indirect IF staining protocols and allowed investigation of host immune factor recruitment to infecting vDNA. We collected evidence that demonstrates sequential recruitment of host restriction factors (PML-NB constituent proteins) and PRRs (IFI16) to vDNA (Figure 12, 19, and 23). These findings inspired additional work which collectively allowed us to conclude that intrinsic and innate arms of intracellular immunity are temporally and functionally distinct from one another. It also allowed us to conclude that defect(s) in the recruitment of PML-NB constituent proteins to vDNA in some cell types correlates with their enhanced permissiveness to infection.

Bio-orthogonal chemistry detection of vDNA has many other applications that fall beyond the scope of this project (Sekine et al. 2017, Dembowski and DeLuca 2015). It provides a valuable tracking tool that allows detailed investigation and quantitative analysis of aspects related to early viral genome dynamics during lytic infection. Indeed, this technique has been recently utilized to investigate uncoating events of HSV-1 genomes, where temporal shifts in HSV-1 genome condensation have been observed upon viral genome delivery to the nucleus (Sekine et al. 2017). Viral genomes remained in a condensed state in the absence of active transcription. Active transcription induced "genome congregation" followed by de-condensation that was enhanced over time as the infection progressed (Sekine et al. 2017). Parallel analysis of alpha-, beta, and gamma-herpesviruses using click chemistry may provide a qualified comparison, with insight into the similarities and differences among different types of human herpesviruses in terms of nuclear uptake of viral genomes, intracellular trafficking, uncoating, and organization.

The utility of click chemistry-mediated detection of vDNA extends to tracing the fate of viral genomes and association with cellular proteins in latently/quiescently-infected cells which remain technically challenging at a molecular and single-cell level. This is key, as the establishment of latency and periodic reactivation represent important aspects in the life cycle of HSV-1 infection.

The major limitation of click chemistry-mediated detection of vDNA is the incompatibility with live cell microscopy. This is particularly important giving that virus-cell interactions are very rapid, often transient, and asynchronous. Developing a method to detect vDNA entry into the nucleus under conditions of synchronous delivery would be useful for this purpose. Overall, further development of minimally invasive labeling techniques of viral components, and advancement in microscopic imaging technology will provide valuable means for obtaining detailed mechanistic insights about the earliest stages of infection that have a significant bearing on the outcome of infection.

7.2. Multi-roles for PML in host immunity

PML-NBs play key roles in many vital cellular processes, such as tumor suppression, DNA repair, gene regulation, apoptosis, and antiviral response (Guan and Kao 2015, Geoffroy and Chelbi-Alix 2011, Tavalai and Stamminger 2009). In plaque-edge assays, PML-NB constituent proteins (PML, SP100, Daxx, ATRX, PIAS-1, and MORC3) have been shown to alter their nuclear distribution and become recruited to sites in close proximity of incoming ΔICP0 HSV-1 genomes. These recruitment phenotypes correlated with intrinsic antiviral activity and repression of viral replication (Brown et al. 2016, Everett et al. 2008, Everett et al. 2006, Glass and Everett 2013, Lukashchuk and Everett 2010). Although intrinsic repression has been shown to occur independently of IFN pathway, these recruitment phenotypes were reported under experimental setting that is now known to induce host innate immune response (Figure 25-27) (Everett et al. 2008). Click chemistry-mediated detection of vDNA enabled recruitment studies of host restriction factors to viral genomes under infection conditions that have not triggered the induction of innate immunity. PML-NB proteins are rapidly recruited to viral genomes as soon as they are delivered to the nucleus (90 mpi). 3D image reconstruction has demonstrated that vDNA is entrapped within PML-NBs in a similar fashion to that observed in quiescently or latently-infected cells (Figure 12) (Catez et al. 2012, Maroui et al. 2016, Everett et al. 2007). Importantly, this phenotype was observed during both WT and ΔICP0 HSV-1 infection. In order to release viral genomes entrapped within PML-NBs, HSV-1 expresses ICP0 which employs both SUMO-dependent and independent mechanisms to induce PML degradation leading to the dispersal of PML-NBs (Figure 16) (Chelbi-Alix and de The 1999, Everett et al. 1998, Everett and Maul 1994). This process is dependent on the ICP0 RING finger domain and attributable to its ubiquitin ligase activity (Boutell et al. 2002, Maul and Everett 1994).

It remains to be determined how HSV-1 genomes can express ICP0 if they are entrapped within PML-NBs upon nuclear entry (Figure 12). We have noticed

that PML localization to vDNA is less efficient at very early time points (15-60 minutes post-addition of virus) (Alandijany et al. 2018). Given that the tegument protein VP16 that drives ICP0 expression and vDNA are simultaneously delivered to the nucleus, one may expect that initiation of ICP0 expression occurs prior to PML-NB mediated entrapment (Gerster and Roeder 1988, Triezenberg et al. 1988). It is also known that PML-NBs are highly dynamic, with many transient proteins actively associating and dissociating from these bodies (Jensen et al. 2001, Chen et al. 2008). It is plausible, thereby, to speculate that vDNA has a chance to stimulate the transcription of ICP0 prior to silencing. Another hypothesis is that the release of entrapped viral genomes is mediated by ICP0 tegument-associated protein, although this is unlikely because *de novo* ICP0 is required for PML degradation (Delboy et al. 2010, Maul et al. 1996).

Under low MOI conditions, ΔICP0 HSV-1 remained entrapped in PML-NBs and failed to initiate plaque formation (Figure 17, 24, and 25). PML depletion enhanced the plaque formation of ΔICP0 (Figure 18). However, it did not fully complement for ICP0 function, demonstrating the presence of other host restriction factors which repress viral gene expression independently of PML (Glass and Everett 2013, Everett et al. 2008, Everett et al. 2006). Interestingly, the efficient recruitment of PML to vDNA was significantly influenced by ATRX depletion (Alandijany et al. 2018). This finding was important giving that permissive cell lines (U2OS and SAOS) lack ATRX protein, and the recruitment of PML to vDNA is impaired in these cells (Figure 42) (McFarlane and Preston 2011, Lukashchuk and Everett 2010, Alandijany et al. 2018). Collectively, our data identify a correlation between the stable entrapment of vDNA within PML-NBs and cell line permissiveness to ΔICP0 HSV-1 infection.

Importantly, entrapment of ΔICP0 HSV-1 vDNA within PML-NBs in restrictive cells occurred in the absence of PRR IFI16 recruitment and ISG induction (Figure 19 and 25). These findings reveal that vDNA entry into the nucleus alone is not sufficient to induce host innate immunity. Saturation of intrinsic immunity at a high MOI, which enables plaque formation, stimulated IFI16 recruitment and ISG expression (Figure 23-25). Notably, the nuclear

distribution of PML is altered under these conditions. PML forms string-like structures at vDNA replication compartments within the body of a developing plaque, while localizes to sites of incoming viral genomes in newly infected cells (Figure 23) (Everett et al. 2004b). Cytoplasmic translocation of PML has also been reported (Burkham et al. 2001). Such findings raise the possibility of other antiviral roles mediated by PML during HSV-1 infection. Indeed, the efficient induction of ISGs during HSV-1 infection was dependent on the presence of PML (Figure 39). Correspondingly, JAK inhibition failed to enhance ΔICP0 HSV-1 yields in the absence of PML (Figure 37). These data identify PML as a key regulator of innate immunity during HSV-1 infection. Previous studies have demonstrated an important role for PML in the induction of ISG expression in response to exogenous IFN treatment and other viral infections (Atwan et al. 2016, Chen et al. 2015, Scherer and Stamminger 2016, Scherer et al. 2015, Kim and Ahn 2015, El Asmi et al. 2014). PML.IV has been shown to interact with peptidyl-prolyl isomerase Pin1 and recruit it to PML-NBs in order to inhibit the degradation of activated IRF-3 and sustain ISG induction (El Asmi et al. 2014). Another study suggested that PML.II stimulates the recruitment of IRF3 to type I IFN promoter and enhances IFN production. It also enhances the binding of NF-κB/STAT1/CBP transcriptional complex to ISG promoters (Chen et al. 2015). The key role of PML in regulating host innate immunity extends to type II IFN-mediated response, as PML has been shown to enhance STAT1 phosphorylation and binding to gamma-activated receptors on IRF1 (El Bougrini et al. 2011, Scherer et al. 2015). The fact that IFNγ plays a critical role in modulating adaptive immunity suggests that PML might also have a role in regulating adaptive immune factors. In support of this hypothesis, it has been shown that PML.II interact with class II transactivator (CIITA) and recruits it to PML-NBs. This process prevents CIITA from proteasome-dependent degradation, induces IFNγ-mediated expression of MHC class II, and enhances antigen presentation to T cells (Gialitakis et al. 2010). The presence of PML also seems important for efficient activation and differentiation of T cells and B cells (Lai et al. 2016).

Collectively, these reports demonstrated the emerging multi-roles of PML in modulating different factors of host immunity, particularly with regards to the

regulation of IFN signaling cascade. However, it is unclear how post-translational modifications of PML can affect PML-mediated ISG induction. It is also unclear whether infected host cells induce alternative splicing to favor expression of specific isoforms. These hypotheses are important given that PML clearly alters its subcellular localization and PML-NB organization under infection conditions that stimulate host innate immune response (Figure 23) (Everett et al. 2004b, Burkham et al. 2001). Another potential mechanism by how PML mediates IFN production and ISG expression is through the epigenetic regulation of ISG promoters taking into consideration that many PML-NB proteins (e.g., Daxx, ATRX, and HIRA) have major roles in histone deposition (Rai et al. 2017, Delbarre et al. 2017, Salomoni 2013).

To sum up, PML is not just an intrinsic repressor. Instead, it is a regulator that facilitates the coordination of all three branches of host immunity (intrinsic, innate, and adaptive). Further investigations are required to fully understand the underlying mechanisms for these processes. The viral ubiquitin ligase ICP0 disrupts PML-NBs not only to overcome intrinsic immunity, but also to interfere with IFN- and other cell-mediated immune responses.

7.3. ISG products play a key role in the intracellular restriction of HSV-1 replication

Innate immunity, unlike intrinsic immunity, is induced in response to infection. Central to this arm of immunity are PRRs which collectively contribute to the induction of IFN production and ISG expression (Knipe 2015, Paludan et al. 2011). vDNA is one of the most potent inducers of innate immunity. Several cytosolic vDNA sensors (e.g., DHX9, DHX36, and cGAS) have been identified. (Kim et al. 2010, Sun et al. 2013). However, these sensors have limited access to vDNA in the cytoplasm of most cell types due to the presence of viral capsids (Miyamoto and Morgan 1971, Pasdeloup et al. 2009, Sodeik et al. 1997, Wolfstein et al. 2006). In recent years, the PYHIN protein IFI16 has received significant

attention due to its ability to sense nuclear and cytosolic vDNA (Cuchet-Lourenco et al. 2013, Diner et al. 2016, Orzalli et al. 2012, Unterholzner et al. 2010). IFI16 acts as a cytosolic sensor in macrophages where the viral capsid is targeted for proteasome-dependent degradation in the cytoplasm exposing the vDNA for recognition (Horan et al. 2013). In fibroblasts, however, the nuclear import of viral genomes is necessary for IFI16-mediated sensing (Orzalli et al. 2012). IFI16 is nuclear diffuse in human fibroblasts (Figure 19 and 21). ChIP analyses demonstrate a direct interaction between vDNA and IFI16 (Johnson et al.) (Johnson et al. 2014). Microscopy studies showed transient IFI16 puncta which were formed at the nuclear periphery of infected cells (Diner et al. 2016, Everett 2015). It was proposed that these IFI16 puncta were localized to infecting viral genomes as soon as they are delivered to the nucleus. However, no direct evidence of vDNA was shown in these studies, and the number of IFI16 puncta observed did not correlate with the MOI (MOI of 10 to 50 PFU/cell) used. Regardless, applying such high MOI conditions is known to saturate intrinsic immunity and, thus, is suboptimal to study the temporal regulation of intrinsic and innate immunity (Everett et al. 2004a). One of the main advantages of our study is the direct detection of vDNA under low MOI conditions. Under these experimental settings, we have collected evidence that IFI16 is not stably recruited to infecting viral genomes upon their delivery to the nucleus (Figure 19) (Alandijany et al. 2018). Instead, IFI16 is only stably localized to vDNA that initiated productive infection, as demonstrated by ICP4 protein expression (Figure 23). Previous plaque-edge recruitment studies showed that IFI16 is localized to ICP4 dot-like complexes that are known to contain vDNA (Cuchet-Lourenco et al. 2013, Orzalli et al. 2013). Our modified plaque-edge recruitment assay agreed with these findings, but also showed that IFI16 failed to recognize viral genomes that are yet to initiate viral gene expression (Figure 23) (Alandijany et al. 2018). Length and structure, but not nucleotide content, of vDNA are crucial for IFI16-mediated sensing and ISG induction (Unterholzner et al. 2010). Indeed, IFI16 has high affinity to high order DNA structures (e.g., DNA Quadruplex) which are accumulated in abundance during vDNA replication (Artusi et al. 2016, Haronikova et al. 2016). PAA treatment blocks the production of high order DNA structures, and inhibited ISG induction in a dose-dependent manner (Figure 28) (Artusi et al. 2016). Collectively, these findings demonstrate

a clear temporal context in the recruitment of host cell restriction factors and PRRs to infecting viral genomes. Delivery of viral genomes into the nucleus and initiation of vDNA replication triggers host intrinsic and innate immune responses, respectively.

The HIN domain of IFI16 mediates its interaction with sugar-phosphate backbone of vDNA. This process activates the pyrin domain, and induces acetylation of the NLS leading to cytoplasmic translocation of IFI16 (Ansari et al. 2015, Jin et al. 2012, Li et al. 2012). IFI16 interacts with cGAS and other adaptor proteins leading to STING activation, IFN production, and ISG expression (Almine et al. 2017, Bowie et al. 2017, Dutta et al. 2015, Orzalli et al. 2015). Apart from few studies (section 1.6.2.4.), It remains largely unknown which ISG products confer effective antiviral response. Mx1, ISG54, ISG56, and ISG15 have been shown to mediate host defense against several viruses (Staeheli et al. 1988, Schnorr et al. 1993, Lenschow et al. 2007, Frese et al. 1996, Fernandez et al. 1997, Perwitasari et al. 2011, Fensterl et al. 2012, Cho et al. 2013, Terenzi et al. 2008). In addition, they are the most robustly induced during ΔICP0 HSV-1 infection (Mossman et al. 2001), but it remains to be determined if these ISGs directly restrict HSV-1 replication.

The inability of some normal (RPE and HaCaT) and tumor-derived (U2OS and SAOS) cell lines to induce robust ISG expression in response to infection is worthy of further investigation (Figure 43 and 44). It is likely that these cells are defective in signaling pathways upstream of IFN production (e.g., recognition of PAMPs) as they were responsive to exogenous IFN treatment. In support of this hypothesis, U2OS cells have been shown to express a low level of STING, and overexpression of STING in these cells partially recovered their ability to induce IFN-mediated antiviral response to ΔICP0 HSV-1 infection (Deschamps and Kalamvoki 2017b).

Both WT and ΔICP0 HSV-1 are sensitive to exogenous IFN treatment (Figure 46, 47, 48, and 49). In type I IFN-treated cells, HSV-1 replication is

restricted prior to the expression of IE proteins (Oberman and Panet 1988, Gloger and Panet 1984). To our knowledge, it is not entirely clear whether viral genomes remain in the cytoplasm during transport, the capsid fails to eject vDNA into the nucleus, or vDNA is imported but fails to initiate active transcription/translation. The use of click-chemistry detection of vDNA in combination with indirect IF staining protocols may provide insight into these aspects. Type II IFN appears to act downstream of ICP0 expression (Klotzbucher et al. 1990), which raises the question whether type II IFN treatment influences the subcellular localization and biochemical activity of ICP0 rending the virus vulnerable to host immune factors. Indeed, IFNγ induces PML.Ib expression; a cytoplasmic PMl isoform has been shown to sequester ICP0 within the cytoplasm and restrict HSV-1 infection (McNally et al. 2008)). Lastly, little information is available with regards to IFNλ-mediated immune response to HSV-1 infection. Finding a model cell line (e.g., HaCaT cells; Figure 49) that is responsive to all three types of IFN is valuable for direct comparison between these distinct IFN responses (Li et al. 2011, Lopusna et al. 2014).

8. Conclusion remarks

Intrinsic and innate immunity are two distinct arms of host response to HSV-1 infection by virtue of their temporal induction and effects on viral replication. Intrinsic immunity is the first line of defense that acts almost instantly following nuclear entry of viral genomes. It is mainly mediated by PML-NB constituent proteins which are stably recruited to infecting viral genomes to prevent the onset of viral gene expression. Saturation of this intrinsic immune response leads to the induction of ISGs; a process that is dependent on the initiation of vDNA replication. This innate immune response constricts viral propagation and limits the spread of infection. PML plays dual roles in the temporal regulation of intrinsic and innate immunity to HSV-1 infection. However, both arms of intracellular immunity are counteracted by the viral ubiquitin ligase ICP0 which targets many intrinsic and innate factors (e.g., PML and IFI16) for degradation.

9. References

ADVANI SJ, BRANDIMARTI R, WEICHSELBAUM RR AND ROIZMAN B. 2000. The disappearance of cyclins A and B and the increase in activity of the G(2)/M-phase cellular kinase cdc2 in herpes simplex virus 1-infected cells require expression of the alpha22/U(S)1.5 and U(L)13 viral genes. Journal of virology 74: 8-15.

ADVANI SJ, WEICHSELBAUM RR AND ROIZMAN B. 2003. Herpes simplex virus 1 activates cdc2 to recruit topoisomerase II alpha for post-DNA synthesis expression of late genes. Proceedings of the National Academy of Sciences of the United States of America 100: 4825-4830.

AHMAD-NEJAD P, HACKER H, RUTZ M, BAUER S, VABULAS RM AND WAGNER H. 2002. Bacterial CpG-DNA and lipopolysaccharides activate Toll-like receptors at distinct cellular compartments. European journal of immunology 32: 1958-1968.

ALANDIJANY T, ROBERTS APE, CONN KL, LONEY C, MCFARLANE S, ORR A AND BOUTELL C. 2018. Distinct temporal roles for the promyelocytic leukaemia (PML) protein in the sequential regulation of intracellular host immunity to HSV-1 infection. PLoS pathogens 14: e1006769.

ALEXOPOULOU L, HOLT AC, MEDZHITOV R AND FLAVELL RA. 2001. Recognition of double-stranded RNA and activation of NF-kappaB by Toll-like receptor 3. Nature 413: 732-738.

ALMINE JF, O'HARE CA, DUNPHY G, HAGA IR, NAIK RJ, ATRIH A, CONNOLLY DJ, TAYLOR J AND KELSALL IR. 2017. IFI16 and cGAS cooperate in the activation of STING during DNA sensing in human keratinocytes. 8: 14392.

AMELIO AL, GIORDANI NV, KUBAT NJ, O'NEIL J E AND BLOOM DC. 2006. Deacetylation of the herpes simplex virus type 1 latency-associated transcript (LAT) enhancer and a decrease in LAT abundance precede an increase in ICP0 transcriptional permissiveness at early times postexplant. Journal of virology 80: 2063-2068.

ANDERSON P, YIP YK AND VILCEK J. 1982. Specific binding of 125I-human interferon-gamma to high affinity receptors on human fibroblasts. The Journal of biological chemistry 257: 11301-11304.

ANSARI MA, DUTTA S, VEETTIL MV, DUTTA D, IQBAL J, KUMAR B, ROY A, CHIKOTI L, SINGH VV AND CHANDRAN B. 2015. Herpesvirus Genome Recognition Induced Acetylation of Nuclear IFI16 Is Essential for Its Cytoplasmic Translocation, Inflammasome and IFN-beta Responses. PLoS pathogens 11: e1005019.

ARNHEITER H AND HALLER O. 1988. Antiviral state against influenza virus neutralized by microinjection of antibodies to interferon-induced Mx proteins. The EMBO journal 7: 1315-1320.

ARTHUR JL, SCARPINI CG, CONNOR V, LACHMANN RH, TOLKOVSKY AM AND EFSTATHIOU S. 2001. Herpes simplex virus type 1 promoter activity during latency establishment, maintenance, and reactivation in primary dorsal root neurons in vitro. Journal of virology 75: 3885-3895.

ARTUSI S, PERRONE R, LAGO S, RAFFA P, DI IORIO E, PALU G AND RICHTER SN. 2016. Visualization of DNA G-quadruplexes in herpes simplex virus 1-infected cells. Nucleic acids research 44: 10343-10353.

ATWAN Z, WRIGHT J, WOODMAN A AND LEPPARD KN. 2016. Promyelocytic leukemia protein isoform II inhibits infection by human adenovirus type 5 through effects on HSP70 and the interferon response. The Journal of general virology 97: 1955-1967.

AVITABILE E, FORGHIERI C AND CAMPADELLI-FIUME G. 2007. Complexes between herpes simplex virus glycoproteins gD, gB, and gH detected in cells by complementation of split enhanced green fluorescent protein. Journal of virology 81: 11532-11537.

BALDWIN S AND WHITLEY RJ. 1989. Intrauterine herpes simplex virus infection. Teratology 39: 1-10.

BARLOW PN, LUISI B, MILNER A, ELLIOTT M AND EVERETT R. 1994. Structure of the C3HC4 domain by 1H-nuclear magnetic resonance spectroscopy. A new structural class of zinc-finger. Journal of molecular biology 237: 201-211.

BEARD PM AND BAINES JD. 2004. The DNA cleavage and packaging protein encoded by the UL33 gene of herpes simplex virus 1 associates with capsids. Virology 324: 475-482.

BIENIASZ PD. 2004. Intrinsic immunity: a front-line defense against viral attack. Nature immunology 5: 1109-1115.

BIGALKE JM, HEUSER T, NICASTRO D AND HELDWEIN EE. 2014. Membrane deformation and scission by the HSV-1 nuclear egress complex. Nature communications 5: 4131.

BINDER PS. 1977. Herpes simplex keratitis. Surv Ophthalmol 21: 313-331.

BLONDEAU C, PELCHEN-MATTHEWS A, MLCOCHOVA P, MARSH M, MILNE RS AND TOWERS GJ. 2013. Tetherin restricts herpes simplex virus 1 and is antagonized by glycoprotein M. Journal of virology 87: 13124-13133.

BODDY MN, HOWE K, ETKIN LD, SOLOMON E AND FREEMONT PS. 1996. PIC 1, a novel ubiquitin-like protein which interacts with the PML component of a multiprotein complex that is disrupted in acute promyelocytic leukaemia. Oncogene 13: 971-982.

BOHREN KM, NADKARNI V, SONG JH, GABBAY KH AND OWERBACH D. 2004. A M55V polymorphism in a novel SUMO gene (SUMO-4) differentially activates heat shock transcription factors and is associated with susceptibility to type I diabetes mellitus. The Journal of biological chemistry 279: 27233-27238.

BOSNJAK L, MIRANDA-SAKSENA M, KOELLE DM, BOADLE RA, JONES CA AND CUNNINGHAM AL. 2005. Herpes simplex virus infection of human dendritic cells induces apoptosis and allows cross-presentation via uninfected dendritic cells. Journal of immunology (Baltimore, Md : 1950) 174: 2220-2227.

BOUTELL C, CUCHET-LOURENCO D, VANNI E, ORR A, GLASS M, MCFARLANE S AND EVERETT RD. 2011. A viral ubiquitin ligase has substrate preferential SUMO targeted ubiquitin ligase activity that counteracts intrinsic antiviral defence. PLoS pathogens 7: e1002245.

BOUTELL C AND EVERETT RD. 2013. Regulation of alphaherpesvirus infections by the ICP0 family of proteins. The Journal of general virology 94: 465-481.

BOUTELL C, SADIS S AND EVERETT RD. 2002. Herpes simplex virus type 1 immediate-early protein ICP0 and is isolated RING finger domain act as ubiquitin E3 ligases in vitro. Journal of virology 76: 841-850.

BOWIE AG ET AL. 2017. IFI16 is required for DNA sensing in human macrophages by promoting production and function of cGAMP. Nature communications 8: 14391.

BRONIARCZYK J, MASSIMI P, BERGANT M AND BANKS L. 2015. Human Papillomavirus Infectious Entry and Trafficking Is a Rapid Process. Journal of virology 89: 8727-8732.

BROWN JR, CONN KL, WASSON P, CHARMAN M, TONG L, GRANT K, MCFARLANE S AND BOUTELL C. 2016. SUMO Ligase Protein Inhibitor of Activated STAT1 (PIAS1) Is a Constituent Promyelocytic Leukemia Nuclear Body Protein That Contributes to the Intrinsic Antiviral Immune Response to Herpes Simplex Virus 1. J Virol 90: 5939-5952.

BURKHAM J, COEN DM, HWANG CB AND WELLER SK. 2001. Interactions of herpes simplex virus type 1 with ND10 and recruitment of PML to replication compartments. Journal of virology 75: 2353-2367.

CAI W, ASTOR TL, LIPTAK LM, CHO C, COEN DM AND SCHAFFER PA. 1993. The herpes simplex virus type 1 regulatory protein ICP0 enhances virus replication during acute infection and reactivation from latency. Journal of virology 67: 7501-7512.

CAMARENA V, KOBAYASHI M, KIM JY, ROEHM P, PEREZ R, GARDNER J, WILSON AC, MOHR I AND CHAO MV. 2010. Nature and duration of growth factor signaling through receptor tyrosine kinases regulates HSV-1 latency in neurons. Cell host & microbe 8: 320-330.

CANTIN E, TANAMACHI B AND OPENSHAW H. 1999. Role for gamma interferon in control of herpes simplex virus type 1 reactivation. Journal of virology 73: 3418-3423.

CANTIN EM, HINTON DR, CHEN J AND OPENSHAW H. 1995. Gamma interferon expression during acute and latent nervous system infection by herpes simplex virus type 1. Journal of virology 69: 4898-4905.

CATEZ F, PICARD C, HELD K, GROSS S, ROUSSEAU A, THEIL D, SAWTELL N, LABETOULLE M AND LOMONTE P. 2012. HSV-1 genome subnuclear positioning and associations with host-cell PML-NBs and centromeres regulate LAT locus transcription during latency in neurons. PLoS pathogens 8: e1002852.

CHANG YE AND ROIZMAN B. 1993. The product of the UL31 gene of herpes simplex virus 1 is a nuclear phosphoprotein which partitions with the nuclear matrix. Journal of virology 67: 6348-6356.

CHEE AV, LOPEZ P, PANDOLFI PP AND ROIZMAN B. 2003. Promyelocytic leukemia protein mediates interferon-based anti-herpes simplex virus 1 effects. Journal of virology 77: 7101-7105.

CHEHREHASA F, MEEDENIYA AC, DWYER P, ABRAHAMSEN G AND MACKAY-SIM A. 2009. EdU, a new thymidine analogue for labelling proliferating cells in the nervous system. Journal of neuroscience methods 177: 122-130.

CHELBI-ALIX MK AND DE THE H. 1999. Herpes virus induced proteasome-dependent degradation of the nuclear bodies-associated PML and Sp100 proteins. Oncogene 18: 935-941.

CHEN Y, WRIGHT J, MENG X AND LEPPARD KN. 2015. Promyelocytic Leukemia Protein Isoform II Promotes Transcription Factor Recruitment To Activate Interferon Beta and Interferon-Responsive Gene Expression. Molecular and cellular biology 35: 1660-1672.

CHEN YC, KAPPEL C, BEAUDOUIN J, EILS R AND SPECTOR DL. 2008. Live cell dynamics of promyelocytic leukemia nuclear bodies upon entry into and exit from mitosis. Molecular biology of the cell 19: 3147-3162.

CHENG H, TUMPEY TM, STAATS HF, VAN ROOIJEN N, OAKES JE AND LAUSCH RN. 2000. Role of macrophages in restricting herpes simplex virus type 1 growth after ocular infection. Investigative ophthalmology & visual science 41: 1402-1409.

CHENG X AND KAO HY. 2012. Post-translational modifications of PML: consequences and implications. Frontiers in oncology 2: 210.

CHEW T, TAYLOR KE AND MOSSMAN KL. 2009. Innate and adaptive immune responses to herpes simplex virus. Viruses 1: 979-1002.

CHIU YH, MACMILLAN JB AND CHEN ZJ. 2009. RNA polymerase III detects cytosolic DNA and induces type I interferons through the RIG-I pathway. Cell 138: 576-591.

CHO H, SHRESTHA B, SEN GC AND DIAMOND MS. 2013. A role for Ifit2 in restricting West Nile virus infection in the brain. Journal of virology 87: 8363-8371.

CHOI MK ET AL. 2009. A selective contribution of the RIG-I-like receptor pathway to type I interferon responses activated by cytosolic DNA. Proceedings of the National Academy of Sciences of the United States of America 106: 17870-17875.

CHRISTENSEN MH ET AL. 2016. HSV-1 ICP27 targets the TBK1-activated STING signalsome to inhibit virus-induced type I IFN expression. 35: 1385-1399.

CIECHANOVER A, HELLER H, ELIAS S, HAAS AL AND HERSHKO A. 1980. ATP-dependent conjugation of reticulocyte proteins with the polypeptide required for protein degradation. Proceedings of the National Academy of Sciences of the United States of America 77: 1365-1368.

CIECHANOVER A, HELLER H, KATZ-ETZION R AND HERSHKO A. 1981. Activation of the heat-stable polypeptide of the ATP-dependent proteolytic system. Proceedings of the National Academy of Sciences of the United States of America 78: 761-765.

CLIFFE AR, GARBER DA AND KNIPE DM. 2009. Transcription of the herpes simplex virus latency-associated transcript promotes the formation of facultative heterochromatin on lytic promoters. Journal of virology 83: 8182-8190.

COEN DM. 1990. Antiviral drug resistance. Ann N Y Acad Sci 616: 224-237.

COLLINS SE, NOYCE RS AND MOSSMAN KL. 2004. Innate cellular response to virus particle entry requires IRF3 but not virus replication. Journal of virology 78: 1706-1717.

CONDEMINE W, TAKAHASHI Y, ZHU J, PUVION-DUTILLEUL F, GUEGAN S, JANIN A AND DE THE H. 2006. Characterization of endogenous human promyelocytic leukemia isoforms. Cancer research 66: 6192-6198.

CONN KL, WASSON P, MCFARLANE S, TONG L, BROWN JR, GRANT KG, DOMINGUES P AND BOUTELL C. 2016. Novel Role for Protein Inhibitor of Activated STAT 4 (PIAS4) in the Restriction of Herpes Simplex Virus 1 by the Cellular Intrinsic Antiviral Immune Response. Journal of virology 90: 4807-4826.

COOK WJ, KRAMER MF, WALKER RM, BURWELL TJ, HOLMAN HA, COEN DM AND KNIPE DM. 2004. Persistent expression of chemokine and chemokine receptor RNAs at primary and latent sites of herpes simplex virus 1 infection. Virology journal 1: 5.

COPELAND AM, NEWCOMB WW AND BROWN JC. 2009. Herpes simplex virus replication: roles of viral proteins and nucleoporins in capsid-nucleus attachment. Journal of virology 83: 1660-1668.

CRUMPACKER CS, SCHNIPPER LE, ZAIA JA AND LEVIN MJ. 1979. Growth inhibition by acycloguanosine of herpesviruses isolated from human infections. Antimicrobial agents and chemotherapy 15: 642-645.

CUCHET-LOURENCO D, ANDERSON G, SLOAN E, ORR A AND EVERETT RD. 2013. The viral ubiquitin ligase ICP0 is neither sufficient nor necessary for degradation of the cellular DNA sensor IFI16 during herpes simplex virus 1 infection. Journal of virology 87: 13422-13432.

CUCHET-LOURENCO D, BOUTELL C, LUKASHCHUK V, GRANT K, SYKES A, MURRAY J, ORR A AND EVERETT RD. 2011. SUMO pathway dependent recruitment of cellular repressors to herpes simplex virus type 1 genomes. PLoS pathogens 7: e1002123.

CUCHET-LOURENCO D, VANNI E, GLASS M, ORR A AND EVERETT RD. 2012. Herpes simplex virus 1 ubiquitin ligase ICP0 interacts with PML isoform I and induces its SUMO-independent degradation. Journal of virology 86: 11209-11222.

CUCHET D, SYKES A, NICOLAS A, ORR A, MURRAY J, SIRMA H, HEEREN J, BARTELT A AND EVERETT RD. 2011. PML isoforms I and II participate in PML-dependent restriction of HSV-1 replication. Journal of cell science 124: 280-291.

DAVIDO DJ, VON ZAGORSKI WF, LANE WS AND SCHAFFER PA. 2005. Phosphorylation site mutations affect herpes simplex virus type 1 ICP0 function. Journal of virology 79: 1232-1243.

DAVIS ME AND GACK MU. 2015. Ubiquitination in the antiviral immune response. Virology 479-480: 52-65.

DE LA CRUZ-HERRERA CF ET AL. 2014. Activation of the double-stranded RNA-dependent protein kinase PKR by small ubiquitin-like modifier (SUMO). The Journal of biological chemistry 289: 26357-26367.

DELBARRE E, IVANAUSKIENE K, SPIRKOSKI J, SHAH A, VEKTERUD K, MOSKAUG JO, BOE SO, WONG LH, KUNTZIGER T AND COLLAS P. 2017. PML protein organizes heterochromatin domains where it regulates histone H3.3 deposition by ATRX/DAXX. Genome research 27: 913-921.

DELBOY MG, SIEKAVIZZA-ROBLES CR AND NICOLA AV. 2010. Herpes simplex virus tegument ICP0 is capsid associated, and its E3 ubiquitin ligase domain is important for incorporation into virions. Journal of virology 84: 1637-1640.

DELUCA NA AND SCHAFFER PA. 1985. Activation of immediate-early, early, and late promoters by temperature-sensitive and wild-type forms of herpes simplex virus type 1 protein ICP4. Molecular and cellular biology 5: 1997-2008.

DEMBOWSKI JA AND DELUCA NA. 2015. Selective recruitment of nuclear factors to productively replicating herpes simplex virus genomes. PLoS pathogens 11: e1004939.

DENG L, WANG C, SPENCER E, YANG L, BRAUN A, YOU J, SLAUGHTER C, PICKART C AND CHEN ZJ. 2000. Activation of the IkappaB kinase complex by TRAF6 requires a dimeric ubiquitin-conjugating enzyme complex and a unique polyubiquitin chain. Cell 103: 351-361.

DESAI P, WATKINS SC AND PERSON S. 1994. The size and symmetry of B capsids of herpes simplex virus type 1 are determined by the gene products of the UL26 open reading frame. Journal of virology 68: 5365-5374.

DESCHAMPS T AND KALAMVOKI M. 2017a. Evasion of the STING DNA-Sensing Pathway by VP11/12 of Herpes Simplex Virus 1. Journal of virology 91.

DESCHAMPS T AND KALAMVOKI M. 2017b. Impaired STING Pathway in Human Osteosarcoma U2OS Cells Contributes to the Growth of ICP0-Null Mutant Herpes Simplex Virus. Journal of virology 91.

DESHMANE SL AND FRASER NW. 1989. During latency, herpes simplex virus type 1 DNA is associated with nucleosomes in a chromatin structure. Journal of virology 63: 943-947.

DESHPANDE SP, ZHENG M, DAHESHIA M AND ROUSE BT. 2000. Pathogenesis of herpes simplex virus-induced ocular immunoinflammatory lesions in B-cell-deficient mice. Journal of virology 74: 3517-3524.

DESTERRO JM, RODRIGUEZ MS, KEMP GD AND HAY RT. 1999. Identification of the enzyme required for activation of the small ubiquitin-like protein SUMO-1. The Journal of biological chemistry 274: 10618-10624.

DIAO L, ZHANG B, FAN J, GAO X, SUN S, YANG K, XIN D, JIN N, GENG Y AND WANG C. 2005. Herpes virus proteins ICP0 and BICP0 can activate NF-kappaB by catalyzing IkappaBalpha ubiquitination. Cellular signalling 17: 217-229.

DINER BA, LUM KK, JAVITT A AND CRISTEA IM. 2015. Interactions of the Antiviral Factor Interferon Gamma-Inducible Protein 16 (IFI16) Mediate Immune Signaling and Herpes Simplex Virus-1 Immunosuppression. Molecular & cellular proteomics : MCP 14: 2341-2356.

DINER BA, LUM KK, TOETTCHER JE AND CRISTEA IM. 2016. Viral DNA Sensors IFI16 and Cyclic GMP-AMP Synthase Possess Distinct Functions in Regulating Viral Gene Expression, Immune Defenses, and Apoptotic Responses during Herpesvirus Infection. mBio 7.

DJEU JY, STOCKS N, ZOON K, STANTON GJ, TIMONEN T AND HERBERMAN RB. 1982. Positive self regulation of cytotoxicity in human natural killer cells by production of interferon upon exposure to influenza and herpes viruses. The Journal of experimental medicine 156: 1222-1234.

DOMKE-OPITZ I, STRAUB P AND KIRCHNER H. 1986. Effect of interferon on replication of herpes simplex virus types 1 and 2 in human macrophages. Journal of virology 60: 37-42.

DU T, ZHOU G AND ROIZMAN B. 2011. HSV-1 gene expression from reactivated ganglia is disordered and concurrent with suppression of latency-associated transcript and miRNAs. Proceedings of the National Academy of Sciences of the United States of America 108: 18820-18824.

DUFFY C, LAVAIL JH, TAUSCHER AN, WILLS EG, BLAHO JA AND BAINES JD. 2006. Characterization of a UL49-null mutant: VP22 of herpes simplex virus type 1 facilitates viral spread in cultured cells and the mouse cornea. Journal of virology 80: 8664-8675.

DUPREZ E, SAURIN AJ, DESTERRO JM, LALLEMAND-BREITENBACH V, HOWE K, BODDY MN, SOLOMON E, DE THE H, HAY RT AND FREEMONT PS. 1999. SUMO-1 modification of the acute promyelocytic leukaemia protein PML: implications for nuclear localisation. Journal of cell science 112 (Pt 3): 381-393.

DUTRIEUX J, MAARIFI G, PORTILHO DM, ARHEL NJ, CHELBI-ALIX MK AND NISOLE S. 2015. PML/TRIM19-Dependent Inhibition of Retroviral Reverse-Transcription by Daxx. PLoS pathogens 11: e1005280.

DUTTA D, DUTTA S, VEETTIL MV, ROY A, ANSARI MA, IQBAL J, CHIKOTI L, KUMAR B, JOHNSON KE AND CHANDRAN B. 2015. BRCA1 Regulates IFI16 Mediated Nuclear Innate Sensing of Herpes Viral DNA and Subsequent Induction of the Innate Inflammasome and Interferon-beta Responses. PLoS pathogens 11: e1005030.

EGAN KP, WU S, WIGDAHL B AND JENNINGS SR. 2013. Immunological control of herpes simplex virus infections. Journal of neurovirology 19: 328-345.

EIDSON KM, HOBBS WE, MANNING BJ, CARLSON P AND DELUCA NA. 2002. Expression of herpes simplex virus ICP0 inhibits the induction of interferon-stimulated genes by viral infection. Journal of virology 76: 2180-2191.

EL ASMI F, MAROUI MA, DUTRIEUX J, BLONDEL D, NISOLE S AND CHELBI-ALIX MK. 2014. Implication of PMLIV in both intrinsic and innate immunity. PLoS pathogens 10: e1003975.

EL BOUGRINI J, DIANOUX L AND CHELBI-ALIX MK. 2011. PML positively regulates interferon gamma signaling. Biochimie 93: 389-398.

ELION GB, FURMAN PA, FYFE JA, DE MIRANDA P, BEAUCHAMP L AND SCHAEFFER HJ. 1977. Selectivity of action of an antiherpetic agent, 9-(2-hydroxyethoxymethyl) guanine. Proceedings of the National Academy of Sciences of the United States of America 74: 5716-5720.

ELLERMANN-ERIKSEN S, JUSTESEN J AND MOGENSEN SC. 1986. Genetically determined difference in the antiviral action of alpha/beta interferon in cells from mice resistant or susceptible to herpes simplex virus type 2. The Journal of general virology 67 (Pt 9): 1859-1866.

EVERETT RD. 1988. Analysis of the functional domains of herpes simplex virus type 1 immediate-early polypeptide Vmw110. Journal of molecular biology 202: 87-96.

EVERETT RD. 1989. Construction and characterization of herpes simplex virus type 1 mutants with defined lesions in immediate early gene 1. The Journal of general virology 70 (Pt 5): 1185-1202.

EVERETT RD. 2013. The spatial organization of DNA virus genomes in the nucleus. PLoS pathogens 9: e1003386.

EVERETT RD. 2015. Dynamic Response of IFI16 and Promyelocytic Leukemia Nuclear Body Components to Herpes Simplex Virus 1 Infection. Journal of virology 90: 167-179.

EVERETT RD, BARLOW P, MILNER A, LUISI B, ORR A, HOPE G AND LYON D. 1993a. A novel arrangement of zinc-binding residues and secondary structure in the C3HC4 motif of an alpha herpes virus protein family. Journal of molecular biology 234: 1038-1047.

EVERETT RD, BOUTELL C AND ORR A. 2004a. Phenotype of a herpes simplex virus type 1 mutant that fails to express immediate-early regulatory protein ICP0. Journal of virology 78: 1763-1774.

EVERETT RD, BOUTELL C, PHEASANT K, CUCHET-LOURENCO D AND ORR A. 2014. Sequences related to SUMO interaction motifs in herpes simplex virus 1 protein ICP0 act cooperatively to stimulate virus infection. Journal of virology 88: 2763-2774.

EVERETT RD, CROSS A AND ORR A. 1993b. A truncated form of herpes simplex virus type 1 immediate-early protein Vmw110 is expressed in a cell type dependent manner. Virology 197: 751-756.

EVERETT RD, FREEMONT P, SAITOH H, DASSO M, ORR A, KATHORIA M AND PARKINSON J. 1998. The disruption of ND10 during herpes simplex virus infection correlates with the Vmw110- and proteasome-dependent loss of several PML isoforms. Journal of virology 72: 6581-6591.

EVERETT RD AND MAUL GG. 1994. HSV-1 IE protein Vmw110 causes redistribution of PML. The EMBO journal 13: 5062-5069.

EVERETT RD AND MURRAY J. 2005. ND10 components relocate to sites associated with herpes simplex virus type 1 nucleoprotein complexes during virus infection. Journal of virology 79: 5078-5089.

EVERETT RD, MURRAY J, ORR A AND PRESTON CM. 2007. Herpes simplex virus type 1 genomes are associated with ND10 nuclear substructures in quiescently infected human fibroblasts. Journal of virology 81: 10991-11004.

EVERETT RD AND ORR A. 2009. Herpes simplex virus type 1 regulatory protein ICP0 aids infection in cells with a preinduced interferon response but does not impede interferon-induced gene induction. Journal of virology 83: 4978-4983.

EVERETT RD, PARADA C, GRIPON P, SIRMA H AND ORR A. 2008. Replication of ICP0-null mutant herpes simplex virus type 1 is restricted by both PML and Sp100. Journal of virology 82: 2661-2672.

EVERETT RD, RECHTER S, PAPIOR P, TAVALAI N, STAMMINGER T AND ORR A. 2006. PML contributes to a cellular mechanism of repression of herpes simplex virus type 1 infection that is inactivated by ICP0. Journal of virology 80: 7995-8005.

EVERETT RD, SOURVINOS G, LEIPER C, CLEMENTS JB AND ORR A. 2004b. Formation of nuclear foci of the herpes simplex virus type 1 regulatory protein ICP4 at early times of infection: localization, dynamics, recruitment of ICP27, and evidence for the de novo induction of ND10-like complexes. Journal of virology 78: 1903-1917.

FENSTERL V, WETZEL JL, RAMACHANDRAN S, OGINO T, STOHLMAN SA, BERGMANN CC, DIAMOND MS, VIRGIN HW AND SEN GC. 2012. Interferon-induced Ifit2/ISG54 protects mice from lethal VSV neuropathogenesis. PLoS pathogens 8: e1002712.

FERNANDEZ M, QUIROGA JA, MARTIN J, COTONAT T, PARDO M, HORISBERGER MA AND CARRENO V. 1997. Impaired interferon induction of human MxA protein in chronic hepatitis B virus infection. Journal of medical virology 51: 332-337.

FIELDS BN, KNIPE DMDM- AND HOWLEY PM 2013. Fields virology (6th ed). United States: Philadelphia : Wolters Kluwer Health/Lippincott Williams & Wilkins.

FITZGERALD KA, MCWHIRTER SM, FAIA KL, ROWE DC, LATZ E, GOLENBOCK DT, COYLE AJ, LIAO SM AND MANIATIS T. 2003. IKKepsilon and TBK1 are essential components of the IRF3 signaling pathway. Nature immunology 4: 491-496.

FONTAINE-RODRIGUEZ EC AND KNIPE DM. 2008. Herpes simplex virus ICP27 increases translation of a subset of viral late mRNAs. Journal of virology 82: 3538-3545.

FRESE M, KOCHS G, FELDMANN H, HERTKORN C AND HALLER O. 1996. Inhibition of bunyaviruses, phleboviruses, and hantaviruses by human MxA protein. Journal of virology 70: 915-923.

FROBERT E ET AL. 2014. Resistance of herpes simplex viruses to acyclovir: an update from a ten-year survey in France. Antiviral Res 111: 36-41.

FU J, XIONG Y, XU Y, CHENG G AND TANG H. 2011. MDA5 is SUMOylated by PIAS2beta in the upregulation of type I interferon signaling. Molecular immunology 48: 415-422.

FU XY, KESSLER DS, VEALS SA, LEVY DE AND DARNELL JE, JR. 1990. ISGF3, the transcriptional activator induced by interferon alpha, consists of multiple interacting polypeptide chains. Proceedings of the National Academy of Sciences of the United States of America 87: 8555-8559.

FURLONG D, SWIFT H AND ROIZMAN B. 1972. Arrangement of herpesvirus deoxyribonucleic acid in the core. Journal of virology 10: 1071-1074.

GACK MU ET AL. 2007. TRIM25 RING-finger E3 ubiquitin ligase is essential for RIG-I-mediated antiviral activity. Nature 446: 916-920.

GALISSON F, MAHROUCHE L, COURCELLES M, BONNEIL E, MELOCHE S, CHELBI-ALIX MK AND THIBAULT P. 2011. A novel proteomics approach to identify SUMOylated proteins and their modification sites in human cells. Molecular & cellular proteomics : MCP 10: M110.004796.

GAO M, MATUSICK-KUMAR L, HURLBURT W, DITUSA SF, NEWCOMB WW, BROWN JC, MCCANN PJ, 3RD, DECKMAN I AND COLONNO RJ. 1994. The protease of herpes simplex virus type 1 is essential for functional capsid formation and viral growth. Journal of virology 68: 3702-3712.

GELMAN IH AND SILVERSTEIN S. 1985. Identification of immediate early genes from herpes simplex virus that transactivate the virus thymidine kinase gene. Proceedings of the National Academy of Sciences of the United States of America 82: 5265-5269.

GEOFFROY MC AND CHELBI-ALIX MK. 2011. Role of promyelocytic leukemia protein in host antiviral defense. Journal of interferon & cytokine research : the official journal of the International Society for Interferon and Cytokine Research 31: 145-158.

GERAGHTY RJ, KRUMMENACHER C, COHEN GH, EISENBERG RJ AND SPEAR PG. 1998. Entry of alphaherpesviruses mediated by poliovirus receptor-related protein 1 and poliovirus receptor. Science (New York, NY) 280: 1618-1620.

GERSTER T AND ROEDER RG. 1988. A herpesvirus trans-activating protein interacts with transcription factor OTF-1 and other cellular proteins. Proceedings of the National Academy of Sciences of the United States of America 85: 6347-6351.

GIALITAKIS M, ARAMPATZI P, MAKATOUNAKIS T AND PAPAMATHEAKIS J. 2010. Gamma interferon-dependent transcriptional memory via relocalization of a gene locus to PML nuclear bodies. Molecular and cellular biology 30: 2046-2056.

GIANNI T, AMASIO M AND CAMPADELLI-FIUME G. 2009. Herpes simplex virus gD forms distinct complexes with fusion executors gB and gH/gL in part through the C-terminal profusion domain. The Journal of biological chemistry 284: 17370-17382.

GIBSON W AND ROIZMAN B. 1971. Compartmentalization of spermine and spermidine in the herpes simplex virion. Proceedings of the National Academy of Sciences of the United States of America 68: 2818-2821.

GLASS M AND EVERETT RD. 2013. Components of promyelocytic leukemia nuclear bodies (ND10) act cooperatively to repress herpesvirus infection. Journal of virology 87: 2174-2185.

GLAUSER DL, STRASSER R, LAIMBACHER AS, SAYDAM O, CLEMENT N, LINDEN RM, ACKERMANN M AND FRAEFEL C. 2007. Live covisualization of competing adeno-associated virus and herpes simplex virus type 1 DNA replication: molecular mechanisms of interaction. Journal of virology 81: 4732-4743.

GLOGER I AND PANET A. 1984. Synthesis of herpes simplex virus proteins in interferon-treated human cells. The Journal of general virology 65 (Pt 6): 1107-1111.

GREBER UF, SUOMALAINEN M, STIDWILL RP, BOUCKE K, EBERSOLD MW AND HELENIUS A. 1997. The role of the nuclear pore complex in adenovirus DNA entry. The EMBO journal 16: 5998-6007.

GREENLUND AC, MORALES MO, VIVIANO BL, YAN H, KROLEWSKI J AND SCHREIBER RD. 1995. Stat recruitment by tyrosine-phosphorylated cytokine receptors: an ordered reversible affinity-driven process. Immunity 2: 677-687.

GRESSER I, TOVEY MG, MAURY C AND BANDU MT. 1976. Role of interferon in the pathogenesis of virus diseases in mice as demonstrated by the use of anti-interferon serum. II. Studies with herpes simplex, Moloney sarcoma, vesicular stomatitis, Newcastle disease, and influenza viruses. The Journal of experimental medicine 144: 1316-1323.

GRUBOR-BAUK B, ARTHUR JL AND MAYRHOFER G. 2008. Importance of NKT cells in resistance to herpes simplex virus, fate of virus-infected neurons, and level of latency in mice. Journal of virology 82: 11073-11083.

GRUNEWALD K, DESAI P, WINKLER DC, HEYMANN JB, BELNAP DM, BAUMEISTER W AND STEVEN AC. 2003. Three-dimensional structure of herpes simplex virus from cryo-electron tomography. Science (New York, NY) 302: 1396-1398.

GU H. 2016. Infected cell protein 0 functional domains and their coordination in herpes simplex virus replication. World J Virol 5: 1-13.

GUAN D AND KAO HY. 2015. The function, regulation and therapeutic implications of the tumor suppressor protein, PML. Cell & bioscience 5: 60.

GULDNER HH, SZOSTECKI C, SCHRODER P, MATSCHL U, JENSEN K, LUDERS C, WILL H AND STERNSDORF T. 1999. Splice variants of the nuclear dot-associated Sp100 protein contain homologies to HMG-1 and a human nuclear phosphoprotein-box motif. Journal of cell science 112 (Pt 5): 733-747.

GUO D ET AL. 2004. A functional variant of SUMO4, a new I kappa B alpha modifier, is associated with type 1 diabetes. Nat Genet 36: 837-841.

HALFORD WP, BALLIET JW AND GEBHARDT BM. 2004. Re-evaluating natural resistance to herpes simplex virus type 1. Journal of virology 78: 10086-10095.

HALFORD WP, GEBHARDT BM AND CARR DJ. 1996. Persistent cytokine expression in trigeminal ganglion latently infected with herpes simplex virus type 1. Journal of immunology (Baltimore, Md : 1950) 157: 3542-3549.

HALLER O, FRESE M, ROST D, NUTTALL PA AND KOCHS G. 1995. Tick-borne thogoto virus infection in mice is inhibited by the orthomyxovirus resistance gene product Mx1. Journal of virology 69: 2596-2601.

HAN KJ, JIANG L AND SHU HB. 2008. Regulation of IRF2 transcriptional activity by its sumoylation. Biochemical and biophysical research communications 372: 772-778.

HANNOUN Z, MAARIFI G AND CHELBI-ALIX MK. 2016. The implication of SUMO in intrinsic and innate immunity. Cytokine & growth factor reviews 29: 3-16.

HARONIKOVA L, COUFAL J, KEJNOVSKA I, JAGELSKA EB, FOJTA M, DVORAKOVA P, MULLER P, VOJTESEK B AND BRAZDA V. 2016. IFI16 Preferentially Binds to DNA with Quadruplex Structure and Enhances DNA Quadruplex Formation. PloS one 11: e0157156.

HEATON SM, BORG NA AND DIXIT VM. 2016. Ubiquitin in the activation and attenuation of innate antiviral immunity. The Journal of experimental medicine 213: 1-13.

HENSELEIT U, ROSENBACH T AND KOLDE G. 1996. Induction of apoptosis in human HaCaT keratinocytes. Archives of dermatological research 288: 676-683.

HERR W. 1998. The herpes simplex virus VP16-induced complex: mechanisms of combinatorial transcriptional regulation. Cold Spring Harb Symp Quant Biol 63: 599-607.

HERSHKO A, CIECHANOVER A, HELLER H, HAAS AL AND ROSE IA. 1980. Proposed role of ATP in protein breakdown: conjugation of protein with multiple chains of the polypeptide of ATP-dependent proteolysis. Proceedings of the National Academy of Sciences of the United States of America 77: 1783-1786.

HERSHKO A AND HELLER H. 1985. Occurrence of a polyubiquitin structure in ubiquitin-protein conjugates. Biochemical and biophysical research communications 128: 1079-1086.

HERSHKO A, HELLER H, ELIAS S AND CIECHANOVER A. 1983. Components of ubiquitin-protein ligase system. Resolution, affinity purification, and role in protein breakdown. The Journal of biological chemistry 258: 8206-8214.

HERSHKO A, HELLER H, EYTAN E AND REISS Y. 1986. The protein substrate binding site of the ubiquitin-protein ligase system. The Journal of biological chemistry 261: 11992-11999.

HILL TJ, BLYTH WA AND HARBOUR DA. 1978. Trauma to the skin causes recurrence of herpes simplex in the mouse. The Journal of general virology 39: 21-28.

HOLLENBACH AD, MCPHERSON CJ, MIENTJES EJ, IYENGAR R AND GROSVELD G. 2002. Daxx and histone deacetylase II associate with chromatin through an interaction with core histones and the chromatin-associated protein Dek. Journal of cell science 115: 3319-3330.

HOLLINSHEAD M, JOHNS HL, SAYERS CL, GONZALEZ-LOPEZ C, SMITH GL AND ELLIOTT G. 2012. Endocytic tubules regulated by Rab GTPases 5 and 11 are used for envelopment of herpes simplex virus. The EMBO journal 31: 4204-4220.

HONDA K AND TANIGUCHI T. 2006. IRFs: master regulators of signalling by Toll-like receptors and cytosolic pattern-recognition receptors. Nature reviews Immunology 6: 644-658.

HONESS RW AND ROIZMAN B. 1974. Regulation of herpesvirus macromolecular synthesis. I. Cascade regulation of the synthesis of three groups of viral proteins. Journal of virology 14: 8-19.

HONESS RW AND ROIZMAN B. 1975. Regulation of herpesvirus macromolecular synthesis: sequential transition of polypeptide synthesis requires functional viral polypeptides. Proceedings of the National Academy of Sciences of the United States of America 72: 1276-1280.

HONESS RW AND WATSON DH. 1977. Herpes simplex virus resistance and sensitivity to phosphonoacetic acid. Journal of virology 21: 584-600.

HORAN KA ET AL. 2013. Proteasomal degradation of herpes simplex virus capsids in macrophages releases DNA to the cytosol for recognition by DNA sensors. Journal of immunology (Baltimore, Md : 1950) 190: 2311-2319.

IBIRICU I, HUISKONEN JT, DOHNER K, BRADKE F, SODEIK B AND GRUNEWALD K. 2011. Cryo electron tomography of herpes simplex virus during axonal transport and secondary envelopment in primary neurons. PLoS pathogens 7: e1002406.

IBIRICU I, MAURER UE AND GRUNEWALD K. 2013. Characterization of herpes simplex virus type 1 L-particle assembly and egress in hippocampal neurones by electron cryo-tomography. Cellular microbiology 15: 285-291.

IGARASHI K, GAROTTA G, OZMEN L, ZIEMIECKI A, WILKS AF, HARPUR AG, LARNER AC AND FINBLOOM DS. 1994. Interferon-gamma induces tyrosine phosphorylation of interferon-gamma receptor and regulated association of protein tyrosine kinases, Jak1 and Jak2, with its receptor. The Journal of biological chemistry 269: 14333-14336.

ISHOV AM, SOTNIKOV AG, NEGOREV D, VLADIMIROVA OV, NEFF N, KAMITANI T, YEH ET, STRAUSS JF, 3RD AND MAUL GG. 1999. PML is critical for ND10 formation and recruits the PML-interacting protein daxx to this nuclear structure when modified by SUMO-1. The Journal of cell biology 147: 221-234.

IYER LM, ABHIMAN S AND ARAVIND L. 2008. MutL homologs in restriction-modification systems and the origin of eukaryotic MORC ATPases. Biol Direct 3: 8.

JACKSON PK. 2001. A new RING for SUMO: wrestling transcriptional responses into nuclear bodies with PIAS family E3 SUMO ligases. Genes & development 15: 3053-3058.

JENSEN E. 2014. Technical review: In situ hybridization. Anatomical record (Hoboken, NJ : 2007) 297: 1349-1353.

JENSEN K, SHIELS C AND FREEMONT PS. 2001. PML protein isoforms and the RBCC/TRIM motif. Oncogene 20: 7223-7233.

JIN T ET AL. 2012. Structures of the HIN domain:DNA complexes reveal ligand binding and activation mechanisms of the AIM2 inflammasome and IFI16 receptor. Immunity 36: 561-571.

JOHNSON AJ, CHU CF AND MILLIGAN GN. 2008a. Effector CD4+ T-cell involvement in clearance of infectious herpes simplex virus type 1 from sensory ganglia and spinal cords. Journal of virology 82: 9678-9688.

JOHNSON KE, BOTTERO V, FLAHERTY S, DUTTA S, SINGH VV AND CHANDRAN B. 2014. IFI16 restricts HSV-1 replication by accumulating on the hsv-1 genome, repressing HSV-1 gene expression, and directly or indirectly modulating histone modifications. PLoS pathogens 10: e1004503.

JOHNSON KE, SONG B AND KNIPE DM. 2008b. Role for herpes simplex virus 1 ICP27 in the inhibition of type I interferon signaling. Virology 374: 487-494.

JOHNSTONE RW, KERSHAW MH AND TRAPANI JA. 1998. Isotypic variants of the interferon-inducible transcriptional repressor IFI 16 arise through differential mRNA splicing. Biochemistry 37: 11924-11931.

JOVASEVIC V, LIANG L AND ROIZMAN B. 2008. Proteolytic cleavage of VP1-2 is required for release of herpes simplex virus 1 DNA into the nucleus. Journal of virology 82: 3311-3319.

KAGEY MH, MELHUISH TA AND WOTTON D. 2003. The polycomb protein Pc2 is a SUMO E3. Cell 113: 127-137.

KAHLE T, VOLKMANN B, EISSMANN K, HERRMANN A, SCHMITT S, WITTMANN S, MERKEL L, REUTER N, STAMMINGER T AND GRAMBERG T. 2015. TRIM19/PML Restricts HIV Infection in a Cell Type-Dependent Manner. Viruses 8.

KAMITANI T, KITO K, NGUYEN HP, FUKUDA-KAMITANI T AND YEH ET. 1998a. Characterization of a second member of the sentrin family of ubiquitin-like proteins. The Journal of biological chemistry 273: 11349-11353.

KAMITANI T, KITO K, NGUYEN HP, WADA H, FUKUDA-KAMITANI T AND YEH ET. 1998b. Identification of three major sentrinization sites in PML. The Journal of biological chemistry 273: 26675-26682.

KASSIM SH, RAJASAGI NK, ZHAO X, CHERVENAK R AND JENNINGS SR. 2006. In vivo ablation of CD11c-positive dendritic cells increases susceptibility to herpes simplex virus type 1 infection and diminishes NK and T-cell responses. Journal of virology 80: 3985-3993.

KASTNER P, PEREZ A, LUTZ Y, ROCHETTE-EGLY C, GAUB MP, DURAND B, LANOTTE M, BERGER R AND CHAMBON P. 1992. Structure, localization and transcriptional properties of two classes of retinoic acid receptor alpha fusion proteins in acute promyelocytic leukemia

(APL): structural similarities with a new family of oncoproteins. The EMBO journal 11: 629-642.

KELLY BJ, FRAEFEL C, CUNNINGHAM AL AND DIEFENBACH RJ. 2009. Functional roles of the tegument proteins of herpes simplex virus type 1. Virus research 145: 173-186.

KESSLER DS, VEALS SA, FU XY AND LEVY DE. 1990. Interferon-alpha regulates nuclear translocation and DNA-binding affinity of ISGF3, a multimeric transcriptional activator. Genes & development 4: 1753-1765.

KHANNA KM, BONNEAU RH, KINCHINGTON PR AND HENDRICKS RL. 2003. Herpes simplex virus-specific memory CD8+ T cells are selectively activated and retained in latently infected sensory ganglia. Immunity 18: 593-603.

KIM EJ, PARK JS AND UM SJ. 2008. Ubc9-mediated sumoylation leads to transcriptional repression of IRF-1. Biochemical and biophysical research communications 377: 952-956.

KIM ET, KIM KK, MATUNIS MJ AND AHN JH. 2009. Enhanced SUMOylation of proteins containing a SUMO-interacting motif by SUMO-Ubc9 fusion. Biochemical and biophysical research communications 388: 41-45.

KIM T ET AL. 2010. Aspartate-glutamate-alanine-histidine box motif (DEAH)/RNA helicase A helicases sense microbial DNA in human plasmacytoid dendritic cells. Proceedings of the National Academy of Sciences of the United States of America 107: 15181-15186.

KIM YE AND AHN JH. 2015. Positive role of promyelocytic leukemia protein in type I interferon response and its regulation by human cytomegalovirus. PLoS pathogens 11: e1004785.

KING CG ET AL. 2006. TRAF6 is a T cell-intrinsic negative regulator required for the maintenance of immune homeostasis. Nature medicine 12: 1088-1092.

KLOTZBUCHER A, MITTNACHT S, KIRCHNER H AND JACOBSEN H. 1990. Different effects of IFN gamma and IFN alpha/beta on "immediate early" gene expression of HSV-1. Virology 179: 487-491.

KNICKELBEIN JE, KHANNA KM, YEE MB, BATY CJ, KINCHINGTON PR AND HENDRICKS RL. 2008. Noncytotoxic lytic granule-mediated CD8+ T cell inhibition of HSV-1 reactivation from neuronal latency. Science (New York, NY) 322: 268-271.

KNIPE DM. 2015. Nuclear sensing of viral DNA, epigenetic regulation of herpes simplex virus infection, and innate immunity. Virology 479-480: 153-159.

KOMATSU T, NAGATA K AND WODRICH H. 2016. The Role of Nuclear Antiviral Factors against Invading DNA Viruses: The Immediate Fate of Incoming Viral Genomes. Viruses 8.

KOTENKO SV, GALLAGHER G, BAURIN VV, LEWIS-ANTES A, SHEN M, SHAH NK, LANGER JA, SHEIKH F, DICKENSHEETS H AND DONNELLY RP. 2003. IFN-lambdas mediate antiviral protection through a distinct class II cytokine receptor complex. Nature immunology 4: 69-77.

KRISTENSSON K, LYCKE E, ROYTTA M, SVENNERHOLM B AND VAHLNE A. 1986. Neuritic transport of herpes simplex virus in rat sensory neurons in vitro. Effects of substances interacting with microtubular function and axonal flow [nocodazole, taxol and erythro-9-3-(2-hydroxynonyl)adenine]. The Journal of general virology 67 (Pt 9): 2023-2028.

KRUG A, LUKER GD, BARCHET W, LEIB DA, AKIRA S AND COLONNA M. 2004. Herpes simplex virus type 1 activates murine natural interferon-producing cells through toll-like receptor 9. Blood 103: 1433-1437.

KUBAT NJ, AMELIO AL, GIORDANI NV AND BLOOM DC. 2004. The herpes simplex virus type 1 latency-associated transcript (LAT) enhancer/rcr is hyperacetylated during latency independently of LAT transcription. Journal of virology 78: 12508-12518.

KUBOTA T, MATSUOKA M, CHANG TH, TAILOR P, SASAKI T, TASHIRO M, KATO A AND OZATO K. 2008. Virus infection triggers SUMOylation of IRF3 and IRF7, leading to the negative regulation of type I interferon gene expression. The Journal of biological chemistry 283: 25660-25670.

KUKLIN NA, DAHESHIA M, CHUN S AND ROUSE BT. 1998. Role of mucosal immunity in herpes simplex virus infection. Journal of immunology (Baltimore, Md : 1950) 160: 5998-6003.

KURT-JONES EA, CHAN M, ZHOU S, WANG J, REED G, BRONSON R, ARNOLD MM, KNIPE DM AND FINBERG RW. 2004. Herpes simplex virus 1 interaction with Toll-like receptor 2

contributes to lethal encephalitis. Proceedings of the National Academy of Sciences of the United States of America 101: 1315-1320.

KWIATKOWSKI DL, THOMPSON HW AND BLOOM DC. 2009. The polycomb group protein Bmi1 binds to the herpes simplex virus 1 latent genome and maintains repressive histone marks during latency. Journal of virology 83: 8173-8181.

LAI P-Y, LO Y-H AND LAI M-Z. 2016. The role of PML in the activation and the differentiation of T cells and B cells. The Journal of Immunology 196: 125.127-125.127.

LANFRANCA MP, MOSTAFA HH AND DAVIDO DJ. 2014. HSV-1 ICP0: An E3 Ubiquitin Ligase That Counteracts Host Intrinsic and Innate Immunity. Cells 3: 438-454.

LAWMAN MJ, ROUSE BT, COURTNEY RJ AND WALKER RD. 1980. Cell-mediated immunity against herpes simplex induction of cytotoxic T lymphocytes. Infection and immunity 27: 133-139.

LAYCOCK KA, LEE SF, BRADY RH AND PEPOSE JS. 1991. Characterization of a murine model of recurrent herpes simplex viral keratitis induced by ultraviolet B radiation. Investigative ophthalmology & visual science 32: 2741-2746.

LEE GW, MELCHIOR F, MATUNIS MJ, MAHAJAN R, TIAN Q AND ANDERSON P. 1998. Modification of Ran GTPase-activating protein by the small ubiquitin-related modifier SUMO-1 requires Ubc9, an E2-type ubiquitin-conjugating enzyme homologue. The Journal of biological chemistry 273: 6503-6507.

LEIB DA, HARRISON TE, LASLO KM, MACHALEK MA, MOORMAN NJ AND VIRGIN HW. 1999. Interferons regulate the phenotype of wild-type and mutant herpes simplex viruses in vivo. The Journal of experimental medicine 189: 663-672.

LENSCHOW DJ ET AL. 2007. IFN-stimulated gene 15 functions as a critical antiviral molecule against influenza, herpes, and Sindbis viruses. Proceedings of the National Academy of Sciences of the United States of America 104: 1371-1376.

LESTER JT AND DELUCA NA. 2011. Herpes simplex virus 1 ICP4 forms complexes with TFIID and mediator in virus-infected cells. Journal of virology 85: 5733-5744.

LI H, LEO C, ZHU J, WU X, O'NEIL J, PARK EJ AND CHEN JD. 2000. Sequestration and inhibition of Daxx-mediated transcriptional repression by PML. Molecular and cellular biology 20: 1784-1796.

LI J, HU S, ZHOU L, YE L, WANG X, HO J AND HO W. 2011. Interferon lambda inhibits herpes simplex virus type I infection of human astrocytes and neurons. Glia 59: 58-67.

LI SJ AND HOCHSTRASSER M. 1999. A new protease required for cell-cycle progression in yeast. Nature 398: 246-251.

LI T, DINER BA, CHEN J AND CRISTEA IM. 2012. Acetylation modulates cellular distribution and DNA sensing ability of interferon-inducible protein IFI16. Proceedings of the National Academy of Sciences of the United States of America 109: 10558-10563.

LIANG Y, VOGEL JL, NARAYANAN A, PENG H AND KRISTIE TM. 2009. Inhibition of the histone demethylase LSD1 blocks alpha-herpesvirus lytic replication and reactivation from latency. Nature medicine 15: 1312-1317.

LIU T, KHANNA KM, CHEN X, FINK DJ AND HENDRICKS RL. 2000. CD8(+) T cells can block herpes simplex virus type 1 (HSV-1) reactivation from latency in sensory neurons. The Journal of experimental medicine 191: 1459-1466.

LIUM EK AND SILVERSTEIN S. 1997. Mutational analysis of the herpes simplex virus type 1 ICP0 C3HC4 zinc ring finger reveals a requirement for ICP0 in the expression of the essential alpha27 gene. Journal of virology 71: 8602-8614.

LONG MC, LEONG V, SCHAFFER PA, SPENCER CA AND RICE SA. 1999. ICP22 and the UL13 protein kinase are both required for herpes simplex virus-induced modification of the large subunit of RNA polymerase II. Journal of virology 73: 5593-5604.

LOPEZ C. 1975. Genetics of natural resistance to herpesvirus infections in mice. Nature 258: 152-153.

LOPUSNA K, REZUCHOVA I, KABAT P AND KUDELOVA M. 2014. Interferon lambda induces antiviral response to herpes simplex virus 1 infection. Acta virologica 58: 325-332.

LORET S, GUAY G AND LIPPE R. 2008. Comprehensive characterization of extracellular herpes simplex virus type 1 virions. Journal of virology 82: 8605-8618.

LOVEJOY CA ET AL. 2012. Loss of ATRX, genome instability, and an altered DNA damage response are hallmarks of the alternative lengthening of telomeres pathway. PLoS genetics 8: e1002772.

LUKASHCHUK V AND EVERETT RD. 2010. Regulation of ICP0-null mutant herpes simplex virus type 1 infection by ND10 components ATRX and hDaxx. Journal of virology 84: 4026-4040.

LUKER GD, PRIOR JL, SONG J, PICA CM AND LEIB DA. 2003. Bioluminescence imaging reveals systemic dissemination of herpes simplex virus type 1 in the absence of interferon receptors. Journal of virology 77: 11082-11093.

LUND J, SATO A, AKIRA S, MEDZHITOV R AND IWASAKI A. 2003. Toll-like receptor 9-mediated recognition of Herpes simplex virus-2 by plasmacytoid dendritic cells. The Journal of experimental medicine 198: 513-520.

LYCKE E, HAMARK B, JOHANSSON M, KROTOCHWIL A, LYCKE J AND SVENNERHOLM B. 1988. Herpes simplex virus infection of the human sensory neuron. An electron microscopy study. Arch Virol 101: 87-104.

MADOR N, GOLDENBERG D, COHEN O, PANET A AND STEINER I. 1998. Herpes simplex virus type 1 latency-associated transcripts suppress viral replication and reduce immediate-early gene mRNA levels in a neuronal cell line. Journal of virology 72: 5067-5075.

MAHAJAN R, DELPHIN C, GUAN T, GERACE L AND MELCHIOR F. 1997. A small ubiquitin-related polypeptide involved in targeting RanGAP1 to nuclear pore complex protein RanBP2. Cell 88: 97-107.

MAHER SG, SHEIKH F, SCARZELLO AJ, ROMERO-WEAVER AL, BAKER DP, DONNELLY RP AND GAMERO AM. 2008. IFNalpha and IFNlambda differ in their antiproliferative effects and duration of JAK/STAT signaling activity. Cancer biology & therapy 7: 1109-1115.

MARCOS-VILLAR L ET AL. 2013. SUMOylation of p53 mediates interferon activities. Cell cycle (Georgetown, Tex) 12: 2809-2816.

MAROUI MA ET AL. 2016. Latency Entry of Herpes Simplex Virus 1 Is Determined by the Interaction of Its Genome with the Nuclear Environment. PLoS pathogens 12: e1005834.

MATUNIS MJ, COUTAVAS E AND BLOBEL G. 1996. A novel ubiquitin-like modification modulates the partitioning of the Ran-GTPase-activating protein RanGAP1 between the cytosol and the nuclear pore complex. The Journal of cell biology 135: 1457-1470.

MAUL GG AND EVERETT RD. 1994. The nuclear location of PML, a cellular member of the C3HC4 zinc-binding domain protein family, is rearranged during herpes simplex virus infection by the C3HC4 viral protein ICP0. The Journal of general virology 75 (Pt 6): 1223-1233.

MAUL GG, ISHOV AM AND EVERETT RD. 1996. Nuclear domain 10 as preexisting potential replication start sites of herpes simplex virus type-1. Virology 217: 67-75.

MCCLELLAND DA, AITKEN JD, BHELLA D, MCNAB D, MITCHELL J, KELLY SM, PRICE NC AND RIXON FJ. 2002. pH reduction as a trigger for dissociation of herpes simplex virus type 1 scaffolds. Journal of virology 76: 7407-7417.

MCFARLANE S AND PRESTON CM. 2011. Human cytomegalovirus immediate early gene expression in the osteosarcoma line U2OS is repressed by the cell protein ATRX. Virus research 157: 47-53.

MCNALLY BA, TRGOVCICH J, MAUL GG, LIU Y AND ZHENG P. 2008. A role for cytoplasmic PML in cellular resistance to viral infection. PloS one 3: e2277.

MELCHJORSEN J, RINTAHAKA J, SOBY S, HORAN KA, POLTAJAINEN A, OSTERGAARD L, PALUDAN SR AND MATIKAINEN S. 2010. Early innate recognition of herpes simplex virus in human primary macrophages is mediated via the MDA5/MAVS-dependent and MDA5/MAVS/RNA polymerase III-independent pathways. Journal of virology 84: 11350-11358.

MELCHJORSEN J, SIREN J, JULKUNEN I, PALUDAN SR AND MATIKAINEN S. 2006. Induction of cytokine expression by herpes simplex virus in human monocyte-derived macrophages

and dendritic cells is dependent on virus replication and is counteracted by ICP27 targeting NF-kappaB and IRF-3. The Journal of general virology 87: 1099-1108.

MELROE GT, SILVA L, SCHAFFER PA AND KNIPE DM. 2007. Recruitment of activated IRF-3 and CBP/p300 to herpes simplex virus ICP0 nuclear foci: Potential role in blocking IFN-beta induction. Virology 360: 305-321.

MEREDITH M, ORR A, ELLIOTT M AND EVERETT R. 1995. Separation of sequence requirements for HSV-1 Vmw110 multimerisation and interaction with a 135-kDa cellular protein. Virology 209: 174-187.

METTENLEITER TC, KLUPP BG AND GRANZOW H. 2009. Herpesvirus assembly: an update. Virus research 143: 222-234.

METTENLEITER TC, MULLER F, GRANZOW H AND KLUPP BG. 2013. The way out: what we know and do not know about herpesvirus nuclear egress. Cellular microbiology 15: 170-178.

MI Z, FU J, XIONG Y AND TANG H. 2010. SUMOylation of RIG-I positively regulates the type I interferon signaling. Protein & cell 1: 275-283.

MIMURA Y, TAKAHASHI K, KAWATA K, AKAZAWA T AND INOUE N. 2010. Two-step colocalization of MORC3 with PML nuclear bodies. Journal of cell science 123: 2014-2024.

MITCHELL AM, HIRSCH ML, LI C AND SAMULSKI RJ. 2014. Promyelocytic leukemia protein is a cell-intrinsic factor inhibiting parvovirus DNA replication. Journal of virology 88: 925-936.

MITCHELL BM AND STEVENS JG. 1996. Neuroinvasive properties of herpes simplex virus type 1 glycoprotein variants are controlled by the immune response. Journal of immunology (Baltimore, Md : 1950) 156: 246-255.

MIYAMOTO K AND MORGAN C. 1971. Structure and development of viruses as observed in the electron microscope. XI. Entry and uncoating of herpes simplex virus. Journal of virology 8: 910-918.

MORDSTEIN M ET AL. 2010. Lambda interferon renders epithelial cells of the respiratory and gastrointestinal tracts resistant to viral infections. Journal of virology 84: 5670-5677.

MOSSMAN KL, MACGREGOR PF, ROZMUS JJ, GORYACHEV AB, EDWARDS AM AND SMILEY JR. 2001. Herpes simplex virus triggers and then disarms a host antiviral response. Journal of virology 75: 750-758.

MOSSMAN KL, SAFFRAN HA AND SMILEY JR. 2000. Herpes simplex virus ICP0 mutants are hypersensitive to interferon. Journal of virology 74: 2052-2056.

MOSSMAN KL AND SMILEY JR. 2002. Herpes simplex virus ICP0 and ICP34.5 counteract distinct interferon-induced barriers to virus replication. Journal of virology 76: 1995-1998.

MULLEN MA, CIUFO DM AND HAYWARD GS. 1994. Mapping of intracellular localization domains and evidence for colocalization interactions between the IE110 and IE175 nuclear transactivator proteins of herpes simplex virus. Journal of virology 68: 3250-3266.

NAKAGAWA K AND YOKOSAWA H. 2002. PIAS3 induces SUMO-1 modification and transcriptional repression of IRF-1. FEBS letters 530: 204-208.

NEGOREV DG, VLADIMIROVA OV, IVANOV A, RAUSCHER F, 3RD AND MAUL GG. 2006. Differential role of Sp100 isoforms in interferon-mediated repression of herpes simplex virus type 1 immediate-early protein expression. Journal of virology 80: 8019-8029.

NEWCOMB WW, FONTANA J, WINKLER DC, CHENG N, HEYMANN JB AND STEVEN AC. 2017. The Primary Enveloped Virion of Herpes Simplex Virus 1: Its Role in Nuclear Egress. mBio 8.

NEWCOMB WW, HOMA FL, THOMSEN DR, BOOY FP, TRUS BL, STEVEN AC, SPENCER JV AND BROWN JC. 1996. Assembly of the herpes simplex virus capsid: characterization of intermediates observed during cell-free capsid formation. Journal of molecular biology 263: 432-446.

NEWCOMB WW, HOMA FL, THOMSEN DR, TRUS BL, CHENG N, STEVEN A, BOOY F AND BROWN JC. 1999. Assembly of the herpes simplex virus procapsid from purified components and identification of small complexes containing the major capsid and scaffolding proteins. Journal of virology 73: 4239-4250.

NEWCOMB WW, JUHAS RM, THOMSEN DR, HOMA FL, BURCH AD, WELLER SK AND BROWN JC. 2001. The UL6 gene product forms the portal for entry of DNA into the herpes simplex virus capsid. Journal of virology 75: 10923-10932.

NEWCOMB WW, TRUS BL, BOOY FP, STEVEN AC, WALL JS AND BROWN JC. 1993. Structure of the herpes simplex virus capsid. Molecular composition of the pentons and the triplexes. Journal of molecular biology 232: 499-511.

NGUYEN EK, NEMEROW GR AND SMITH JG. 2010. Direct evidence from single-cell analysis that human {alpha}-defensins block adenovirus uncoating to neutralize infection. Journal of virology 84: 4041-4049.

NICOLA AV, HOU J, MAJOR EO AND STRAUS SE. 2005. Herpes simplex virus type 1 enters human epidermal keratinocytes, but not neurons, via a pH-dependent endocytic pathway. Journal of virology 79: 7609-7616.

NICOLA AV, MCEVOY AM AND STRAUS SE. 2003. Roles for endocytosis and low pH in herpes simplex virus entry into HeLa and Chinese hamster ovary cells. Journal of virology 77: 5324-5332.

NICOLA AV AND STRAUS SE. 2004. Cellular and viral requirements for rapid endocytic entry of herpes simplex virus. Journal of virology 78: 7508-7517.

O'HARE P AND HAYWARD GS. 1985a. Evidence for a direct role for both the 175,000- and 110,000-molecular-weight immediate-early proteins of herpes simplex virus in the transactivation of delayed-early promoters. Journal of virology 53: 751-760.

O'HARE P AND HAYWARD GS. 1985b. Three trans-acting regulatory proteins of herpes simplex virus modulate immediate-early gene expression in a pathway involving positive and negative feedback regulation. Journal of virology 56: 723-733.

OBERMAN F AND PANET A. 1988. Inhibition of transcription of herpes simplex virus immediate early genes in interferon-treated human cells. The Journal of general virology 69 (Pt 6): 1167-1177.

OKURA T, GONG L, KAMITANI T, WADA T, OKURA I, WEI CF, CHANG HM AND YEH ET. 1996. Protection against Fas/APO-1- and tumor necrosis factor-mediated cell death by a novel protein, sentrin. Journal of immunology (Baltimore, Md : 1950) 157: 4277-4281.

OLESKY M, MCNAMEE EE, ZHOU C, TAYLOR TJ AND KNIPE DM. 2005. Evidence for a direct interaction between HSV-1 ICP27 and ICP8 proteins. Virology 331: 94-105.

OLIVO PD, NELSON NJ AND CHALLBERG MD. 1988. Herpes simplex virus DNA replication: the UL9 gene encodes an origin-binding protein. Proceedings of the National Academy of Sciences of the United States of America 85: 5414-5418.

OLSON LC, BUESCHER EL, ARTENSTEIN MS AND PARKMAN PD. 1967. Herpesvirus infections of the human central nervous system. N Engl J Med 277: 1271-1277.

ORCHANSKY P, NOVICK D, FISCHER DG AND RUBINSTEIN M. 1984. Type I and Type II interferon receptors. J Interferon Res 4: 275-282.

ORZALLI MH, BROEKEMA NM, DINER BA, HANCKS DC, ELDE NC, CRISTEA IM AND KNIPE DM. 2015. cGAS-mediated stabilization of IFI16 promotes innate signaling during herpes simplex virus infection. Proceedings of the National Academy of Sciences of the United States of America 112: E1773-1781.

ORZALLI MH, BROEKEMA NM AND KNIPE DM. 2016. Relative Contributions of Herpes Simplex Virus 1 ICP0 and vhs to Loss of Cellular IFI16 Vary in Different Human Cell Types. Journal of virology 90: 8351-8359.

ORZALLI MH, CONWELL SE, BERRIOS C, DECAPRIO JA AND KNIPE DM. 2013. Nuclear interferon-inducible protein 16 promotes silencing of herpesviral and transfected DNA. Proceedings of the National Academy of Sciences of the United States of America 110: E4492-4501.

ORZALLI MH, DELUCA NA AND KNIPE DM. 2012. Nuclear IFI16 induction of IRF-3 signaling during herpesviral infection and degradation of IFI16 by the viral ICP0 protein. Proceedings of the National Academy of Sciences of the United States of America 109: E3008-3017.

ORZALLI MH AND KNIPE DM. 2014. Cellular sensing of viral DNA and viral evasion mechanisms. Annual review of microbiology 68: 477-492.

OWEN DJ, CRUMP CM AND GRAHAM SC. 2015. Tegument Assembly and Secondary Envelopment of Alphaherpesviruses. Viruses 7: 5084-5114.

PALADINO P, COLLINS SE AND MOSSMAN KL. 2010. Cellular localization of the herpes simplex virus ICP0 protein dictates its ability to block IRF3-mediated innate immune responses. PloS one 5: e10428.

PALMA-OCAMPO HK, FLORES-ALONSO JC, VALLEJO-RUIZ V, REYES-LEYVA J, FLORES-MENDOZA L, HERRERA-CAMACHO I, ROSAS-MURRIETA NH AND SANTOS-LOPEZ G. 2015. Interferon lambda inhibits dengue virus replication in epithelial cells. Virology journal 12: 150.

PALUDAN SR, BOWIE AG, HORAN KA AND FITZGERALD KA. 2011. Recognition of herpesviruses by the innate immune system. Nature reviews Immunology 11: 143-154.

PANAGIOTIDIS CA, LIUM EK AND SILVERSTEIN SJ. 1997. Physical and functional interactions between herpes simplex virus immediate-early proteins ICP4 and ICP27. Journal of virology 71: 1547-1557.

PANDEY S, KAWAI T AND AKIRA S. 2014. Microbial sensing by Toll-like receptors and intracellular nucleic acid sensors. Cold Spring Harbor perspectives in biology 7: a016246.

PARKINSON J AND EVERETT RD. 2001. Alphaherpesvirus proteins related to herpes simplex virus type 1 ICP0 induce the formation of colocalizing, conjugated ubiquitin. Journal of virology 75: 5357-5362.

PASDELOUP D, BLONDEL D, ISIDRO AL AND RIXON FJ. 2009. Herpesvirus capsid association with the nuclear pore complex and viral DNA release involve the nucleoporin CAN/Nup214 and the capsid protein pUL25. Journal of virology 83: 6610-6623.

PASTERNACK MS, BEVAN MJ AND KLEIN JR. 1984. Release of discrete interferons by cytotoxic T lymphocytes in response to immune and nonimmune stimuli. Journal of immunology (Baltimore, Md : 1950) 133: 277-280.

PEDERSEN EB, HAAHR S AND MOGENSEN SC. 1983. X-linked resistance of mice to high doses of herpes simplex virus type 2 correlates with early interferon production. Infect Immun 42: 740-746.

PENFOLD ME, ARMATI P AND CUNNINGHAM AL. 1994. Axonal transport of herpes simplex virions to epidermal cells: evidence for a specialized mode of virus transport and assembly. Proceedings of the National Academy of Sciences of the United States of America 91: 6529-6533.

PENG K, MURANYI W, GLASS B, LAKETA V, YANT SR, TSAI L, CIHLAR T, MULLER B AND KRAUSSLICH HG. 2014. Quantitative microscopy of functional HIV post-entry complexes reveals association of replication with the viral capsid. eLife 3: e04114.

PEREIRA RA, SIMON MM AND SIMMONS A. 2000. Granzyme A, a noncytolytic component of CD8(+) cell granules, restricts the spread of herpes simplex virus in the peripheral nervous systems of experimentally infected mice. Journal of virology 74: 1029-1032.

PERI P, MATTILA RK, KANTOLA H, BROBERG E, KARTTUNEN HS, WARIS M, VUORINEN T AND HUKKANEN V. 2008. Herpes simplex virus type 1 Us3 gene deletion influences toll-like receptor responses in cultured monocytic cells. Virology journal 5: 140.

PERRY JJ, TAINER JA AND BODDY MN. 2008. A SIM-ultaneous role for SUMO and ubiquitin. Trends Biochem Sci 33: 201-208.

PERRY LJ, RIXON FJ, EVERETT RD, FRAME MC AND MCGEOCH DJ. 1986. Characterization of the IE110 gene of herpes simplex virus type 1. The Journal of general virology 67 (Pt 11): 2365-2380.

PERWITASARI O, CHO H, DIAMOND MS AND GALE M, JR. 2011. Inhibitor of kappaB kinase epsilon (IKK(epsilon)), STAT1, and IFIT2 proteins define novel innate immune effector pathway against West Nile virus infection. The Journal of biological chemistry 286: 44412-44423.

PICA F, VOLPI A, GAZIANO R AND GARACI E. 2010. Interferon-lambda in immunocompetent individuals with a history of recurrent herpes labialis. Antivir Ther 15: 737-743.

POFFENBERGER KL AND ROIZMAN B. 1985. A noninverting genome of a viable herpes simplex virus 1: presence of head-to-tail linkages in packaged genomes and requirements for circularization after infection. Journal of virology 53: 587-595.

POLLARA G, JONES M, HANDLEY ME, RAJPOPAT M, KWAN A, COFFIN RS, FOSTER G, CHAIN B AND KATZ DR. 2004. Herpes simplex virus type-1-induced activation of myeloid dendritic cells: the roles of virus cell interaction and paracrine type I IFN secretion. Journal of immunology (Baltimore, Md : 1950) 173: 4108-4119.

POTT J, MAHLAKOIV T, MORDSTEIN M, DUERR CU, MICHIELS T, STOCKINGER S, STAEHELI P AND HORNEF MW. 2011. IFN-lambda determines the intestinal epithelial antiviral host defense. Proceedings of the National Academy of Sciences of the United States of America 108: 7944-7949.

PURIFOY DJ, LEWIS RB AND POWELL KL. 1977. Identification of the herpes simplex virus DNA polymerase gene. Nature 269: 621-623.

QUINTAS-CARDAMA A ET AL. 2010. Preclinical characterization of the selective JAK1/2 inhibitor INCB018424: therapeutic implications for the treatment of myeloproliferative neoplasms. Blood 115: 3109-3117.

RABKIN SD AND HANLON B. 1990. Herpes simplex virus DNA synthesis at a preformed replication fork in vitro. Journal of virology 64: 4957-4967.

RABKIN SD AND HANLON B. 1991. Nucleoprotein complex formed between herpes simplex virus UL9 protein and the origin of DNA replication: inter- and intramolecular interactions. Proceedings of the National Academy of Sciences of the United States of America 88: 10946-10950.

RADTKE K, KIENEKE D, WOLFSTEIN A, MICHAEL K, STEFFEN W, SCHOLZ T, KARGER A AND SODEIK B. 2010. Plus- and minus-end directed microtubule motors bind simultaneously to herpes simplex virus capsids using different inner tegument structures. PLoS pathogens 6: e1000991.

RAI TS, GLASS M, COLE JJ, RATHER MI, MARSDEN M, NEILSON M, BROCK C, HUMPHREYS IR, EVERETT RD AND ADAMS PD. 2017. Histone chaperone HIRA deposits histone H3.3 onto foreign viral DNA and contributes to anti-viral intrinsic immunity. Nucleic acids research 45: 11673-11683.

RAIZMAN MB AND FOSTER CS. 1988. Passive transfer of anti-HSV-1 IgG protects against stromal keratitis in mice. Curr Eye Res 7: 823-829.

RAN Y, LIU TT, ZHOU Q, LI S, MAO AP, LI Y, LIU LJ, CHENG JK AND SHU HB. 2011. SENP2 negatively regulates cellular antiviral response by deSUMOylating IRF3 and conditioning it for ubiquitination and degradation. Journal of molecular cell biology 3: 283-292.

RASMUSSEN SB, SORENSEN LN, MALMGAARD L, ANK N, BAINES JD, CHEN ZJ AND PALUDAN SR. 2007. Type I interferon production during herpes simplex virus infection is controlled by cell-type-specific viral recognition through Toll-like receptor 9, the mitochondrial antiviral signaling protein pathway, and novel recognition systems. Journal of virology 81: 13315-13324.

REICHELT M, WANG L, SOMMER M, PERRINO J, NOUR AM, SEN N, BAIKER A, ZERBONI L AND ARVIN AM. 2011. Entrapment of viral capsids in nuclear PML cages is an intrinsic antiviral host defense against varicella-zoster virus. PLoS pathogens 7: e1001266.

REYNOLDS AE, RYCKMAN BJ, BAINES JD, ZHOU Y, LIANG L AND ROLLER RJ. 2001. U(L)31 and U(L)34 proteins of herpes simplex virus type 1 form a complex that accumulates at the nuclear rim and is required for envelopment of nucleocapsids. Journal of virology 75: 8803-8817.

REYNOLDS AE, WILLS EG, ROLLER RJ, RYCKMAN BJ AND BAINES JD. 2002. Ultrastructural localization of the herpes simplex virus type 1 UL31, UL34, and US3 proteins suggests specific roles in primary envelopment and egress of nucleocapsids. Journal of virology 76: 8939-8952.

RICE SA, LONG MC, LAM V, SCHAFFER PA AND SPENCER CA. 1995. Herpes simplex virus immediate-early protein ICP22 is required for viral modification of host RNA polymerase II and establishment of the normal viral transcription program. Journal of virology 69: 5550-5559.

ROCK DL AND FRASER NW. 1983. Detection of HSV-1 genome in central nervous system of latently infected mice. Nature 302: 523-525.

ROCK DL AND FRASER NW. 1985. Latent herpes simplex virus type 1 DNA contains two copies of the virion DNA joint region. Journal of virology 55: 849-852.

RODE K, DOHNER K, BINZ A, GLASS M, STRIVE T, BAUERFEIND R AND SODEIK B. 2011. Uncoupling uncoating of herpes simplex virus genomes from their nuclear import and gene expression. Journal of virology 85: 4271-4283.

ROLLER RJ AND ROIZMAN B. 1992. The herpes simplex virus 1 RNA binding protein US11 is a virion component and associates with ribosomal 60S subunits. Journal of virology 66: 3624-3632.

ROLLER RJ, ZHOU Y, SCHNETZER R, FERGUSON J AND DESALVO D. 2000. Herpes simplex virus type 1 U(L)34 gene product is required for viral envelopment. Journal of virology 74: 117-129.

ROSATO PC AND LEIB DA. 2014. Intrinsic innate immunity fails to control herpes simplex virus and vesicular stomatitis virus replication in sensory neurons and fibroblasts. Journal of virology 88: 9991-10001.

ROUSE BT AND LAWMAN MJ. 1980. Induction of cytotoxic T lymphocytes against herpes simplex virus type i: role of accessory cells and amplifying factor. Journal of immunology (Baltimore, Md : 1950) 124: 2341-2346.

ROWLAND SL, TREMBLAY MM, ELLISON JM, STUNZ LL, BISHOP GA AND HOSTAGER BS. 2007. A novel mechanism for TNFR-associated factor 6-dependent CD40 signaling. Journal of immunology (Baltimore, Md : 1950) 179: 4645-4653.

RYTINKI MM, KAIKKONEN S, PEHKONEN P, JAASKELAINEN T AND PALVIMO JJ. 2009. PIAS proteins: pleiotropic interactors associated with SUMO. Cellular and molecular life sciences : CMLS 66: 3029-3041.

SACKS WR AND SCHAFFER PA. 1987. Deletion mutants in the gene encoding the herpes simplex virus type 1 immediate-early protein ICP0 exhibit impaired growth in cell culture. Journal of virology 61: 829-839.

SAINZ B, JR. AND HALFORD WP. 2002. Alpha/Beta interferon and gamma interferon synergize to inhibit the replication of herpes simplex virus type 1. Journal of virology 76: 11541-11550.

SALIC A AND MITCHISON TJ. 2008. A chemical method for fast and sensitive detection of DNA synthesis in vivo. Proceedings of the National Academy of Sciences of the United States of America 105: 2415-2420.

SALOMONI P. 2013. The PML-Interacting Protein DAXX: Histone Loading Gets into the Picture. Frontiers in oncology 3: 152.

SAMPATH P AND DELUCA NA. 2008. Binding of ICP4, TATA-binding protein, and RNA polymerase II to herpes simplex virus type 1 immediate-early, early, and late promoters in virus-infected cells. Journal of virology 82: 2339-2349.

SANCHEZ R AND MOHR I. 2007. Inhibition of cellular 2'-5' oligoadenylate synthetase by the herpes simplex virus type 1 Us11 protein. Journal of virology 81: 3455-3464.

SANDRI-GOLDIN RM. 1998. ICP27 mediates HSV RNA export by shuttling through a leucine-rich nuclear export signal and binding viral intronless RNAs through an RGG motif. Genes & development 12: 868-879.

SATOH T ET AL. 2008. PILRalpha is a herpes simplex virus-1 entry coreceptor that associates with glycoprotein B. Cell 132: 935-944.

SAWTELL NM AND THOMPSON RL. 1992. Rapid in vivo reactivation of herpes simplex virus in latently infected murine ganglionic neurons after transient hyperthermia. Journal of virology 66: 2150-2156.

SCHANG LM, ROSENBERG A AND SCHAFFER PA. 2000. Roscovitine, a specific inhibitor of cellular cyclin-dependent kinases, inhibits herpes simplex virus DNA synthesis in the presence of viral early proteins. Journal of virology 74: 2107-2120.

SCHERER M, OTTO V, STUMP JD, KLINGL S, MULLER R, REUTER N, MULLER YA, STICHT H AND STAMMINGER T. 2015. Characterization of Recombinant Human Cytomegaloviruses

Encoding IE1 Mutants L174P and 1-382 Reveals that Viral Targeting of PML Bodies Perturbs both Intrinsic and Innate Immune Responses. Journal of virology 90: 1190-1205.

SCHERER M AND STAMMINGER T. 2016. Emerging Role of PML Nuclear Bodies in Innate Immune Signaling. Journal of virology 90: 5850-5854.

SCHNEIDER-SCHAULIES S, SCHNEIDER-SCHAULIES J, SCHUSTER A, BAYER M, PAVLOVIC J AND TER MEULEN V. 1994. Cell type-specific MxA-mediated inhibition of measles virus transcription in human brain cells. Journal of virology 68: 6910-6917.

SCHNORR JJ, SCHNEIDER-SCHAULIES S, SIMON-JODICKE A, PAVLOVIC J, HORISBERGER MA AND TER MEULEN V. 1993. MxA-dependent inhibition of measles virus glycoprotein synthesis in a stably transfected human monocytic cell line. Journal of virology 67: 4760-4768.

SCHRAG JD, PRASAD BV, RIXON FJ AND CHIU W. 1989. Three-dimensional structure of the HSV1 nucleocapsid. Cell 56: 651-660.

SCHWARZ SE, MATUSCHEWSKI K, LIAKOPOULOS D, SCHEFFNER M AND JENTSCH S. 1998. The ubiquitin-like proteins SMT3 and SUMO-1 are conjugated by the UBC9 E2 enzyme. Proceedings of the National Academy of Sciences of the United States of America 95: 560-564.

SEGAL AL, KATCHER AH, BRIGHTMAN VJ AND MILLER MF. 1974. Recurrent herpes labialis, recurrent aphthous ulcers, and the menstrual cycle. J Dent Res 53: 797-803.

SEKINE E, SCHMIDT N, GABORIAU D AND O'HARE P. 2017. Spatiotemporal dynamics of HSV genome nuclear entry and compaction state transitions using bioorthogonal chemistry and super-resolution microscopy. PLoS pathogens 13: e1006721.

SEN J, LIU X, ROLLER R AND KNIPE DM. 2013. Herpes simplex virus US3 tegument protein inhibits Toll-like receptor 2 signaling at or before TRAF6 ubiquitination. Virology 439: 65-73.

SHARMA S, TENOEVER BR, GRANDVAUX N, ZHOU GP, LIN R AND HISCOTT J. 2003. Triggering the interferon antiviral response through an IKK-related pathway. Science (New York, NY) 300: 1148-1151.

SHAW AR, CHAN JK, REID S AND SEEHAFER J. 1985. HLA-DR synthesis induction and expression in HLA-DR-negative carcinoma cell lines of diverse origins by interferon-gamma but not by interferon-beta. J Natl Cancer Inst 74: 1261-1268.

SHEN G, WANG K, WANG S, CAI M, LI ML AND ZHENG C. 2014. Herpes simplex virus 1 counteracts viperin via its virion host shutoff protein UL41. Journal of virology 88: 12163-12166.

SHEN Z, PARDINGTON-PURTYMUN PE, COMEAUX JC, MOYZIS RK AND CHEN DJ. 1996. Associations of UBE2I with RAD52, UBL1, p53, and RAD51 proteins in a yeast two-hybrid system. Genomics 37: 183-186.

SHEPARD AA AND DELUCA NA. 1991. A second-site revertant of a defective herpes simplex virus ICP4 protein with restored regulatory activities and impaired DNA-binding properties. Journal of virology 65: 787-795.

SHEPARD AA, IMBALZANO AN AND DELUCA NA. 1989. Separation of primary structural components conferring autoregulation, transactivation, and DNA-binding properties to the herpes simplex virus transcriptional regulatory protein ICP4. Journal of virology 63: 3714-3728.

SHERIDAN BS, CHERPES TL, URBAN J, KALINSKI P AND HENDRICKS RL. 2009. Reevaluating the CD8 T-cell response to herpes simplex virus type 1: involvement of CD8 T cells reactive to subdominant epitopes. Journal of virology 83: 2237-2245.

SHIP, II, MILLER MF AND RAM C. 1977. A retrospective study of recurrent herpes labialis (RHL) in a professional population, 1958-1971. Oral Surg Oral Med Oral Pathol 44: 723-730.

SHOWALTER SD, ZWEIG M AND HAMPAR B. 1981. Monoclonal antibodies to herpes simplex virus type 1 proteins, including the immediate-early protein ICP 4. Infection and immunity 34: 684-692.

SHUAI K, STARK GR, KERR IM AND DARNELL JE, JR. 1993a. A single phosphotyrosine residue of Stat91 required for gene activation by interferon-gamma. Science (New York, NY) 261: 1744-1746.

SHUAI K, ZIEMIECKI A, WILKS AF, HARPUR AG, SADOWSKI HB, GILMAN MZ AND DARNELL JE. 1993b. Polypeptide signalling to the nucleus through tyrosine phosphorylation of Jak and Stat proteins. Nature 366: 580-583.

SHUKLA D, LIU J, BLAIKLOCK P, SHWORAK NW, BAI X, ESKO JD, COHEN GH, EISENBERG RJ, ROSENBERG RD AND SPEAR PG. 1999. A novel role for 3-O-sulfated heparan sulfate in herpes simplex virus 1 entry. Cell 99: 13-22.

SILVENNOINEN O, IHLE JN, SCHLESSINGER J AND LEVY DE. 1993. Interferon-induced nuclear signalling by Jak protein tyrosine kinases. Nature 366: 583-585.

SLOAN E, ORR A AND EVERETT RD. 2016. MORC3, a Component of PML Nuclear Bodies, Has a Role in Restricting Herpes Simplex Virus 1 and Human Cytomegalovirus. Journal of virology 90: 8621-8633.

SLOAN E, TATHAM MH, GROSLAMBERT M, GLASS M, ORR A, HAY RT AND EVERETT RD. 2015. Analysis of the SUMO2 Proteome during HSV-1 Infection. PLoS pathogens 11: e1005059.

SMITH CA, BATES P, RIVERA-GONZALEZ R, GU B AND DELUCA NA. 1993. ICP4, the major transcriptional regulatory protein of herpes simplex virus type 1, forms a tripartite complex with TATA-binding protein and TFIIB. Journal of virology 67: 4676-4687.

SODEIK B, EBERSOLD MW AND HELENIUS A. 1997. Microtubule-mediated transport of incoming herpes simplex virus 1 capsids to the nucleus. The Journal of cell biology 136: 1007-1021.

SOMMEREYNS C, PAUL S, STAEHELI P AND MICHIELS T. 2008. IFN-lambda (IFN-lambda) is expressed in a tissue-dependent fashion and primarily acts on epithelial cells in vivo. PLoS pathogens 4: e1000017.

SPEAR PG, SHIEH MT, HEROLD BC, WUDUNN D AND KOSHY TI. 1992. Heparan sulfate glycosaminoglycans as primary cell surface receptors for herpes simplex virus. Adv Exp Med Biol 313: 341-353.

SPRUANCE SL. 1992. The natural history of recurrent oral-facial herpes simplex virus infection. Semin Dermatol 11: 200-206.

STAEHELI P, GROB R, MEIER E, SUTCLIFFE JG AND HALLER O. 1988. Influenza virus-susceptible mice carry Mx genes with a large deletion or a nonsense mutation. Molecular and cellular biology 8: 4518-4523.

STARK GR, KERR IM, WILLIAMS BR, SILVERMAN RH AND SCHREIBER RD. 1998. How cells respond to interferons. Annual review of biochemistry 67: 227-264.

STEPP WH, MEYERS JM AND MCBRIDE AA. 2013. Sp100 provides intrinsic immunity against human papillomavirus infection. mBio 4: e00845-00813.

STERN S, TANAKA M AND HERR W. 1989. The Oct-1 homoeodomain directs formation of a multiprotein-DNA complex with the HSV transactivator VP16. Nature 341: 624-630.

STERNSDORF T, JENSEN K, REICH B AND WILL H. 1999. The nuclear dot protein sp100, characterization of domains necessary for dimerization, subcellular localization, and modification by small ubiquitin-like modifiers. The Journal of biological chemistry 274: 12555-12566.

STERNSDORF T, JENSEN K AND WILL H. 1997. Evidence for covalent modification of the nuclear dot-associated proteins PML and Sp100 by PIC1/SUMO-1. The Journal of cell biology 139: 1621-1634.

STOW ND AND STOW EC. 1986. Isolation and characterization of a herpes simplex virus type 1 mutant containing a deletion within the gene encoding the immediate early polypeptide Vmw110. The Journal of general virology 67 (Pt 12): 2571-2585.

SU C, ZHANG J AND ZHENG C. 2015. Herpes simplex virus 1 UL41 protein abrogates the antiviral activity of hZAP by degrading its mRNA. Virology journal 12: 203.

SU C AND ZHENG C. 2017. Herpes Simplex Virus 1 Abrogates the cGAS/STING-Mediated Cytosolic DNA-Sensing Pathway via Its Virion Host Shutoff Protein, UL41. Journal of virology 91.

SUN L, WU J, DU F, CHEN X AND CHEN ZJ. 2013. Cyclic GMP-AMP synthase is a cytosolic DNA sensor that activates the type I interferon pathway. Science (New York, NY) 339: 786-791.

TAKAOKA A ET AL. 2007. DAI (DLM-1/ZBP1) is a cytosolic DNA sensor and an activator of innate immune response. Nature 448: 501-505.

TAO H, SIMMONS BN, SINGIREDDY S, JAKKIDI M, SHORT KM, COX TC AND MASSIAH MA. 2008. Structure of the MID1 tandem B-boxes reveals an interaction reminiscent of intermolecular ring heterodimers. Biochemistry 47: 2450-2457.

TATHAM MH, JAFFRAY E, VAUGHAN OA, DESTERRO JM, BOTTING CH, NAISMITH JH AND HAY RT. 2001. Polymeric chains of SUMO-2 and SUMO-3 are conjugated to protein substrates by SAE1/SAE2 and Ubc9. The Journal of biological chemistry 276: 35368-35374.

TAVALAI N AND STAMMINGER T. 2009. Interplay between Herpesvirus Infection and Host Defense by PML Nuclear Bodies. Viruses 1: 1240-1264.

TERENZI F, SAIKIA P AND SEN GC. 2008. Interferon-inducible protein, P56, inhibits HPV DNA replication by binding to the viral protein E1. The EMBO journal 27: 3311-3321.

TERNI M, CACCIALANZA P, CASSAI E AND KIEFF E. 1971. Aseptic meningitis in association with herpes progenitalis. N Engl J Med 285: 503-504.

TOKUNAGA F ET AL. 2009. Involvement of linear polyubiquitylation of NEMO in NF-kappaB activation. Nature cell biology 11: 123-132.

TRIEZENBERG SJ, KINGSBURY RC AND MCKNIGHT SL. 1988. Functional dissection of VP16, the trans-activator of herpes simplex virus immediate early gene expression. Genes & development 2: 718-729.

TRUS BL, BOOY FP, NEWCOMB WW, BROWN JC, HOMA FL, THOMSEN DR AND STEVEN AC. 1996. The herpes simplex virus procapsid: structure, conformational changes upon maturation, and roles of the triplex proteins VP19c and VP23 in assembly. Journal of molecular biology 263: 447-462.

TRUS BL, HOMA FL, BOOY FP, NEWCOMB WW, THOMSEN DR, CHENG N, BROWN JC AND STEVEN AC. 1995. Herpes simplex virus capsids assembled in insect cells infected with recombinant baculoviruses: structural authenticity and localization of VP26. Journal of virology 69: 7362-7366.

UMBACH JL, KRAMER MF, JURAK I, KARNOWSKI HW, COEN DM AND CULLEN BR. 2008. MicroRNAs expressed by herpes simplex virus 1 during latent infection regulate viral mRNAs. Nature 454: 780-783.

UNTERHOLZNER L ET AL. 2010. IFI16 is an innate immune sensor for intracellular DNA. Nature immunology 11: 997-1004.

UPRICHARD SL AND KNIPE DM. 1997. Assembly of herpes simplex virus replication proteins at two distinct intranuclear sites. Virology 229: 113-125.

VALLABHAPURAPU S, MATSUZAWA A, ZHANG W, TSENG PH, KEATS JJ, WANG H, VIGNALI DA, BERGSAGEL PL AND KARIN M. 2008. Nonredundant and complementary functions of TRAF2 and TRAF3 in a ubiquitination cascade that activates NIK-dependent alternative NF-kappaB signaling. Nature immunology 9: 1364-1370.

VAN LINT AL, MURAWSKI MR, GOODBODY RE, SEVERA M, FITZGERALD KA, FINBERG RW, KNIPE DM AND KURT-JONES EA. 2010. Herpes simplex virus immediate-early ICP0 protein inhibits Toll-like receptor 2-dependent inflammatory responses and NF-kappaB signaling. Journal of virology 84: 10802-10811.

VANNI E, GATHERER D, TONG L, EVERETT RD AND BOUTELL C. 2012. Functional characterization of residues required for the herpes simplex virus 1 E3 ubiquitin ligase ICP0 to interact with the cellular E2 ubiquitin-conjugating enzyme UBE2D1 (UbcH5a). Journal of virology 86: 6323-6333.

VEERANKI S AND CHOUBEY D. 2012. Interferon-inducible p200-family protein IFI16, an innate immune sensor for cytosolic and nuclear double-stranded DNA: regulation of subcellular localization. Molecular immunology 49: 567-571.

VERPOOTEN D, MA Y, HOU S, YAN Z AND HE B. 2009. Control of TANK-binding kinase 1-mediated signaling by the gamma(1)34.5 protein of herpes simplex virus 1. The Journal of biological chemistry 284: 1097-1105.

VERTEGAAL AC, ANDERSEN JS, OGG SC, HAY RT, MANN M AND LAMOND AI. 2006. Distinct and overlapping sets of SUMO-1 and SUMO-2 target proteins revealed by quantitative proteomics. Molecular & cellular proteomics : MCP 5: 2298-2310.

VOLLSTEDT S, ARNOLD S, SCHWERDEL C, FRANCHINI M, ALBER G, DI SANTO JP, ACKERMANN M AND SUTER M. 2004. Interplay between alpha/beta and gamma interferons with B, T, and natural killer cells in the defense against herpes simplex virus type 1. Journal of virology 78: 3846-3850.

WADSWORTH S, JACOB RJ AND ROIZMAN B. 1975. Anatomy of herpes simplex virus DNA. II. Size, composition, and arrangement of inverted terminal repetitions. Journal of virology 15: 1487-1497.

WANG IH, SUOMALAINEN M, ANDRIASYAN V, KILCHER S, MERCER J, NEEF A, LUEDTKE NW AND GREBER UF. 2013a. Tracking viral genomes in host cells at single-molecule resolution. Cell host & microbe 14: 468-480.

WANG QY, ZHOU C, JOHNSON KE, COLGROVE RC, COEN DM AND KNIPE DM. 2005. Herpesviral latency-associated transcript gene promotes assembly of heterochromatin on viral lytic-gene promoters in latent infection. Proceedings of the National Academy of Sciences of the United States of America 102: 16055-16059.

WANG S, WANG K, LIN R AND ZHENG C. 2013b. Herpes simplex virus 1 serine/threonine kinase US3 hyperphosphorylates IRF3 and inhibits beta interferon production. Journal of virology 87: 12814-12827.

WARNER MS, GERAGHTY RJ, MARTINEZ WM, MONTGOMERY RI, WHITBECK JC, XU R, EISENBERG RJ, COHEN GH AND SPEAR PG. 1998. A cell surface protein with herpesvirus entry activity (HveB) confers susceptibility to infection by mutants of herpes simplex virus type 1, herpes simplex virus type 2, and pseudorabies virus. Virology 246: 179-189.

WATLING D ET AL. 1993. Complementation by the protein tyrosine kinase JAK2 of a mutant cell line defective in the interferon-gamma signal transduction pathway. Nature 366: 166-170.

WEBER F, WAGNER V, RASMUSSEN SB, HARTMANN R AND PALUDAN SR. 2006. Double-stranded RNA is produced by positive-strand RNA viruses and DNA viruses but not in detectable amounts by negative-strand RNA viruses. Journal of virology 80: 5059-5064.

WEIR HM, CALDER JM AND STOW ND. 1989. Binding of the herpes simplex virus type 1 UL9 gene product to an origin of viral DNA replication. Nucleic acids research 17: 1409-1425.

WHITLEY RJ. 2002. Herpes simplex virus infection. Semin Pediatr Infect Dis 13: 6-11.

WHITLEY RJ, LEVIN M, BARTON N, HERSHEY BJ, DAVIS G, KEENEY RE, WHELCHEL J, DIETHELM AG, KARTUS P AND SOONG SJ. 1984. Infections caused by herpes simplex virus in the immunocompromised host: natural history and topical acyclovir therapy. The Journal of infectious diseases 150: 323-329.

WILKINSON DE AND WELLER SK. 2003. The role of DNA recombination in herpes simplex virus DNA replication. IUBMB Life 55: 451-458.

WITTELS M AND SPEAR PG. 1991. Penetration of cells by herpes simplex virus does not require a low pH-dependent endocytic pathway. Virus research 18: 271-290.

WOLFSTEIN A, NAGEL CH, RADTKE K, DOHNER K, ALLAN VJ AND SODEIK B. 2006. The inner tegument promotes herpes simplex virus capsid motility along microtubules in vitro. Traffic 7: 227-237.

WU CA, NELSON NJ, MCGEOCH DJ AND CHALLBERG MD. 1988. Identification of herpes simplex virus type 1 genes required for origin-dependent DNA synthesis. Journal of virology 62: 435-443.

WU J, SUN L, CHEN X, DU F, SHI H, CHEN C AND CHEN ZJ. 2013. Cyclic GMP-AMP is an endogenous second messenger in innate immune signaling by cytosolic DNA. Science (New York, NY) 339: 826-830.

WYSOCKA J AND HERR W. 2003. The herpes simplex virus VP16-induced complex: the makings of a regulatory switch. Trends Biochem Sci 28: 294-304.

XING J, NI L, WANG S, WANG K, LIN R AND ZHENG C. 2013. Herpes simplex virus 1-encoded tegument protein VP16 abrogates the production of beta interferon (IFN) by inhibiting NF-kappaB activation and blocking IFN regulatory factor 3 to recruit its coactivator CBP. Journal of virology 87: 9788-9801.

XING J, WANG S, LIN R, MOSSMAN KL AND ZHENG C. 2012. Herpes simplex virus 1 tegument protein US11 downmodulates the RLR signaling pathway via direct interaction with RIG-I and MDA-5. Journal of virology 86: 3528-3540.

XUE Y, GIBBONS R, YAN Z, YANG D, MCDOWELL TL, SECHI S, QIN J, ZHOU S, HIGGS D AND WANG W. 2003. The ATRX syndrome protein forms a chromatin-remodeling complex with Daxx and localizes in promyelocytic leukemia nuclear bodies. Proceedings of the National Academy of Sciences of the United States of America 100: 10635-10640.

YAN N AND CHEN ZJ. 2012. Intrinsic antiviral immunity. Nature immunology 13: 214-222.

YANG K AND BAINES JD. 2006. The putative terminase subunit of herpes simplex virus 1 encoded by UL28 is necessary and sufficient to mediate interaction between pUL15 and pUL33. Journal of virology 80: 5733-5739.

YANG K, WILLS EG AND BAINES JD. 2011. A mutation in UL15 of herpes simplex virus 1 that reduces packaging of cleaved genomes. Journal of virology 85: 11972-11980.

YAO F AND SCHAFFER PA. 1995. An activity specified by the osteosarcoma line U2OS can substitute functionally for ICP0, a major regulatory protein of herpes simplex virus type 1. Journal of virology 69: 6249-6258.

YIN Z ET AL. 2012. Type III IFNs are produced by and stimulate human plasmacytoid dendritic cells. Journal of immunology (Baltimore, Md : 1950) 189: 2735-2745.

YOKOTA S, YOKOSAWA N, KUBOTA T, SUZUTANI T, YOSHIDA I, MIURA S, JIMBOW K AND FUJII N. 2001. Herpes simplex virus type 1 suppresses the interferon signaling pathway by inhibiting phosphorylation of STATs and janus kinases during an early infection stage. Virology 286: 119-124.

YONEYAMA M ET AL. 2005. Shared and unique functions of the DExD/H-box helicases RIG-I, MDA5, and LGP2 in antiviral innate immunity. Journal of immunology (Baltimore, Md : 1950) 175: 2851-2858.

YOSHIDA A, KOIDE Y, UCHIJIMA M AND YOSHIDA TO. 1994. IFN-gamma induces IL-12 mRNA expression by a murine macrophage cell line, J774. Biochemical and biophysical research communications 198: 857-861.

ZAWATZKY R, GRESSER I, DEMAEYER E AND KIRCHNER H. 1982. The role of interferon in the resistance of C57BL/6 mice to various doses of herpes simplex virus type 1. The Journal of infectious diseases 146: 405-410.

ZENNER HL, MAURICIO R, BANTING G AND CRUMP CM. 2013. Herpes simplex virus 1 counteracts tetherin restriction via its virion host shutoff activity. Journal of virology 87: 13115-13123.

ZERIAL A, HOVANESSIAN AG, STEFANOS S, HUYGEN K, WERNER GH AND FALCOFF E. 1982. Synergistic activities of type I (alpha, beta) and type II (gamma) murine interferons. Antiviral Res 2: 227-239.

ZHANG D, SU C AND ZHENG C. 2016. Herpes Simplex Virus 1 Serine Protease VP24 Blocks the DNA-Sensing Signal Pathway by Abrogating Activation of Interferon Regulatory Factor 3. Journal of virology 90: 5824-5829.

ZHANG J, WANG K, WANG S AND ZHENG C. 2013. Herpes simplex virus 1 E3 ubiquitin ligase ICP0 protein inhibits tumor necrosis factor alpha-induced NF-kappaB activation by interacting with p65/RelA and p50/NF-kappaB1. Journal of virology 87: 12935-12948.

ZHANG SY ET AL. 2007. TLR3 deficiency in patients with herpes simplex encephalitis. Science (New York, NY) 317: 1522-1527.

ZHENG C. 2018. Evasion of Cytosolic DNA-Stimulated Innate Immune Responses by Herpes Simplex Virus 1. Journal of virology 92.

ZHENG Y, SAMRAT SK AND GU H. 2016. A Tale of Two PMLs: Elements Regulating a Differential Substrate Recognition by the ICP0 E3 Ubiquitin Ligase of Herpes Simplex Virus 1. Journal of virology 90: 10875-10885.

ZHONG S, MULLER S, RONCHETTI S, FREEMONT PS, DEJEAN A AND PANDOLFI PP. 2000. Role of SUMO-1-modified PML in nuclear body formation. Blood 95: 2748-2752.

ZHOU C AND KNIPE DM. 2002. Association of herpes simplex virus type 1 ICP8 and ICP27 proteins with cellular RNA polymerase II holoenzyme. Journal of virology 76: 5893-5904.

ZHOU ZH, CHEN DH, JAKANA J, RIXON FJ AND CHIU W. 1999. Visualization of tegument-capsid interactions and DNA in intact herpes simplex virus type 1 virions. Journal of virology 73: 3210-3218.

ZHOU ZH, HE J, JAKANA J, TATMAN JD, RIXON FJ AND CHIU W. 1995. Assembly of VP26 in herpes simplex virus-1 inferred from structures of wild-type and recombinant capsids. Nature structural biology 2: 1026-1030.

Distinct temporal roles for the promyelocytic leukaemia (PML) protein in the sequential regulation of intracellular host immunity to HSV-1 infection

Thamir Alandijany[1,2], Ashley P. E. Roberts[1], Kristen L. Conn[1,3], Colin Loney[1], Steven McFarlane[1], Anne Orr[1], Chris Boutell[1]*

1 MRC-University of Glasgow Centre for Virus Research (CVR), Garscube Campus, Glasgow, Scotland, United Kingdom, **2** Department of Medical Laboratory Technology, Faculty of Applied Medical Sciences, King Abdulaziz University, Jeddah, Saudi Arabia, **3** Department of Biochemistry, University of Alberta, Edmonton, AB, Canada

* chris.boutell@glasgow.ac.uk

Abstract

Detection of viral nucleic acids plays a critical role in the induction of intracellular host immune defences. However, the temporal recruitment of immune regulators to infecting viral genomes remains poorly defined due to the technical difficulties associated with low genome copy-number detection. Here we utilize 5-Ethynyl-2'-deoxyuridine (EdU) labelling of herpes simplex virus 1 (HSV-1) DNA in combination with click chemistry to examine the sequential recruitment of host immune regulators to infecting viral genomes under low multiplicity of infection conditions. Following viral genome entry into the nucleus, PML-nuclear bodies (PML-NBs) rapidly entrapped viral DNA (vDNA) leading to a block in viral replication in the absence of the viral PML-NB antagonist ICP0. This pre-existing intrinsic host defence to infection occurred independently of the vDNA pathogen sensor IFI16 (Interferon Gamma Inducible Protein 16) and the induction of interferon stimulated gene (ISG) expression, demonstrating that vDNA entry into the nucleus alone is not sufficient to induce a robust innate immune response. Saturation of this pre-existing intrinsic host defence during HSV-1 ICP0-null mutant infection led to the stable recruitment of PML and IFI16 into vDNA complexes associated with ICP4, and led to the induction of ISG expression. This induced innate immune response occurred in a PML-, IFI16-, and Janus-Associated Kinase (JAK)-dependent manner and was restricted by phosphonoacetic acid, demonstrating that vDNA polymerase activity is required for the robust induction of ISG expression during HSV-1 infection. Our data identifies dual roles for PML in the sequential regulation of intrinsic and innate immunity to HSV-1 infection that are dependent on viral genome delivery to the nucleus and the onset of vDNA replication, respectively. These intracellular host defences are counteracted by ICP0, which targets PML for degradation from the outset of nuclear infection to promote vDNA release from PML-NBs and the onset of HSV-1 lytic replication.

Author summary

Intrinsic and innate immunity act to restrict the replication of many clinically important viral pathogens. However, the temporal regulation of these two arms of host immunity during virus infection remains poorly defined. A key aspect in the regulation of these intracellular immune defences during herpesvirus infection is the rapid recruitment of constitutively expressed immune regulators to infecting viral genomes. Here we show that at physiologically low multiplicities of infection, PML-NBs rapidly entrap HSV-1 genomes upon nuclear entry. Saturation of this pre-existing intrinsic host defence led to the stable recruitment of the vDNA pathogen sensor IFI16 to HSV-1 vDNA and the induction of ISG expression, an induced innate immune response dependent on the initiation of vDNA replication. Importantly, both intrinsic and innate arms of host immunity required PML, the principle scaffolding protein of PML-NBs. Our research identifies dual roles for PML in the sequential regulation of intracellular host immunity during HSV-1 infection, and highlights distinct phases in host immune factor recruitment to infecting viral genomes required for the temporal regulation of intracellular host immune defences during herpesvirus infection.

Introduction

Intrinsic, innate, and adaptive arms of host immunity cooperatively supress the replication and spread of invading viral pathogens. Conferred by constitutively expressed host-cell restriction factors, intrinsic immunity is the first line of intracellular defence against infection (reviewed in [1–3]). In contrast, innate immune defences are upregulated following the activation of Pattern Recognition Receptors (PRRs) that detect Pathogen-Associated Molecular Patterns (PAMPs) unique to microbial pathogens, including foreign viral nucleic acids. PRR activation induces downstream signalling events that culminate in the expression of antiviral host genes, principally cytokines (including interferons) and interferon stimulated gene (ISG) products (reviewed in [4–6]). This induced innate immune response confers a broadly refractory antiviral state that limits virus propagation and stimulates adaptive immune responses. Consequently, many viruses have evolved counter measures to antagonize intrinsic and innate immune defences to promote their efficient propagation and transmission to new hosts.

A key event in the regulation of intracellular immune defences during herpesvirus infection is the rapid recruitment of constitutively expressed host factors to sites in close proximity to infecting viral genomes upon nuclear entry (reviewed in [1, 7]). These factors include core constituent proteins of Promyelocytic Leukaemia Nuclear Bodies (PML-NBs; notably PML, Sp100, Daxx and ATRX; [8–10]), innate immune regulators (IFI16, cGAS, and STING; [11–14]), DNA Damage Response (DDR) proteins (γH2AX, Mdc1, 53BP1, and BRCA1; [15]), and core component proteins of the SUMOylation pathway (SUMO-1, SUMO-2/3, PIAS1, and PIAS4 [16–19]). The recruitment of these host factors represents the earliest detectable nuclear responses to infection, and have been linked to the repression of viral gene expression and PRR activation in the regulation of intrinsic and innate immune defences, respectively. The importance of PML-NB constituent proteins and IFI16 in the regulation of intracellular immunity is highlighted by the fact that many viruses have evolved strategies to antagonise these key immune regulators (reviewed in [1, 4, 6, 20, 21]). One of the first viral proteins to be expressed during Herpes Simplex Virus 1 (HSV-1) infection is ICP0, a viral RING-finger ubiquitin ligase that promotes the degradation and dispersal of host factors, including PML and IFI16 [11, 22–31], away from infecting viral genomes (reviewed in [7, 32]). This activity

inhibits viral genome silencing and the induction of ISG expression, thereby promoting the efficient onset of HSV-1 gene expression and replication. Viral mutants that do not express ICP0, or carry mutations that impair its ubiquitin ligase activity, are highly susceptible to host-cell restriction at low multiplicities of infection (MOI) and are hypersensitive to interferon (IFN) treatment [33–38]. The use of such mutants has been critical in defining many aspects relating to the regulation of intrinsic and innate immunity during herpesvirus infection. Studies analysing the recruitment of host immune regulators to infecting viral genomes have typically relied on high MOI conditions due to the technical challenges associated with low genome copy-number detection. A defining hallmark of intrinsic immunity, however, is that this host defence is readily saturated under high MOI conditions due to limiting levels of pre-existing host factors. Thus, much of the mechanistic detail of immune regulator recruitment to infecting HSV-1 genomes has been established using viral mutants at input genome levels that saturate intrinsic host defences. Consequently, the temporal recruitment of intrinsic and innate immune regulators to infecting viral genomes remains poorly defined, specifically under low MOI conditions pertinent to wild-type (WT) herpesvirus infections observed in a clinical setting.

Here we use fluorophore conjugation by click chemistry to investigate the temporal recruitment of intrinsic and innate immune regulators to 5-Ethynyl-2'-deoxyuridine (EdU) labelled HSV-1 genomes under physiologically low MOI conditions (0.1 to 3 PFU/cell). HSV-1 genomes were readily detected in the nucleus within 30 minutes of infection (post-addition of virus) and to be stably entrapped within PML-NBs in restrictive cell types prior to PML-NB disruption and genome release by ICP0. PML-NB entrapment of vDNA occurred independently of the PRR sensor IFI16 and ISG expression, demonstrating that this intrinsic host response does not directly contribute to the induction of innate immunity. Saturation of this host defence during HSV-1 ICP0-null mutant infection led to the stable recruitment of PML and IFI16 into vDNA complexes associated with ICP4, and the subsequent induction of ISGs. This induced innate immune response occurred in a PML-, IFI16-, and Janus associated kinase (JAK) dependent manner, which could be suppressed by the vDNA polymerase inhibitor phosphonoacetic acid (PAA). These data demonstrate that vDNA entry into the nucleus alone under low MOI conditions is not sufficient to stimulate a robust innate immune response to HSV-1 nuclear infection, which only occurs after the onset of vDNA replication. We show that intrinsic and innate arms of intracellular host immunity act sequentially, as inhibition of innate immune signalling could not relieve the intrinsic cellular restriction of an HSV-1 ICP0-null mutant, but instead led to significantly enhanced virus yields under infection conditions that enabled the onset of vDNA replication. Collectively, our data demonstrate that intrinsic and innate arms of host immunity are temporally distinct immune events activated in response to vDNA nuclear entry and the onset of vDNA replication, respectively. Our data identifies distinct roles for PML in the sequential regulation of these intracellular immune defences to HSV-1 infection, findings that are likely to be highly pertinent in the cellular restriction of many nuclear replicating viral pathogens.

Results

Direct visualization of bio-orthogonally labelled input HSV-1 genomes at low MOI

Microscopy studies have played pivotal roles in the identification of host factors and signalling pathways that contribute to the intracellular regulation of intrinsic and innate immunity during herpesvirus infection (reviewed in [1, 4, 7, 32, 39]). However, the detection of viral genomes under low MOI conditions, which do not saturate intrinsic host defences, remains a

significant technical challenge. To date, viral genome localization studies have relied on the indirect detection of vDNA through immunolabelling or fluorescent tagging of vDNA binding proteins, for example the viral immediate early (IE) transcription factor ICP4 or the early (E) single-stranded vDNA binding protein ICP8 [8–10, 13, 14, 40]. The use of vDNA binding proteins limits temporal resolution of host factor recruitment to infecting viral genomes, as genome detection requires the successful expression of viral gene products that may compete with, or displace, host factors bound to vDNA. Consequently, this strategy is suboptimal for the examination of early intrinsic host immune defences that influence the cellular restriction of viral gene expression. While direct vDNA labelling strategies have been employed, most notably fluorescent *in situ* hybridization (FISH; [8, 10]), such approaches require harsh denaturing conditions which impair host antigen detection ([41], personal communication J. Brown), and have not been widely adopted. Recent advances in direct bio-orthogonal nucleic acid labelling, using Ethynyl-tagged deoxynucleotides in combination with fluorescent labelling by click chemistry techniques, have enabled the direct visualization of vDNA during both Adeno- and Herpesvirus infection ([42–46]). We sought to apply this technique by purifying either EdU or EdC labelled HSV-1 virions (HSV-1^{EdU} or HSV-1^{EdC}, respectively) and infecting cells at low MOI (≤ 3 PFU/cell) to examine the temporal recruitment of intrinsic and innate immune regulators to input viral genomes following nuclear entry.

Successful labelling of vDNA and the purification of high titre WT or ICP0-null mutant HSV-1^{EdU} or HSV-1^{EdC} stocks was achieved by infecting Retinal Pigmented Epithelial (RPE) cells (see Materials and methods; S1A–S1C Fig). Notably, many laboratory cell lines were unable to support efficient viral propagation at nucleotide concentrations exceeding 1 μM in an Ethynyl-tag dependent manner (S1 Table, S1D–S1F Fig). As RPE cells were restrictive to HSV-1 ICP0-null mutant replication (see below) and sensitive to Ethynyl-tagged deoxynucleotide labelling in the absence of ICP0 (S1G–S1I Fig), we selected the lowest dose of 0.5 μM EdU or EdC for genome labelling to enable comparative recruitment studies to input viral genomes in the presence or absence of ICP0. *In vitro* genome release assays demonstrated that $\geq 60\%$ of virions contained EdU or EdC labelled viral genomes detectable by click chemistry following partial denaturation of the HSV-1 capsid by 2M guanidine hydrochloride (GuHCl, Fig 1A–1C, S2 Fig; [47]). Particle to plaque forming unit (PFU) analysis of virus preparations grown in the presence of EdU demonstrated that HSV-1^{EdU} labelled virions had a roughly equivalent ratio to that of unlabelled control virus preparations (within 3-fold; S2 Table). These data demonstrate that EdU labelling of vDNA was not significantly detrimental to virion production or infectivity under these labelling conditions.

A time course of infection of human foreskin fibroblast (HFt) cells with WT (HSV-1^{EdU}) or ICP0-null (ΔICP0^{EdU}) mutant HSV-1 demonstrated that vDNA could be readily detected within the nuclei of infected cells as early as 30 minutes post-infection (mpi; post-addition of virus), with $> 70\%$ of nuclei containing at least 1 (median average of 2) HSV-1^{EdU} genome foci by 120 mpi (Fig 1D, 1F and 1G). Signal detection was dependent on both HSV-1 infection and EdU vDNA labelling, demonstrating that fluorescent click signal(s) were specific to input EdU labelled vDNA (Fig 1E), with the majority of genome signals ($\geq 70\%$) observed within the nucleus (Fig 1H). Notably, qPCR analysis (S2 Table) revealed that the majority of particles ($> 50\%$) had yet to release their genomes by 120 mpi (post-addition of virus). As vDNA is undetectable within native capsids (S2 Fig), these data suggest that the process of nuclear infection is still ongoing at 120 mpi. We note that under equivalent MOI conditions, ΔICP0^{EdU} infected cells had a reduced number of vDNA positive nuclei at each time point (Fig 1F–1H), a phenotype that likely reflects the efficiency of ICP0-null mutant EdU vDNA labelling in restrictive RPE cells (S1G–S1I Fig).
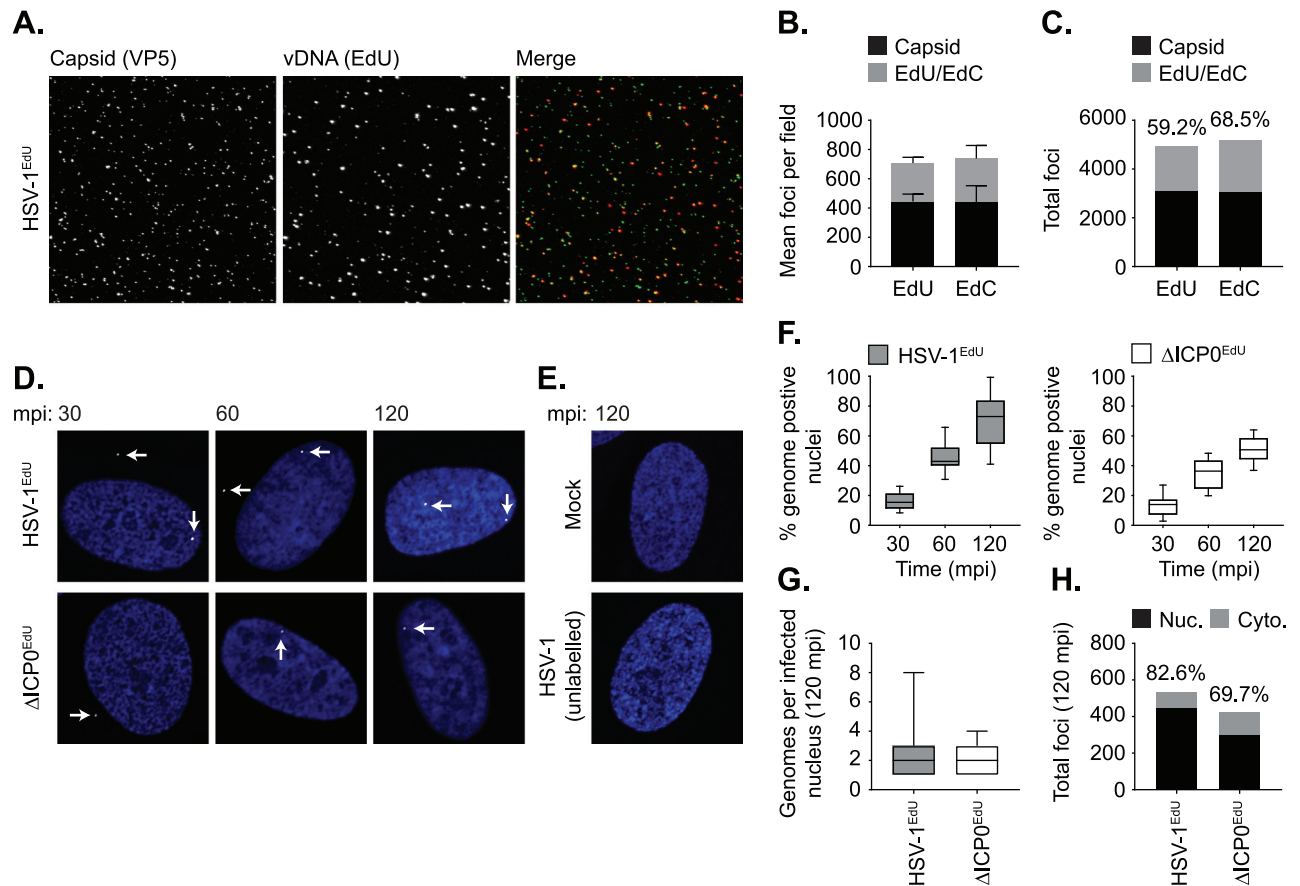
Fig 1. Direct visualization of bio-orthogonally labelled HSV-1 genomes. Quantitation of bio-orthogonally labelled vDNA in HSV-1 virions. HSV-1^{EdU} or HSV-1^{EdC} virions were subjected to partial denaturation with 2M GuHCl at 4°C for 60 mins to release vDNA [47]. vDNA (red) was detected by click chemistry and capsid (green) by indirect immunofluorescence staining. (A) Representative confocal images showing vDNA release and expansion from partially denatured HSV-1^{EdU} virions following GuHCl treatment. (B,C) Stack plots showing the relative population of EdU or EdC positive vDNA labelled HSV-1 virions. $n \geq 3000$ particles per population derived from 3 independent experiments. Minimum estimates for viral genome labelling efficiency are shown (%). (D,E) HFt cells were mock or HSV-1 infected with either unlabelled or EdU labelled WT (HSV-1^{EdU}) or ICP0-null mutant HSV-1 (ΔICP0^{EdU}) at an MOI of 3 PFU/cell. Cells were fixed and permeabilized at the indicated times minutes post-infection (mpi; post-addition of virus). vDNA was detected by click chemistry (white arrows) and nuclei stained with DAPI (blue). Representative confocal images showing the nuclear accumulation of HSV-1^{EdU} and ΔICP0^{EdU} genomes over time (30–120 mpi; as indicated), with genome detection specific to input EdU labelled virus. (F) Quantitation of HSV-1^{EdU} or ΔICP0^{EdU} genome positive nuclei over time (as in D). Boxes: 25th to 75th percentile range; black line: median; whiskers: 5th to 95th percentile range. $n \geq 300$ cells per sample population derived from a minimum of 3 independent experiments. (G) Number of genomes detected within infected nuclei at 120 mpi. Boxes: 25th to 75th percentile range; black line: median; whiskers: minimum and maximum range of sample. $n \geq 200$ cells per sample population derived from a minimum of 3 independent experiments. (H) Nuclear (Nuc.) and cytoplasmic (Cyto.) distribution of genome foci detected at 120 mpi. $n \geq 300$ cells per sample population derived from a minimum of 3 independent experiments. Percentage of total genomes detected within the nucleus is shown (%).

https://doi.org/10.1371/journal.ppat.1006769.g001

PML-NBs entrap WT HSV-1 genomes upon nuclear entry

With the ability to detect input vDNA within the nuclei of infected cells as early as 30 mpi (post-addition of virus), we next assessed the utility of this approach to investigate the recruitment of intrinsic immune factors to infecting WT HSV-1^{EdU} genomes over a short time-course of infection (30 to 90 mpi; Fig 2). Using a combination of click chemistry to detect vDNA and immuno-labelling to detect PML-NB intrinsic host factors, PML (the main scaffolding protein of PML-NBs; [48]) and Daxx (a core constituent protein of PML-NBs; [48]) were observed to stably colocalize with vDNA over the time course of infection (30–90 mpi;
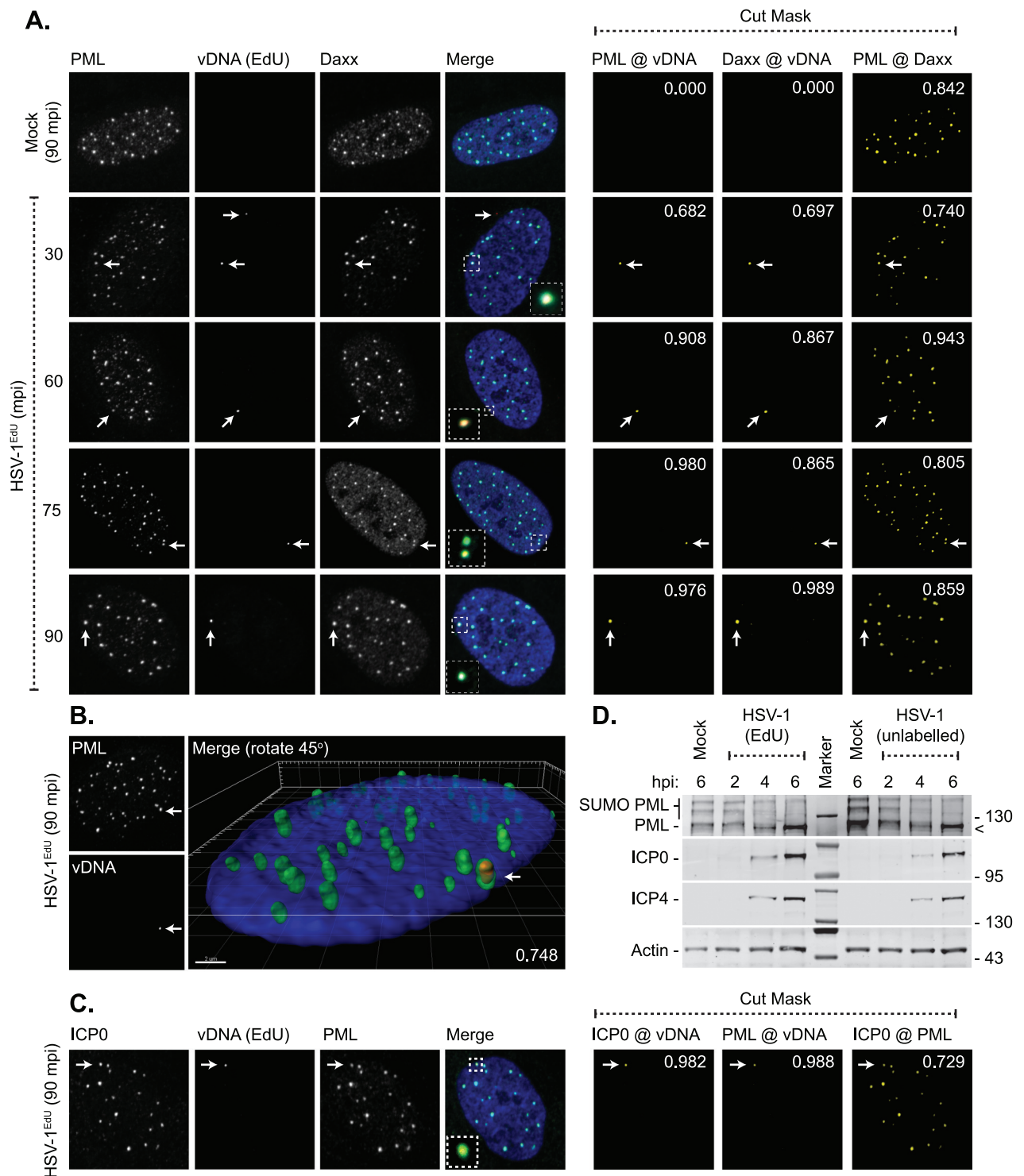
Fig 2. PML-NBs stably entrap vDNA upon nuclear entry. HFt cells were mock or HSV-1^{EdU} infected at an MOI of 3 PFU/cell. Cells were fixed and permeabilized at the indicated times (mpi; post-addition of virus). vDNA, or PML-NB host factors and ICP0, were detected by click chemistry and indirect immunofluorescence staining, respectively. (A) Localization of PML (green) and Daxx (cyan) to HSV-1 vDNA (red, white arrows) at 30–90 mpi (as indicated). Insets show magnified regions of interest (dashed boxes) highlighting PML-NB colocalization with vDNA. Cut mask (yellow) highlights regions of colocalization between PML, Daxx, and vDNA (as indicated). Weighted colocalization coefficients are shown. (B) 3D reconstruction of high-resolution confocal Z-series images showing PML (green) entrapment of vDNA (red, white arrow) at 90 mpi. Single channel maximum intensity projections (left-

hand panels) and 3D rendered image (right-hand panel). Pearson coefficient for PML-vDNA colocalization is shown. Scale bar 2 μm. (C) Nuclear localization of ICP0 (green) to vDNA (red, white arrow) and PML (cyan) in HSV-1^{EdU} infected cells at 90 mpi. Cut mask (yellow) highlights regions of colocalization between ICP0, PML, and vDNA (as indicated). Weighted colocalization coefficients are shown. Nuclei stained with DAPI (blue). (D) EdU labelling of viral genomes does not affect the initiation of infection. HFt cells were mock or HSV-1 infected with unlabelled (HSV-1) or EdU labelled (HSV-1^{EdU}) HSV-1 at an MOI of 3 PFU/cell. Whole cell lysates were collected at the indicated times (hours post-infection; hpi) for western blot analysis to monitor the rate of PML degradation and the accumulation of the viral immediate early (IE) gene products (ICP0, ICP4). Actin is shown as a loading control. Molecular mass markers are shown, < denotes the detection of a non-specific background band.

Fig 2A). High-resolution Z-series imaging revealed input vDNA to be encased in PML following nuclear infection (Fig 2B). At 90 mpi, ICP0 could be observed to colocalize with PML-NBs prior to PML degradation and PML-NB disruption (Fig 2C and 2D; [22, 25–27]). ICP0 localization at multiple PML-NBs demonstrates that vDNA entrapment within any single PML-NB is not sufficient to target ICP0 to that specific body (Fig 2C). Western blotting of infected cell lysates demonstrated that EdU labelling of vDNA was not detrimental to the initiation of IE gene expression (ICP0, ICP4) or the degradation of PML (Fig 2D). Collectively, these data that demonstrate infecting WT HSV-1 genomes are rapidly encased by PML-NB intrinsic host factors from the outset of nuclear infection prior to the onset of lytic replication. Our data contrast with previous recruitment studies, which have reported PML-NB constituent proteins to localize to sites in close proximity to infecting viral genomes [8–10, 40]. However, we note that these studies have typically relied on higher MOI conditions ($\geq$ 10 PFU/cell; [10]), the use of vDNA binding proteins to enable genome detection by proxy, or time points post-infection where vDNA replication proteins are readily detectable. We conclude that PML-NB host factors rapidly entrap viral genomes shortly after nuclear entry prior to the robust onset of viral gene expression (Fig 2D).

Asynchronous plaque-edge recruitment studies have shown that PML-NB host factors are independently recruited to infecting viral genomes [49, 50] in an IFI16-dependent manner [11, 12, 14], where *de novo* PML-NB like foci are reformed [10]. We therefore assessed the composition of vDNA containing PML-NBs, as well as the localization of the PRR IFI16, to infecting WT HSV-1^{EdU} or HSV-1^{EdC} genomes (Fig 3, S3 Fig). High colocalization frequencies (weighted colocalization coefficients > 0.7) were observed for all PML-NB component proteins examined (PML, Daxx, Sp100, ATRX, and SUMO2/3) to infecting viral genomes irrespective of genome label, with equivalent paired colocalization frequencies observed for resident PML-NB proteins in mock-infected cells (Fig 3A–3D and 3F, S3 Fig). These data demonstrate that PML-NBs that contained vDNA were indistinguishable in composition from other PML-NBs within the same infected cell or in mock-infected cells at 90 mpi. Surprisingly, the colocalization frequency between IFI16 and input viral genomes was below coincident threshold levels (weighted colocalization coefficients < 0.2; solid line), demonstrating that IFI16 does not stably localize with viral genomes entrapped within PML-NBs at 90 mpi (Fig 3E and 3F, S3 Fig). These data again contrast with published asynchronous plaque-edge recruitment studies that have used vDNA binding proteins for genome detection, which have shown IFI16 and PML to both localize to infecting HSV-1 ICP0-null mutant genomes [11, 13, 14]. As ICP0 has been reported to promote the degradation of IFI16 [11, 28–31], we examined the recruitment of IFI16 to ΔICP0^{EdU} genomes to investigate the potential effect of ICP0 expression on IFI16 localization to vDNA. No stable localization of IFI16 could be observed to infecting ΔICP0^{EdU} genomes (S4 Fig), demonstrating that a lack of stable IFI16 recruitment to viral genomes was not due to low levels of ICP0 expression at 90 mpi (Fig 2C). We note that IFI16 localization to viral genomes has been reported to be highly dynamic [12, 14], which could potentially be inhibited by PML-NB entrapment of vDNA. We therefore investigated the influence of MOI (1, 10, and 50 PFU/cell) and time (15 or 30 mpi) on the recruitment of
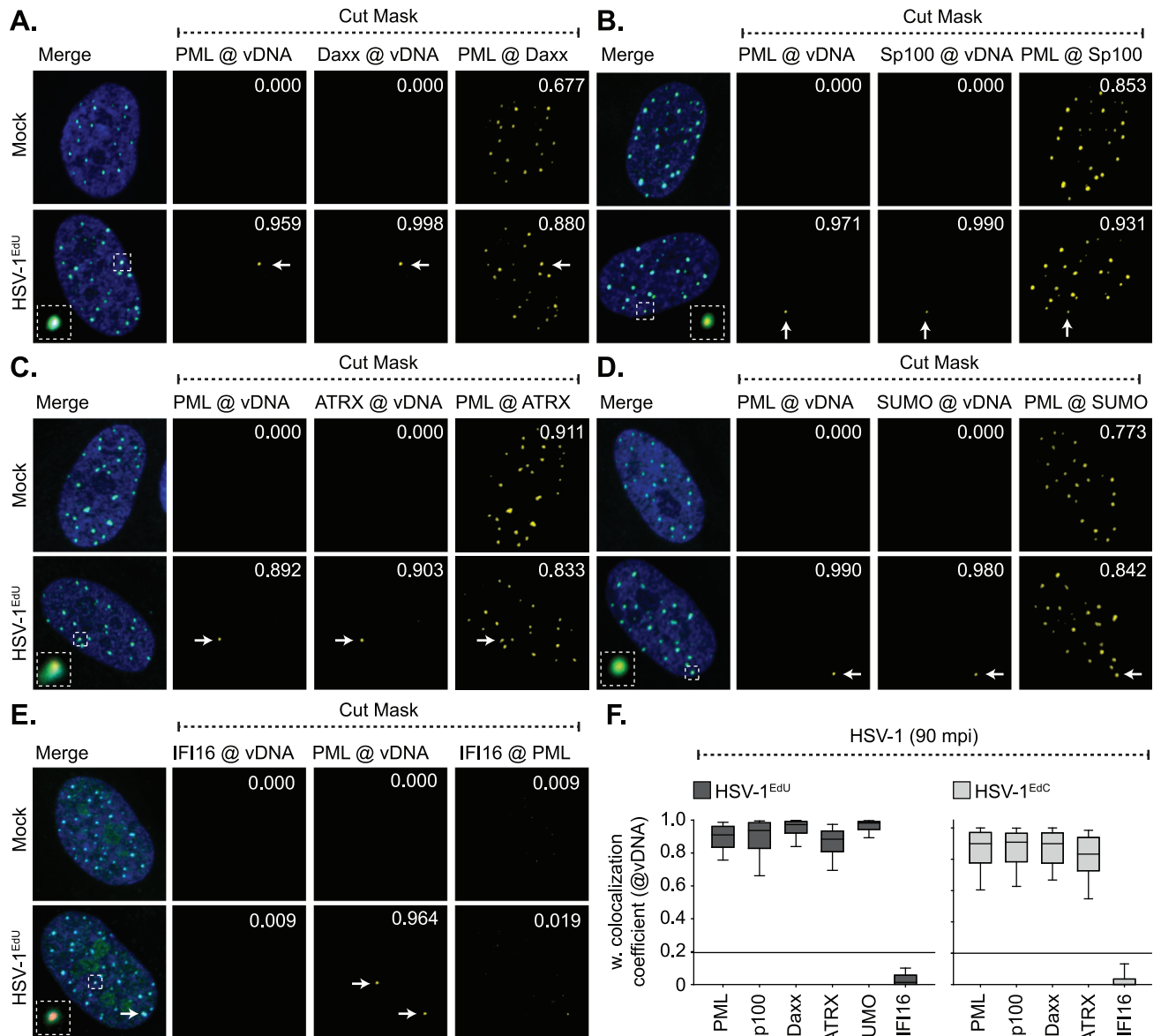
Fig 3. Core PML-NB proteins, but not IFI16, associate with infecting HSV-1 genomes. HFt cells were mock or infected with either HSV-1[EdU] or HSV-1[EdC] at an MOI of 3 PFU/cell. Cells were fixed and permeabilized at the indicated times (mpi; post-addition of virus). vDNA and PML-NB host factors were detected by click chemistry and indirect immunofluorescence staining, respectively. (A-E) Localization of PML (green), and either Daxx, Sp100, ATRX, SUMO2/3 (SUMO), or IFI16 (cyan; as indicated) to infecting HSV-1[EdU] vDNA (red, white arrows). Insets show magnified regions of interest (dashed boxes) highlighting host protein localization with vDNA. Cut mask (yellow) highlights regions of colocalization between host proteins and vDNA (as indicated). Weighted colocalization coefficients are shown. Individual channel images shown in S3 Fig. Nuclei were stained with DAPI (blue). (F) Quantitation of host protein recruitment to infecting viral genomes labelled with EdU (as shown in A-E) or EdC. Boxes: 25th to 75th percentile range; black line: median weighted (w.) colocalization coefficient; whiskers: 5th to 95th percentile range. Solid line indicates coincident threshold level (weighted colocalization coefficients < 0.2). n ≥ 50 vDNA foci per sample population from a minimum of three independent infections.

IFI16 and PML to nuclear infecting HSV-1[EdU] genomes (S5 Fig). While vDNA-IFI16 colocalization could be observed under very high MOI conditions (50 PFU/cell; S5A Fig), quantitation (n ≥ 250 genomes) revealed the frequency of these colocalization events was not significantly altered by MOI or time (S5B–S5E Fig). In contrast, PML colocalization with vDNA was

significantly reduced in a MOI dependent manner (1–50 PFU/cell), indicative of PML-NB saturation by viral genomes or disruption by ICP0 under these high MOI conditions. PML recruitment to vDNA also occurred in a time dependent manner, with a significant increase in colocalization frequency between 15 and 30 mpi (MOI of 10 PFU/cell). As bio-orthogonal nucleic acid labelling is incompatible with live-cell kinetic studies, we conclude that IFI16 does not form a stable association with input vDNA following genome entry into the nucleus.

IFI16 recruitment to input viral genomes is not enhanced in the absence of PML

To test if PML-NBs competitively exclude IFI16 from binding vDNA following nuclear entry, we investigated the recruitment of IFI16 and Daxx (as a positive control; [49]) to input HSV-1^{EdU} and ΔICP0^{EdU} genomes in cells depleted of PML (Fig 4, S6 Fig). HFt cells were stably transduced with lentiviral vectors expressing non-targeting control or PML-targeting short hairpin RNAs (shCtrl and shPML, respectively; [49]). qRT-PCR and western blotting confirmed PML depletion without influencing Daxx or IFI16 expression (Fig 4A and 4B). HSV-1^{EdU} or ΔICP0^{EdU} infection of shCtrl cells recapitulated observations made in parental HFt cells (Fig 3, S3 Fig, S4 Fig), demonstrating that lentiviral transduction, shRNA expression, or puromycin selection did not affect PML-NB entrapment of vDNA or alter IFI16 localization (Fig 4C–4E). PML depletion did not increase the frequency of IFI16 colocalization with vDNA during either HSV-1^{EdU} or ΔICP0^{EdU} infection (Fig 4D and 4E, S6 Fig), demonstrating that PML-NBs do not competitively exclude IFI16 from binding vDNA. In contrast, while Daxx colocalized with vDNA in a subset of PML depleted cells (Fig 4C, S6A Fig), quantitation (n ≥ 100 genomes) revealed that the frequency of this colocalization was significantly reduced compared to control cells irrespective of ICP0 expression (Fig 4E). These data contrast with asynchronous plaque-edge recruitment studies, where Daxx recruitment to infecting viral genomes occurs in a PML independent manner under high MOI conditions [49]. We conclude that under infection conditions that do not saturate or disrupt PML-NBs by 90 mpi (MOI < 10 PFU/cell; S5 Fig), Daxx colocalization with vDNA is stabilized by PML at PML-NBs where Daxx is a resident protein (Figs 2–4, S3 Fig; [48]).

Live cell microscopy studies and asynchronous plaque-edge recruitment assays have reported that IFI16 is required for PML and Daxx recruitment to infecting viral genomes [11, 12, 14], although no direct evidence of IFI16 colocalization with vDNA or deposition within PML-NBs was reported to support this hypothesis. We therefore investigated if IFI16 played a role in PML-NB entrapment of vDNA (Fig 5). HFt cells were stably transduced with lentiviral vectors expressing non-targeting control or IFI16-targeting short hairpin RNAs (shCtrl and shIFI16, respectively; [11]). qRT-PCR and western blotting confirmed IFI16 depletion without influencing PML or Daxx expression (Fig 5A and 5B). HSV-1^{EdU} infection of shCtrl or shIFI16 cells demonstrated that both PML and Daxx strongly colocalized with vDNA independently of IFI16 (Fig 5C–5E). We conclude that IFI16 does not play an essential role in the entrapment of vDNA within PML-NBs. As we failed to observe any significant recruitment of IFI16 to infecting HSV-1 genomes under a range of infection conditions, our data suggest that the stable recruitment of PML and IFI16 to infecting viral genomes occurs with temporally distinct kinetics.

vDNA entry into the nucleus is not sufficient to induce ISG expression

As asynchronous plaque-edge recruitment assays have played a key role in defining the recruitment of IFI16 to infecting HSV-1 genomes [11, 13, 14], we conducted analogous assays to assess the temporal recruitment of PML and IFI16 to both vDNA and ICP4, an IE vDNA
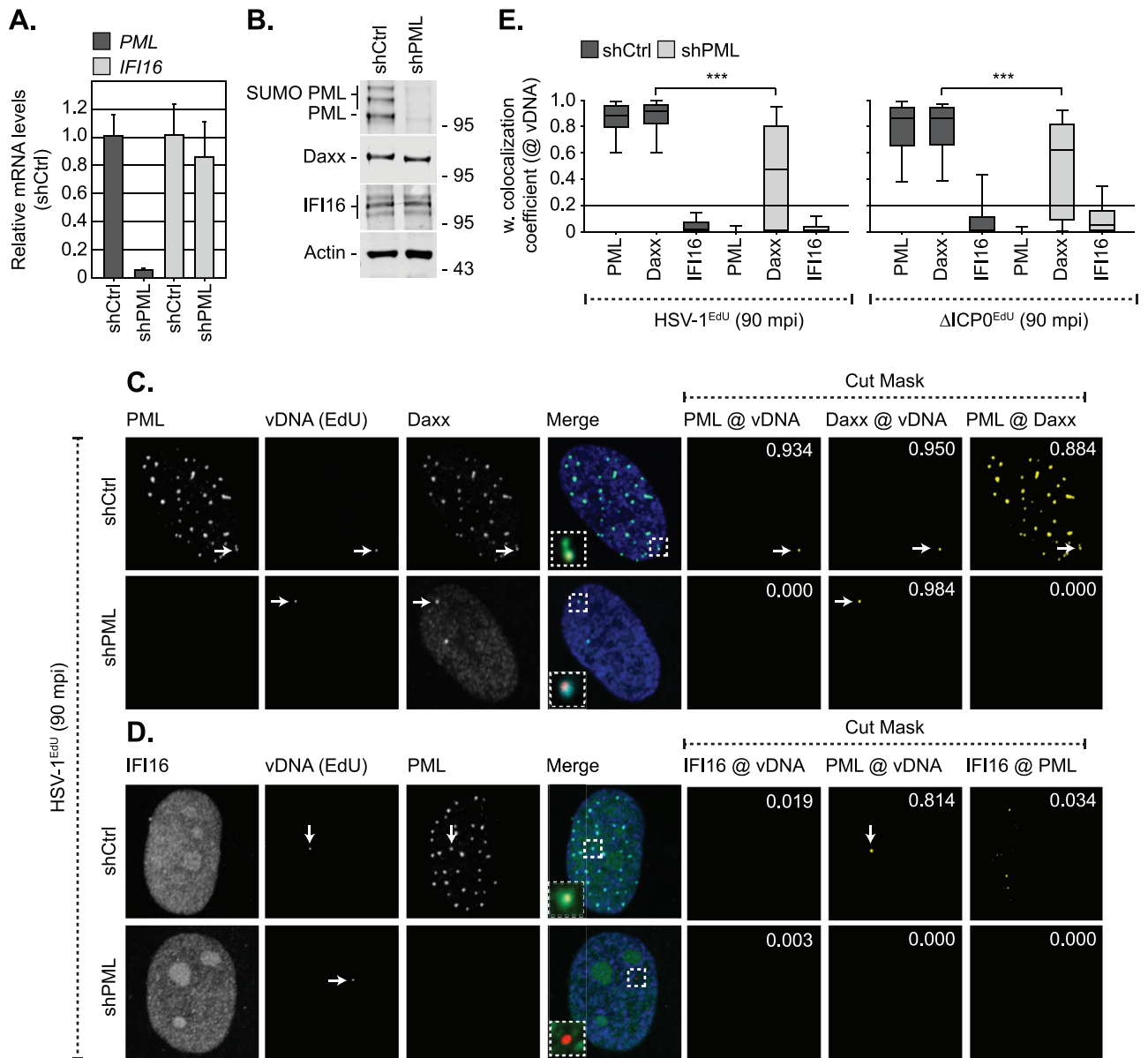
Fig 4. Depletion of PML does not enhance the recruitment of IFI16 to infecting viral genomes. HFt cells were stably transduced with lentiviruses expressing PML-targeting (shPML) or non-targeting control (shCtrl) shRNAs. (A) qRT-PCR quantitation of *PML* or *IFI16* mRNA levels in HFt shCtrl and shPML cells. Mean (RQ) and standard deviation (RQmin/max) shown and expressed relative to HFt shCtrl cells (1). (B) Western blot analysis of the expression levels of PML, Daxx and IFI16 in whole cell lysates derived from HFt shCtrl and shPML cells. Actin is shown as a loading control. Molecular mass markers are shown. (C, D) Localization of PML (green), and either Daxx or IFI16 (cyan; as indicated), to infecting HSV-1^{EdU} vDNA (red, white arrows) in HFt shCtrl and shPML cells at 90 mpi (post-addition of virus). Cells were infected with HSV-1^{EdU} or ΔICP0^{EdU} at an MOI of 3 PFU/cell. Insets show magnified regions of interest (dashed boxes) highlighting host protein localization with vDNA. Cut mask (yellow) highlights regions of colocalization between PML, IFI16, Daxx, and vDNA (as indicated). Weighted colocalization coefficients are shown. Nuclei were stained with DAPI (blue). Images for ΔICP0^{EdU} infected cells are shown in S6 Fig. (E) Quantitation of host protein recruitment to infecting viral genomes (as shown in C, D, S6). Boxes: 25th to 75th percentile range; black line: median weighted (w.) colocalization coefficient; whiskers: 5th to 95th percentile range. Solid line indicates coincident threshold level (weighted colocalization coefficients < 0.2). n ≥ 50 vDNA foci per sample population from a minimum of four independent infections. *** $P < 0.001$, Mann-Whitney U-test.
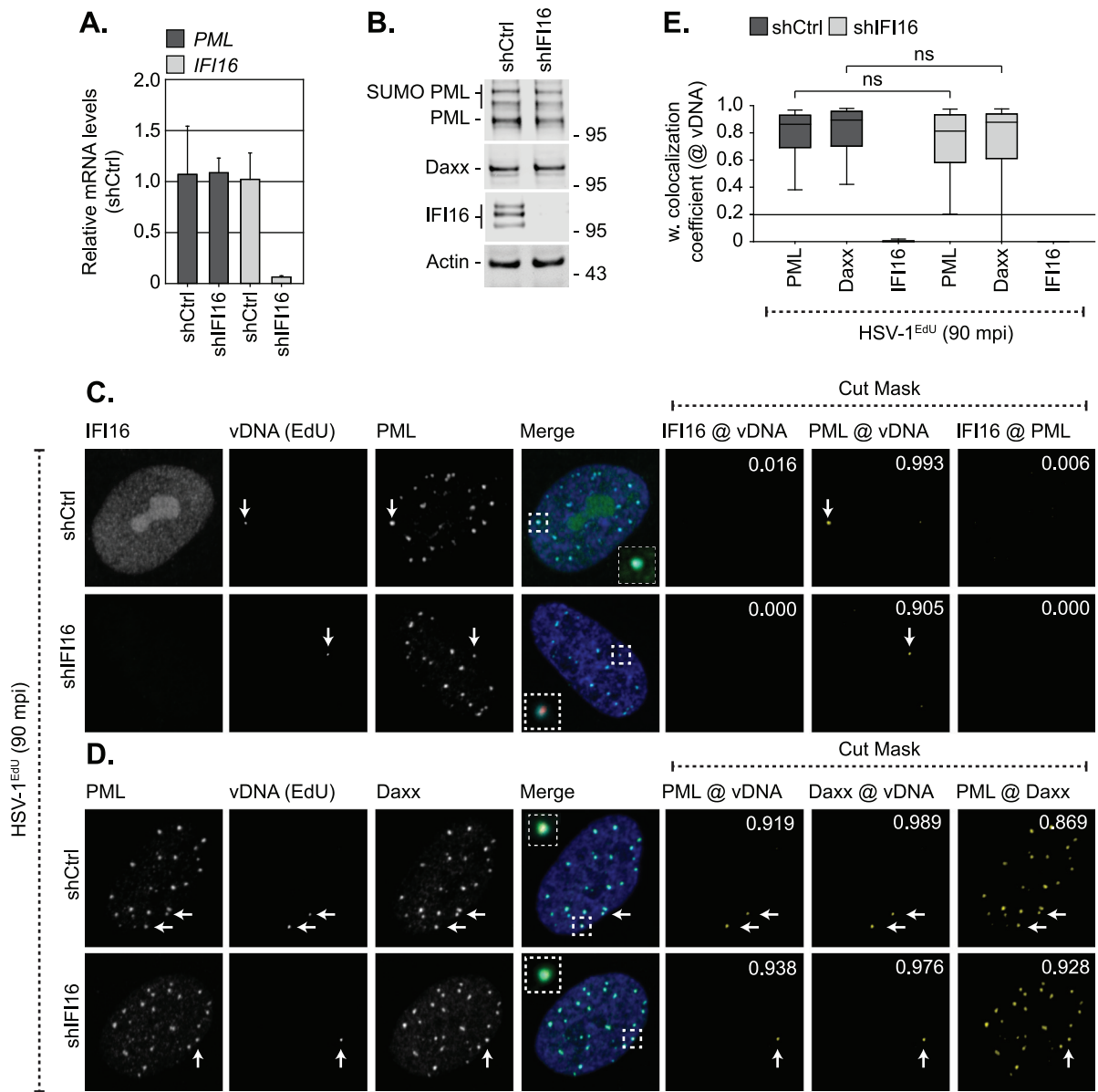
Fig 5. IFI16 does not influence the recruitment of PML or Daxx to infecting viral genomes. HFt cells were stably transduced with lentiviruses expressing IFI16-targeting (shIFI16) or non-targeting control (shCtrl) shRNAs. (A) qRT-PCR quantitation of *IFI16* or *PML* mRNA levels in HFt shCtrl and shIFI16 cells. Mean (RQ) and standard deviation (RQmin/max) shown and expressed relative to HFt shCtrl cells (1). (B) Western blot analysis of the expression levels of IFI16, PML, and Daxx in whole cell lysates from HFt shCtrl and shIFI16 cells. Actin is shown as a loading control. Molecular mass markers are shown. (C, D) Localization of PML (green), and either IFI16 or Daxx (cyan; as indicated) to infecting HSV-1^{EdU} vDNA (red, white arrows) in HFt shCtrl and shIFI16 cells at 90 mpi (post-addition of virus). Cells were infected with HSV-1^{EdU} at an MOI of 3 PFU/cell. Insets show magnified regions of interest (dashed boxes) highlighting host protein localization with vDNA. Cut mask (yellow) highlights regions of colocalization between IFI16, PML, Daxx, and vDNA (as indicated). Weighted colocalization coefficients are shown. Nuclei were stained with DAPI (blue). (E) Quantitation of host protein recruitment to infecting viral genomes (as shown in C, D). Boxes: 25th to 75th percentile range; black line: median weighted (w.) colocalization coefficient; whiskers: 5th to 95th percentile range. Solid line indicates coincident threshold level (weighted colocalization coefficients < 0.2). n ≥ 50 vDNA foci per sample population from a minimum of four independent infections. ns (not significant), Mann-Whitney *U*-test.

binding protein commonly utilized as a proxy for vDNA in genome recruitment studies [9–11, 14, 40]. Viral DNA labelling was achieved by pulse labelling HSV-1 ICP0-null mutant infected

cell monolayers at 24 hours post-infection (hpi) with 1 μM EdU for 6 h. Under these conditions, DNA replication compartments within the body of a developing plaque were clearly detected (S7 Fig). Cells on the periphery of the plaque-edge were readily observed to contain EdU positive vDNA foci asymmetrically distributed around the nuclear rim prior to ICP4 detection (Figs 6A, 6C top panels, S7), indicative of input EdU labelled viral genomes that have yet to initiate a productive gene expression programme. The recruitment of PML to infecting viral genomes occurred independently of ICP4 expression, with many genome foci observed to localise in close proximity to PML foci (Fig 6A and 6B). In contrast, IFI16 recruitment only occurred in cells that expressed ICP4 localized to vDNA at the nuclear rim (ICP4 NR; Fig 6C and 6D, S7 Fig). These data support previous asynchronous recruitment studies that have used ICP4 as a proxy for genome detection [11, 14] and demonstrate that PML and IFI16 are recruited to infecting viral genomes with temporally distinct kinetics, which in the case of IFI16 correlates with the expression and localization of viral gene products with vDNA (Fig 6D). Importantly, these data suggest that vDNA entry into the nucleus alone may not be sufficient to stimulate the induction of an IFI16-dependent innate immune response, but instead require the expression of specific viral gene products or the initiation of vDNA replication.

To test this hypothesis, we examined the induction of Mx1, a well-characterized ISG product [51], during HSV-1 ICP0-null mutant infection by confocal microscopy. HFt cells were mock treated, stimulated with IFN-β (as a positive control), or infected with ΔICP0^{EdU} at input levels which either restrict or permit the initiation of HSV-1 ICP0-null mutant replication and plaque formation at 24 hpi (MOI 0.1 and 1.0 PFU/cell, respectively; Fig 6E). vDNA was readily detectible within the nuclei of infected cells under restrictive MOI conditions (0.1 PFU/cell) with a frequency close its expected input genome ratio (Fig 6F) and copy number (1–2 genomes/infected cell; Fig 6G, S2 Table). Notably, the number of genomes per infected cell nuclei under permissive conditions (MOI 1 PFU/cell) was lower than expected based on our input qPCR analysis (~ 25 genomes/cell; Fig 6G, S2 Table). These data indicate that under MOI conditions that begin to saturate intrinsic host defences (~ 10–20 genome copies/nuclei), ΔICP0^{EdU} genome detection is lost following the onset of vDNA replication by 24 hpi.

As expected, IFN-β stimulation efficiently induced Mx1 expression 24 h post-treatment (Fig 6H and 6I). In contrast, infection with ICP0-null mutant HSV-1 only stimulated Mx1 expression at genome input levels sufficient to stimulate the onset of viral replication and plaque formation (MOI 1.0 PFU/cell; Fig 6E, 6H and 6I). High-resolution Z-series imaging revealed that viral genomes remained stably entrapped within PML-NBs under restrictive MOI conditions (0.1 PFU/cell) at 24 hpi (Fig 6J). These data demonstrate that under infection conditions that restrict the initiation of ICP0-null mutant HSV-1 replication, viral genome entry into the nucleus alone is not sufficient to stimulate the induction Mx1 ISG expression.

vDNA replication is required for the induction of innate immunity

As PML-NB entrapped HSV-1 ICP0-null mutant genomes failed to stimulate the induction of Mx1 expression, we next examined the kinetics of ISG induction during HSV-1 infection under MOI conditions that enabled the onset of viral replication (MOI 1 PFU/cell; Fig 7). As expected, HSV-1 ICP0-null mutant infection efficiently induced the transcription (by 8–9 hpi) and expression (by 16 hpi) of three independent ISG products (*Mx1*, *ISG15*, and *ISG54*), a host response that was significantly impaired during WT HSV-1 infection (Fig 7A–7C). Importantly, the induction of ISGs only occurred under infection conditions that enabled the onset of ICP0-null mutant HSV-1 replication and plaque-formation (≥ 1.0 PFU/cell; Figs 6E and 7D). Consistent with our microscopy observations (Fig 6H and 6I), these data demonstrate that saturation of intrinsic host defences is required for the robust induction of ISGs during
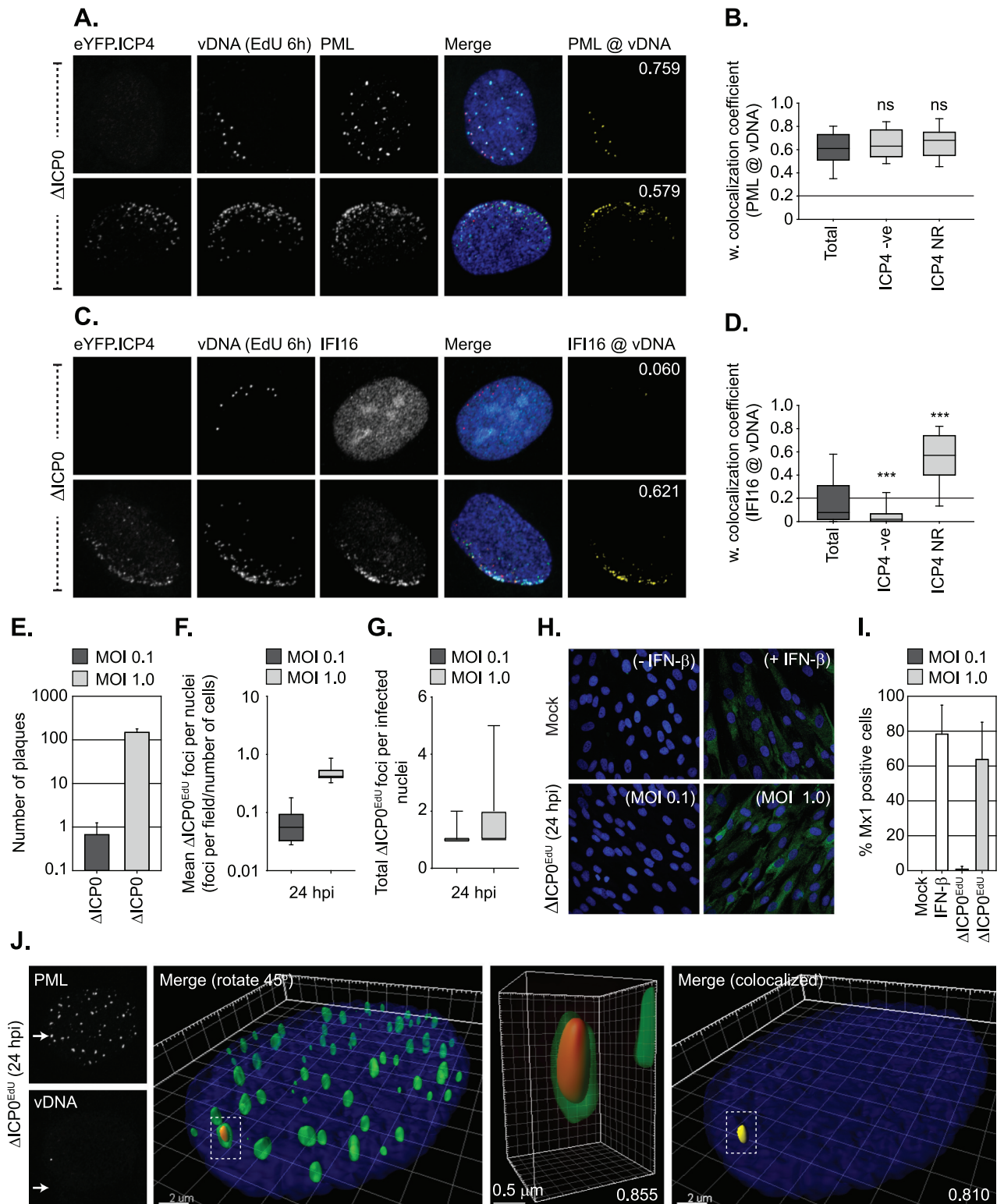
Fig 6. Nuclear entry of vDNA is not sufficient to induce robust Mx1 ISG expression. (A-D) Recruitment of PML, IFI16, and eYFP.ICP4 to ΔICP0 infecting viral genomes in an asynchronous plaque-edge recruitment assay (as described in [10]). HFt cells were infected with ΔICP0 expressing eYFP.ICP4 under conditions (MOI 2 PFU/cell) that enable plaque-formation to occur. Cells were pulse labelled at 24 hpi with 1 μM EdU for 6h to label vDNA. (A, C) Localization of eYFP.ICP4 (green), PML or IFI16 (cyan; as indicated) to vDNA (red) in newly infected cells on the periphery of a developing plaque-edge.

Cut mask (yellow) highlights regions of colocalization between either PML or IFI16 and vDNA (as indicated). Weighted (w.) colocalization coefficients shown. (B, D) Quantitation of PML and IFI16 recruitment to infecting vDNA in the presence or absence of eYFP.ICP4 at the nuclear rim (ICP4 NR and ICP4 -ve, respectively; as shown in A and C). Boxes: 25th to 75th percentile range; black line: median weighted (w.) colocalization coefficient; whiskers: 5th to 95th percentile range. Solid line indicates coincident threshold level (weighted colocalization coefficients < 0.2). n = 100 plaque-edge cells +ve for vDNA per PML or IFI16 sample population from 4 independent infections. *** $P < 0.001$, ns (not significant), Mann-Whitney U-test. (E-I) Mx1 expression is only induced under infection conditions that permit ΔICP0 plaque formation. (E) Number of plaques detected at 24 hpi following ΔICP0 infection of HFt cells at an input MOI of 0.1 or 1 PFU/cell (as indicated). n = 3, means and standard deviations shown. (F) Quantitation of ΔICP0^{EdU} nuclear genomes in HFt cells (as infected in E). Boxes: 25th to 75th percentile range; black line: median; whiskers: 5th to 95th percentile range. n ≥ 250 cells derived from 3 independent experiments per condition. (G) Frequency of ΔICP0^{EdU} genomes detected within infected cell nuclei (as described in E/F). Boxes: 25th to 75th percentile range; black line: median; whiskers: minimum and maximum range of sample. (H) HFt cells were mock treated, IFN-β stimulated (100 IU/ml), or infected with ΔICP0 at a MOI of 0.1 or 1 PFU/cell. Samples were fixed at 24 post-treatment and analysed by confocal microscopy for Mx1 (green) ISG expression. (I) Quantitation of Mx1 positive cells (as shown in H). n ≥ 250 cells derived from 3 independent experiments per condition. (J) PML-NB entrapment of vDNA is maintained under low MOI conditions (0.1 PFU/cell) that restrict ΔICP0^{EdU} replication and plaque formation at 24 hpi. 3D reconstruction of high-resolution Z-series confocal images showing PML entrapment of ΔICP0^{EdU} vDNA. Single channel maximum intensity projection images (left), 3D rendered images of the whole nucleus showing PML (green) and vDNA (red), with a single vDNA focus entrapped by PML (dashed box; right). Scale bar 2 μm. Enlargement of PML entrapped vDNA (centre-right). Scale bar 0.5 μm. Cut mask (yellow) highlights colocalization between PML and vDNA (far-right). Pearson coefficient for PML-vDNA colocalization shown. Nuclei were stained with DAPI (blue).

https://doi.org/10.1371/journal.ppat.1006769.g006

HSV-1 ICP0-null mutant infection. As IFI16 binds to a range of DNA structures that may be produced during vDNA replication [52], we next investigated the role of vDNA replication in the induction of ISGs. ISG transcript levels were monitored in the presence of the vDNA replication inhibitors PAA (phosphonoacetic acid) and ACG (acycloguanosine), two well-characterized herpesvirus DNA replication inhibitors [53–57]. PAA efficiently inhibited the induction of both *Mx1* and *ISG15* transcript levels in a dose-dependent manner (Fig 7E), while ACG treatment had only a modest inhibitory effect at concentrations sufficient to restrict HSV-1 plaque formation (≥ 50 μM; Fig 7F, S1 Table). Inhibition of ISG induction by PAA was virus-specific, as ISG transcript levels were readily induced by IFN-β stimulation in the presence of PAA (Fig 7G). By way of contrast, JAK inhibition by Ruxolitinib (Ruxo) effectively blocked ISG induction following IFN-β stimulation (Fig 7G; [58, 59]), consistent with a key role for JAK in IFN-mediated innate immune signalling [60]. JAK inhibition also effectively blocked ISG induction during HSV-1 ICP0-null mutant infection (Fig 7H). Importantly, this inhibition occurred in the presence 50 μM ACG (Fig 7I), demonstrating that JAK activity is specifically required to induce ISG expression during the initiating cycle(s) of HSV-1 ICP0-null mutant vDNA replication by 9 hpi. Together with our microscopy observations (Fig 6), these data demonstrate that the onset of vDNA replication is required for the robust induction of ISG expression during HSV-1 ICP0-null mutant infection.

Dual roles for both PML and IFI16 in the regulation of intrinsic and innate immunity to HSV-1 infection

As the induction of innate immunity during HSV-1 ICP0-null mutant infection was inhibited by Ruxolitinib, we next examined the effect of JAK inhibition on WT and ICP0-null mutant HSV-1 replication (Fig 8). At a concentration sufficient to inhibit ISG induction (5 μM; Fig 7G–7I), Ruxolitinib treatment had no effect on the relative plaque formation efficiency (PFE) of either WT or ICP0-null mutant HSV-1 (Fig 8A). These data indicate that innate immune signalling and the induction of ISGs does not directly contribute to the cellular restriction and plaque-formation defect of an HSV-1 ICP0-null mutant observed in restrictive cell types (≥ 1000 fold; [33, 35, 61]). In contrast, virus yield assays demonstrated that Ruxolitinib treatment enhanced the levels of ICP0-null mutant, but not WT, HSV-1 propagation (Fig 8B). Thus, under infection conditions that saturate intrinsic host defences and enable the onset of HSV-1 ICP0-null mutant replication (MOI of ≥ 1 PFU/cell; Fig 6E), innate immune defences act to restrict virus propagation. By way of contrast, depletion of IFI16 or PML enhanced both the PFE and virus yield of an HSV-1 ICP0-null mutant (Fig 8C and 8D; [11, 49]). Importantly,
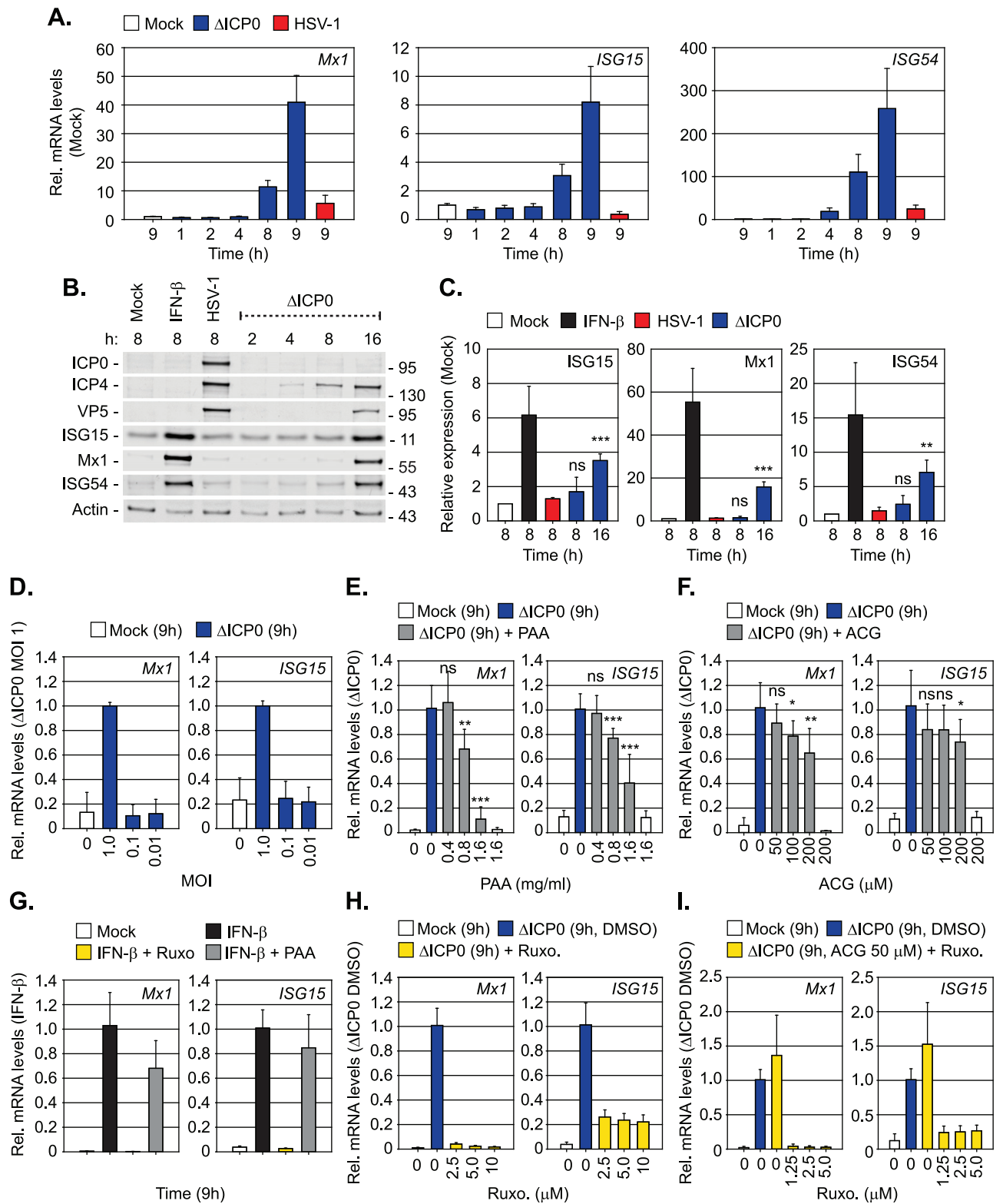
Fig 7. Inhibition of vDNA replication impairs the induction of innate immunity during HSV-1 infection. HFt cells were mock, WT, or ΔICP0 HSV-1 infected at an MOI of 1 PFU/cell (unless stated otherwise). Samples were collected at the indicated times (hours; h) post-treatment or infection. (A) Relative

mRNA levels of *Mx1*, *ISG15*, and *ISG54* during WT or ΔICP0 HSV-1 infection. n = 2, means (RQ) and standard deviations (RQmin/max) are shown and expressed relative to mock (1). (B) Western blot analysis of the expression levels of ISGs (ISG15, Mx1, ISG54), viral proteins (ICP0, ICP4, VP5), and actin (as a loading control), from whole cell lysates of mock, IFN-β stimulated (100 IU/ml), WT or ΔICP0 HSV-1 infected HFt cells at the indicated times. Molecular mass markers are shown. (C) Quantitation of ISG expression levels (as shown in B). n = 3, means and standard deviations shown expressed relative to mock (1). ** $P < 0.01$, *** $P < 0.001$, ns (not significant); two-tailed t-test. (D) Relative mRNA levels of *Mx1* and *ISG15* in mock or ΔICP0 infected HFt cells (MOI of 0.01 to 1 PFU/cell, as indicated). n = 3, means (RQ) and standard deviations (RQmin/max) are shown and expressed relative to ΔICP0 MOI 1 (1). (E, F) Relative mRNA levels of *Mx1* and *ISG15* in mock or ΔICP0 infected HFt cells in the presence of phosphonoacetic acid (PAA) or acycloguanosine (ACG) at the indicated concentrations. n = 3, means (RQ) and standard deviations (RQmin/max) are shown and expressed relative to ΔICP0 (1). * $P < 0.05$, ** $P < 0.01$, *** $P < 0.001$, ns (not significant); two-tailed t-test. (G) Relative mRNA levels of *Mx1* and *ISG15* in mock or IFN-β stimulated (100 IU/ml) HFt cells co-incubated in the presence Ruxolitinib (5 μM; Ruxo) or PAA (1.6 mg/ml), as indicated. n = 2, means (RQ) and standard deviations (RQmin/max) are shown and expressed relative to IFN-β treatment (1). (H, I) Relative *Mx1* and *ISG15* mRNA levels in mock or ΔICP0 infected HFt cells treated with Ruxo (2.5–10 μM, as indicated) or Ruxo (5 μM) and ACG (50 μM), as indicated. n = 2, means (RQ) and standard deviations (RQmin/max) are shown and expressed relative to ΔICP0 infection (1).

https://doi.org/10.1371/journal.ppat.1006769.g007

no additional increase in virus yield was observed on Ruxolitinib treatment of IFI16 or PML depleted cells (Fig 8D), indicative of an impaired innate immune response in these cells during HSV-1 ICP0-null mutant infection. Correspondingly, qRT-PCR demonstrated that the induction of ISGs (*Mx1*, *ISG15*, *ISG54*) was significantly impaired in both IFI16 or PML depleted cells in response to HSV-1 ICP0-null mutant infection at 9 hpi (Fig 8E and 8F). These data identify a novel role for PML in the induction of ISGs and the regulation of innate immunity during HSV-1 infection. Collectively, our data demonstrate that PML plays dual roles in the temporal regulation of intrinsic and innate immune defences that are dependent on viral genome delivery to the nucleus and the onset of vDNA replication, respectively.

As intrinsic and innate immune defences to HSV-1 infection are known to be cell-type dependent [34, 35, 62], we next investigated if there was a correlation between cell line permissiveness to HSV-1 ICP0-null mutant replication and the entrapment of viral genomes by PML-NB host factors (Fig 9). Relative to permissive osteosarcoma cells (U2OS, SAOS), which do not require ICP0 to stimulate the onset of HSV-1 replication [34], RPE cells demonstrated equivalent levels of HSV-1 ICP0-null mutant restriction to HFt cells ($\geq$ 1000-fold reduction in PFE, Fig 9A). Western blot analysis revealed that all these cell lines expressed similar levels of PML, Daxx, and IFI16 (Fig 9B). However, infection with HSV-1^{EdU} demonstrated a significant reduction in the colocalization frequency of PML and Daxx to infecting viral genomes between permissive (U2OS, SAOS) and restrictive (HFt, RPE) cell-types (Fig 9C and 9D). Importantly, in many instances neither PML nor Daxx was observed to localize with infecting viral genomes in permissive cell types (Fig 9C, bottom panels). Thus, we have identified a correlation between the stable entrapment of vDNA by PML-NBs and the requirement for ICP0 to stimulate the efficient onset of HSV-1 infection in restrictive (HFt, RPE), but not permissive (U2OS, SAOS), cell-types. As U2OS and SAOS cells do not express ATRX (Fig 9B; [63, 64]), a known core constituent protein of PML-NBs and an intrinsic antiviral regulator to HSV-1 infection [64–66], we investigated the requirement for ATRX to mediate PML-NB entrapment of vDNA. HFt cells were stably transduced with lentiviral vectors expressing non-targeting control or ATRX-targeting short hairpin RNAs (shCtrl and shATRX, respectively; [65]). qRT-PCR and western blotting confirmed ATRX depletion, which had a modest effect on PML mRNA transcript levels without influencing PML or Daxx expression levels (Fig 9E and 9F). HSV-1^{EdU} infection of shCtrl or shATRX cells demonstrated that depletion of ATRX led to a distinct population of viral genomes with a reduced colocalization frequency with PML (left-hand dotted box; Fig 9G). Notably, low levels of ATRX colocalization were still observed with vDNA in a significant proportion of ATRX depleted cells (right-hand dotted box; Fig 9G). Quantitation (n $\geq$ 200 genomes per condition) revealed that there was a significant difference in PML recruitment to vDNA in ATRX depleted cells (Fig 9H). We conclude that ATRX, either directly or indirectly, contributes to the entrapment of vDNA within PML-NBs following nuclear entry.
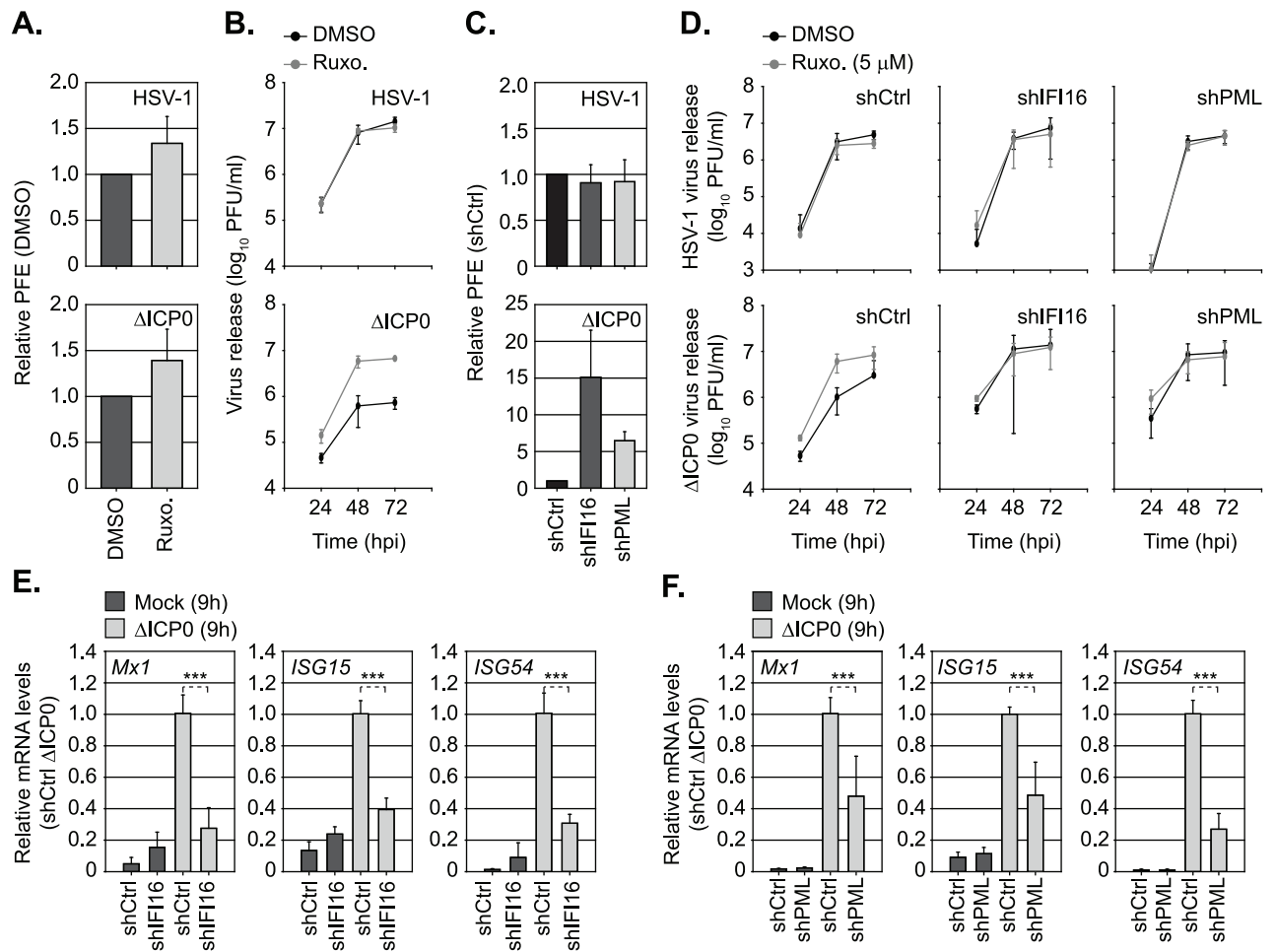
Fig 8. Dual roles for PML and IFI16 in the regulation of intrinsic and innate immunity to HSV-1 infection. (A) HFt cells were DMSO or Ruxolitinib (5μM; Ruxo) treated and infected with serial dilutions of WT or ΔICP0 HSV-1 for 24 h prior to immuno-staining for plaque formation. Plaque counts expressed relative to control cell monolayers (# of plaques treated / # of plaques DMSO control) at equivalent serial dilutions of virus and presented as relative plaque formation efficiency (PFE). n ≥ 3, means and standard deviations shown. (B) HFt cells were DMSO or Ruxo treated and infected with WT (MOI 0.001 PFU/cell) or ΔICP0 (MOI 1 PFU/cell) HSV-1. Cell released virus (CRV) was harvested at the indicated times (hpi) and CRV titres determined on U2OS cells. n = 3, means and standard deviations shown. (C) Stably transduced HFt cells expressing non-targeting control (shCtrl), or targeting IFI16 (shIFI16) or PML (shPML) shRNAs, were infected with WT or ΔICP0 HSV-1 (as in A). Plaque counts expressed relative to infected shCtrl cell monolayer plaque counts (1) and presented as relative PFE. n = 3, means and standard deviations shown. (D) shCtrl, shIFI16, or shPML HFt cells were treated with DMSO or Ruxo and infected with either WT or ΔICP0 HSV-1 (as in B). CRV was collected at the indicated times (hpi) and titres determined on U2OS cells. n = 3, means and standard deviations shown. (E, F) Relative *Mx1*, *ISG15*, and *ISG54* mRNA levels in HFt shCtrl, shIFI16, or shPML cells mock or ΔICP0 infected (MOI 1 PFU/cell) at 9 hpi. n = 3, means (RQ) and standard deviations (RQmin/max) shown and expressed relative to ΔICP0 infected shCtrl (1). *** $P < 0.001$; two-tailed t-test.

Finally, we compared restrictive (HFt, RPE) and permissive (U2OS, SAOS; [62]) cell types to mount an innate immune response to HSV-1 ICP0-null mutant infection under infection conditions that permitted the onset of viral replication (MOI 1 PFU/cell). Surprisingly, qRT-PCR analysis demonstrated that only HFt cells induced ISG (*Mx1*, *ISG15*, *ISG54*) expression during HSV-1 ICP0-null mutant infection (Fig 10A, top panels; [62]). This was not due to a defect in IFN pathway signalling, as all four cell-types were responsive to exogenous IFN-β stimulation (Fig 10A, bottom panels). Correspondingly, only HFt cells showed enhanced levels of HSV-1 ICP0-null mutant propagation following JAK inhibition by Ruxolitinib (Fig 10B). We conclude that RPE cells, which are highly restrictive to HSV-1 ICP0-null mutant
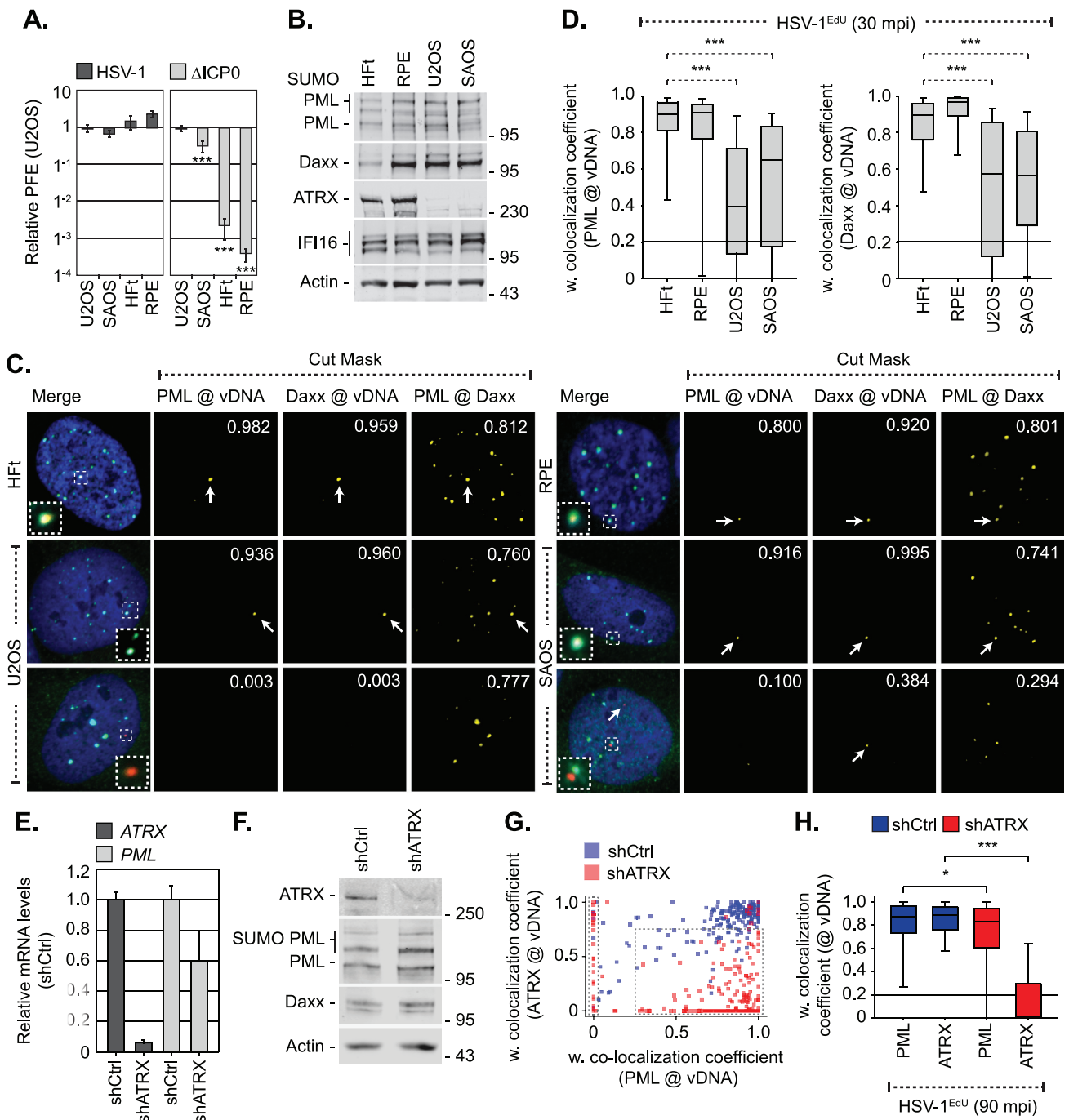
Fig 9. PML-NB entrapment of infecting HSV-1 vDNA occurs in a cell type and ATRX dependent manner. (A) U2OS, SAOS, RPE, and HFt cells were infected with serial dilutions of WT or ΔICP0 HSV-1 for 24 h. Plaque counts expressed relative to U2OS, a cell line permissive to ΔICP0 replication [34], (# of plaques / # of plaques U2OS control) at equivalent serial dilutions of virus and presented as relative plaque formation efficiency (PFE). n ≥ 3, means and standard deviations shown. (B) Western blot analysis of the relative expression levels of PML, Daxx, ATRX, and IFI16 in whole cell lysates derived from HFt, RPE, U2OS and SAOS cells. Actin is shown as a loading control. Molecular mass markers are indicated. (C) Localization of PML (green) and Daxx (cyan) to HSV-1^{EdU} vDNA (red, white arrows) in restrictive (HFt, RPE) and permissive (U2OS, SAOS) cell types at 30 mpi (post-addition of virus; MOI of 3 PFU/cell). Insets show magnified regions of interest (dashed boxes) highlighting host protein localization with vDNA. Cut mask (yellow) highlights regions of colocalization between PML, Daxx, and vDNA (as indicated). Weighted (w.) colocalization coefficients shown. (D) Quantitation of PML and Daxx recruitment to infecting vDNA in restrictive (HFt, RPE) and permissive (U2OS, SAOS) cell lines (as shown in C). Boxes: 25th to 75th percentile range; black line: median weighted (w.) colocalization coefficient; whiskers: 5th to 95th percentile range. Solid line indicates coincident threshold level (weighted colocalization coefficients < 0.2). n ≥ 50 vDNA foci per sample population from 4 independent infections. (E-H) ATRX is required for efficient PML-NB

entrapment of vDNA. HFt cells were stably transduced with lentiviruses expressing ATRX-targeting (shATRX) or non-targeting control (shCtrl) shRNAs. (E) qRT-PCR quantitation of *ATRX* or *PML* mRNA levels in HFt shCtrl and shATRX cells. Mean (RQ) and standard deviation (RQmin/max) shown and expressed relative to HFt shCtrl cells (1). (F) Western blot analysis of the relative expression levels of ATRX, PML, and Daxx in whole cell lysates from HFt shCtrl and shATRX cells. Actin is shown as a loading control. Molecular mass markers are shown. (G) Scatter plot showing paired w. colocalization coefficients of ATRX and PML to individual nuclear infecting viral genomes in shCtrl (blue) and shATRX (red) cells infected with HSV-1^{EdU} at an MOI of 3 PFU/cell at 90 mpi (post-addition of virus). n ≥ 200 genomes per sample population. Dotted boxes highlight genome populations identified to have altered distribution of colocalization frequency in comparison to infected shCtrl cells. (H) Quantitation of PML and ATRX recruitment to infecting viral genomes (as shown in G). Boxes: 25th to 75th percentile range; black line: median weighted (w.) colocalization coefficient; whiskers: 5th to 95th percentile range. Solid line indicates coincident threshold level (weighted colocalization coefficients < 0.2). * $P < 0.05$, *** $P < 0.001$; Mann-Whitney U-test.

replication (Fig 9A), are defective in aspects relating to intracellular innate signalling in response to HSV-1 infection. These data support our microscopy observations (Fig 6) and inhibitor studies (Figs 7 and 8), and collectively demonstrate that intrinsic and innate host immune responses to HSV-1 infection are temporally distinct and functionally separable arms of host immunity.

In summary, we show that the temporal recruitment of host immune regulators to infecting viral genomes plays an important role in the sequential regulation of intrinsic and innate immunity during HSV-1 infection. We identify PML-NBs to entrap vDNA shortly after nuclear entry in an ATRX-dependent and IFI16-independent manner. We identify a novel role for PML in the induction of innate immunity in response to HSV-1 infection that correlates with the recruitment of IFI16 into vDNA complexes associated with ICP4 and the onset of vDNA replication. These intracellular host defences are counteracted by ICP0, which
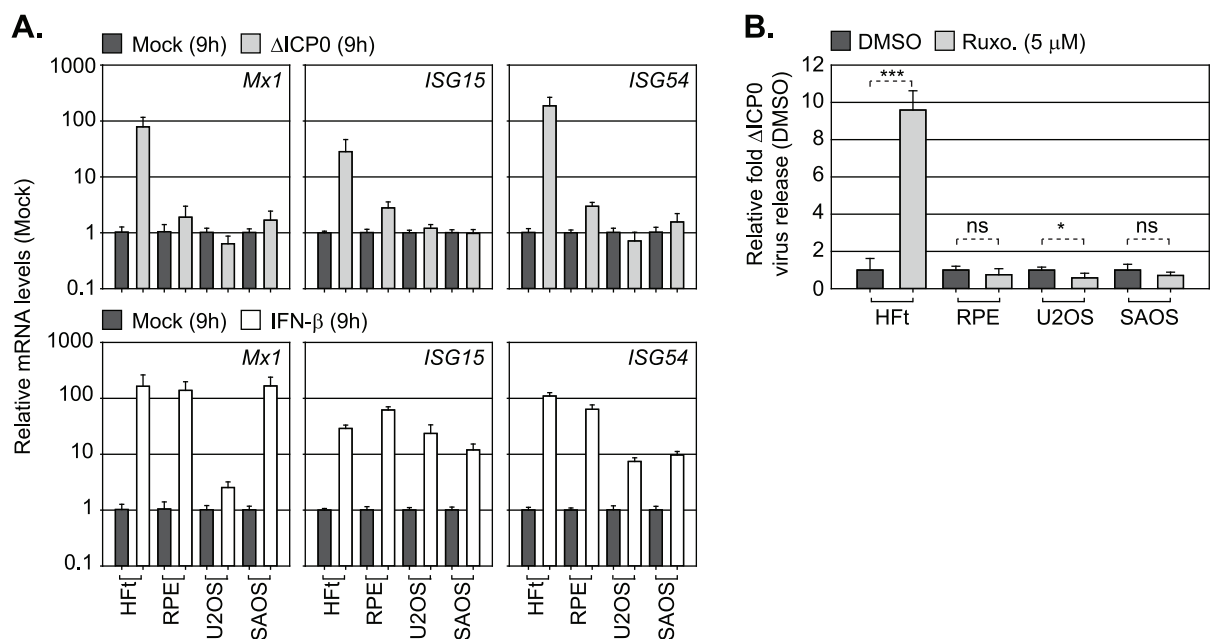
Fig 10. PML-NB entrapment of vDNA does not lead to the induction of innate immunity. (A) Relative *Mx1*, *ISG15*, and *ISG54* mRNA levels in cell lines restrictive (HFt, RPE) or permissive (U2OS, SAOS) to HSV-1 ICP0-null mutant (ΔICP0) infection. Cells were mock treated, IFN-β (100 IU/ml) stimulated, or infected with ΔICP0 at an MOI of 1 PFU/cell for 9 h. n = 3, means (RQ) and standard deviations (RQmin/max) are shown and expressed relative to mock for each cell line (1). (B) Restrictive (HFt, RPE) or permissive (U2OS, SAOS) cell lines were infected with ΔICP0 at an MOI of 1 PFU/cell and treated with either DMSO or Ruxolitinib (Ruxo, 5μM). CRV was harvested at 48 hpi and titres determined on U2OS cells. n = 3, means and standard deviations shown and expressed as relative fold-change to DMSO titres (1) for each cell line. * $P < 0.05$, *** $P < 0.001$, ns (not significant); two-tailed t-test.

induces the degradation of PML from the outset of infection to release viral genomes entrapped within PML-NBs to stimulate the onset of HSV-1 lytic replication.

Discussion

A key aspect in the regulation of intracellular host immunity during herpesvirus infection is the rapid recruitment of host immune factors to infecting viral genomes. This nuclear response to infection has been linked to viral genome silencing, as part of a pre-existing intrinsic immune defence, and the activation of innate immune signalling pathways (reviewed in [1, 4, 32]). However, the temporal recruitment of these host immune regulators to infecting viral genomes upon vDNA entry into the nucleus has remained poorly defined due to the technical challenges associated with low genome copy-number detection.

Microscopy studies have historically relied on the use of viral mutants, high MOI conditions, and vDNA binding proteins to investigate the recruitment of host immune regulators to infecting viral genomes. Whilst informative, such approaches can readily saturate intrinsic host defences that restrict the initiation of viral gene expression due to high input genome loads [35]. Consequently, the temporal sequence of events that influence the sequential regulation of intracellular host immunity upon vDNA entry into the nucleus has remained poorly defined, specifically during WT herpesvirus infections that express a full complement of immune antagonists. Here we quantitatively examine the recruitment of intrinsic and innate immune regulators to infecting WT and ICP0-null mutant HSV-1 genomes under a range of relatively low MOI conditions ($\leq$ 3 PFU/cell) within the first 15–90 mpi (post-addition of virus). We show that PML, the principle scaffolding protein of PML-NBs [48], plays temporally distinct and functionally separable roles in the regulation of intrinsic and innate immune defences activated in response to HSV-1 infection through the entrapment of viral genomes (Figs 2 and 6) and the induction of ISG expression following the onset of vDNA replication (Fig 7), respectively. These observations reconcile many longstanding issues within the field as to the importance of PML and PML-NBs during primary herpesvirus infection and the requirement for ICP0 to stimulate the onset of HSV-1 lytic replication, as discussed below.

Immuno-FISH experiments conducted by Gerd Maul and colleagues over 20 years ago originally identified that infecting HSV-1 genomes localize in close proximity to PML-NBs under infection conditions that enabled detection of ICP8 [8], an essential component of the vDNA replication complex [67]. These pioneering observations have stimulated a field of research that has uncovered fundamental roles for many PML-NB associated proteins in the regulation of intracellular host immunity against a range of DNA and RNA viral pathogens (reviewed in [1, 20, 21, 68]). PML-NBs are highly dynamic nuclear sub-domains, with resident proteins (PML, Sp100, and Daxx) in constant exchange with the surrounding nucleoplasm [10]. Correspondingly, asynchronous plaque-edge recruitment assays (examples of which are shown in Fig 6, S7 Fig; [9]) have shown that many PML-NB component proteins re-localize to sites in close proximity to infecting HSV-1 genomes under high MOI conditions, where *de novo* PML-NB like foci are reformed [10]. These observations have set the paradigm for intrinsic immunity during herpesvirus infection, where pre-existing PML-NB host factors re-localize to infecting viral genomes to mediate the transcriptional repression of viral gene expression [19, 49, 50, 69]. However, recent live-cell microscopy studies have proposed an alternate mechanism, whereby vDNA becomes transiently associated with host factor(s) within the nucleoplasm (notably Daxx and IFI16; [12, 14]) prior to deposition at PML-NBs, although no evidence for Daxx or IFI16 colocalization with vDNA or deposition within PML-NBs was reported. Using click chemistry, we demonstrate for the first time that infecting WT and ICP0-null mutant HSV-1 genomes are rapidly entrapped within PML-NBs following nuclear

entry (30–90 mpi; Figs 2 and 6J). While we cannot rule out a recruitment model of genome entrapment, specifically the re-localization of PML-NB host factors that are in immediate proximity to nuclear infecting viral genomes, our data support a deposition model as: (i) PML-NBs that contained vDNA were indistinguishable in composition from other PML-NBs within the same infected nucleus or mock-infected cells (Fig 3A–3D, S3 Fig); (ii) Depletion of PML reduced Daxx colocalization with vDNA, indicative of a transient association stabilized by PML at PML-NBs where Daxx is a resident protein (Fig 4E; [48, 49]); (iii) Depletion of ATRX, a binding partner of Daxx [70], reduced the frequency of PML colocalization with vDNA in a significant subset of infected cells (Fig 9E–9H). These observations support a deposition model of vDNA entrapment at pre-existing PML-NBs that contain a core complement of PML-NB host factors and implicate the Daxx/ATRX complex in this process, consistent with live-cell microscopy observations [12]. These observations are consistent with co-depletion experiments [19, 50, 69], which have shown PML-NB proteins to act cooperatively to restrict the initiation of HSV-1 ICP0-null mutant replication under low MOI conditions (≤ 1 PFU/cell, 6E; < 25 genome copies/cell, S2 Table). We therefore provide spatial context to these studies, as repressed viral genomes remain stably entrapped within PML-NBs at 24 hpi (Fig 6J), a host response that is impaired in cell types permissive to HSV-1 ICP0-null mutant replication which lack ATRX (U2OS, SAOS; Fig 9A–9D; [34, 63, 64]). Thus, we identify PML-NB entrapment of vDNA as a key intrinsic antiviral host defence to WT herpesvirus nuclear infection, a conclusion consistent with genome localization studies in HSV-1 latently infected cells by immuno-FISH [71–73]. We demonstrate that this intrinsic PML-NB host defence occurs in a range of restrictive cell types relevant to primary HSV-1 infection (Figs 2 and 9) and independently of the induction of ISG expression (Figs 6H–6J, 7D and 10A), demonstrating that this host response does not directly contribute to the sensing of viral nucleic acids that leads to the induction of innate immunity.

Our data highlights the importance of ICP0 to promote the onset of WT HSV-1 infection under low MOI conditions [33–35]. ICP0 is known to localize to PML-NBs from the outset of infection in a PML isoform and SUMO-dependent manner [17, 22, 74, 75], where it targets PML and other SUMO-modified component proteins for ubiquitination and proteasome-dependent degradation [17, 25–27, 74, 75]. As ICP0 does not preferentially localize to PML-NBs that contain vDNA (Fig 2C), our data indicate that these vDNA containing nuclear bodies are likely to be equivalent in their respective PML isoform composition and SUMO modification status at this extremely early stage of nuclear infection. Thus, cell-wide PML-NB disruption through ICP0 mediated degradation of PML ensures viral genome release and the dispersal of associated PML-NB host factors that repress the onset of viral gene expression [19, 49, 50, 66, 69]. This hypothesis is supported by our depletion experiments that show reduced Daxx localization with vDNA in PML depleted cells (Fig 4E), and accounts for why many PML-NB resident host factors known to restrict HSV-1 ICP0-null mutant replication (including Daxx, ATRX, and PIAS1) are not directly targeted for degradation by ICP0 [19, 66]. Thus, the correct complement of host factors within pre-existing PML-NBs is likely to play an important role in mediating the cellular restriction of viral gene expression from the outset of nuclear infection. These observations account for why many herpesviruses encode IE gene products that disrupt the structural organization of PML-NBs (reviewed in [1, 68]), and the respective abilities of these proteins to complement the replication and plaque-forming defect of an HSV-1 ICP0-null mutant in restrictive cell types [76–79].

Our observation that repressed HSV-1 ICP0-null mutant genomes remain stably entrapped within PML-NBs without inducing ISG expression (Figs 6E–6J and 7D) has significant implications with respect to host PRR sensing of vDNA and the regulation of innate immunity during herpesvirus infection. The sensing of foreign DNA and the activation of innate immune

signalling pathways can occur through multiple pathways and PRRs, including TLR9, RIG-I, MAVS, AIM2, DNA-PK, cGAS, and IFI16 (reviewed in [4–6]). Of these, IFI16 has received significant attention due to its role as a vDNA PRR in the induction of ISG expression and type-I IFN production during herpesvirus infection [28, 29, 80–84]. Correspondingly, microscopy assays have shown IFI16 to be recruited to infecting HSV-1 genomes in a pyrin domain-dependent manner in association with PML-NB host factors [11, 12, 14]. This host response was initially reported to be antagonized by the ubiquitin ligase activity of ICP0 [28, 29], although subsequent studies have shown other viral and cellular factors are likely to be involved [11, 30, 31]. IFI16 recruitment studies have relied on the use of vDNA binding proteins to enable viral genome detection by proxy, or on extrapolation of altered patterns in IFI16 nuclear localization to infer IFI16-vDNA association in restrictive cell types. Thus, the temporal kinetics of IFI16 recruitment to vDNA and its subsequent association with PML-NB host factors has remained poorly defined, specifically under MOI conditions relevant to WT herpesvirus infections. In contrast to PML-NB host factors, we failed to observe any significant frequency of stable colocalization between IFI16 and vDNA up to 90 mpi (post-addition of virus; Figs 3 and 5, S5 Fig), even in the absence of PML or ICP0 (Fig 4E). While we cannot exclude the possibility of highly transient IFI16 interactions with vDNA (S5A Fig; [12, 14]), our data indicates that IFI16 does not play an essential role in the entrapment of viral genomes by PML-NBs (Fig 5; [11, 14]). Importantly, under infection conditions that do not saturate or antagonize intrinsic PML-NB host defences (HSV-1 ICP0-null mutant MOI < 1 PFU/cell, Fig 6E; < 25 genome copies/cell, S2 Table), we demonstrate vDNA entry into the nucleus alone is not sufficient to stimulate a robust innate immune response (Figs 6E–6J and 7D). Induction of innate immunity only occurred under MOI conditions sufficient to saturate intrinsic host defences leading to the onset of HSV-1 ICP0-null mutant replication and plaque-formation (MOI ≥ 1 PFU/cell; Figs 6E and 7D). Under such conditions, we identified a clear kinetic difference in the stable recruitment of PML and IFI16 to infecting viral genomes, which in the case of IFI16 correlated with the recruitment of ICP4 (the major IE viral transcription factor) to vDNA and the onset of viral gene expression (Fig 6A–6D). Thus, we have identified a temporal boundary in the recruitment of intrinsic and innate immune regulators to infecting viral genomes that could represent a shift in host response; from an intrinsic defence centred on the repression of viral gene expression to the induction of innate immune signalling that promotes an antiviral state to restrict virus propagation. This hypothesis is supported by our observation that the induction of innate immunity requires the onset of vDNA replication (Fig 7E and 7I). IFI16 is reported to recognise nucleosome free DNA in a sequence independent manner [85–87], with high binding affinity for G quadraplex, branched or cruciform DNA structures [52]. Thus, it likely that the recruitment of IFI16 to infecting viral genomes is stabilised following the onset of vDNA replication that produces an abundance of such DNA structures [57]. This hypothesis may account for why PAA, but not ACG, is capable of inhibiting the induction of ISG expression (Fig 7E and 7F). As inactivation of the vDNA polymerase by PAA would be expected to impair the initiation of vDNA replication [53, 57], while ACG treatment would lead to the accumulation of stalled vDNA replication products [54]. Thus, we hypothesize that the topology of replicating vDNA is important for the stable recruitment of IFI16 on to vDNA that leads to the induction of ISG expression and type-I IFN production during herpesvirus infection. We note that other viral and cellular factors are likely to contribute to the induction of innate immunity under alternative infection conditions, for example excessively high MOI, UV inactivation, or the use of viral mutants defective in multiple genes, which may deliver or generate PAMPs for PRR detection at different stages of infection.

While it is clear that IFI16 plays a key role in the induction of ISG expression during herpesvirus infection, we have also identified an important and novel role for PML in this host

response to HSV-1 infection (Fig 8). Depletion of PML significantly reduced the levels of ISG transcript accumulation observed at 9 hpi during HSV-1 ICP0-null mutant infection (Fig 8F), a time point which proceeds ISG expression (16 hpi; Fig 7B). Thus, under infection conditions that saturate intrinsic PML-NB host defences during HSV-1 ICP0-null mutant infection (MOI ≥ 1 PFU/cell, ~ 25 genome copies/cell), PML plays a significant role in mediating the induction of ISG transcription. Correspondingly, pharmacological inhibition of JAK signalling by Ruxolitinib [58, 59] did not enhance HSV-1 ICP0-null mutant propagation in either IFI16 or PML depleted cells (Fig 8D). Collectively, these data demonstrate that PML plays an important role in the induction of innate immunity in response to HSV-1 infection that restricts the propagation of HSV-1 following the successful saturation of PML-NB intrinsic host defences. These observations are consistent with reports highlighting a role for PML to mediate the induction of innate immunity in response to other human herpesviruses [88–90], and a growing body of literature suggesting that specific PML isoforms play an important role in mediating the transcriptional regulation of cytokine signalling (reviewed in [91]). Notably, PML has been reported to mediate the recruitment of activated STAT1 and 2, along with HDAC1 and 2, onto ISG promoters (*ISG54*, *CXCL10*) during human cytomegalovirus (HCMV) infection [90]. This host response is antagonized by the HCMV IE gene product IE1 [88, 90], a viral protein known to disrupt PML-NBs and to relieve the intrinsic cellular restriction of an HSV-1 ICP0-null mutant [78]. As JAK activity is well known to be required for STAT phosphorylation [60], these observations are consistent with our inhibitor studies (Figs 7H, 7I, 8B and 8D), which show JAK activity to play an important role in the induction of ISGs during HSV-1 ICP0-null mutant vDNA replication at 9 hpi. Consistent with STAT1 depletion studies [61], JAK inhibition did not influence the intrinsic restriction of an HSV-1 ICP0-null mutant (Fig 8A). These data contrast with depletion studies, which show a clear cooperative role for PML-NB host factors to restrict the initiation of HSV-1 ICP0-null replication [19, 50, 69]. Taken together with our observations in RPE cells (Figs 9A and 10), which are restrictive to ICP0-null HSV-1 replication but defective in innate immune signalling, these data show that PML plays dual roles in the temporal regulation of both intrinsic and innate immunity in response to HSV-1 infection. Host defences that are counteracted by ICP0 through the degradation of PML and disruption of PML-NBs from the outset of infection.

In conclusion, we have shown for the first time that the differential recruitment of host immune regulators to infecting viral genomes plays a fundamental role in the sequential regulation of intrinsic and innate immune defences following HSV-1 nuclear infection. We have identified dual roles for PML in the regulation of these intracellular defences to HSV-1 infection that are dependent on vDNA entry into the nucleus and the onset of vDNA replication, respectively. Our analysis reconciles many long-standing questions as to the importance of PML and PML-NBs in the regulation of intracellular host immunity during HSV-1 infection. Our data highlights the importance of viral antagonists that disrupt PML-NBs to inactivate and evade key intracellular immune defences from the outset of infection, thereby promoting the onset of replication, propagation, and ultimately transmission to new hosts. Moreover, we demonstrate the versatility and sensitivity of bio-orthogonal labelling of viral nucleic acid to investigate the temporal recruitment of host immune regulators to infecting viral genomes during infection.

Materials and methods

Cells and drugs

Primary human foreskin fibroblast cells (HFs) were obtained from Thomas Stamminger (Department of Urology, University of Erlangen; [49]) and immortalized (HFt) by retrovirus

transduction to express the catalytic subunit of human telomerase, as previously described [18]. HFt, retinal pigmented epithelial (RPE-1; ATCC, CRL-4000), Human osteosarcoma (U2OS and SAOS; ECACC, 92022711 and 89050205), primary human foetal lung fibroblast (MRC-5; ATCC, CCL-171), and adult human keratinocyte (HaCat; a gift of F. Rixon, MRC-UoG CVR) cells were grown in Dulbecco's Modified Eagle Medium (DMEM; Life Technologies, 41966). HFt cells were cultured in the presence of 5 µg/ml of Hygromycin (Invitrogen, 10687–010) to maintain hTERT expression. Transduced HFt cells expressing shRNAs were cultured in the presence of Puromycin (Sigma-Aldrich, P8833; 1 µg/ml or 0.5 µg/ml for selection or maintenance, respectively). Primary human embryonic lung fibroblast (HEL 299; ECACC, 87042207) cells were maintained in Minimum Essential Medium Eagle (MEM; Sigma-Aldrich M5650) supplemented with 2 mM L-Glutamine (Life Technologies, 25030–024) and 1 mM Sodium Pyruvate (Life Technologies, 11360–039). Baby hamster kidney fibroblast (BHK-21 C13; a gift of R. Everett, MRC-UoG CVR) cells were grown in Glasgow Minimum Essential Medium (GMEM; Life Technologies, 21710–025) supplemented with 10% Tryptose Phosphate Broth (TPB; Life Technologies, 18050–039). Medium for all cell lines was supplemented with 10% foetal bovine serum (FBS; Life Technologies, 10270), 100 units/ml penicillin, and 100 µg/ml streptomycin (Life Technologies, 15140–122). All cell lines were maintained at 37°C in 5% CO_2. 5-Ethynyl-2'-deoxyuridine (EdU; Sigma-Aldrich, T511285), 5-Ethynyl-2'-deoxycytidine (EdC; Sigma-Aldrich, T511307), 2'-deoxyuridine (dU; Sigma-Aldrich, D5412), and Ruxolitinib (Ruxo; Sellechchem, S1378) were prepared in DMSO and used at the indicated concentrations. Acycloguanosine (ACG, Sigma-Aldrich, A4669), Phosphonoacetic acid (PAA, Sigma-Aldrich, 284270), and Interferon beta (IFN-β; Calbiochem, 407318) were prepared in Milli-Q H_2O and used at the indicated concentrations.

Viruses

Wild-type HSV-1 strain 17syn+ (HSV-1), its ICP0-null mutant derivative *dl*1403 (ΔICP0; [33]), and their respective variants that express eYFP.ICP4 [40] were propagated and titrated as described [35]. For EdU labelling of viral genomes, RPE cells were infected with either HSV-1 (MOI 0.001 PFU/cell) or ΔICP0 (MOI 0.5 PFU/cell). At 24 h post-infection (hpi), EdU or EdC was added at a final concentration of 0.5 µM, unless otherwise indicated. Fresh EdU/EdC was pulsed into infected cultures at 24 h intervals until extensive cytopathic effect was observed, typically 3 to 4 days post-infection. Supernatants containing labelled cell released virus (CRV) were clarified by centrifugation (423 x*g* for 10 min) and filtered through a 0.45 µm sterile filter and pelleted using a Beckman TLA100 Ultracentrifuge (33,800 x*g* for 3h at 4°C). Virion pellets were resuspended and pooled in 500 µl complete DMEM medium, and titrated in U2OS cells as described [35].

Plasmids and lentiviral transduction

Plasmids encoding short hairpin (sh) RNAs against a non-targeted control sequence (shCtrl; 5'-TTATCGCGCATATCACGCG-3'), PML (shPML; 5'-AGATGCAGCTGTATCCAAG-3'), ATRX (shATRX; 5'- CGACAGAAACTAACCCTGTAA-3'), or IFI16 (shIFI16; 5'-CCAC AATCTACGAAATTCA-3') were used to generate lentiviral supernatant stocks for transduction of HFt cells as described [11, 49, 65]. Pooled and stably transduced cells were used for experimentation.

Antibodies

The following antibodies were used for immunofluorescence or western blotting: Primary rabbit polyclonal: anti-actin (Sigma-Aldrich, A5060), anti-Daxx (Upstate, 07–471), anti-ATRX

(Santa Cruz, H300), anti-PML (Bethyl Laboratories, A301-167A; Jena Biosciences, ABD-030), anti-Sp100 (GeneTex, GTX131569), anti-SUMO2/3 (Abcam, ab22654), anti-Mx1 (Santa Cruz, sc-50509;ProteinTech, 13750-1-AP), anti-ISG15 (ProteinTech, 15981-1-AP), and anti-ISG54 (IFIT2, proteinTech, 12604-1-AP). Primary mouse monoclonal: anti-ICP0 (11060, [92]), anti-ICP4 (58s, [93]), anti-VP5 (DM165, [94]), anti-SUMO2/3 (Abcam, ab81371), anti-PML (abcam, ab96051), anti-IFI16 (abcam, ab55328; Santa Cruz, sc-8023). Primary antibodies were detected using the following secondary antibodies: DyLight-680 or -800 conjugated anti-rabbit or -mouse (Thermo; 35568 and SA5-35571), Alexa -488, -555, or -647 conjugated anti-rabbit, or -mouse (Invitrogen; A21206, A21202, A31572, A31570, A31573, A31571), HRP conjugated anti-mouse (Sigma-Aldrich, A4416).

Plaque Forming Efficiency (PFE)

Unless otherwise stated, cells were infected with serial dilutions of HSV-1 or ΔICP0 and rocked every 10 min for 1 h prior to overlay with medium supplemented with 2% Human Serum (HS; MP Biomedicals, 2931149). 24 to 36 hpi, cells were washed twice in PBS (Sigma-Aldrich, D1408), simultaneously fixed and permeabilized in 1.8% formaldehyde (Sigma-Aldrich, F8775) and 0.5% NP40 (BDH, 56009) in PBS for 10 min, then washed twice in 0.1% Tween in PBS (PBST). Cells were blocked with 5% skimmed milk powder (SMP; Marvel) in PBST (blocking buffer) for 30 min before incubation with an anti-VP5 monoclonal antibody diluted in blocking buffer for 90 min. Cells were washed three times with PBST, incubated with HRP conjugated anti-mouse IgG diluted in blocking buffer for 60 min, then washed with PBST three times. Plaques were visualized with True Blue peroxidase developing solution (Insight, 50-78-02) according to the manufacturer's instructions, and washed with Milli-Q H$_2$O prior to plaque counting or imaging using an Axio Observer Z.1 microscope (Zeiss) with differential interference contrast. For plaque formation efficiency (PFE) assays, plaque counts are expressed relative to the number of plaques on control HFt or U2OS infected cell monolayers (as indicated) at the equivalent dilution of input virus. Results presented as relative fold change (number of plaques sample/number of plaques sample control). Plaque diameters were measured using Zen blue (Zeiss) imaging software.

Viral yield assays

Cells were infected with either HSV-1 (MOI 0.001 PFU/cell), or ΔICP0 (MOI 1 or 2 PFU/cell, as indicated) and rocked every 10 min for 1 h prior to overlay with complete medium containing either 5 μM Ruxolitinib or DMSO as a carrier control. Supernatants containing cell released virus (CRV) were collected at the indicated times post-infection. Virus titres were calculated by titration on U2OS cells as described [35].

Particle counting

Equal volumes of virus suspension and polystyrene latex spheres (Agar Scientific, AGS130-02) at a known concentration per ml were mixed in 2 volumes of TNE buffer (20 mM Tris [pH 7.5], 0.5 M NaCl, and 1 mM EDTA). 5 μl of suspension was then added to a glow discharged EM grid (Agar Scientific, S162-4), allowed to rest for 1 min, washed three times in deionised water, and stained with Ammonium Molybdate (2% (w/v) pH 7.2). Dry grids were examined using a JEM2200 FS electron microscope (JEOL) and images captured using an Ultrascan 4000 charge-coupled-device (CCD) camera (Gatan). Multiple images (n ≥ 6) per sample were used for virus particle and latex bead enumeration and used to calculate the number of particles per ml of virus stock inoculum.

Western blotting

Treated or infected cells were washed twice with PBS. Whole cell lysates were collected in SDS-PAGE loading buffer containing 4 M Urea (Sigma-Aldrich, U0631) and 50 mM Dithiothreitol (DTT; Sigma-Aldrich, D0632). Proteins were resolved on NuPAGE 4–12% Bis-Tris Protein gels (Invitrogen, NP0322BOX) in MES (Invitrogen; NP0002) or MOPS buffer (Invitrogen, NP0001) and transferred onto 0.2 μm nitrocellulose membrane (Amersham, 15249794) for 90 min at 30 volts in Novex transfer buffer (Invitrogen, NP0006-1) according to the manufacturer's instructions. Membranes were blocked in PBS with 5% FBS (Block) for a minimum of 1 h at room temperature. Membranes were incubated in primary antibody diluted in Block for a minimum of 1 h, washed three times with PBST for 5 min each, then incubated in secondary antibody diluted in Block for 1 h. Following three 5 min washes in PBST, one 5 min wash in PBS, and one rinse in Milli-Q H_2O, membranes were imaged on an Odyssey Infrared Imager (LiCor). The intensity of protein bands was quantified with Odyssey Image Studio Software.

Immunofluorescence and confocal microscopy

Cells were seeded overnight on to 13 mm coverslips prior to treatment or infection at the indicated MOI and time points at 37˚C. For click chemistry assays, cells were washed in serum free DMEM prior to overlay in complete medium or fixation. At indicated time points, cells were washed twice in CSK buffer (10 mM HEPES, 100 mM NaCl, 300 mM Sucrose, 3 mM $MgCl_2$, 5 mM EGTA), simultaneously fixed and permeabilized in 1.8% formaldehyde and 0.5% Triton-X100 (Sigma-Aldrich, T-9284) in CSK buffer for 10 min, and washed twice in CSK. Coverslips were then blocked with 2% HS in PBS for 30 min prior to click chemistry followed by immunostaining. Where applicable, EdU-labelled vDNA was detected using the Click-iT Plus EdU Alexa Fluor 555 Imaging Kit (ThermoFisher scientific, C10638) according to the manufacturer's instructions. For host and viral protein labelling, cells were incubated with primary antibodies diluted in 2% HS in PBS for 60 min, then washed in PBS three times, before incubation with secondary antibodies and DAPI (Sigma-Aldrich, D9542) in 2% HS in PBS for 60 min. Coverslips were then washed in PBS three times, and twice in Milli-Q H_2O prior to mounting on Citiflour AF1 (Agar Scientific, R1320). Coverslips were examined using a Zeiss LSM 880 confocal microscope using the 63x Plan-Apochromat oil immersion lens (numerical aperture 1.4) using 405 nm, 488 nm, 543 nm, 594 nm, and 633 nm laser lines. Zen black software (Zeiss) was used for image capture, generating cut mask channels, and calculating weighted colocalization coefficients. High-resolution Z-series images were captured under LSM 880 Airy scan deconvolution settings using 1:1:1 capture conditions at 0.035 μm intervals. Images were processed using Imaris (Bitplane) software to produce rendered 3D image reconstructions and to calculate Pearson colocalization coefficients. Exported images were processed with minimal adjustment using Adobe Photoshop and assembled for presentation using Adobe Illustrator.

Virion genome release assay

In vitro virion DNA release assays were conducted as essentially described in [47]. Briefly, $1x10^8$ PFU of virus preparation was diluted in ice-cold TNE buffer in the presence or absence of GuHCl (2M final concentration; Sigma-Aldrich, G3272). Samples were incubated on ice for 60 mins prior to the addition of ice-cold Methanol (final concentration 60%). Samples were dried onto poly-D-lysine (Sigma-Aldrich, P7405) treated coverslips for 60–90 mins at 4˚C prior to fixation in PBS containing 1.8% formaldehyde and 0.5% Triton-X100 for 10 mins at RT. Samples were washed twice in PBS and blocked in PBS containing 2% FBS for 10 mins at

RT. Samples were processed for click chemistry to detect EdU or EdC labelled vDNA and immuno-stained for VP5 to detect viral capsids (as described above). High-resolution Z-series images were captured under LSM 880 Airy scan deconvolution settings at 0.2 μm intervals (as described above) and the number of capsids and EdU or EdC labelled viral genomes were quantified in Zen blue (Zeiss) from maximum intensity projection images.

Plaque-edge recruitment assays

HFt cells were infected with ΔICP0 EYFP.ICP4 at an MOI of 2 PFU/cell to enable the initiation of viral replication and plaque formation, as previously described [9]. At 24 hpi, infected cell monolayers were pulsed with 1 μM EdU for 6h prior to fixation and immunostaining, as described above.

Quantitative RT-PCR

Cells were mock, HSV-1, or ΔICP0-infected at the indicated MOI, and total RNA collected at 9 hrs post-infection unless otherwise stated. Where applicable, all drug treatments were added at the indicated concentration 1 h after inoculum adsorption. Total RNA was isolated using the RNAeasy Plus Kit (Qiagen, 74134) according to the manufacturer's instructions. Reverse transcription (RT) was performed using the TaqMan Reverse Transcription Reagents kit (Life Technologies, N8080234) with oligo(dT) primers. cDNA samples were analyzed in triplicate using TaqMan Fast Universal PCR Master Mix (Life Technologies, 4352042) with the following TaqMan gene specific primer-(FAM/MGB) probe mixes (Life Technologies): PML (assay ID Hs00231241_m1), IFI16 (assay ID Hs00986757_m1), ATRX (assay ID HS00997529_m1), Mx1 (assay ID HS00895608_m1) ISG15 (assay ID HS01921425_s1), ISG54 (assay ID Hs0192 2738_s1), or GAPDH (4333764F) on a 7500 Fast Real time PCR system (Applied Biosystems). Relative mRNA levels were determined using the ΔΔCt method, normalized to GAPDH, and expressed relative to indicated treatments. Data presented is from a minimum of two independent biological replicates, each analysed in triplicate (RQ/RQmin/max). Means (RQ) and standard deviations (RQmin/max) are presented. For input viral genome quantitation, vDNA was extracted from infected HFt cells harvested at 90 mpi. Cells were trypsinised, pelleted by centrifugation (500 xg, 10 min), washed twice in PBS, and resuspended in PBS containing 1% SDS and 300mM Sodium acetate (pH 5.2). Total DNA was isolated by phenol chloroform extraction and ethanol precipitation, and resuspended in Tris buffer (10mM Tris-HCl pH 8.5). qPCR was performed using two virus specific (UL30 and UL36) primer-probe sets with distinct fluorophores (Sigma-Aldrich; S3 Table) in duplex reactions performed in triplicate per biological replicate. Quantitation was performed against standards of known concentration derived from a purified infectious HSV-1 17syn+ BAC clone (SR27 DNA, [95]; a kind gift from Andrew Davison MRC-UoG CVR).

Supporting information

S1 Fig. HSV-1 replication is sensitive to EdU or EdC labelling in a cell type and ICP0-dependent manner. (A, D, G) RPE or HEL cells (as indicated) were infected with 100 PFU of either WT or ΔICP0 HSV-1 and incubated in the presence of DMSO, ACG (50 μM), EdU or EdC (0.5–10 μM, as indicated) for 24 h. Plaque counts were determined and expressed relative to DMSO control (1) and presented as relative PFE. n ≥ 3, means and standard deviations shown. (B, E, H) RPE or HEL cells (as indicated) were infected (as in A) and plaque diameters measured at 24 hpi. Boxes: 25th to 75th percentile range; black line: median plaque size; whiskers: 5th to 95th percentile range. n ≥ 100 plaque measurements from 4 independent infections. (C, F, I) RPE or HEL cells (as indicated) were infected with either WT (MOI 0.001 PFU/cell)

or ΔICP0 (MOI 2 PFU/cell) HSV-1 in the presence of EdU or dU at the indicate concentrations. CRV was collected at 48 hpi and titres determined on U2OS cells. n ≥ 3, means and standard deviations are shown.
(EPS)

S2 Fig. Detection of viral genomes within HSV-1^EdC virions requires permeabilization of the capsid by GuHCl treatment. $1x10^8$ PFU of HSV-1^EdC virions were incubated in TNE buffer or TNE buffer containing 2M GuHCl at 4˚C for 60 mins, as described in [47]. EdC labelled vDNA (red) and capsids (green) were detected by click chemistry and indirect immunofluorescence staining for VP5 (the major capsid protein), respectively.
(EPS)

S3 Fig. PML-NB proteins entrap vDNA upon nuclear entry. Individual channel images for data presented in Fig 3. Localization of PML (green) with HSV-1^EdU vDNA (red, white arrows), and PML-NB constituent proteins (Daxx, Sp100, ATRX, SUMO2/3) or IFI16 (cyan, as indicated) at 90 mpi (post-addition of virus; MOI of 3 PFU/cell) or equivalent mock infected cells (as indicated). Insets show magnified regions of interest (dashed boxes) highlighting host protein localization with vDNA. Cut mask (yellow) highlights regions of colocalization between host proteins and vDNA (as indicated). Weighted colocalization coefficients are shown.
(EPS)

S4 Fig. PML-NBs entrap HSV-1 vDNA in an ICP0-independent manner. Confocal microscopy images as for data presented in Fig 3 for ΔICP0^EdU infection. Localization of PML (green) with infecting ΔICP0^EdU vDNA (red, white arrows) and PML-NB constituent proteins (Daxx, Sp100, ATRX, SUMO2/3) or IFI16 (cyan, as indicated) at 90 mpi (post-addition of virus; MOI of 3 PFU/cell). Insets show magnified regions of interest (dashed boxes) highlighting host protein localization with vDNA. Cut mask (yellow) highlights regions of colocalization between host proteins and vDNA (as indicated). Weighted colocalization coefficients are shown.
(EPS)

S5 Fig. IFI16 and PML colocalization with vDNA over a range of MOI. (A,B) HFt cells were infected with HSV-1^EdU over a range of MOIs (1–50 PFU/cell, as indicated). Cells were fixed and permeabilized at 90 mpi (post-addition of virus). vDNA, IFI16 and PML, were detected by click chemistry and indirect immunofluorescence staining, respectively. (A) Confocal microscopy images showing IFI16 (green) dots at the nuclear rim in association with PML (cyan) and vDNA (red) at an MOI of 50. White arrow highlights vDNA colocalization with IFI16 and PML. Yellow arrow highlights vDNA colocalization with PML only. Correspondingly coloured insets show magnified regions of interest (dashed boxes). Cut mask (yellow) highlights regions of colocalization between IFI16, PML, and vDNA (as indicated). Weighted (w.) colocalization coefficients shown. (B) Scatter plot showing paired w. colocalization coefficients of IFI16 and PML to individual nuclear infecting viral genomes (as described above). n ≥ 250 genomes per sample population derived from a minimum of two independent infections. (C) Quantitation of host protein recruitment to infecting viral genomes (as in B). Boxes: 25th to 75th percentile range; black line: median weighted (w.) colocalization coefficient; whiskers: 5th to 95th percentile range. Solid line indicates coincident threshold level (weighted colocalization coefficients < 0.2). (D) HFt cells were HSV-1^EdU infected at an MOI 10 PFU/cell. Cells were fixed and permeabilized at either 15 or 30 mpi (post-addition of virus). Scatter plot showing paired w. colocalization coefficients of IFI16 and PML to individual nuclear infecting viral genomes. n ≥ 60 genomes per sample population derived from a minimum of two

independent infections. (E) Quantitation of host protein recruitment to infecting viral genomes (as shown in D). Boxes: 25th to 75th percentile range; black line: median weighted (w.) colocalization coefficient; whiskers: 5th to 95th percentile range. Solid line indicates coincident threshold level (weighted colocalization coefficients < 0.2). ** $P < 0.01$, *** $P < 0.001$, ns (not significant); Mann-Whitney U-test.
(EPS)

S6 Fig. Depletion of PML does not enhance IFI16 recruitment to ΔICP0^{EdU} infecting viral genomes. Individual channel images for data presented in Fig 4 for ΔICP0^{EdU} infection. Localization of PML (green), and either Daxx or IFI16 (cyan; as indicated) to infecting ΔICP0^{EdU} vDNA (red, white arrows) in HFt shCtrl and shPML cells at 90 mpi (post-addition of virus; MOI of 3 PFU/cell). Insets show magnified regions of interest (dashed boxes) highlighting host protein localization with vDNA. Cut mask (yellow) highlights regions of colocalization between PML, IFI16, Daxx, and vDNA (as indicated). Weighted colocalization coefficients are shown.
(EPS)

S7 Fig. Recruitment of IFI16 and eYFP.ICP4 to ΔICP0^{EdU} vDNA in an asynchronous plaque-edge recruitment assay. HFt cells were infected with ΔICP0.eYFP.ICP4 at an MOI of 2 PFU/cell for 24h prior to pulse labelling with EdU for 6h. Representative images show the cellular localization of eYFP.ICP4 (green), vDNA (red), and IFI16 (cyan) in cells associated with a developing ΔICP0.eYFP.ICP4 plaque. (Left) Wide-field view of the plaque-body with newly infected cells on the periphery of the plaque-edge highlighted (dashed boxes; regions of interest 1–3). (Right) Single cell images of regions of interest (dashed boxes 1–3, respectively) showing nuclei at different stages of infection. Box 1: Infected nucleus with robust vDNA replication compartments. Box 2: Asymmetrically infected nucleus with early stage vDNA replication compartments. Box 3: Asymmetrically distributed EdU labelled nuclear infecting viral genomes that have yet to initiate viral IE (eYFP.ICP4) gene expression. IFI16 is only detected in association with vDNA that has initiated IE gene expression.
(EPS)

S8 Fig. PML-NB entrapment of vDNA occurs in a cell type dependent manner. Individual channel images from data presented in Fig 10. Localization of PML (green) and Daxx (cyan) with vDNA (red, white arrows) in HSV-1^{EdU} infected HFt, RPE, U2OS, or SAOS cells at 30 mpi (post-addition of virus; MOI 3 PFU/cell). Insets show magnified regions of interest (dashed boxes) highlighting PML and Daxx localization with vDNA. Cut mask (yellow) highlights regions of colocalization between PML or Daxx and vDNA (as indicated). Weighted colocalization coefficients are shown.
(EPS)

S1 Table. EdU or EdC treatment of infected cell monolayers inhibits wild-type (strain 17syn+) and ICP0-null mutant (*dl*1403/ΔICP0) HSV-1 plaque formation efficiency (PFE) in a cell-type and dose-dependent manner. Plaque counts expressed relative to DMSO control monolayers, (# of plaques treated / # of plaques DMSO control) at equivalent serial dilutions of virus and presented as relative plaque formation efficiency (PFE). n ≥ 3, means and standard deviations (in brackets) shown. Small plaque phenotypes at 24–36 hpi highlighted.
(DOCX)

S2 Table. Particle to PFU and genome to PFU ratios of EdU labelled wild-type and ICP0-null mutant (*dl*1403/ΔICP0) HSV-1 stock preparations in permissive (U2OS) and restrictive (HFt) cell types. Mean particles/ml determined from a minimum of 6 independent fields

of view. Mean PFU/ml determined from 3 independent titrations on either U2OS or HFt (as indicated). Mean genome copy number/U2OS PFU determined from triplicate qPCR reactions from 2 independent experiments. *PS*, plate stock (no ultracentrifugation).
(DOCX)

S3 Table. Primer-probe sets used for HSV-1 vDNA quantitation by qPCR.
(DOCX)

Acknowledgments

Author Contributions

Conceptualization: Thamir Alandijany, Ashley P. E. Roberts, Kristen L. Conn, Chris Boutell.

Data curation: Thamir Alandijany, Ashley P. E. Roberts, Chris Boutell.

Formal analysis: Thamir Alandijany, Ashley P. E. Roberts, Chris Boutell.

Funding acquisition: Chris Boutell.

Investigation: Thamir Alandijany, Ashley P. E. Roberts, Colin Loney, Steven McFarlane, Anne Orr, Chris Boutell.

Methodology: Kristen L. Conn, Colin Loney, Chris Boutell.

Project administration: Chris Boutell.

Resources: Chris Boutell.

Supervision: Ashley P. E. Roberts, Kristen L. Conn, Steven McFarlane, Anne Orr, Chris Boutell.

Visualization: Thamir Alandijany, Ashley P. E. Roberts.

Writing – original draft: Thamir Alandijany, Ashley P. E. Roberts, Chris Boutell.

Writing – review & editing: Thamir Alandijany, Ashley P. E. Roberts, Kristen L. Conn, Chris Boutell.

References

1. Komatsu T, Nagata K, Wodrich H. The Role of Nuclear Antiviral Factors against Invading DNA Viruses: The Immediate Fate of Incoming Viral Genomes. Viruses. 2016; 8(10). https://doi.org/10.3390/v8100290 PMID: 27782081; PubMed Central PMCID: PMCPMC5086622.

2. Yan N, Chen ZJ. Intrinsic antiviral immunity. Nat Immunol. 2012; 13(3):214–22. https://doi.org/10.1038/ni.2229 PMID: 22344284; PubMed Central PMCID: PMCPMC3549670.

3. Blanco-Melo D, Venkatesh S, Bieniasz PD. Intrinsic cellular defenses against human immunodeficiency viruses. Immunity. 2012; 37(3):399–411. Epub 2012/09/25. https://doi.org/10.1016/j.immuni.2012.08.013 [pii]. PMID: 22999946.

4. Diner BA, Lum KK, Cristea IM. The emerging role of nuclear viral DNA sensors. J Biol Chem. 2015; 290 (44):26412–21. https://doi.org/10.1074/jbc.R115.652289 PMID: 26354430; PubMed Central PMCID: PMCPMC4646299.

5. Knipe DM. Nuclear sensing of viral DNA, epigenetic regulation of herpes simplex virus infection, and innate immunity. Virology. 2015; 479–480:153–9. https://doi.org/10.1016/j.virol.2015.02.009 PMID: 25742715; PubMed Central PMCID: PMCPMC4424148.

6. Dempsey A, Bowie AG. Innate immune recognition of DNA: A recent history. Virology. 2015;479–480:146–52. https://doi.org/10.1016/j.virol.2015.03.013 PMID: 25816762; PubMed Central PMCID: PMCPMC4424081.

7. Everett RD. The spatial organization of DNA virus genomes in the nucleus. PLoS Pathog. 2013; 9(6): e1003386. https://doi.org/10.1371/journal.ppat.1003386 PMID: 23825941; PubMed Central PMCID: PMCPMC3694854.

8. Maul GG, Ishov AM, Everett RD. Nuclear domain 10 as preexisting potential replication start sites of herpes simplex virus type-1. Virology. 1996; 217(1):67–75. https://doi.org/10.1006/viro.1996.0094 PMID: 8599237.

9. Everett RD, Sourvinos G, Leiper C, Clements JB, Orr A. Formation of nuclear foci of the herpes simplex virus type 1 regulatory protein ICP4 at early times of infection: localization, dynamics, recruitment of ICP27, and evidence for the de novo induction of ND10-like complexes. J Virol. 2004; 78(4):1903–17. Epub 2004/01/30. https://doi.org/10.1128/JVI.78.4.1903-1917.2004 PMID: 14747555; PubMed Central PMCID: PMC369473.

10. Everett RD, Murray J. ND10 components relocate to sites associated with herpes simplex virus type 1 nucleoprotein complexes during virus infection. J Virol. 2005; 79(8):5078–89. https://doi.org/10.1128/JVI.79.8.5078-5089.2005 PMID: 15795293; PubMed Central PMCID: PMCPMC1069553.

11. Cuchet-Lourenco D, Anderson G, Sloan E, Orr A, Everett RD. The viral ubiquitin ligase ICP0 is neither sufficient nor necessary for degradation of the cellular DNA sensor IFI16 during herpes simplex virus 1 infection. J Virol. 2013; 87(24):13422–32. https://doi.org/10.1128/JVI.02474-13 PMID: 24089555; PubMed Central PMCID: PMCPMC3838218.

12. Everett RD. Dynamic Response of IFI16 and Promyelocytic Leukemia Nuclear Body Components to Herpes Simplex Virus 1 Infection. J Virol. 2015; 90(1):167–79. https://doi.org/10.1128/JVI.02249-15 PMID: 26468536; PubMed Central PMCID: PMCPMC4702556.

13. Orzalli MH, Broekema NM, Diner BA, Hancks DC, Elde NC, Cristea IM, et al. cGAS-mediated stabilization of IFI16 promotes innate signaling during herpes simplex virus infection. Proc Natl Acad Sci U S A. 2015; 112(14):E1773–81. https://doi.org/10.1073/pnas.1424637112 PMID: 25831530; PubMed Central PMCID: PMCPMC4394261.

14. Diner BA, Lum KK, Toettcher JE, Cristea IM. Viral DNA Sensors IFI16 and Cyclic GMP-AMP Synthase Possess Distinct Functions in Regulating Viral Gene Expression, Immune Defenses, and Apoptotic Responses during Herpesvirus Infection. MBio. 2016; 7(6). https://doi.org/10.1128/mBio.01553-16 PMID: 27935834; PubMed Central PMCID: PMCPMC5111403.

15. Lilley CE, Chaurushiya MS, Boutell C, Everett RD, Weitzman MD. The intrinsic antiviral defense to incoming HSV-1 genomes includes specific DNA repair proteins and is counteracted by the viral protein ICP0. PLoS Pathog. 2011; 7(6):e1002084. https://doi.org/10.1371/journal.ppat.1002084 PMID: 21698222; PubMed Central PMCID: PMCPMC3116817.

16. Cuchet-Lourenco D, Boutell C, Lukashchuk V, Grant K, Sykes A, Murray J, et al. SUMO pathway dependent recruitment of cellular repressors to herpes simplex virus type 1 genomes. PLoS Pathog. 2011; 7(7):e1002123. https://doi.org/10.1371/journal.ppat.1002123 PMID: 21779164; PubMed Central PMCID: PMCPMC3136452.

17. Boutell C, Cuchet-Lourenco D, Vanni E, Orr A, Glass M, McFarlane S, et al. A viral ubiquitin ligase has substrate preferential SUMO targeted ubiquitin ligase activity that counteracts intrinsic antiviral defence. PLoS Pathog. 2011; 7(9):e1002245. https://doi.org/10.1371/journal.ppat.1002245 PMID: 21949651; PubMed Central PMCID: PMCPMC3174244.

18. Conn KL, Wasson P, McFarlane S, Tong L, Brown JR, Grant KG, et al. Novel Role for Protein Inhibitor of Activated STAT 4 (PIAS4) in the Restriction of Herpes Simplex Virus 1 by the Cellular Intrinsic Antiviral Immune Response. J Virol. 2016; 90(9):4807–26. https://doi.org/10.1128/JVI.03055-15 PMID: 26937035; PubMed Central PMCID: PMCPMC4836348.

19. Brown JR, Conn KL, Wasson P, Charman M, Tong L, Grant K, et al. SUMO Ligase Protein Inhibitor of Activated STAT1 (PIAS1) Is a Constituent Promyelocytic Leukemia Nuclear Body Protein That Contributes to the Intrinsic Antiviral Immune Response to Herpes Simplex Virus 1. J Virol. 2016; 90(13):5939–52. https://doi.org/10.1128/JVI.00426-16 PMID: 27099310; PubMed Central PMCID: PMCPMC4907222.

20. Everett RD, Chelbi-Alix MK. PML and PML nuclear bodies: implications in antiviral defence. Biochimie. 2007; 89(6–7):819–30. https://doi.org/10.1016/j.biochi.2007.01.004 PMID: 17343971.

21. Geoffroy MC, Chelbi-Alix MK. Role of promyelocytic leukemia protein in host antiviral defense. J Interferon Cytokine Res. 2011; 31(1):145–58. Epub 2011/01/05. https://doi.org/10.1089/jir.2010.0111 PMID: 21198351.

22. Everett RD, Maul GG. HSV-1 IE protein Vmw110 causes redistribution of PML. EMBO J. 1994; 13 (21):5062–9. PMID: 7957072; PubMed Central PMCID: PMCPMC395452.

23. Boutell C, Sadis S, Everett RD. Herpes simplex virus type 1 immediate-early protein ICP0 and is isolated RING finger domain act as ubiquitin E3 ligases in vitro. J Virol. 2002; 76(2):841–50. https://doi.org/10.1128/JVI.76.2.841-850.2002 PMID: 11752173; PubMed Central PMCID: PMCPMC136846.

24. Vanni E, Gatherer D, Tong L, Everett RD, Boutell C. Functional characterization of residues required for the herpes simplex virus 1 E3 ubiquitin ligase ICP0 to interact with the cellular E2 ubiquitin-conjugating enzyme UBE2D1 (UbcH5a). J Virol. 2012; 86(11):6323–33. https://doi.org/10.1128/JVI.07210-11 PMID: 22438555; PubMed Central PMCID: PMCPMC3372195.

25. Chelbi-Alix MK, de The H. Herpes virus induced proteasome-dependent degradation of the nuclear bodies-associated PML and Sp100 proteins. Oncogene. 1999; 18(4):935–41. Epub 1999/02/19. https://doi.org/10.1038/sj.onc.1202366 PMID: 10023669.

26. Everett RD, Freemont P, Saitoh H, Dasso M, Orr A, Kathoria M, et al. The disruption of ND10 during herpes simplex virus infection correlates with the Vmw110- and proteasome-dependent loss of several PML isoforms. J Virol. 1998; 72(8):6581–91. PMID: 9658103.

27. Muller S, Matunis MJ, Dejean A. Conjugation with the ubiquitin-related modifier SUMO-1 regulates the partitioning of PML within the nucleus. Embo J. 1998; 17(1):61–70. https://doi.org/10.1093/emboj/17.1.61 PMID: 9427741.

28. Johnson KE, Chikoti L, Chandran B. Herpes simplex virus 1 infection induces activation and subsequent inhibition of the IFI16 and NLRP3 inflammasomes. J Virol. 2013; 87(9):5005–18. https://doi.org/10.1128/JVI.00082-13 PMID: 23427152; PubMed Central PMCID: PMCPMC3624293.

29. Orzalli MH, DeLuca NA, Knipe DM. Nuclear IFI16 induction of IRF-3 signaling during herpesviral infection and degradation of IFI16 by the viral ICP0 protein. Proc Natl Acad Sci U S A. 2012; 109(44):E3008–17. https://doi.org/10.1073/pnas.1211302109 PMID: 23027953; PubMed Central PMCID: PMCPMC3497734.

30. Orzalli MH, Broekema NM, Knipe DM. Relative Contributions of Herpes Simplex Virus 1 ICP0 and vhs to Loss of Cellular IFI16 Vary in Different Human Cell Types. J Virol. 2016; 90(18):8351–9. https://doi.org/10.1128/JVI.00939-16 PMID: 27412599; PubMed Central PMCID: PMCPMC5008076.

31. Diner BA, Lum KK, Javitt A, Cristea IM. Interactions of the Antiviral Factor Interferon Gamma-Inducible Protein 16 (IFI16) Mediate Immune Signaling and Herpes Simplex Virus-1 Immunosuppression. Mol Cell Proteomics. 2015; 14(9):2341–56. https://doi.org/10.1074/mcp.M114.047068 PMID: 25693804; PubMed Central PMCID: PMCPMC4563720.

32. Boutell C, Everett RD. Regulation of alphaherpesvirus infections by the ICP0 family of proteins. J Gen Virol. 2013; 94(Pt 3):465–81. https://doi.org/10.1099/vir.0.048900-0 PMID: 23239572.

33. Stow ND, Stow EC. Isolation and characterization of a herpes simplex virus type 1 mutant containing a deletion within the gene encoding the immediate early polypeptide Vmw110. J Gen Virol. 1986; 67 (Pt 12):2571–85. https://doi.org/10.1099/0022-1317-67-12-2571 PMID: 3025339.

34. Yao F, Schaffer PA. An activity specified by the osteosarcoma line U2OS can substitute functionally for ICP0, a major regulatory protein of herpes simplex virus type 1. J Virol. 1995; 69(10):6249–58. PMID: 7666525; PubMed Central PMCID: PMCPMC189522.

35. Everett RD, Boutell C, Orr A. Phenotype of a herpes simplex virus type 1 mutant that fails to express immediate-early regulatory protein ICP0. J Virol. 2004; 78(4):1763–74. https://doi.org/10.1128/JVI.78.4.1763-1774.2004 PMID: 14747541; PubMed Central PMCID: PMCPMC369471.

36. Leib DA, Harrison TE, Laslo KM, Machalek MA, Moorman NJ, Virgin HW. Interferons regulate the phenotype of wild-type and mutant herpes simplex viruses in vivo. J Exp Med. 1999; 189(4):663–72. PMID: 9989981; PubMed Central PMCID: PMCPMC2192939.

37. Mossman KL, Saffran HA, Smiley JR. Herpes simplex virus ICP0 mutants are hypersensitive to interferon. J Virol. 2000; 74(4):2052–6. PMID: 10644380; PubMed Central PMCID: PMC111685.

38. Harle P, Sainz B Jr., Carr DJ, Halford WP. The immediate-early protein, ICP0, is essential for the resistance of herpes simplex virus to interferon-alpha/beta. Virology. 2002; 293(2):295–304. https://doi.org/10.1006/viro.2001.1280 PMID: 11886249.

39. Everett RD. The use of fluorescence microscopy to study the association between herpesviruses and intrinsic resistance factors. Viruses. 2011; 3(12):2412–24. https://doi.org/10.3390/v3122412 PMID: 22355446; PubMed Central PMCID: PMCPMC3280513.

40. Everett RD, Sourvinos G, Orr A. Recruitment of herpes simplex virus type 1 transcriptional regulatory protein ICP4 into foci juxtaposed to ND10 in live, infected cells. J Virol. 2003; 77(6):3680–9. https://doi.org/10.1128/JVI.77.6.3680-3689.2003 PMID: 12610143; PubMed Central PMCID: PMCPMC149519.

41. Catez F, Rousseau A, Labetoulle M, Lomonte P. Detection of the genome and transcripts of a persistent DNA virus in neuronal tissues by fluorescent in situ hybridization combined with immunostaining. J Vis Exp. 2014;(83):e51091. https://doi.org/10.3791/51091 PMID: 24514006; PubMed Central PMCID: PMCPMC4089569.

42. Wang IH, Suomalainen M, Andriasyan V, Kilcher S, Mercer J, Neef A, et al. Tracking viral genomes in host cells at single-molecule resolution. Cell Host Microbe. 2013; 14(4):468–80. https://doi.org/10.1016/j.chom.2013.09.004 PMID: 24139403.

43. Dembowski JA, DeLuca NA. Selective recruitment of nuclear factors to productively replicating herpes simplex virus genomes. PLoS Pathog. 2015; 11(5):e1004939. https://doi.org/10.1371/journal.ppat.1004939 PMID: 26018390; PubMed Central PMCID: PMCPMC4446364.

44. Dembowski JA, Dremel SE, DeLuca NA. Replication-Coupled Recruitment of Viral and Cellular Factors to Herpes Simplex Virus Type 1 Replication Forks for the Maintenance and Expression of Viral Genomes. PLoS Pathog. 2017; 13(1):e1006166. https://doi.org/10.1371/journal.ppat.1006166 PMID: 28095497; PubMed Central PMCID: PMCPMC5271410.

45. Schmidt N, Hennig T, Serwa RA, Marchetti M, O'Hare P. Remote Activation of Host Cell DNA Synthesis in Uninfected Cells Signaled by Infected Cells in Advance of Virus Transmission. J Virol. 2015; 89 (21):11107–15. https://doi.org/10.1128/JVI.01950-15 PMID: 26311877; PubMed Central PMCID: PMCPMC4621119.

46. Johnson KE, Bottero V, Flaherty S, Dutta S, Singh VV, Chandran B. IFI16 restricts HSV-1 replication by accumulating on the hsv-1 genome, repressing HSV-1 gene expression, and directly or indirectly modulating histone modifications. PLoS Pathog. 2014; 10(11):e1004503. https://doi.org/10.1371/journal.ppat.1004503 PMID: 25375629; PubMed Central PMCID: PMCPMC4223080.

47. Newcomb WW, Brown JC. Induced extrusion of DNA from the capsid of herpes simplex virus type 1. J Virol. 1994; 68(1):433–40. PMID: 8254753; PubMed Central PMCID: PMCPMC236303.

48. Ishov AM, Sotnikov AG, Negorev D, Vladimirova OV, Neff N, Kamitani T, et al. PML is critical for ND10 formation and recruits the PML-interacting protein daxx to this nuclear structure when modified by SUMO-1. J Cell Biol. 1999; 147(2):221–34. PMID: 10525530; PubMed Central PMCID: PMCPMC2174231.

49. Everett RD, Rechter S, Papior P, Tavalai N, Stamminger T, Orr A. PML contributes to a cellular mechanism of repression of herpes simplex virus type 1 infection that is inactivated by ICP0. J Virol. 2006; 80 (16):7995–8005. https://doi.org/10.1128/JVI.00734-06 PMID: 16873256; PubMed Central PMCID: PMCPMC1563828.

50. Everett RD, Parada C, Gripon P, Sirma H, Orr A. Replication of ICP0-null mutant herpes simplex virus type 1 is restricted by both PML and Sp100. J Virol. 2008; 82(6):2661–72. https://doi.org/10.1128/JVI.02308-07 PMID: 18160441; PubMed Central PMCID: PMCPMC2258993.

51. Horisberger MA, McMaster GK, Zeller H, Wathelet MG, Dellis J, Content J. Cloning and sequence analyses of cDNAs for interferon- and virus-induced human Mx proteins reveal that they contain putative guanine nucleotide-binding sites: functional study of the corresponding gene promoter. J Virol. 1990; 64 (3):1171–81. PMID: 2154602; PubMed Central PMCID: PMCPMC249231.

52. Haronikova L, Coufal J, Kejnovska I, Jagelska EB, Fojta M, Dvorakova P, et al. IFI16 Preferentially Binds to DNA with Quadruplex Structure and Enhances DNA Quadruplex Formation. PLoS One. 2016; 11(6):e0157156. https://doi.org/10.1371/journal.pone.0157156 PMID: 27280708; PubMed Central PMCID: PMCPMC4900677.

53. Honess RW, Watson DH. Herpes simplex virus resistance and sensitivity to phosphonoacetic acid. J Virol. 1977; 21(2):584–600. PMID: 189089; PubMed Central PMCID: PMCPMC353861.

54. Elion GB, Furman PA, Fyfe JA, de Miranda P, Beauchamp L, Schaeffer HJ. Selectivity of action of an antiherpetic agent, 9-(2-hydroxyethoxymethyl) guanine. Proc Natl Acad Sci U S A. 1977; 74(12):5716–20. PMID: 202961; PubMed Central PMCID: PMCPMC431864.

55. Crumpacker CS, Schnipper LE, Zaia JA, Levin MJ. Growth inhibition by acycloguanosine of herpesviruses isolated from human infections. Antimicrob Agents Chemother. 1979; 15(5):642–5. PMID: 230783; PubMed Central PMCID: PMCPMC352730.

56. Reardon JE, Spector T. Herpes simplex virus type 1 DNA polymerase. Mechanism of inhibition by acyclovir triphosphate. J Biol Chem. 1989; 264(13):7405–11. PMID: 2540193.

57. Artusi S, Perrone R, Lago S, Raffa P, Di Iorio E, Palu G, et al. Visualization of DNA G-quadruplexes in herpes simplex virus 1-infected cells. Nucleic Acids Res. 2016; 44(21):10343–53. https://doi.org/10.1093/nar/gkw968 PMID: 27794039; PubMed Central PMCID: PMCPMC5137459.

58. Mesa RA. Ruxolitinib, a selective JAK1 and JAK2 inhibitor for the treatment of myeloproliferative neoplasms and psoriasis. IDrugs. 2010; 13(6):394–403. PMID: 20506062.

59. Quintas-Cardama A, Vaddi K, Liu P, Manshouri T, Li J, Scherle PA, et al. Preclinical characterization of the selective JAK1/2 inhibitor INCB018424: therapeutic implications for the treatment of myeloproliferative neoplasms. Blood. 2010; 115(15):3109–17. https://doi.org/10.1182/blood-2009-04-214957 PMID: 20130243; PubMed Central PMCID: PMCPMC3953826.

60. Villarino AV, Kanno Y, Ferdinand JR, O'Shea JJ. Mechanisms of Jak/STAT signaling in immunity and disease. J Immunol. 2015; 194(1):21–7. https://doi.org/10.4049/jimmunol.1401867 PMID: 25527793; PubMed Central PMCID: PMCPMC4524500.

61. Everett RD, Young DF, Randall RE, Orr A. STAT-1- and IRF-3-dependent pathways are not essential for repression of ICP0-null mutant herpes simplex virus type 1 in human fibroblasts. J Virol. 2008; 82 (17):8871–81. https://doi.org/10.1128/JVI.00613-08 PMID: 18579584; PubMed Central PMCID: PMC2519674.

62. Deschamps T, Kalamvoki M. Impaired STING Pathway in Human Osteosarcoma U2OS Cells Contributes to the Growth of ICP0-Null Mutant Herpes Simplex Virus. J Virol. 2017; 91(9). https://doi.org/10.1128/JVI.00006-17 PMID: 28179534; PubMed Central PMCID: PMCPMC5391473.

63. Lovejoy CA, Li W, Reisenweber S, Thongthip S, Bruno J, de Lange T, et al. Loss of ATRX, genome instability, and an altered DNA damage response are hallmarks of the alternative lengthening of telomeres pathway. PLoS Genet. 2012; 8(7):e1002772. https://doi.org/10.1371/journal.pgen.1002772 PMID: 22829774; PubMed Central PMCID: PMCPMC3400581.

64. McFarlane S, Preston CM. Human cytomegalovirus immediate early gene expression in the osteosarcoma line U2OS is repressed by the cell protein ATRX. Virus Res. 2011; 157(1):47–53. https://doi.org/10.1016/j.virusres.2011.02.002 PMID: 21310198.

65. Lukashchuk V, McFarlane S, Everett RD, Preston CM. Human cytomegalovirus protein pp71 displaces the chromatin-associated factor ATRX from nuclear domain 10 at early stages of infection. J Virol. 2008; 82(24):12543–54. https://doi.org/10.1128/JVI.01215-08 PMID: 18922870; PubMed Central PMCID: PMCPMC2593304.

66. Lukashchuk V, Everett RD. Regulation of ICP0-null mutant herpes simplex virus type 1 infection by ND10 components ATRX and hDaxx. J Virol. 2010; 84(8):4026–40. https://doi.org/10.1128/JVI.02597-09 PMID: 20147399; PubMed Central PMCID: PMCPMC2849514.

67. Weller SK, Coen DM. Herpes simplex viruses: mechanisms of DNA replication. Cold Spring Harb Perspect Biol. 2012; 4(9):a013011. https://doi.org/10.1101/cshperspect.a013011 PMID: 22952399; PubMed Central PMCID: PMCPMC3428768.

68. Everett RD, Boutell C, Hale BG. Interplay between viruses and host sumoylation pathways. Nat Rev Microbiol. 2013; 11(6):400–11. https://doi.org/10.1038/nrmicro3015 PMID: 23624814.

69. Glass M, Everett RD. Components of promyelocytic leukemia nuclear bodies (ND10) act cooperatively to repress herpesvirus infection. J Virol. 2013; 87(4):2174–85. https://doi.org/10.1128/JVI.02950-12 PMID: 23221561; PubMed Central PMCID: PMCPMC3571464.

70. Xue Y, Gibbons R, Yan Z, Yang D, McDowell TL, Sechi S, et al. The ATRX syndrome protein forms a chromatin-remodeling complex with Daxx and localizes in promyelocytic leukemia nuclear bodies. Proc Natl Acad Sci U S A. 2003; 100(19):10635–40. https://doi.org/10.1073/pnas.1937626100 PMID: 12953102; PubMed Central PMCID: PMCPMC196856.

71. Catez F, Picard C, Held K, Gross S, Rousseau A, Theil D, et al. HSV-1 genome subnuclear positioning and associations with host-cell PML-NBs and centromeres regulate LAT locus transcription during latency in neurons. PLoS Pathog. 2012; 8(8):e1002852. Epub 2012/08/23. https://doi.org/10.1371/journal.ppat.1002852 [pii]. PMID: 22912575; PubMed Central PMCID: PMC3415458.

72. Maroui MA, Calle A, Cohen C, Streichenberger N, Texier P, Takissian J, et al. Latency Entry of Herpes Simplex Virus 1 Is Determined by the Interaction of Its Genome with the Nuclear Environment. PLoS Pathog. 2016; 12(9):e1005834. https://doi.org/10.1371/journal.ppat.1005834 PMID: 27618691; PubMed Central PMCID: PMCPMC5019400.

73. Everett RD, Murray J, Orr A, Preston CM. Herpes simplex virus type 1 genomes are associated with ND10 nuclear substructures in quiescently infected human fibroblasts. J Virol. 2007; 81(20):10991–1004. https://doi.org/10.1128/JVI.00705-07 PMID: 17670833.

74. Cuchet-Lourenco D, Vanni E, Glass M, Orr A, Everett RD. Herpes simplex virus 1 ubiquitin ligase ICP0 interacts with PML isoform I and induces its SUMO-independent degradation. J Virol. 2012; 86 (20):11209–22. Epub 2012/08/10. doi: JVI.01145-12 [pii] https://doi.org/10.1128/JVI.01145-12 PMID: 22875967; PubMed Central PMCID: PMC3457127.

75. Everett RD, Boutell C, Pheasant K, Cuchet-Lourenco D, Orr A. Sequences related to SUMO interaction motifs in herpes simplex virus 1 protein ICP0 act cooperatively to stimulate virus infection. J Virol. 2014; 88(5):2763–74. https://doi.org/10.1128/JVI.03417-13 PMID: 24352468; PubMed Central PMCID: PMCPMC3958091.

76. Everett RD, Boutell C, McNair C, Grant L, Orr A. Comparison of the biological and biochemical activities of several members of the alphaherpesvirus ICP0 family of proteins. J Virol. 2010; 84(7):3476–87. https://doi.org/10.1128/JVI.02544-09 PMID: 20106921; PubMed Central PMCID: PMCPMC2838103.

77. Everett RD, Bell AJ, Lu Y, Orr A. The replication defect of ICP0-null mutant herpes simplex virus 1 can be largely complemented by the combined activities of human cytomegalovirus proteins IE1 and pp71.

J Virol. 2013; 87(2):978–90. https://doi.org/10.1128/JVI.01103-12 PMID: 23135716; PubMed Central PMCPMC3554063.

78. Lu Y, Everett RD. Analysis of the functional interchange between the IE1 and pp71 proteins of human cytomegalovirus and ICP0 of herpes simplex virus 1. J Virol. 2015; 89(6):3062–75. https://doi.org/10.1128/JVI.03480-14 PMID: 25552717; PubMed Central PMCID: PMCPMC4337537.

79. Lu Y, Orr A, Everett RD. Stimulation of the Replication of ICP0-Null Mutant Herpes Simplex Virus 1 and pp71-Deficient Human Cytomegalovirus by Epstein-Barr Virus Tegument Protein BNRF1. J Virol. 2016; 90(21):9664–73. https://doi.org/10.1128/JVI.01224-16 PMID: 27535048; PubMed Central PMCID: PMCPMC5068519.

80. Unterholzner L, Keating SE, Baran M, Horan KA, Jensen SB, Sharma S, et al. IFI16 is an innate immune sensor for intracellular DNA. Nat Immunol. 2010; 11(11):997–1004. https://doi.org/10.1038/ni.1932 PMID: 20890285; PubMed Central PMCID: PMCPMC3142795.

81. Kerur N, Veettil MV, Sharma-Walia N, Bottero V, Sadagopan S, Otageri P, et al. IFI16 acts as a nuclear pathogen sensor to induce the inflammasome in response to Kaposi Sarcoma-associated herpesvirus infection. Cell Host Microbe. 2011; 9(5):363–75. https://doi.org/10.1016/j.chom.2011.04.008 PMID: 21575908; PubMed Central PMCID: PMCPMC3113467.

82. Ansari MA, Singh VV, Dutta S, Veettil MV, Dutta D, Chikoti L, et al. Constitutive interferon-inducible protein 16-inflammasome activation during Epstein-Barr virus latency I, II, and III in B and epithelial cells. J Virol. 2013; 87(15):8606–23. https://doi.org/10.1128/JVI.00805-13 PMID: 23720728; PubMed Central PMCID: PMCPMC3719826.

83. Gariano GR, Dell'Oste V, Bronzini M, Gatti D, Luganini A, De Andrea M, et al. The intracellular DNA sensor IFI16 gene acts as restriction factor for human cytomegalovirus replication. PLoS Pathog. 2012; 8(1):e1002498. https://doi.org/10.1371/journal.ppat.1002498 PMID: 22291595; PubMed Central PMCID: PMCPMC3266931.

84. Horan KA, Hansen K, Jakobsen MR, Holm CK, Soby S, Unterholzner L, et al. Proteasomal degradation of herpes simplex virus capsids in macrophages releases DNA to the cytosol for recognition by DNA sensors. J Immunol. 2013; 190(5):2311–9. https://doi.org/10.4049/jimmunol.1202749 PMID: 23345332; PubMed Central PMCID: PMCPMC3578088.

85. Stratmann SA, Morrone SR, van Oijen AM, Sohn J. The innate immune sensor IFI16 recognizes foreign DNA in the nucleus by scanning along the duplex. Elife. 2015; 4:e11721. https://doi.org/10.7554/eLife.11721 PMID: 26673078; PubMed Central PMCID: PMCPMC4829420.

86. Jin T, Perry A, Jiang J, Smith P, Curry JA, Unterholzner L, et al. Structures of the HIN domain:DNA complexes reveal ligand binding and activation mechanisms of the AIM2 inflammasome and IFI16 receptor. Immunity. 2012; 36(4):561–71. https://doi.org/10.1016/j.immuni.2012.02.014 PMID: 22483801; PubMed Central PMCID: PMCPMC3334467.

87. Morrone SR, Wang T, Constantoulakis LM, Hooy RM, Delannoy MJ, Sohn J. Cooperative assembly of IFI16 filaments on dsDNA provides insights into host defense strategy. Proc Natl Acad Sci U S A. 2014; 111(1):E62–71. https://doi.org/10.1073/pnas.1313577111 PMID: 24367117; PubMed Central PMCID: PMCPMC3890864.

88. Scherer M, Otto V, Stump JD, Klingl S, Muller R, Reuter N, et al. Characterization of Recombinant Human Cytomegaloviruses Encoding IE1 Mutants L174P and 1–382 Reveals that Viral Targeting of PML Bodies Perturbs both Intrinsic and Innate Immune Responses. J Virol. 2015; 90(3):1190–205. https://doi.org/10.1128/JVI.01973-15 PMID: 26559840; PubMed Central PMCID: PMCPMC4719593.

89. El Asmi F, Maroui MA, Dutrieux J, Blondel D, Nisole S, Chelbi-Alix MK. Implication of PMLIV in both intrinsic and innate immunity. PLoS Pathog. 2014; 10(2):e1003975. https://doi.org/10.1371/journal.ppat.1003975 PMID: 24586174; PubMed Central PMCID: PMCPMC3937294.

90. Kim YE, Ahn JH. Positive role of promyelocytic leukemia protein in type I interferon response and its regulation by human cytomegalovirus. PLoS Pathog. 2015; 11(3):e1004785. https://doi.org/10.1371/journal.ppat.1004785 PMID: 25812002; PubMed Central PMCID: PMCPMC4374831.

91. Maarifi G, Chelbi-Alix MK, Nisole S. PML control of cytokine signaling. Cytokine Growth Factor Rev. 2014; 25(5):551–61. https://doi.org/10.1016/j.cytogfr.2014.04.008 PMID: 24861946.

92. Everett RD, Cross A, Orr A. A truncated form of herpes simplex virus type 1 immediate-early protein Vmw110 is expressed in a cell type dependent manner. Virology. 1993; 197(2):751–6. https://doi.org/10.1006/viro.1993.1651 PMID: 7504367.

93. Showalter SD, Zweig M, Hampar B. Monoclonal antibodies to herpes simplex virus type 1 proteins, including the immediate-early protein ICP 4. Infect Immun. 1981; 34(3):684–92. PMID: 6277788; PubMed Central PMCID: PMCPMC350925.

94. McClelland DA, Aitken JD, Bhella D, McNab D, Mitchell J, Kelly SM, et al. pH reduction as a trigger for dissociation of herpes simplex virus type 1 scaffolds. J Virol. 2002; 76(15):7407–17. https://doi.org/10.1128/JVI.76.15.7407-7417.2002 PMID: 12097553; PubMed Central PMCID: PMCPMC136365.

95. Roberts AP, Abaitua F, O'Hare P, McNab D, Rixon FJ, Pasdeloup D. Differing roles of inner tegument proteins pUL36 and pUL37 during entry of herpes simplex virus type 1. J Virol. 2009; 83(1):105–16. https://doi.org/10.1128/JVI.01032-08 PMID: 18971278; PubMed Central PMCID: PMCPMC2612316.